

Charles University in Prague
First Faculty of Medicine

Degree program: Human Physiology and Pathophysiology
Field of study: Biomedicine



Formalization of Integrative Physiology

by

Marek Mateják

(Dissertation thesis)

Supervisor: Doc. MUDr. Jiří Kofránek, CSc.

Prague, 2015

Prohlášení:

Prohlašuji, že jsem závěrečnou práci zpracoval samostatně a že jsem řádně uvedl a citoval všechny použité prameny a literaturu. Současně prohlašuji, že práce nebyla využita k získání jiného nebo stejného titulu

Souhlasím s trvalým uložením elektronické verze mé práce v databázi systému meziuniverzitního projektu Theses.cz za účelem soustavné kontroly podobnosti kvalifikačních prací.

V Praze, 10.06.2015

Marek Mateják

Identification record

MATEJÁK, MAREK. Formalization of Integrative Physiology. Prague, 2015. 115, 3, 1 CD. Dissertation thesis. Charles University in Prague, First Faculty of Medicine, Institute of Pathological Physiology. Supervisor Doc. MUDr. Jiří Kofránek CSc.

Acknowledgements

This work would never have been completed without the support of my wife and my parents. I also want to thank my tutor, Doc. MUDr. Jiří Kofránek, CSc., for his long years of support for this work, and for contacts he has helped me create with members of the physiology simulation community.

I would like to show my appreciation for the hospitality of Dr. Robert Hester, Professor of Physiology, who has facilitated our cooperation with his department at the University of Mississippi Medical Center, from 2010. Many thanks to Doc. RNDr. Jan Obdržálek, CSc. for providing very useful consultation regarding the physics behind physiological processes. Special thanks must also be given to Prof. MUDr. Emanuel Nečas, DrSc., who made a critical review of our hemoglobin allosteric binding theory, and to Doc. MUDr. Zdeněk Wunsch, CSc., for his review of this thesis.

Last but not least, I want to express my thanks for the graphic design of the icons for the implemented blocks, which were drawn by Verča, Martin, Klára, Stáňa and Zuzana. This graphical representation of the components has really improved the readability of the models.

This work was partially supported by grants from the Ministry of Industry and Trade of the Czech Republic: MPO MSM/2C – e-Golem: medical learning simulator of human physiological functions as a background of e-learning teaching of critical care medicine (2006-2009); and by MPO TIP T13/869 – Virtual patient for medical education (2011-2014).

Dedication

This thesis is dedicated to Dr. Tom G. Coleman, Professor Emeritus at the University of Mississippi Medical Center, whose complex work in the field of integrative physiology at the level of computer simulation was my greatest inspiration, and from whose work I was able to establish my own outlook on integrative physiology formalization.

Abstract

New information technologies bring with them new possibilities for defining and simulating complex physical systems. A huge amount of progress was made in this field with the Modelica language standard, developed by the worldwide nonprofit Modelica Association. Using the Modelica language specification, new chemical, hydraulic, thermal and population components for human physiology were designed for the implementation of the physiological principles in this thesis. The presented free Modelica libraries was named PHYSIOLIBRARY and CHEMICAL. Similarly to the electrical circuits already implemented in the Modelica Standard Library, it is also possible to connect the components of these libraries to the diagrams and, in this way, define more complex components of physiological systems. Using this kind of implementation, this thesis presents an extension and improvement of the HumMod version 1.6 model, developed at the University of Mississippi Medical Center (Jackson, MS), which has more than 5,000 variables. As a result of the use of graphical diagrams, our implementation is more expandable and more modifiable at each point. The precise rules of connections lead to fewer implementation errors. In addition, the visual verification of the model is achieved, because the physiological connections of diagrams are self-describing, which allows them to be directly examined and presented in the form in which they are implemented.

A new acid-base model for blood gas transport was here designed and integrated. This extension of HumMod 1.6 was more appropriate for describing the status of blood during oxygen and carbon dioxide transport, even during respiratory or metabolic acid-base disorders. The presented theory of multiple ligands binding to hemoglobin A is used to describe the equilibrium of oxygenation, carboxylation and oxygen-linked (de)protonation. This integrative approach not only shifts the oxygen-hemoglobin dissociation curve, it can also be used to calculate the carbon dioxide saturation and changes of linked protonation, which are significant for maintaining the pH of blood during blood gas exchange.

As a language for this complex physiological integrations, Modelica can be used—with new proposed physiological libraries behind it—thanks to the already established commercial and noncommercial support.

Abstrakt

Nové informační technologie přinášejí možnosti jak exaktně popsat a simulovat komplexní fyzikální systémy. Pokrok v tomto směru umožnila standardizace jazyka Modelica neziskovou celosvětovou asociací firem, univerzit a jednotlivců Modelica Association. Standard jazyka umožnil v této disertaci vytvořit chemické, hydraulické, tepelné a populační komponenty pro základní principy fyziologie člověka. Tyto nové Modelikové knihovny byly nazvány PHYSIOLIBRARY a CHEMICAL. Jejich základní komponenty je možné v Modelice graficky propojovat a tak vytvářet komplexnější komponenty fyziologických systémů, obdobně jako se v Modelice vytvářejí modely elektronických obvodů ze základních prvků elektronických komponent. Disertace ukazuje, jak lze obdobným způsobem vytvořit i tak komplexní modely jakým je model integrativní fyziologie člověka HumMod 1.6 který má více než 5000 proměnných. A nejen to, tyto modely je potom možné velmi intuitivně modifikovat a rozšiřovat. Disertační práce tak model amerických autorů HumMod 1.6 (www.hummod.org) nejen implementovala, ale i rozšířila o vlastnosti krve a hemoglobinu, které původní model neměl. Při reimplementaci modelu bylo odhaleno (a americkým autorům reportováno) 30 logických, matematických a fyziologických chyb, na které se při důkladné analýze modelu narazilo.

Byl vytvořen a integrován nový model acidobazické rovnováhy a transportu krevních plynů. Toto rozšíření modelu HumMod mnohem věrohodněji popisuje stav acidobazické rovnováhy krve a přenosu krevních plynů i v respiračních a metabolických acidobazických poruchách. Díky integračnímu přístupu byl také navržen nový pohled na přenos krevních plynů pomocí hemoglobinu A. Tento integrační model dokáže popsat nejen disociační křivku hemoglobinu pro kyslík, ale i pro oxid uhličitý a dokonce i pro kyslíkem propojené vodíkové ionty, které se významně podílejí na udržování pH v krvi při výměně krevních plynů.

Prakticky i teoreticky pomocí exaktních definic je v práci ukázáno, že integrace nových poznatků do jednoho komplexního modelu lidské fyziologie je možná a přínosná. Jeho jazykem by mohla být právě Modelica s novými, prací vytvořenými, knihovnami fyziologických komponent díky podpoře velkého množství komerčních i nekomerčních nástrojů.

Abbreviations

Variable	Physical quantity	Physical unit
a	Mole fraction based activity of the substance	1
b	Molality of the substance	$\text{mol} \cdot \text{kg}^{-1}$
c	Molarity of the substance	$\text{mol} \cdot \text{m}^{-3}$
C	Hydraulic compliance of space with elastic walls	$\text{m}^3 \cdot \text{Pa}^{-1}$
c_p	Specific molar heat capacity at constant pressure	$\text{J} \cdot \text{K}^{-1} \cdot \text{mol}^{-1}$
C_p	Specific heat capacity per mass at constant pressure	$\text{J} \cdot \text{K}^{-1} \cdot \text{kg}^{-1}$
D	Donnan's equilibrium ratio of monovalent ion	1
G	Gibbs energy	J
$\Delta_f G^\circ$	Free Gibbs energy of formation of the substance at 25°C, 1bar	$\text{J} \cdot \text{mol}^{-1}$
h	Vertical height between two points	m
H	Enthalpy; Heat energy	J
∂H	Change of heat energy; heat flow	$\text{J} \cdot \text{s}^{-1}$
H_m	Molar enthalpy of the substance	$\text{J} \cdot \text{mol}^{-1}$
$\Delta_f H^\circ$	Free molar enthalpy of formation of the substance at 25°C, 1bar	$\text{J} \cdot \text{mol}^{-1}$
$\Delta_{\text{vap}} H$	Enthalpy of vaporization	$\text{J} \cdot \text{mol}^{-1}$
k_H	Henry's law coefficient as liquid to gas ratio	1
k_C	Kinetics coefficient of chemical process	$\text{mol}^2 \cdot \text{J}^{-1} \cdot \text{s}^{-1}$
K	Dissociation coefficient of the chemical reaction	1
L	Hydraulic inertia	$\text{Pa} \cdot \text{s}^2 \cdot \text{m}^{-3}$
m	Mass	kg
∂m	Change of mass; mass flow	$\text{kg} \cdot \text{s}^{-1}$
M_A	Molar mass of the substance A	$\text{kg}^{-1} \cdot \text{mol}^{-1}$
n	Amount of the substance	mol
∂n	Change of the amount of substance; molar flow	$\text{mol} \cdot \text{s}^{-1}$
p	Pressure	Pa
Q	Electric charge	C
R	Hydraulic resistance	$\text{m}^3 \cdot \text{Pa} \cdot \text{s}$
S	Entropy	$\text{J} \cdot \text{K}^{-1}$
S_m	Molar entropy of the substance	$\text{J} \cdot \text{K}^{-1} \cdot \text{mol}^{-1}$
T	Temperature	K
U	Internal energy	J
v	Stoichiometry coefficient in the chemical reaction	1
V	Volume	m^3
∂V	Change of volume or volumetric flow	$\text{m}^3 \cdot \text{s}^{-1}$
V_m	Molar volume of the substance	$\text{m}^3 \cdot \text{mol}^{-1}$
x	Mole fraction of the substance	$\text{mol} \cdot \text{mol}^{-1}$
z	Electrical charge of one particle of the substance	C
Π	Osmotic pressure	Pa
γ	Mole fraction based activity coefficient of substance	1
μ	Electrochemical potential of the chemical substance	$\text{J} \cdot \text{mol}^{-1}$
φ	Electric potential	V
ϱ	Density	$\text{kg} \cdot \text{m}^{-3}$

Content

1	Introduction	14
1.1	Formalization of Physiology	14
1.2	Models From Mississippi.....	15
1.3	Acid-base and blood gases in HumMod 1.6.....	17
1.4	Goals – integrative model for computer simulation.....	18
2	Methods of first principles formalization	22
2.1	Physical principles.....	22
2.2	Modelica Principles.....	24
2.3	Building Modelica Libraries	28
3	Results of first principles formalization	34
3.1	Chemical domain.....	34
3.2	Thermal domain	40
3.3	Hydraulic domain.....	41
3.4	Population domain	43
4	Methods of integrative physiology formalization	46
5	Result of integrative physiology formalization.....	50
5.1	Cardiovascular system	51
5.2	Body Water	60
5.3	Hormones.....	67
5.4	Electrolytes and Acid-Base	72
5.5	Blood Gases	80
5.6	Nutrients and Metabolism	84
5.7	Thermoregulation.....	89
5.8	Neural Regulations	90
6	Discussion	92
6.1	Selection of first principles.....	92
6.2	Development of integrative physiological theories.....	93
6.3	Sensitivity analysis and identification	94
6.4	Verification.....	95
7	Conclusion.....	98
	References	102
	Appendix A – List of publications of author	116
	Appendix B – Selected Equations	120

Appendix C – Publications in extenso	124
--	-----

Motto:

“Science is a method for deciding whether what we choose to believe has a basis in the laws of nature or not.”

Marcia McNutt

1 INTRODUCTION

Having a detailed computer simulation that can predict the behavior of a system is a dream of many scientists. However, in the world of physics, many predictions are already possible. Even in chemistry, in 2013, M. Karplus, M. Levitt and A. Warshel won the Nobel Prize for the development of multi-scale models for complex chemical systems, which can predict the chemical reaction properties of even the most complex molecules. So why should this kind of computer prediction not be possible in the case of complex physiology? What needs to be done to reach that goal?

I have a strong belief that, for these purposes, physiological processes must be formalized in terms of physical generalization and mathematical integration. Formalization at the level of exact physical description would be a step in the right direction, since physics generalizes the processes in nature. However, the human physiology is very complex and it must be described with respect to this complexity. Thus, the precise and effective integration of physiological knowledge could be the key to achieving these *in silico* predictions.

There have already been many observations concerning relations between physical quantities in physiology. Many of them are statistically significant. However, statistical approximation is not enough if there are more than two variables to be connected. For this reason, the nonphysical empirical relations should be more extensively studied and described using physical processes. The building of mathematical relations between variables in physiology must be represented by designing a theory based on first physical principles. As a result of these basic principles, even a relationship between more than two variables can be easily deduced. This mathematical deduction can strongly maintain the consistency of the theory without contradicting other parts of the theory. However, these theoretical relations must always fit the observations; if they do not fit the measurements, the theory must be rearranged.

The implementation of an exactly formalized theory is called a model. Thanks to mathematical relations, it should be possible to implement the formalized theory into almost any computer language—even into a list of various types of computer processor instructions. However there are huge differences in the effectiveness and readability of these implementations, which are critical for the verification of the model. Given the availability of the most recent generation of computer languages, designed for the implementation of complex physical models, the number of steps from theory to model is minimized and the work can be more focused on the formalization of the theory, as opposed to the implementation of the theory into computer language. Thanks to this new approach in computer science, a complex integrative physiological theory can have almost the same meaning as a complex integrative model.

The formalization of integrative physiology can be understood as a process of determining the basic principles from physics and defining the methods for integrating these basic principles into one complex model of human physiology. This approach was already being pioneered in Mississippi in the 1960s. This thesis follows on from the developments of the University of Mississippi Medical Center, by finding better first principles and better ways to implement the model, and finally, by extending the model with better first principles of chemical processes, such as multi-ligands equilibrium on macromolecule.

1.1 FORMALIZATION OF PHYSIOLOGY

The building of mathematical models is strongly connected with the formalization process. The advantage of formalized description of examined reality using mathematical relations is that

the deduction of the behavior of examined objects can be done by solving the equations. The equations do not need to be solved manually, because typically, this is done by computers. These solutions to differential equations simulate the behavior of real objects over a period of time. This is called a **computer simulation**.

One of the first formalized mathematical models in physiology was a simplified model of a neuron in 1943 by (McCulloch and Pitts, 1943). Five years later, the compartmental approach for pharmacology was invented by (Sheppard, 1948). Following on, a model of excitable neural membrane was published by (Hodgkin and Huxley, 1952). In 1954, two compartmental models of respiration homeostasis was designed by (Grodins, et al., 1954). In the 1960s, with the development of the first computers, more complex models were developed, e.g., the first complex blood gases transport model (Grodins, et al., 1967) and the regulation of blood circulation with body fluid balance (Coleman, et al., 1967). In the 1970s, complex models such as the models by Guyton from Mississippi University (Guyton, et al., 1972) and models of homeostasis and body fluid balance by (Ikeda, et al., 1979) were developed. In the 1980s and 1990s, personal computers rendered mathematical modeling one of the standard methods for use in physiological research.

Nowadays, physiological formalization has a new dimension, thanks to the international project Physiome, the successor of the famous project Genome. The goals of Physiome and the European project called Virtual Physiology Human (VPH) is the formalized description of physiological functions. The framework used includes computers models of physiological parts of the human body (Bassingthwaigte, 2000).

Practical use of these formalized models is today concentrated on education, using smart robotic simulators to emulate real situations in critical care medicine; these include mannequins SimMan (Laerdal Medical AS, Norway) or the METIman (CAE Healthcare Inc, USA). There is also a large set of educational interactive software based on physiological models, starting with HumMod (Hester, et al., 2011a; Hester, et al., 2011b), Physiological Atlas (Kofránek, et al., 2011) and Virtual Patient (Privitzer, et. al., 2014).

New perspectives on the use of complex physiological models include hardware-in-loop devices for the automatic monitoring and curing of patients and improving the product-life-cycle management of pharmacological drugs through, for example, simulated testing prior to conducting clinical trials. Notions pertaining to future use include applying the model for the use of personalized medicine. Simulation of a selected patient is not currently possible, due to a lack of methods for effectively setting all the parameters within the complex model. However, restricting default values or simple scaling to type of pathological problem, height, sex, age, surface of she akin or height is in most instances sufficient for observing the primary implemented physiological principles even for some individuals.

1.2 MODELS FROM MISSISSIPPI

One of the first integrative mathematical models of human physiology was designed by (Guyton, et al., 1972). This model integrates the most necessary relations in order to describe essential hypertension. Since this pathology includes cardiovascular circulation, renal functions, the renin-angiotensin-aldosterone-system (RAAS), vasopressin and fluid balances, the model was quite complex in terms of describing the state of the patient in periods of minutes, days and months. The model was compared and partially fitted to dog nephrectomy experiments. The model well-describes the regulation of the cardiovascular system as it relates to extended water volume, which is caused by kidney function failure. It is also able to provide answers to matters of increased blood flow during an acute phase, as well as an increase of

blood pressure in the chronic phase following hormonal induced vasoconstriction (Guyton, 1991; Guyton and CE Coleman, 1973).

The power of integration in this model was very strong, leading to it becoming the basis for follow-up ongoing developments. Guyton and coworkers noticed the interactions between regulations at different time scales and elegantly described long-term pathological processes. Guyton's Textbook of Medical Physiology (Hall, 2010) became a bestseller that was translated into at least 15 languages and is still upgraded today with new editions.

The development of the model continued with more detailed cardio-vascular and body fluid regulations (Guyton, 1981; Guyton and CE Coleman, 1973; Guyton, et al., 1975). In 1983, Thomas G. Coleman, Guyton's coworker, published the "Human" model (Coleman and Randall, 1983). This model was more interactive and based on standard medical situations and the cures applied by physicians. The user can simulate cardiac failure, renal failure or hemorrhage and can interact during the simulation by applying infusion, transfusion, artificial ventilation, selected drugs and/or dialysis. This model became a virtual simulator designed for teaching medical students. Even its interface was simple; both teacher and student examine the state of the patient (described by physical quantities such as blood pressure, heart rate, ventilation rate, etc.) and apply the necessary response measures. The model was also reimplemented into a web version by Roy D. Meyers, Leo D. Geoffrion and Chris L. Doherty.

This model could be applied for more than simply the description of development of hypertension. Its users were able to examine the microcirculation of tissues, more details regarding the function of kidneys in terms of complex homeostasis, the ventilation system and other areas. The scientific expertise of Mississippi University's Medical Center also evolved as a result of cooperation with NASA on interesting physiological research, for example, the project Digital Astronaut (Summers and Coleman, 2002). Estimation and validation of experiments in microgravity or in artificial environments remain one of the goals of the model. Though there were many types of simulations available, there was only one model describing one organism in different settings and different conditions.

In 2005, the next version of the model, called "Quantitative Circulatory Physiology" (QCP) (Abram, et al., 2007) was released. This model continues in the style of the Human model. Dr. Coleman extracted parameter sets from the model, which allows for creating a patient using separate files with unique parameters. Though there are more than 1000 parameters to the setting, most of them can be copied or scaled.

The next improved version was called "Digital Human" or "Quantitative Human Physiology" (QHP) (Hester, et al., 2008). This model even separates equations from the compiled executable file.

Dr. Coleman defined a new xml-based language of physiology formalization. Using Coleman's tags, it is possible to implement a set of differential equations and implicit equations. To read these xml-files, we designed an xsl-template for Mozilla browser called QHPView, which allows for reading the equation in a more readable style. Furthermore, the graphical user interface was implemented using specific xml-language that allows for designing the application simply by editing these files. This mode has more than four thousand variables, defined mostly as real physical quantities. This model was in 2010 renamed as "HumMod" (Hester, et al., 2011a; Hester, et al., 2011b). With more than 4500 variables based on physical quantities, the HumMod is to date the largest model of the complexity of human physiology.

1.3 ACID-BASE AND BLOOD GASES IN HUMMOD 1.6

In our opinion, acid-base homeostasis and the transport of blood gases are the biggest weakness of the HumMod 1.6 model.

The production of carbon dioxide (CO_2) is in this instance defined in each tissue using a global respiratory quotient, i.e., “Metabolism-RespiratoryQuotient.RQ” (see Source code 1). This quotient can be improved, because the model already contains the metabolic consumption of base nutrients such as glucose, fatty acids, lactate or keto acids or amino acids in each tissue. If these consumption rates are known, then the production of CO_2 is the result of oxygen the rates for burning these nutrients, as well as the respiratory quotients (RQ) of the nutrients, e.g., glucose has RQ=1 and fatty acids with an RQ of around 0.7.

```
[structure: Brain-CO2 ]
[equations]
der( Mass ) = Change
initial equation: Mass = 14.3
errorLimit: 0.14
[definitions]
[block: CalcConc ]
[HCO3] = Mass / Brain-Size.LiquidVol
[HCO3(mEq/L)] = 1000.0 * [HCO3]
Tissue-BaseToGas.[HCO3] := [HCO3]
Tissue-BaseToGas.[SID] := Brain-Ph.[SID]
Tissue-BaseToGas.Calc
PCO2 := Tissue-BaseToGas.pCO2
[block: CalcDerVs ]
K = Brain-Flow.BloodFlow / Brain-Size.LiquidVol
[testcase]
[case]
test = System.Dx >= UNDEFINED
Alpha = 0.0
[case]
test = ( K * System.Dx ) >= 100.0
Alpha = 4E-44
[case]
test = true
Alpha = exp( - K * System.Dx )
InflowGas = Metabolism-RespiratoryQuotient.RQ * Brain-Flow.O2Use
InflowBase = CO2Tools.LitersToMols * InflowGas
Blood-GasToBase.pCO2 := PCO2
Blood-GasToBase.[SID] := BloodIons.[SID]
Blood-GasToBase.Calc
[BloodHCO3] := Blood-GasToBase.[HCO3]
Outflow(0) = Brain-Flow.BloodFlow * ( [BloodHCO3] - CO2Arterys.[HCO3] )
OutflowBase =
( Alpha * Outflow(0) )
+ ( ( 1 - Alpha ) * InflowBase )

Change = InflowBase - OutflowBase
```

Source code 1: Example of carbon dioxide code in neural tissue (file Structure/Brain/Brain-CO2.DES) of the HumMod 1.6.1 (model downloaded from <http://hummod.org> using “Get Started” button), with highlighted assignment of the source of carbon dioxide flow in tissues and strong ion difference as an input for the Henderson-Hasselbalch relation.

More questionable is the calculation of bicarbonate (HCO_3^-) from the strong ion difference (SID), as in Source code 2. In reality, the relation between pH as $-\log_{10}(\text{aH}^+)$ and the partial pressure of carbon dioxide (pCO_2) is driven by the Henderson-Hasselbalch reaction, i.e., $\text{CO}_2 + \text{H}_2\text{O} \leftrightarrow \text{H}^+ + \text{HCO}_3^-$. The relation between SID and pH in blood is the goal of the blood acid-base model. In HumMod 1.6, the relation between pH and SID is questionable, especially in pathological conditions, because the amount of HCO_3^- is not always 23.25% of SID (SID has a normal value of 42 mmol/L) plus 0.36 times pCO_2 in mmHg (pCO_2 in arteries has a normal value of 40 mmHg). This empirical relation in the HumMod is designed to approximate only a

state very close to a normal condition; it does not take into the account the current types and amounts of acid-base buffers. However, a model of proteins in blood plasma has previously been presented; thus, for example, the amount of albumins can be connected to acid-base homeostasis as having significant dependences, as shown by Fige-Fencl (Fijke, 2015). A significant regulator of pH is red blood cells, where hemoglobin and phosphates buffer the H⁺. Furthermore, pH is also dependent on the oxygenation state of hemoglobin (Siggaard-Andersen, 1971). This missing pH-regulation process can also be taken into account, because hematocrit and oxygen saturation are also presented in HumMod 1.6.

```
[structure: Blood-GasToBase ]
[variables]
  [var: pCO2 ]
  [var: [SID] ]
  [var: [HCO3] ]
  [constant: A = 0.2325 ]
  [constant: B = 0.00036 ]
[definitions]
  [block: Calc ]
    [HCO3] = if ( pCO2 > 0.0 ) and ( [SID] > 0.0 ) then ( A * [SID] ) + ( B
* pCO2 ) else 0.0001
```

Source code 2: Model of bicarbonate calculation from pCO₂ and SID in HumMod 1.6.1 from file Structure/CO2/Blood-GasToBase.DES.

The connected oxygen dissociation curve on hemoglobin (ODC) can be shifted according to the effects of pH, pCO₂ and carbon monoxide (CO), as well as temperature (T) in the HumMod model. However, each of these effects is valid only in situations where other effects have normal values. In pathological disorders, it is common for more than one of these effects to be deflected, e.g., during respiratory acidosis and with an acidic pH, and a higher concentration of CO₂, where the effect of CO₂ almost disappears and the Bohr effect (shift of ODC by pH) is also significantly affected by CO₂ (Siggaard-Andersen, 1971). Thus, the implementation of Hill's equation (Hill, 1913) as oxygen saturation in the HumMod is able to describe the correct shape of oxygen saturation curve only in close to normal conditions.

The HumMod 1.6 does not include the binding of CO₂ to hemoglobin. Even though it is only present in a small amount, hemoglobin helps to transport almost 25% of carbon dioxide from tissues to lungs. Behind this transporting power are several processes linked to hemoglobin: when hemoglobin binds to O₂ it releases H⁺, CO₂ and heat; when it releases O₂ it binds to H⁺, CO₂ and heat (Mateják, et al., 2015). This extremely smart mechanism is the basis of blood gas transport and can even be implemented as one integrated model that describes ODC, carbon dioxide saturation and heat transfers. The HumMod 1.6 does not calculate any of these processes, with the exception of the previously-mentioned oxygen saturation.

1.4 GOALS – INTEGRATIVE MODEL FOR COMPUTER SIMULATION

The primary goal of formalization should be to achieve the formal possibility of expressing a theory. All formalized definitions and terms must have unique meanings. Furthermore, the number of first principles must be minimized and their usage and connections should be standardized. As a result of integrative physiology, formalization should give the option for implementing the formalized theory into the computer in order to achieve the computer simulation. However, the formalized theory must be as readable as possible for the sake of verification. For these purposes, the approach to using graphical schemes for describing an integrative model should be designed. These schemes must exactly describe the theory; as a

result, it must be possible to generate computer code from them. A good candidate for this approach appears to be the Modelica language standard.

Modelica® is the most recent generation of computer equation-based object-oriented language for physical modeling and is maintained by the Modelica Association (non-profit organization with members from Europe, USA, Canada and Asia). It contains all the necessary support for an exact definition of elementary physical laws, as well as support for the robust integration of complex systems. Many libraries for electrical, mechanical, magnetic and thermal domains already in use in the industry are already included, particularly among automotive companies, such as Audi, BMW, Daimler, Ford, Toyota and Volkswagen. However, usage of Modelica in chemistry or biology is still in its initial phase. Existing Modelica libraries such as Fluid, HemoltzMedia, BioChem, ADGenKinetics, FCSys, FuelCellLib and NeuralNetwork are not yet well-enough designed for all general physiological purposes. As such, the current thesis should be a pioneering work regarding the use of Modelica in the field of physiology.

Furthermore, because to date no-one knows whether it is really possible, the usability of this language in the field of integrative physiology serves as the primary investigation of this work.

Hypothesis 1 (formalization):

Modelica®, as the most recent generation of object-oriented equation-based computer language designed for the dynamic simulation of large complex physical systems and machines, is suitable for exact formalization of integrative human physiology.

The suitability of Modelica support for the development of the model should be based on giving the user the power to develop complex physical human health simulations simply by dragging, dropping and connecting small amounts of components from prepared libraries into diagrams, such as electrical circuits with connectors independent of the causality of calculation. Each diagram should be able to be used many times in many other diagrams with different values and parameters for each type of tissue, cell, organelle, receptor, macromolecule or any chemical element. To attain such support, physiology should be considered as a science in which all first principles need to be exactly described according to the laws of nature. Without a physical description, the data becomes more valuable than their interpolation, or worse, extrapolation functions. A much better approach should be to use physics to describe the experimental setting and results using physical quantities and physical units. When this will be the case, well-known and valid relations from physics and physical chemistry can also be used.

Nowadays, physiological research is more focused on unknown elementary interactions, typically concerning one type of gene or molecule. These results should be integrated in order to gain a complex picture of physiological functions. Of course, the goal of the present work is not to integrate all of these interactions; however, it should provide the rules, the basis and the motivation for integrating them within Modelica.

Hypothesis 2 (integrative):

Mathematical formalizations of physiological knowledge about one organism can be integrated using graphical hierarchical physical diagrams into one complex physiological model, which will simulate all integrated physiological experiments.

Considering the long history of HumMod development described in section 1.2, integration into one complex model of human physiology appears possible. Therefore, the support designed for physiology in Modelica should be used for re-implementation of the HumMod to

graphical hierarchical physical diagrams and even more so in the case of integrating the new acid-base and gases transport phenomena into one complex model of human physiology.

The final goal of the thesis is to implement this complex model using hierarchical graphical diagrams in Modelica, which will render it readable at any selected level, even for medical students. Similarly, the graphical diagrams already used only for illustrative purposes in some physiological textbooks, such as in (Kittnar and Mlček, 2009). However, these diagrams in Modelica are the real implementation for attaining a runnable physiological model that can be simulated using selected settings and its dynamical results are the analogies of measurable physical quantities of the body, such as blood pressure, chemical concentrations, temperatures, etc.

The additional goal of the thesis is to design a new acid-base, new blood gases transport and new integrative hemoglobin O₂, CO₂ and H⁺ binding model as an extension of the complex model of integrative physiology.

2 METHODS OF FIRST PRINCIPLES FORMALIZATION

2.1 PHYSICAL PRINCIPLES

Generalization of physical laws leads to similar principles existing between many physical domains. The motivation is not only to have similar mathematical expressions, but also to apply prepared methodologies to more than one domain. For example, an electrical circuit diagram that can be generalized for chemical, osmotic, hydraulic or other non-electrical systems. To do this, it is necessary to find analogies in physical quantities and physical laws.

Using only two quantities, the state of subsystems at interfaces can be described. One of these variables is flow in term of Kirchhoff's law, i.e., the sum of connected flows is zero at each place in the diagram. The second variable has to be nonflow, i.e., it has the same value in each connected side. The flows are usually changes in some quantity over time such as volumetric flow, molar flow, heat flow, electric current, magnetic flux or mechanical force. The nonflows should be some type of effort such as pressure, electrochemical potential, temperature, electric potential, magnetic potential or space position. Most of the physical laws from the already mentioned physical domains can be represented using equations that mention flow and nonflow physical quantities, for example, hydraulic resistance, diffusion, thermal conduction, Ohm's law, etc.

2.1.1 International system of units

As a result of a very long tradition in medicine, values are still represented in "medical" units instead of physical units of international standard (SI). Even recently manufactured medical devices still use mmHg, calories and degrees in Celsius, among others. The problem is that these units primarily indicate their type of their measurement rather than their usability in terms of how they calculate physical laws. However, almost always exist the simple recalculation between "medical" non-SI and physical SI units. In Modelica, there is consensus that the running simulation is always in SI-units and recalculation from/to "medical" units can be done only prior to starting or after finishing the simulation.

Table I: Selected non-SI units.

Unit conversion table

x kcal	=	4186.8*x	J
x kcal/min	=	69.78*x	W
x mmHg	=	133.322387415*x	Pa
x degC	=	273.15 + x	K
x meq	=	96.4853365*x	C
x meq/min	=	1.60808894*x	A
x mosm	=	0.001*x	mol
x literSTP	=	0.044031617*x	mol
x literSATP	=	0.040339548*x	mol
x literNIST	=	0.041571200*x	mol
x iu of Erythropoietin	=	?	mol/m ³

Energy in medicine and chemistry has been observed for a very long period of time. However, one must not be confused by its different units and definitions. The researcher must be aware of the multiple definitions related to 'calorie', such as the international calorie, the

15°C calorie, the thermal calorie or ‘Calorie’ with a capital “C”. The origin of this unit lies within the amount of thermal energy needed to heat one gram of water by one degree Celsius. However, because measurement conditions may differ, alternative definitions are necessary. In physiology, it is recommended that only international calorie, as defined in Table I, be used. The flow of heat/energy is usually calculated in kcal/min; however, in physics, this is called ‘power’ and expressed in the SI unit of watts.

Pressure units in medicine are also primarily based on historical measurements. For many years, blood pressure was measured by the mercury sphygmomanometer, where the pressure is represented by the change in mercury hydrostatic column height. Since the scale of units on the column is in millimeters, the pressure unit is called millimeter of mercury, ‘mmHg’. There also exists a very small difference between this unit and torr, which is caused by variance in measurement conditions.

Many physiological processes are based on electrical principles within the human body. The main cause of this is that each cell has a nonconductive membrane with molecular structures called channels, through which the fluxes of electrolytes can be precisely regulated. Even more, the cells use energy created by the metabolism to retain a small amount of electric potential, both internally and externally. This view gave rise to a unit called equivalents or “eq”. A charge of 1eq, for example, has 1mol of sodium cations (Na^+). The fluxes of electrically charged ions can be in meq/min; however, in physics, the SI unit ‘ampere’ is more generally used.

Another odd unit describing the amount of substance is the osmol (“osm”), which has the same value as mol, but highlights the property that this substance cannot cross the membrane together with the flux of its solvent.

For gases, it is common to measure the amount as volume, which for specific measurement conditions is equivalent to the number of molecules. The International Union of Pure and Applied Chemistry (IUPAC) set this standard condition for temperature and pressure (STP) precisely at 0°C and 100kPa. However, other standards also exist. For example, SATP is measured at 25°C and 100kPa, or alternatively, at the standard measurement condition of the National Institute of Standards and Technology (NIST), which is 20°C and 101.325kPa.

Chemical substances can be quantified in many ways, typically as the amount of substance in moles, which after multiplication by the Avogadro constant ($6.02214129(27) \times 10^{23} \text{ mol}^{-1}$) yields the number of substance particles. The amount of pure substance can be expressed from its molar mass, as each atom has known and recorded its molar mass in a table of elements, usually in the unit Dalton (gram per one mole). However, each substance has different molar mass and as a result, the conversion from mass to moles is always dependent on type (composition) of substance.

In physiology, units for directly-immeasurable substances are also used. Small concentrations such as 10^{-12} moles per liter are almost impossible to measure directly and only indirect measurements with immunoreactions or biological effects are known. However, the effect of some substances at these small concentrations can be crucial enough that they nonetheless need to be calculated somehow within physiological models. Most of these substances are called hormones, but some may be also enzymes (renin) or cytokines (erythropoietin). Pharmacological international units of these substances are defined as ratios to some extracted and purified standardized sample, which also has an unknown molar concentration, but known and well-described biological effects. As a result, the pharmacological international unit of substances often has no equivalent in SI units, but nonetheless needs to be used in physiological calculations as is. The danger of using these units is significant, especially in pathologies, because their biological activity is often times species dependent and is usually defined within a “normal” population. For example, in diabetes mellitus type 2 is presented an insulin resistance; therefore, the biological activity of the same amount of insulin for these individuals is entirely different than in a healthy individual.

2.1.2 Redundant physical quantities

Some standardization should be conducted regarding the definitions of physical quantities. For example, each two variables in reciprocal relation, connected only by the trivial equation $a=1/b$, where the handling of both does not bring any additional information to the model, because their physical meaning is the same. Even the zero-infinity numerical problem can be easily solved by selecting variables such as the smallest representable floating point number or the highest representable floating point number, which are typically far enough from tolerance limits even for very long simulations.

The above reciprocal quantities are derivable from almost each physiological parameter such as hydraulic conductance, hydraulic resistance, hydraulic compliance, hydraulic elasticity, frequency, time period, solubility, volatility, dissociation coefficient, association coefficient, etc. To simplify this situation, it is better to select only one of each pair and build the physiological and chemical laws above as is usually done in physics, which will assist significantly in the elimination of redundancies inside shared interfaces.

Bad practice also includes using a unitless logarithm or other non-units, as well as non-physical variables in interfaces, even if the user has good documentation of how to convert these values. Values should always have an analogy in physical quantity, as this is more user-friendly and more intuitive for follow-up developments.

2.1.3 Conservation laws

The next step of physiology formalization is the identification of physiological systems as physical systems. Based on interactions with environment, there exist closed and open systems. An example of an open system is oxygen transport, where there is non-zero flow of oxygen from the environment to the body. In a closed system, there are not interactions between the body and the environment. For example, the chemical system of elementary particles in all its forms and in all places within the body that partakes in no exchange with the external environment is a closed particle system.

The laws of conservation applies to closed systems. Neither energy, mass, an amount of substance or electric charge can be created from nothing. In dynamic models, it is very intuitive, because there is a rule stating that input flow to one component is always output flow from another component. However, in a steady state calculation (section 2.3.3), this system equation must be written explicitly, which is often not as intuitive; this is because in a steady state, flows from/to components are equal to zero.

2.2 MODELICA PRINCIPLES

Modelica is an object-oriented, equation-based computer language that is standardized and maintained by the Modelica Association (www.modelica.org). The non-proprietary standard of this language is supported by many other projects, companies and organizations. As a result, there are a range of different environments available for this language. For example, Dymola, OpenModelica, SimulationX, JModelica, CATIA Systems, CyModelica, MapleSim and Wolfram SystemModeler.

My Modelica extensions called Chemical (section 3.1), Physiolibrary (section 3.2, 3.3 and 3.4) and Physiomodel (section 5) should be able to run in all these environments, which support the Modelica standard 3.3 and Modelica Standard Library 3.2.1.

2.2.1 Floating point numbers

From a mathematical point of view, the domain of real numbers is infinite. How then is it possible that it can be represented by a finite number of bits, i.e., 32 or 64? The answer is that it does so via approximations. There must always be some limits to precisions, some tolerances. Floating point numbers are represented by scientific notation with mantissa (a) and exponent (b) as $a \cdot 10^b$. Both mantissa and exponent are represented by a fixed number of bits. At single-precision floating point format there is one bit for a sign, 8 bits for an exponent and 23 bits for mantissa. This representation provides the smallest number as 10^{-127} , the biggest number as 10^{127} and eps (the biggest number, e.g., $1.0 + \text{eps} = 1.0$) as $<10^{-6}$. This 32-bit precision is sufficient in most common cases; however, for specific calculations, better precision exists. For 64-bit, the double-precision floating-point format has 11 as the exponent (with a theoretical range from 10^{-1027} to 10^{1027}) and 52 bits for mantissa (with $\text{eps} < 10^{-15}$).

Though ranges and precisions are limited, floating points calculations can also present the user with other obstacles. The first of these is expressing the equality of real numbers. For example, what does it mean if we say that x is equal to zero, such as the condition $x == 0$? If the number x is set to zero by the user and it does not by calculation change, its value truly remains zero; however, if it is calculated, it is always calculated with some precision. This means that a test of equality has sense only within this tolerance range. If we have set tolerance to 10^{-3} , then we should be satisfied with numbers greater than -0.001 and numbers less than 0.001. Otherwise, the solver may reach the tolerance limits and as a result, will no longer reach equality.

The user tolerance definition for elementary non-iterative mathematical operations is not needed, but it is necessary for iterative numerical methods. The most common of these methods are numerical solving of differential equations (such as the Euler method, DASSL and others) or the numerical solving of non-linear equations by iterative approximations (such as the Newton method). At first glance, it seems that the tolerance for each tested variable is needed in error conditions of the iterative algorithms. However, this can be handled only by one relative tolerance and scaling of the variables. For this scaling, Modelica uses the attribute ‘nominal’, which can be included in all real variables.

2.2.2 Object-oriented programming

Object oriented programming has been one of the most significant developments in computer science to date. The programing of large applications and systems becomes more simplified when re-using and extending already defined objects. The notion of an object as a definition is particularly intuitive, because it copies human language and thinking. Each defined term is an object, which can have more occurrences; occurrence of the object is called an instance.

Each object can have properties. These properties can be a primitive variable such as a number, text, a true/false value or an object. This can create hierarchical decomposition within one system as one object to its subsystems as more and more detailed definitions of the owner parts. Particularly in physiology, these patterns are everywhere. When an object is present for a chemical reaction, a chemical substance, organelle, membrane channel, cell, membrane, tissue or physiological system, it is possible to compose new detailed objects such as large models of physiology, by using already described objects and by choosing the correct parameters of these new instances.

It is not necessary to make decomposition of problem from up to down¹ or vice versa, because object-oriented thinking just support to start everywhere. There is only one condition for effective object-oriented programming: *the minimization of object numbers at the same time as the minimization of instance numbers to describe the same system according to the same rules.* This process is already used in mathematics and physical sciences, where the science can be exactly built from a small number of base rules by a finite minimized number of definitions.

The above idea can also be found in medicine books, where many principles or objects are generalized and finally applied to many parts of the body's systems. For example, one family of membrane receptors can be used in many pathways and can interact with many different effectors.

Computer language principles are fairly straightforward. As a simple example, we defined two objects: class A and class B. Class B has only one parameter p, which can in each instance of B have a different value. Class A, as an example of class composition, contains two instances of class B, first with the parameter set at 1 and second with the parameter set at a value of 2.

```

class B "Definition of class B"
  parameter Real p "Real number parameter";
end B;

class A "Definition of class A"
  B b1(p=1) "First instance of class B";
  B b2(p=2) "Second instance of class B";
  B bArray[100](each p=3) "Array of one hundred instances of class B";
end A;

```

It is good practice to write the names of classes as starting with a capital letter and the names of instances starting in lower case. The object-oriented pattern includes any combination of parameters, variables and instances within the class definition. Other more sophisticated rules of object-oriented programming in Modelica can be described as modifications of this principle. The instances, variables and parameters can be hidden or publish outside the class by using the prefixes 'private', 'protected' and 'public', which provides useful restrictions for other users; this is referred to as encapsulation.

Modelica language provides an analogy of these classic textual representations using graphical diagrams. Generally, a definition of each class is accessible as an icon on the left side of the Modelica environment, called the 'Package Browser'. These classes can be as simple as elementary mathematical operations or very complex classes, which may be hierarchically composed from other classes.

To make an instance from any class in the 'Package Browser' it is necessary to have opened your class in diagram mode, then drag the selected class from 'Package Browser' and drop it to diagram. In general, it is not possible to modify integrated library classes; therefore, it is first necessary to create a 'new model' (using menu command: File > New > Model) with the unique name 'MyClass'. Any class instance can be added to 'MyClass' just by dragging and dropping icons from the 'Package Browser' to the new model. Care must be taken, however, because double clicking any class in the 'Package Browser' can cause switches in class definitions.

¹ Decomposition from up to down means starting with the whole and dividing it to smaller pieces.
Decomposition from down to up means starting with many small pieces and joining them together.

The restricted class called ‘model’ without connectors can be flattened, translated and simulated with all its instance trees. This is because they have section ‘equation’, where all the equations and connections between instances are defined that is needed to calculate complete behavior (defined by the same number of equations as the number of unknowns). In the first step of this model, the [Open Modelica Compiler](#) translates structures into a flat model, where the same equation and algorithm are extracted, but without using object-oriented class definitions. This step can be done fully automatic and can generate a large amount of code compared to the original object-oriented representation. Then, the compiler automatically translate this flattened model into lower level computer language such as [C/C++](#). This code is then run as a typical computer program; it has inputs such as initial setting and outputs such as the results of the simulation during the simulation time interval.

2.2.3 Connections

Each library class has some possibilities for connecting their instances together. In the case of restricted classes, referred to as ‘block’, they are only causal connectors, which can be ‘input’ or ‘output’ variables. The restricted class, referred to as ‘connector’ is in this case used only as a substitution elementary type for the real number (‘Real’) and with a causality direction prefix. After inserting any block instance to ‘MyClass’, all input and output connectors will be visible. Connections of these types of connectors are intuitive – each output can be connected to many inputs and connected variables will always have the same value.

Since the complex parts of a model can have many inputs and outputs, there exists in Modelica a special class called ‘expandable connector’. This connector does not have an explicitly defined list of variables or their causal direction, since this can be automatically generated from connections. For example, if we connect connector ‘c’ to this expandable connector called ‘busConnector’ as variable ‘busConnector.c3’, it automatically creates an implicit definition from the ‘c’ connector. This is designed only for large models and sends values from one branch to another branch of instances. Generally, it does not make sense to use expandable connectors for models where instances at the top level are composed only of elementary classes.

What allows for creating models such as electrical circuits is a connector defined by two variables: nonflow and flow. The flow variable has the prefix ‘flow’. It is possible to connect any number of connector instances of one definition together. These connections generate expected rules of circuits, where connected nonflows are equal and the sum of connected flows is zero.

The best practice in computer science is to use negative flow values for outflowing from the component and positive for inflowing to the component.

2.2.4 Conditional inputs

The Modelica library for physiology can be designed to have the minimal number of components that are necessary for describing any processes inside the human body. Thanks to the support of steady state interfaces, the same components exist for dynamic and for equilibrium calculations. The conditional Modelica principle is also used for switching between parameters and for input to the block. These inputs are called conditional inputs and they are arranged in the same pattern as some components in MSL, for example, the component “Modelica.Analog.Basic.Resistor”.

2.3 BUILDING MODELICA LIBRARIES

Due to Modelica principles, it is possible to describe with a relatively small amount of physical types the basic rules of selected physical domains. First, we were implemented in Modelica complex models such as Guyton's 'Overall Circulation' (Guyton, et al., 1972; Kofránek, et al., 2009), Ikeda's 'Body Fluids' (Ikeda, et al., 1979; Mateják and Kofránek, 2010), Siggaard's 'Oxygen Status Algorithm' (Mateják, et al., 2012; Siggaard-Andersen and Siggaard-Andersen, 1990), 'Quantitative Human Physiology' (Mateják and Kofránek, 2010) and finally Coleman's 'HumMod' model (Mateják and Kofránek, 2011). We can argue that reimplementations of models does not bring about new knowledge, but we nonetheless hope that this is not entirely correct and that my methodology will be useful for researchers designing their own theories, as well as for the integration of models.

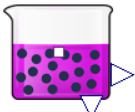
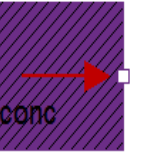
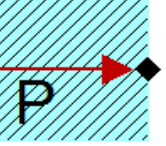
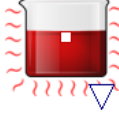
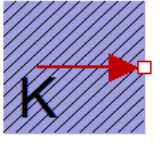
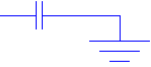
As proof that new theories can be based on the physical laws already implemented in the Physiolibrary, we presented some of our models in physiological articles. The first concerns the modeling of pulsatile circulations (Kulhánek, et al., 2014a; Kulhánek, et al., 2014b), the second concerns the modeling of oxygen, carbon dioxide and hydrogen ions binding to hemoglobin (Mateják, et al., 2015). The integration of models works well because of object-oriented programming with well-defined interfaces using physical SI units, physical quantities, physical connectors and physical laws. The primary result of the integration of the above-mentioned models is the Physiomodel.

Table II: Physical connectors in the Physiolibrary and Chemical libraries, compared to electrical connectors of the Modelica Standard Library.

Connector:	Nonflow variable	Flow variable
■□ Substance	electrochemical potential μ [J.mol ⁻¹]	molar flow ∂n [mol.s ⁻¹]
◆◆ Hydraulic	Pressure p [Pa]	volumetric flow ∂V [m ³ .s ⁻¹]
■□ Thermal	Temperature T [K]	heat flow ∂H [W]
■□ Population	size of population sz [1]	change of population ∂sz [s ⁻¹]
■□ Electrical	electric potential u [V]	electric current i [A]

Each connector of the Physio- or Chemical library belongs to one physical domain (see Table), where the components can be connected using appropriate connector definitions. As seen in Table III, most of the components are analogous throughout the domains. For example, the resistor in electrical circuits are analogous to those in the chemical domain (as diffusion), because the molar flow of substance is driven by an electrochemical potential gradient in the same manner as an electric current is driven by voltage gradient. To define these mathematical analogies in Table III, the symbols e – as in the effort for connector nonflow variables – and f – as in the flow for connector flow variables – are selected. If more connectors are present in the component, they are differentiated by index.

Table III: Analogies of new proposed Physiolibrary and Chemical library components, based on proposed connectors from Table II and with electrical components from the Modelica Standard Library.

Resistance	Accumulation	Stream	Inertia	Effort source
$f_1 = G*(e_1 - e_2)$ $f_1 + f_2 = 0$	$\int f = a$ $a = C*e$	$f_1 = \begin{cases} F e_1, & F \geq 0 \\ F e_2, & F < 0 \end{cases}$ $f_1 + f_2 = 0$	$f_1 = \int \frac{e_1 - e_2}{L}$ $f_1 + f_2 = 0$	$e = E$
G... conductance	C...capacitance	F...stream flow	L...inertia	E..effort
			not applicable	
<i>Chemical diffusion</i>	<i>Chemical substance</i>	<i>Solution stream</i>		<i>Mole Fraction</i>
		not applicable		
<i>Hydraulic resistance</i>	<i>Elastic vessel</i>		<i>Inertia</i>	<i>Pressure</i>
			not applicable	
<i>Heat convection</i>	<i>Heat accumulation</i>	<i>Heated mass flow</i>		<i>Temperature</i>
not applicable			not applicable	not applicable
	<i>Population</i>	<i>Growth, Differentiation</i>		
		not applicable		
<i>Electrical resistor</i>	<i>Electrical capacitor</i>		<i>Inductor</i>	<i>Voltage</i>

2.3.1 Types

Most of the variables in mathematical models are real numbers and can be defined only by using an elementary type, i.e., ‘Real’. Why then does the Physiolibrary need so many elementary types for real numbers? Even the ‘Real’ is a simple type, which represents the number as described in the section [Floating point numbers](#); in Modelica, it can have attributes that differentiate between the meaning of values. This meaning is aimed at being user-friendly through the use of library components. With the help of these attributes, the Modelica environments can:

- find incompatible physical quantities in connections or equations
- recalculate the physical units in dialogs or in outputs
- assert the simulation when the values are not in their domain of definition
- increase the precision of results and speed up calculations

Checking physical quantities is extremely useful, especially for simple input/output connectors, which are in the Physiolibrary specified for each type in the package ‘Types.RealIO’. Using this type of connector instead of simple RealInput/RealOutput ones, a warning can be generated or even an error each time the user tries to connect, for example, an output connector of pressure value with an input connector expecting volume value.

Setting parameters using dialogs during implementation of the model can be simplified by the correct specification of physical units. Some environments can recalculate many non-SI units into expected SI units within models, but they need to know at which SI unit the value is (see the following section: [International system of units](#)). For the dialog setting of only one value within the model, constants are prepared for each type in the package ‘Types.Constants’. However, if the user applies any Physiolibrary types for his parameter or variable, the recalculations of this entire unit should also be automatically recognized.

The min/max assertions are not always set as the default debug feature for environments, but if they are, they can recognize bad results such as negative volumes, negative masses and temperatures less than 0 K. In correct physical models, these values should not be reached; however, the user always has the option to implement whatever equation they wish. Furthermore, because the correctness of each model cannot be decided automatically, any warning or assertion can be very useful.

Due to the compatibility of all Modelica libraries and models, all values should be calculated in SI units. This rule can generate strange dimensions for some values. For example, the SI unit for volume is cubic meter; however, in the body, compartments are measured in volumes of milliliters. Therefore, the numbers used for calculation will be a million times smaller than those generally used by a physiologist. However, this does not matter, because in the Physiolibrary, these types are defined as having ‘nominal’ attributes, which move the tolerance level from SI units to the typical values used in physiology.

2.3.2 Blocks

The reason why Physiolibrary defines blocks is because they are missing in the Modelica Standard Library 3.2 (MSL). The blocks in the Physiolibrary are graphical implementations of simple mathematical operations such as reciprocity and power, among others, as well as more complex blocks for the interpolation of value by cubic function. This type of interpolation is needed for the implementation of empirical dependences between two variables, for which the physical explanation lies beyond the scope of the model. The interpolation can be implemented in different ways. The linear MSL look-up table approximates the value between known points using linear segments, which generates once derivation discontinuities. To solve this problem,

we selected a cubic **spline** interpolation curve, which also has continuous first derivations. The curve is defined by a set of points with the coordinates x, y and slope. Approximated value v (coordinate y) is calculated from u (coordinate x), where point (u,v) lies on the curve. First, a segment of curve is selected, which is defined by the nearest curve points. During initialization, each segment has a prepared coefficient a, b, c and d of cubic equation $ax^3+bx^2+cx+d=y$ as a means for reaching these definition points at defined coordinates and slopes.

2.3.2.1 Factors

Special patterns are used in the Physiolibrary in the form of factors. This idea has been applied in many physiological models in which multiplication effects are relative. In normal conditions, this effect is at value one. When it increases the base value twice its value is two; when it decreases the resulting value to half its value is 0.5. The resulting value can be affected by many factors, because at normal conditions, the product of ones is one. The graphical block for a factor always has one input at the top for an unaffected value and one output on the bottom for a resulting value, which is calculated as the effect multiplied by the unaffected value. The calculation of effects differentiates the factors from one another. The ‘Blocks.Factors’ package contains not only linear or cubic interpolations, there are also factors, which could quickly or slowly adapt the effect in time to the left-located input. This adaptation is called ‘**lag**’ and a simple mathematical filter is defined for it by Equation 1:

$$y(t) = \int k \cdot (x(t) - y(t)) dt \quad \begin{matrix} \text{Equation 1,} \\ \text{Lag} \end{matrix}$$

where t is time, x is an input, y is an output as adapted value and k is a parameter. The meaning of parameter k can be solved from a hypothetical situation where x is constant during simulation and y has another initial value than x. The solution to this simplification as a simple differential equation of one unknown function y shows that the halftime of y’s adaptation to x’s value is exactly $\ln(2)/k$; this is because in the case of constant input x, the result is always $y(\ln(2)/k) = x + (y(0)-x)/2$.

2.3.3 Steady states

Each integrator is implemented in Physiolibrary 2.3 using a steady state interface. This provides support for changing the convergent system of differential equations to a system without derivations and with direct calculation of the fixed converging state. This feature is not designed for non-convergent systems such as oscillating or divergent systems. Though periodical processes in physiology are common, e.g., heartbeat, breathing, pericardial cycle or menstrual cycle, they can be implemented as a convergent system.

A convergent system does not have typical oscillating behavior; instead, oscillation is generally simplified to mean values and frequencies (frequency equals reciprocal period time). Surprisingly, for most variables, this significant simplification does not change the impact on other processes also calculated in mean values. Another example is if we want to view the specific current points in an oscillating period. This type of calculation delivers significant complexity in the form of additional processes, which can be neglected in a convergent system. For example, if we calculate to include convergent blood circulation, we can successively use mean pressures and mean blood flows with only two types of equation for elastic vessels and hydraulic resistor. However, if we want to calculate the values of pressure and blood flow continuously beat-by-beat, many other physical laws must also be included for precise dynamic calculation such as the opening and closing of valves, the inertia of mass flow, pressure waves with reflections in a 3D net of vessels, a fluid convection model inside the

vessels and many others that disappear completely during the time the process takes place. Sometimes, these dynamic effects must also be calculated; however, for the long-term simulation of a typically healthy patient in typical conditions they can be eliminated without loss of generality.

Having a convergent system of differential equations, the point of convergence can be calculated by setting derivations to zero. This static time-independent situation is known as steady state. Typically, it can be used for very quick processes that converge in much shorter times than the time of simulation. Solving these processes dynamically using differential equations leads to stiff-equations, which can cause many problems in numerical solutions. Avoiding these very slow numerical calculations and their uncertain results can be effected by instead calculating the steady state (equilibrium) immediately.

The main problem with defining the steady state is that the swapping of branches in Equation 2 can generate dependent equations, especially when changing from a dynamic state to a steady state. For each dependent equation one additional equation should be added. These additional equations typically describe the state of the system, e.g., Conservation laws or the environmental conditions.

$$x = \begin{cases} \partial y, & \text{dynamic state: } y(t) = \int x(t) dt \\ 0, & \text{steady state: } y(t) \text{ is constant} \end{cases}$$

Equation 2: Steady state.

For example, chemical equilibrium is the steady state in the chemical domain. The chemical reaction can be so fast that for long-term simulation, a dissociation constant with sufficient precision is always reached, rendering it unnecessary to calculate the dynamic for reaching a chemical equilibrium within the model. One solution to this issue is to implement the system only as equilibrium; however, the physical reality is the same as it is for models, where this dynamic is necessary. A better approach is therefore to implement the process with the possibility of selecting the option for dynamic or steady state calculation according to parameters prior to simulation. This implementation can be used for both short-term and long-term simulations.

Steady state does not always infer zero flow. For example, the steady state of a cardiovascular system is the state of non-zero, meaning cardiac output typically around five liters per minute. However, the total number of derivations, which increase or decrease the mean volume inside vessels remains zero, as defined by the steady state. Constant mean vessel volumes lead to constant mean pressures, driven only by hydraulic resistances. Furthermore, the systemic or pulmonary circulation at steady state can be calculated as systemic or pulmonary resistance without any dynamic adaptations caused by the spillover of blood volume.

3 RESULTS OF FIRST PRINCIPLES FORMALIZATION

The primary result of this work is “[Physilibrary](#)”, a Modelica library for physiology, as well as a general Modelica library for chemical and electrochemical processes called “[Chemical](#)”. The whole of this section is dedicated to a description of first principles behind these libraries, which serve as the basis for the model “[Physiomodel](#)” described in section 6.

3.1 CHEMICAL DOMAIN

The chemical connector provides the molar flow “ ∂n_A ” of substance A. The amount of substance “ n_A ” can be expressed by the integration of this molar flow, as shown in Equation 3. In equilibrium, changes in substance “ ∂n_A ” remain zero and the amount of the substance “ n_A ” remains constant.

$$n_A = \int \partial n_A \quad \text{Equation 3: Amount of substance.}$$



From the amount of the substance “ n_A ” its mole fraction “ x_A ”, molar concentration “ c_A ” or molality “ b_A ” can be expressed in the solution. If the amount of all particles in the solution is “ n_T ”, the volume of the entire solution is “ V_T ” and the mass of the solvent is “ m_S ”, and the relation between mole fraction, concentration and molarity is Equation 4.

$$x_A = \frac{n_A}{n_T} = \frac{V_T}{n_T} \cdot c_A = \frac{m_S}{n_T} \cdot b_A \quad \text{Equation 4: Mole fraction of the substance.}$$

For example, one liter of typical blood plasma, as presented in (Raftos, et al., 1990), has a total number of particles “ n_T ” of about 51.8 mol and contains water as a solvent in a mass of 0.93 kg. The mole fraction of water is about 0.995 mol/mol and the mole fraction of chloride in the molar concentration 100 mmol/L is 0.00193 mol/mol.

Inside the cell, the situation is different. For example, in the red blood cells of (Raftos, et al., 1990), the total number of particles “ n_T ” is roughly 38.7 mole per liter and the mass of water is only 0.69 kg per liter of intracellular fluid. However, these values yield the same mole fraction of water as in plasma (0.995 mol/mol). The mole fraction of chloride, the molar concentration of which is in erythrocyte around 50 mol/L, is 0.0013 mol/mol.

The current theory of physical chemistry requires a correction coefficient between different ways of measuring a substance within a solution. This correction is called activity coefficient γ_A . For the ideal substance, this is 1. However, it can vary for electrolytes, as predicted by Debey and Huckel (Debye and Huckel, 1923), Davies and Robinson-Stokes (Stokes and Robinson, 1948) and others. As a reason of this non-ideal behavior an activity of the substance “ a_A ” should be inserted to the equation of the chemical potential instead of its mole fraction x_A .

$$a_A = \gamma_A \cdot x_A \quad \text{Equation 5: Activity of the substance.}$$

Each chemical process will endeavor to equilibrate the electrochemical potentials of the substances. Electrochemical potential (Equation 6) describes the free Gibbs energy of one mole of the substance in the solution at defined conditions. This definition is the base equation for the physical chemistry (Mortimer, 2008).

$$\bar{\mu}_A = \mu_A^o + R \cdot T \cdot \ln(a_A) + z_A \cdot F \cdot \varphi$$

*Equation 6:
Electrochemical
potential.*

$$\mu_A = \mu_A^o + R \cdot T \cdot \ln(a_A)$$

*Equation 7:
Chemical
potential.*

where T is the temperature of the solution, φ is electric potential of the solution, R is gas constant (8.314), z_A is the number of ion charge (0 is the substance and is not an ion), F is Faraday constant and μ_A^o is the chemical potential of the pure substance.

A typical chemical solution has electric potential equal to zero ($\varphi=0$), so that the electrochemical potential is the same as the chemical potential (Mortimer, 2008). Additionally, for all chemical processes in one homogenous chemical solution, the electrical part of electrochemical potential can potentially be neglected, because it is algebraically eliminated (the electric potential is the same in both sides of electrochemical equality for each chemical substance). After removing the electrical part of the electrochemical potential, only the chemical potential remains. However, for processes between different solutions, the electric part must be present. As a result, non-zero electric potentials can be presented between solutions.

3.1.1 Chemical substance transports

The most intuitive equilibrium of electrochemical potentials is reached by equilibrating diffusion in order to attain one homogenous mixture with the same activities of all substances in all places.



It is somewhat complicated to imagine the equilibrium of uncharged substances through a semipermeable membrane. The electric part of the potential is zero, because the substance has zero charge ($z=0$). Therefore, only the chemical parts of the potential on both sides of the membrane are equilibrated. As it is the same substance on both sides, equilibrium of both pressure and chemical potential is reached if the activities are the same in both sides of the membrane. This equilibration of permeable particles is usually called osmosis and is the reason why water has the same mole fraction in plasma as in the intracellular fluids of erythrocytes. A second view of the same calculation can sometimes be simplified by impermeable particles, because a higher level of impermeable particles causes lower mole fractions in each permeable substance. In some cases, the mathematical simplification “ $\ln(1-x) \approx x$ ” can be used, e.g., for such small x as mole fraction of plasmatic proteins on capillary membranes, where $\ln(x_{\text{Permeants}}) = \ln(1-x_{\text{Impermeants}}) \approx x_{\text{Impermeants}}$. In this case, it appears as if there is equilibration of osmolarities (molar concentration of impermeable substances); however, in reality this is equilibration of electrochemical potentials for each permeable substance as expressed in [Equation 8](#), where μ_A^o must be extended alongside the pressure dependence of its state of matter, as we do with constant molar volume $V_{m,A}$ in case of incompressible substances.

$$\bar{\mu}_{A,in} = \bar{\mu}_{A,out}$$

*Equation 8:
Osmotic pressure
gradient across
the membrane for
uncharged
incompressible
permeable
substance A.*

$$\Pi_{in \rightarrow out} = p_{in} - p_{out} = \frac{\mu_{A,in}^o(p_{in}) - \mu_{A,out}^o(p_{out})}{V_{m,A}} = \frac{R \cdot T}{V_{m,A}} \ln \left(\frac{a_{A,out}}{a_{A,in}} \right)$$

The other equilibrium is reached for chloride on cellular membrane of erythrocyte. Chloride can freely cross the membrane through a membrane channel, a process called chloride-shift. In

contrast with electroneutral water, chloride has a charge number, -1, which takes membrane potential into the equation of the equilibrium. If we reorder this relation, we get the Nernst membrane potential equation as a relation between the ratio of chloride inside and outside the red blood cells.

$$\bar{\mu}_{Cl-,in} = \bar{\mu}_{Cl-,out}$$

$$R \cdot T \cdot \ln(a_{Cl-,in}) + z_{Cl-} \cdot F \cdot \varphi_{in} = R \cdot T \cdot \ln(a_{Cl-,out}) + z_{Cl-} \cdot F \cdot \varphi_{out}$$

$$\varphi_{membrane} = \varphi_{in} - \varphi_{out} = \frac{R \cdot T}{z_{Cl-} \cdot F} \cdot \ln\left(\frac{a_{Cl-,out}}{a_{Cl-,in}}\right) = \frac{R \cdot T}{F} \cdot \ln\left(\frac{Cl^{-}_{in}}{Cl^{-}_{out}}\right)$$

*Equation 9:
Algebraic
derivation of
Nernst equilibrium
of passive ion
transport across
membrane.*

Donnan's equilibrium is present on the red blood cell membranes, which generates a Donnan's ratio of about 0.5 for each permeable anion of charge -1 (Raftos, et al., 1990). This ratio reflects a measurable electric potential of about -12 mV (Gedde and Huestis, 1997). For chloride, it appears that we can assume almost the same activity coefficients for the same substance on both side of the membrane, because the ratio of activities is the same as Donnan's ratio of concentrations.

3.1.2 The chemical substance formations

In all of the above types of substance transport equilibrating, we worked with the same substance in the same phase and in the same solvent. This rendered the equilibrium independent of the base chemical potentials of the pure substance (μ_A^0), because both sides of the equation had the same value. However, if the chemical process created a new substance or changed its phase, μ_A^0 was changed to a new substance. We called this process the formation of the substance A; if the reference substances from which the substances formed (e.g. H₂(gas), O₂(gas), N₂(gas), C(graphite), Na(solid), etc.) had been carefully selected, we were able to measure the relative (to these reference substances; marked by the degree symbol “°”) formulate energies from the entire formation process in order to describe μ_A^0 for any new formed substance in the chemical system by using Equation 10.

$$\mu_A^0 = \Delta_f G_A^0 = \Delta_f H_A^0 - T \cdot \Delta_f S_A^0$$

*Equation 10 :
Chemical potential
of the pure
substance.*

where T is temperature, $\Delta_f G_A^0$ is free Gibbs energy of formation of substance A (relative to selected reference substances), $\Delta_f H_A^0$ is free formation enthalpy (heat energy consumed by the formation) of substance A (relative to selected reference substances) and $\Delta_f S_A^0$ is free formation entropy (the function of changed microstates by the formation) of substance A (relative to selected reference substances). The relation between enthalpy H, entropy S and Gibbs energy G ($G = H - T \cdot S$) is a primary relationship of chemical thermodynamics (Mortimer, 2008). Typical in this situation is the formation of enthalpy $\Delta_f H_A^0$, as well as Gibbs energy tabulated value $\Delta_f G_A^0$ at $T_0 = 25^\circ\text{C}$ and pressure $p_0 = 100 \text{ kPa}$.

This description of molar Gibbs energies in substances is a dual way for describing the equilibrium coefficient of chemical processes. For example, the dissociation constant of chemical reaction A<->B in a solution without electric potential, defined as $K=[B]/[A]$, has a relationship to the Gibbs energy of the reaction. If we set A as the reference substance ($\Delta_f G_A^0 = 0$), then $\Delta_f G_B^0 = -R \cdot T \cdot \ln(K)$. This is also the result of the equilibrium of the chemical potentials, which defines the free Gibbs energy of reaction $\Delta_r G^o$:



$$\begin{aligned}\mu_A &= \mu_B \\ \mu_A^o + R \cdot T \cdot \ln(a_A) &= \mu_B^o + R \cdot T \cdot \ln(a_B) \\ \Delta_r G^o = \mu_B^o - \mu_A^o &= R \cdot T \cdot \ln(a_A) - R \cdot T \cdot \ln(a_B) = -R \cdot T \cdot \ln(K)\end{aligned}$$

*Equation 11:
Algebraic derivation
of free Gibbs energy
from the reaction of
its dissociation
coefficient.*

Using free Gibbs energies instead of dissociation constants is much better, because it automatically fulfills the principle of detailed balance (Shiryeva, 2010). This fundamental principle can be also translated as follows: the product of dissociation constants must be equal to 1 for each closed chemical cycle (closed system of the reactions, which ends with the same substances, phases, enthalpies and entropies as it starts). This relation of dissociation constants is not as intuitive as thermodynamic meaning, i.e., the free Gibbs energy of each closed chemical cycle is 0, which means that an isolated system does not consume or produce new energy. Mathematically stated, this can be stated as: the logarithm of 1 is 0.

As shown in the example of the simple reaction A<->B, the free Gibbs energy of the reaction ($\Delta_r G^o$) is the difference between the free Gibbs energies of product and substrate ($\mu_B^o - \mu_A^o$). This rule is called Hess' law and can be used for any chemical process with any number of substances and with any stoichiometric coefficients "v". If we use the positive-negative stoichiometric coefficient notations (e.g., $v_B=2$, $v_A=-3$ for reaction 3 A <-> 2 B), we can extend the equilibrium to any number of reactants and products:

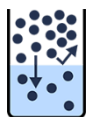
$$\sum (v_i \cdot \mu_i^o) = 0$$

$$\Delta_r G^o = \sum (v_i \cdot \mu_i^o) = -R \cdot T \cdot \ln(K), \quad K = \prod a_i^{v_i}$$

*Equation 12: Hess's
law in the
equilibrium of
chemical reaction
 $0 <-> v_1 A_1 + v_2 A_2 + \dots$*

For example the equilibrium of the Henderson-Hasselbalch reaction $H_2O + CO_2 <-> HCO_3^- + H^+$ in red blood cells at 37°C can be calculated from the tabulated formation energies (shifted from 25°C to 37°C) of substances, as in $\mu_{H+(aq)}^o = 0$, $\mu_{H_2O(l)}^o = -235 \text{ kJ.mol}^{-1}$, $\mu_{CO_2(aq)}^o = -385 \text{ kJ.mol}^{-1}$, $\mu_{HCO_3-(aq)}^o = -583 \text{ kJ.mol}^{-1}$ as reaction free Gibbs energy $\Delta_r G^o = \mu_{HCO_3-(aq)}^o + \mu_{H+(aq)}^o - \mu_{CO_2(aq)}^o - \mu_{H_2O(l)}^o = 37.4 \text{ kJ.mol}^{-1}$. Thus, the negative decimal logarithm of the dissociation constant is $pK=6.3$. However, the bicarbonate is an anion and must therefore be corrected by activity coefficient $\gamma_A = 0.85$ in order to reach its physiologically measured intracellular concentration of 11.6 mmol/L ($x_{HCO_3}=3e-4$, $a_{HCO_3}=1.9e-4$) at $pH=7.2=-\log_{10}(a_{H^+})$ ($a_{H^+}=6.31e-8$), where the mole fraction of the free dissolved carbon dioxide $x_{CO_2}=a_{CO_2}=3.22e-5$ and the mole fraction of water $x_{H_2O}=a_{H_2O}=0.995$ as in data presented by Raftos et al. (Raftos, et al., 1990). The same pattern with the same activity coefficient of bicarbonate can be applied to blood plasma in order to reach a typical concentration of bicarbonate 24 mmol/L at pH=7.4 and at the same mole fraction of carbon dioxide $x_{CO_2}=a_{CO_2}=3.22e-5$.

In our example, we calculated the free dissolved gas in liquid. Gases such as carbon dioxide or oxygen are equilibrated in the lungs between their gaseous and aqueous states of matter. The equilibrium of this process is in physical chemistry described as Henry's law. Thanks to this fixed linear dependence between gaseous and aqueous forms, it is possible to exchange the meaning of the partial pressures of gases with their concentration as a free dissolved form. The relation between mole fraction $x_{A,g}$ and partial pressure p_A of the substance A in a gas of total pressure p_T is $x_{A,g}=p_A/p_T$. Henry's coefficient can be defined as $kH = x_{A,l} / x_{A,g}$, where $x_{A,l}$ is a



mole fraction of free dissolved substance A in a liquid. Additionally, this coefficient can be rewritten to Gibbs energy in a chemical process:

$$\begin{aligned}\mu_{A,d} &= \mu_{A,g} \\ \mu_{A,l}^o + R \cdot T \cdot \ln(a_{A,d}) &= \mu_{A,g}^o + R \cdot T \cdot \ln(a_{A,g}) \\ \Delta_{dis}G^o &= \mu_{A,d}^o - \mu_{A,g}^o = -R \cdot T \cdot \ln(kH)\end{aligned}$$

*Equation 13:
Algebraic derivation of free Gibbs energy of the gas dissolution in liquid using its Henry's coefficient.*

The primary problem with these parameters is that they are shifted from mole fraction to molality in water such as in NIST (U.S. Department of Commerce, National Institute of Standard and Technology) tables. Therefore, if we use a value from NIST, e.g., 0.034 mol/kg/bar for CO₂, it should be recalculated to mole fraction units using water molar mass 0.018 kg/mol as kH=0.034*0.018. Furthermore, the calculation of mole fraction of free dissolved CO₂ at pCO₂=40 mmHg in blood is x_{CO₂}=0.034*0.018*40/760=3.22e-5. The molar concentration in erythrocytes can be expressed by the multiplication of the total amount of substances 38.7 mol in one liter of intracellular fluid and the resulting value of 1.24 mmol/L is in good agreement with Siggaard's data (Siggaard-Andersen and Siggaard-Andersen, 1990).

3.1.3 Change of phase of the substance

Change of phase is in physiology primarily connected with evaporation of water in the lungs or as sweat through the skin. In terms of a chemical equation, this also means the equilibration of chemical potentials in the water in the liquid and gaseous phases.

$$\begin{aligned}\mu_{H_2O(l)} &= \mu_{H_2O(g)} \\ \mu_{H_2O(l)}^o + R \cdot T \cdot \ln(a_{H_2O(l)}) &= \mu_{H_2O(g)}^o + R \cdot T \cdot \ln(a_{H_2O(g)}) \\ \Delta_{vap}G^o &= \mu_{H_2O(l)}^o - \mu_{H_2O(g)}^o = R \cdot T \cdot \ln\left(\frac{p_{H_2O}}{p \cdot x_{H_2O}}\right)\end{aligned}$$

*Equation 14:
Algebraic derivation of equilibrium in water evaporation.*

The free formation enthalpy of liquid water is -285.8 kJ/mol and for gaseous water, it is -241.8 kJ/mol. The free formation Gibbs energy of liquid water is -237.1 kJ/mol and for gaseous water -228.6 kJ/mol at 25°C and 100kPa. From these values, free entropy of formation can be expressed as -163.14 J/mol/K for liquid water and -44.27 J/mol/K for gaseous water at 25°C and 100kPa using Equation 15. As a result of almost constant enthalpy and entropy of formation, the free Gibbs energy of vaporization to temperature T at pressure 100kPa can be recalculated.

$$\begin{aligned}\mu^o &= \Delta_f H^o - T \cdot \Delta_f S^o \\ \Delta_{vap}G^o &= \Delta_{vap}H^o - T \cdot \Delta_{vap}S^o\end{aligned}$$

*Equation 15:
Water evaporation molar energies.*

The free Gibbs energy of vaporization is -44030+118.867*T and the vapor pressure of water is x_{H2O}*exp((-44030/T+118.867)/8.314) bar. Using this relation for pure water at a body temperature of 310 K (37°C) and normal atmospheric pressure of 100kPa we get the vapor pressure 6.22 kPa (47.2mmHg) at equilibrium of the vaporization process. This value is close to the observation of 6.28 kPa (47.7mmHg).

3.1.4 Stream, degradation and clearance

The chemical substance can be transported together with their chemical solution. The component modeling volumetric flow of solution is called the **stream**. Typically, the stream is



used alongside the air transportation of oxygen or carbon dioxide during ventilation, as well as for the transportation of substances using blood circulation. The calculated molar flow of an entrained substance labeled as ∂n_A is in this instance the molar flow of the entire solution ∂n multiplied by the mole fraction x_A in the original stream, as shown in Equation 16.

$$\partial n_A = \partial n \cdot x_A$$

*Equation 16:
Stream.*

$$\partial n_A = Clearance \cdot \rho_m \cdot x_A$$

*Equation 17:
Clearance.*

An analogy of stream calculation is in medicine referred to as **clearance**, which is used for calculating extracting substances from the body such as kidney excretion, liver metabolism, enzymatic processes, etc. For a defined substance, the *Clearance* parameters are measured as an amount of solution flow that has been fully cleared from the substance. Since we use the mole fraction instead of molar concentration, we need to convert mole fraction to molar concentration using the mole density of the solution ρ_m [mol.m⁻³], which is the total amount of the substances per volume unit. In contrast with stream, there is not loss of solution.

One must be careful, because clearance is not only one possible way of removing substances from the body. In some cases, there is also the passive **degradation** of molecules in the entire solution volume (Equation 18). In contrast with clearance, degradation is dependent on the distribution space of a substance. If there is no other change in the substance and only degradation in the constant amount of solution n takes place, then the concentration reverts to half the amount following the amount of time expressed as the parameter *HalfTime*. In the condition of the constant solution amount this can also be rewritten to Clearance = $(n/\rho_m) * \ln(2)/\text{HalfTime}$.

$$\frac{\partial n_A}{n} = \frac{\ln 2}{\text{HalfTime}} \cdot x_A$$

*Equation 18:
Degradation.*

The simplest chemical components for chemical substances can be gained by simply putting a prescribed number as molar flow of substance; this is referred to as **Pump**. This molar flow is usually calculated by user-defined diagrams, for example, using normal flow as a parameter affected by factors such as those described in the section Blocks.

3.1.5 Macromolecule equilibria

Macromolecules in physiology are common and include, for example, proteins, DNA and RNA. These molecules are typically polymers composed from small amounts of base elements such as amino acids for proteins or nucleotides for DNA. Through the polymerization of these base elements one strand of macromolecule is created, where not only the order of the base elements are critical for future functions, but where the entire space with all the types of presented bounds determine the function of the macromolecule.

From a chemical point of view, there are many distinguishable forms of macromolecules. For example the side chains of some amino acids can be presented as base or conjugate acids, while some can even be presented in an acid or conjugate base form at the typical cellular or interstitial pH. Fortunately, reactions with ligands can be independent on different sites in macromolecules, which simplifies the calculation of equilibrium. The mole fraction of the specific state “sQ” (defined by selected quaternary conformation “Q” and by the state of each independent site “i” at equilibrium) is calculated by Equation 19. The equation can be read as the probability of the selected form in quaternary conformation (x_{sQ}), which is the probability

of quaternary conformation (x_Q) multiplied by the probability of each selected site form in the quaternary conformation (x_i/x_Q).

$$x_{sQ} = x_Q \cdot \prod_i \frac{x_i}{x_Q}$$

Equation 19:
Speciation.

As a result of these general equations for attaining equilibrium of macromolecules, changes between quaternary conformations can be easily expressed. For example, the allosteric effect on hemoglobin can be described by tensed and relaxed conformation of hemoglobin tetramer molecules, where the binding of oxygen is in each conformation independent. However, the affinity of oxygen in tensed conformation is much higher than in relaxed conformation. This simplification was first presented in a model by Monod-Wyman-Changeux in 1965 as the basis of all allosteric regulations. However, they are only calculating the very simplified one ligand situation.

Our research pertaining to these allosteric effects is able to extend the model of allostery with many possible quaternary states and with many ligands. The example of usage this extended revolutionary approach is the first paper in appendix (Mateják, et al., 2015) I designed the mathematical description of the hemoglobin model including oxygenation, carboxylation, Bohr's effects and heat balance. Co-author Stanislav Matoušek completed the review and scientific language support for the paper. Co-author Tomáš Kulhánek identified the parameters of the model in order to fit experimental data. As shown in what follows, the model describes the interconnection of all phenomena that are joined together nonlinearly. Therefore, it is not possible to describe the phenomena separately as independent processes.

3.2 THERMAL DOMAIN

It should not be surprising that in the thermal domain, heat energy is accumulated as shown in Equation 20. From **accumulated heat H [J]**, temperature T [K] can be calculated using the properties of materials such as their specific heat C_p [$\text{J}\cdot\text{kg}^{-1}\cdot\text{T}^{-1}$] and mass m [kg] (Equation 21). Since in human physiology temperature is regulated to 37°C ($=310.15$ K), relative heat is shifted to this value. The negative value of heat means a lack of heat to 37°C while the positive value of relative heat means heat excess and a higher temperature.

$$H = \int \partial H \quad \text{Equation 20: Heat.}$$

$$T = 310.15 + \frac{H}{m \cdot C_p} \quad \text{Equation 21: Temperature.}$$



The connectors in heat domains use temperature T [K] as nonflow and heat flow ∂H [$\text{J}\cdot\text{s}^{-1}$] in establishing meanings of change in heat energy. The connector was inherited from the package Thermal.HeatTransfer of Modelica Standard Library (MSL 3.2.1), which creates compatibility with all standard thermal components of that package.

Heat conduction is driven by a temperature gradient as shown in Equation 22. Heat is transferred from a warmer to colder environment until the temperature is equilibrated. The speed of conduction is determined by the parameter $Cond$, which can also be expressed as the reciprocal value of heat resistance.



$$\partial H = Cond \cdot (T_{in} - T_{out})$$

*Equation 22:
Conduction.*

Heat is also transported together with mass. Each loss of mass will decrease absolute heat, but it does not change temperature. This situation is an analogy of substance molar flow when the entire solution is outflowing. Additionally, Equation 16 and Equation 23 are similar, but the meaning of variables is different. The **heat stream** is based on mass flow ∂m [kg.s⁻¹] not molar flow and there is no molar fraction, but a “concentration of heat energy” expressed as the multiplication of temperature [K] with the specific heat of the substance [J.kg⁻¹.K⁻¹].

$$\partial H = \partial m \cdot (T \cdot C_p + \Delta_{vap}H \cdot M_{H2O})$$

*Equation 23:
Heat change by
water
evaporation.*

Typically, the microcirculation is so effective that the outgoing blood from capillary nets has the same temperature as the tissue around the capillaries. The principle of heat transfer from blood to tissue acts like an **ideal radiator**, because the radiator also overflows with heated liquid. The specific heat [J.kg⁻¹.K⁻¹] of this liquid is named C_p . The amount of transferred heat to the environment is proportional to the flow of the liquid inside the radiator, called ∂m [kg.s⁻¹]. Maximal heat flow to the environment can be limited by the equilibrium of temperatures of outflowing liquid and the environment around the radiator can be controlled as in Equation 24. Equation 25 states that all heat energy of the inflowing liquid ($T_i * C_p$) is divided only to heat energy transferred to the environment ($\partial H / \partial m$) and the heat energy of the outflowing liquid ($T_o * C_p$).

$$T_o = T_{env}$$

*Equation 24:
Ideal radiator.*

$$\partial H = \partial m \cdot (T_i - T_o) \cdot C_p$$

*Equation 25:
Heat flow.*

However, blood can transfer about 5% more heat from working muscles to the lungs than is calculated by Equation 25, due to the endothermic behavior of hemoglobin deoxygenation (Mateják, et al., 2015). This additional heat is not accumulated to mass when temperature changes, but released by chemical reactions when the form of molecules changes as described in the above sections (chemical enthalpy). This type of chemical enthalpy also takes place during sweating, in the water change phase from liquid to gas. This process effectively cools down the skin even when the environment temperature is higher than the temperature of the skin.

3.3 HYDRAULIC DOMAIN

The modeling of the cardiovascular system is based on hydraulic principles where volume V [m³] in **elastic vessels** generates pressure p [Pa] and the pressure drives blood flow ∂V [m³.s⁻¹] through circulation. The main component in the accumulation of volume is called ElasticVessel and is described with Equation 26 and Equation 27. As a result of the elastic properties of blood vessels, there is an increase in pressure, together with an increase in the volume inside this component. This proportional dependence is set by the compliance parameter C [m³.Pa⁻¹], which is the property of the wall of the blood vessel. For example, compliance is bigger for systemic veins, where the same additional volume does not increase

the pressure as much as in systemic arteries. The walls do not generate positive pressure within when the volume decreases below V_0 and they lose tension. The result is the same pressure inside as outside the vessel.

$$V = \int \partial V$$

Equation 26:
Volume.

$$p = \begin{cases} \frac{V - V_0}{C} + P_{Ext}, & V_0 \leq V \\ P_{Ext}, & V \leq V_0 \end{cases}$$

Equation 27:
Elastic
Vessel.

Fortunately, the typical working state of elastic vessels at each place during each phase in the heart period is at the first branch, where $V > V_0$. The second additional branch solves critical situations, which may appear, for example, after massive hemorrhage. The external pressure around vessels P_{Ext} are typically set to zero with the exception of a local bandage or intrathorax pressure. Negative intrathorax pressure around -500 Pa is a result of respiration quotient. Inside the lungs, more oxygen is bound by hemoglobin than carbon dioxide is released from the blood, leading to a lack of molecules within properly working alveoli. This causes a small pressure debt to the intrathorax extravascular pressure during the entire respiration period.

The volumetric flow through segments of vessel is driven by the pressure gradient. This component is called the **conductor** or hydraulic resistor. Flow moves from a higher to a lower pressure; its value is determined with conductance $Cond$ [$m^3 \cdot s^{-1} \cdot Pa^{-1}$], which can be expressed with a reciprocal value in the form of hydraulic resistance [$Pa \cdot s \cdot m^3$].

$$\partial V = Cond \cdot (p_{in} - p_{out})$$

Equation 28:
Conductance.



Conductance is dependent on the current radius of the vessel. Vasoconstriction and vasodilation changes the radius, which in turn changes conductance. Higher conductance means higher flow for the same pressure gradient.

Pressure in liquid is also generated by gravity. Hydrostatic pressure is dependent on depth below the surface, on the density of the liquid and on gravitational acceleration. For example, pressure gradient of one atmosphere is at the bottom of a 0.76 m high column of mercury or at the bottom of a roughly 10 m high column of water. This phenomenon causes additional blood pressure in the lower parts of circulation and lower blood pressure in the upper parts, as expressed by Equation 29. The classic formula (gravity*density*height) is here extended with pumping effect ($pumpE$), which significantly helps to break the **hydrostatic column** within the vein's valves.

$$p_{down} = p_{up} + G \cdot \rho \cdot h \cdot pumpE$$

Equation 29:
Hydrostatic
pressure
gradient.



Typically, one point is selected for circulation (e.g., heart aortic valve). Height below this point is positive. Height above this point is negative. Change in the orthostatic position of the body during standing or lying is represented by changing the height of computed vessels. Gravitational acceleration (*gravity*) in the earth's surface is always set to 9.8 [$m \cdot s^{-2}$]. The

pumping effect changes with movement of the legs, because the segments of leg veins between valves can push the blood up only when the leg's skeletal muscles periodically contract and relax.

 **Ideal valve** is a designed hydraulic component that acts as conductor, but with different resistance for each flow direction. Forward flow has high conductance (low resistance) G_{on} and backward flow has low conductance (high resistance) G_{off} . The second branch of Equation 30 is valid during the opened phase (pressure gradient > 0); otherwise, if the valve is closed, the first branch occurs instead. At the break point defined by pressure gradient 0 both branches with zero are valid.

$$\partial V = \begin{cases} G_{off} \cdot (p_{in} - p_{out}), & \text{closed} \\ G_{on} \cdot (p_{in} - p_{out}), & \text{open} \end{cases} \quad \begin{array}{l} \text{Equation 30:} \\ \text{Valve.} \end{array}$$

Backward conductance is typically very small; small volumetric flow in the case of a closed valve can be generated. However, this flow can be so small that it can be described by the swelling of the valve membrane without any direct connection between liquids on both sides.

 The resistance of mass to any change in motion is called **inertia**. Volumetric flow has the tendency to continue forward and as a result, volumetric flow will continuously react to changes in pressure. The other view to the Equation 31 concerns generating pressure proportionally to the change of flow. The higher parameter *Inertance* [$\text{Pa.m}^{-3} \cdot \text{s}^2$] means the higher pressure gradient answers to the same changes in volumetric flow.

$$\partial V = \int \frac{p_{in} - p_{out}}{\text{Inertance}} dt \quad \begin{array}{l} \text{Equation 31:} \\ \text{Inertia.} \end{array}$$

The inertance of fluid in the vessel segment can be expressed as the density*length/cross-sectional area. Typically, inertia is most important in the aorta, where in each heart cycle blood flow starts and stops from the left ventricle.

3.4 POPULATION DOMAIN

 Physiology models must also take into account organisms, cells, viruses, bacteria, etc. As in a predator-prey model, there is also an accumulation of the members of the **populations** that can reproduce or die. Even though all the calculations are in real numbers (as in Equation 32), the results can be rounded to integers quite easily. The number of cells is typically very high and this approximation, alongside floating point numbers, is able to count any large amount of members.

$$sz = \int \partial sz \quad \begin{array}{l} \text{Equation 32:} \\ \text{Population.} \end{array}$$

 The number of members is called sz . An increase or decrease in members is called population change ∂sz . One type of cell is generally selected as representing the population; for example, red blood cells, which are produced by erythropoiesis in bone marrow. Furthermore, as a population can be implemented, so can one phase of cell maturation, differentiation or reproduction, in which the properties that differentiate these cells from others exist.

Reproduction, mortality and stream are represented by the same equation. The main idea is the proportional dependence of population change on population size, as expressed in Equation 33.

$$\partial sz = \partial szpm * sz$$

Equation 33:
Change.

The parameter $\partial szpm$ (change of population per its one member) can be recalculated from lifetime or half-life, where $lifetime = \ln(2) * half-life$ and $\partial szpm = 1 / lifetime$. Even though these conditions and behavior has been simplified, it can nonetheless illustrate the primary trends of dynamics and can fit the steady states of the system.

4 METHODS OF INTEGRATIVE PHYSIOLOGY FORMALIZATION

The integrative model of human physiology is a representation of physiological theory. As in all natural sciences, physiology must also be based on real experiments and logic. The model of physiological functions must be proven with measurements and the power of deduction regarding proven models can be used to prove new facts or identify questionable situations. All approaches must be deterministic and there cannot be any mathematical controversy.

The following exact logical definitions and theorems claim that it is possible to develop by *integration*, *reduction* and *extension* from previous models a model that must be *at least as good as* the previous models. Robustness (the ‘at least as good as’ operator) of the model must take into account all *real experiments* behind the models (the ‘be described’ operator) and the dimensions and size of the *image* of the model (number and type of results). This comparison of models can be defined by a comparison of all their real experiments. Integration of new knowledge can be done without losing any potential of the model in order to solve previously described real experimental data. The extension of the image of the model with new physiological definitions of new variables should also be noted as an improvement. On the other hand, an extension with new and unnecessary parameters and with new inputs is unwanted, because it brings correlations and problems needing unique identification to individual objects. The reduction of *domain* (number and type of parameters) will also be exactly defined to gain a model at least as good as the original. As a result of these rules of development, the better model should describe more data with more outputs and less parameters. Having logical proof at each instance that the new version of the model is better than the previous version will indicate that the new version is better than each preceding model in its history.

<i>Definition 1: Real Experiment</i>	$R^{(D_R, I_R)}$
Real experiment R with settings from <u>domain of definition</u> D_R giving data to <u>image domain</u> I_R , where for each setting s is the run of the experiment giving reproducible measurable data $R(s)$.	
	$\forall s \in D_R: \exists! R(s) \in I_R$

Each experiment must be reproducible with the same output at the same settings and without any other assumed conditions. The range and type of these value settings will determine the domain of the definition. For example, if we have only a parameter s_1 , which can reach values from 0 to 1, then the domain of the experiment is one-dimensional interval $<0,1>$. Outputs must be handled similarly, for example, as values from -10 to 10 and having image as a one-dimensional interval $<-10,10>$. Typically, settings remain constant during the experiment and the data can vary during the experiment in the form of measured outputs.

<i>Definition 2: Default Setting</i>	s_D^0
Default setting s_D^0 are fixed values in domain D , which represent the selected state as a set of parameters and inputs for all experiments.	
	$s_D^0 \in D$

Default settings must be consistent, which can be achieved by measuring all values for one individual object, at well-defined conditions within the specified fixed time. This snapshot of all values is typically used for parameters, which can be ignored or neglected in experiments to reduce the complexity and dimension of domain D . This is very comfortable, because by using default settings experiments can be designed with only a few parameters, which directly determines the outputs. Default settings should be selected to represent the normal state of a normal patient in normal conditions in order to achieve reasonably normal data $R(s_D^0)$ even for long-term experiment $R^{(D,I)}$. If it is not really necessary, default values should not be changed during development.

<i>Definition 3: Model</i>	$M^{(D_M, I_M)}$
Theoretical model M with settings from <u>domain</u> D_M giving data to <u>image</u> I_M , where for each setting s is the simulation of the model M giving a deterministic simulation output $M(s)$.	
$\forall s \in D_M: \exists! M(s) \in I_M$	

A model is always an approximation of reality. Even if we use fundamental physical relations, we should not be sure that a model will exactly match the reality. There is the same assumption when working with a model as for conducting a real experiment: the unique results for each parameter of the model (reproducibility=determinism). In other words, all necessary settings should be known before both real and theoretical experiments. For this reason, parameters and inputs are usually defined as physical quantities with physical units. Additionally, the model setting s typically remains constant during the simulation and the outputs can vary over time. This dynamic behavior is caused by a differential equation, which can dynamically react to prescribed changes of the settings. Each model M in domain D should give the reasonable results $M(s_D^0)$ for the default values s_D^0 . However, this condition is not part of the model definition, but simply a logical proposition.

<i>Definition 4: Experiment is described by model</i>	$R^{(D_R, I_R)} \in_{\epsilon} M^{(D_M, I_M)}$
Let d_{IR} is a <u>metric</u> of I_R . Let ϵ is a small real number. Experiment R is described by model M from domain $D_R \cap D_M$ to image I_R with precision ϵ using metric d_{IR} if and only if the image of the experiment I_R is a subset of the image of the model I_M and the distance between experiment output and simulation output for each setting is less than ϵ .	
$(I_R \subset I_M) \& (\forall s_{RM} \in (D_R \cap D_M), \forall s_R \in (D_R \setminus D_M): d_{IR}(R(s_{RM}, s_R), M(s_{RM}, s_{D_M \setminus D_R}^0)) < \epsilon)$	

The setting $s=[s_{RM}, s_R]$ arises from the design of experiment. The model can reduce this setting only to the primary information necessary for determining the right behavior in each case (as setting s_{RM}). Comparison of the measured data $R(s_{RM}, s_R)$ with the results of the simulation $M(s_{RM}, s_{D_M \setminus D_R}^0)$ can be done in different ways. An error calculation called a metric must always be used, which provides the information about how similar the curves are. Any mathematical norm can be used. For example, having points in a specific time, the sum of square distances between the simulation and measured points can be used. The value of precision ϵ must be selected appropriately for the precision of measurements and for the selected metric. The ideal value of precision ϵ is 0.5% of default values for the Euclidean norm. However, this precision is too difficult for most physiological measurements; therefore, even a 25% error for the worst case is currently tolerated by the Physiomodel.

Definition 5: Model Comparison	$M_1^{(D_1, I_1)} \geq_{\epsilon} M_2^{(D_2, I_2)}$
Model M_1 is at least as good as M_2 if and only if it can describe all experiments that can be described by M_2 .	
$\forall R \in_{\epsilon} M_2^{(D_2, I_2)} : R \in_{\epsilon} M_1^{(D_1, I_1)}$	

Almost all debates about different models that represents the same thing revolves around recognizing which model is better. This definition cannot be used to compare all models, because there may exist a setting accurate only for the second model, even if in other setting, only the results of the first model are correct. This operator, “be at least as good as”, can therefore be applied if all real experiments described by the “worse” model can also be described by the “better” model. From the “is described” operator, this new operator inherits the following useful properties: ($I_2 \subset I_1$). Therefore, the better model has a number of output variables at least as big as the worse model. The equality of models in precision ϵ occurs when $M_1^{(D_1, I_1)} \geq_{\epsilon} M_2^{(D_2, I_2)}$ and $M_2^{(D_2, I_2)} \geq_{\epsilon} M_1^{(D_1, I_1)}$. In this situation, the direct result is the equality of images ($I_1=I_2$) and the same set of experiments, which are described by both models. The other property of the operator ‘at least as good as’ is transitivity, which means that if $M_1^{(D_1, I_1)} \geq_{\epsilon} M_2^{(D_2, I_2)}$ and $M_2^{(D_2, I_2)} \geq_{\epsilon} M_3^{(D_3, I_3)}$ then $M_1^{(D_1, I_1)} \geq_{\epsilon} M_3^{(D_3, I_3)}$. This transitive relation is a result of definitions of both “be described” relations as ($I_3 \subset I_2 \subset I_1$) & ($\forall R \in_{\epsilon} M_3^{(D_3, I_3)} : R \in_{\epsilon} M_2^{(D_2, I_2)} : R \in_{\epsilon} M_1^{(D_1, I_1)}$), which is the definition of the “be at least as good as” operator between M_1 and M_3 . Having the transitive “is at least as great as” operator for model comparison is critical for model development, because if the new version is at least as good as the previous version of the model during each phase of development, then the new version must also be at least as good as all versions in the history of the model’s development.

Definition 6: Incomparable Models	$M_1^{(D_1, I_1)} \parallel_{\epsilon} M_2^{(D_2, I_2)}$
Model M_1 is incomparable with M_2 if and only if M_1 is not at least as good as M_2 (in precision ϵ) and M_2 is not at least as good as M_1 (in precision ϵ).	
$\neg(M_1^{(D_1, I_1)} \geq_{\epsilon} M_2^{(D_2, I_2)}) \& \neg(M_2^{(D_2, I_2)} \geq_{\epsilon} M_1^{(D_1, I_1)})$	

Negation of this relation between two models must render one of the models at least as good as the other model. In other words, if the models are not incomparable then they are comparable. The incomparable operator is commutative, so if $M_1 \parallel_{\epsilon} M_2$ then $M_2 \parallel_{\epsilon} M_1$.

Definition 7: Integration	$M_{AB}^{(D_{AB}, I_{AB})} = M_A^{(D_A, I_A)} \cup_{\epsilon} M_B^{(D_B, I_B)}$
M_{AB} is an integration of two models M_A and M_B in precision ϵ if and only if M_{AB} describes all data that are described using the model M_A or the model M_B	
$(M_{AB}^{(D_{AB}, I_{AB})} \geq_{\epsilon} M_A^{(D_A, I_A)}) \& (M_{AB}^{(D_{AB}, I_{AB})} \geq_{\epsilon} M_B^{(D_B, I_B)})$	

Having models for different types of experiments, there must be an option for how to merge them into one model, which will be able to describe all of these experiments. This integration is the most problematic stage of model development, because for each process, only one relation must be selected, even if it is described in both models differently. The new integrated model must generally be re-implemented with a new theory that describes both types of

experiments. If it is not possible to establish a smooth mathematical relation for both groups of behavior, it can be always be implemented as an “if-then-else-” solution. The existence of conditional integration is proof of the integration theorem, which states that there must exist some integration for each of the two models.

Integration theorem: $\forall M_A \forall M_B \exists M_{AB}: (M_{AB} \geq_{\epsilon} M_A) \& (M_{AB} \geq_{\epsilon} M_B)$

For example, if we have two models of aortic valve, one for an opened valve and a second for a closed valve, then we can integrate them by using conditions pertaining to the opening and closing of valves. If the integration is based on improved physical theories, then the final model can achieve much higher potential for solving more complicated experiments than the original experiments based on the once separate, but now integrated models. This integration phenomenon was observed when we integrated, for example, the new physical chemistry theory with HumMod 1.6. The original HumMod 1.6 was based on the equilibration of molar concentration and osmolarity. However, using these old relations, it was not possible to describe equilibrium on the erythrocyte membrane. Using a new physical theory, however, we solved not only this problem, but also brought to the model a solution for all electrochemical processes, which is based on new physical chemistry relations, as noted in section 3.

<i>Definition 8: Domain reduction</i>	$M_r^{(D_r,I)} = \text{reduction}(M^{(D,I)}, \epsilon)$
M_r is a reduction of the model M in precision ϵ to new domain D_r if and only if its domain D_r is a subset of the domain D and M_r describes all experiments described by the original model M in the same image.	
	$(D_r \subset D) \& (M_r^{(D_r,I)} \geq_{\epsilon} M^{(D,I)})$

The model after domain reduction is at least as good as the original model. The image remains the same. The domain is reduced ($D_r \subset D$), typically by removing correlating parameters or making parameters more invariant in order to have the same default values during all experiments (parameters become constants). Making values more invariant has long tradition in physiology, typically in terms of scaling values according to weight, skin surface, height, age, sex, etc.

<i>Definition 9: Image extension</i>	$M_e^{(D,I_e)} = \text{extension}(M^{(D,I)}, \epsilon)$
M_e is an extension of the model M if and only if the original image I is a subset of the extended image I_e and M_e describes all data described by the original model M in the extended image I_e with precision ϵ .	
	$(I \subset I_e) \& (M_e^{(D,I_e)} \geq_{\epsilon} M^{(D,I)})$

The model after extension of the image is at least as good as the original model, as only the image was extended ($I \subset I_e$). The domain and the experiments remain the same.

Development using these rules of integration, image extension and domain reduction always consistently provides the next version of the model with all previously integrated knowledge. However, it is necessary to collect the knowledge of integrated real experiments and their measured data in order to know exactly the limits of the current version of the model. These references to scientific research are an inseparable part of any complex model.

5 RESULT OF INTEGRATIVE PHYSIOLOGY FORMALIZATION

The result of integration is one runnable complex model of integrative human physiology called the Physiomodel (Diagram 1). The model is composed of 10 subsystems and one block containing settings. Each of the subsystems is described in the following subsections.

The implementation of each subsystem can be simulated separately, which is very helpful when debugging the model. The inputs are stored in one file, which is comparable with the inputs of the original HumMod 1.6 model, except for new states and parameters of the newly implemented acid-base and new hemoglobin binding model. Each subsystem also contains a large set of references to existing literature that was used for estimating parameters and relations within the model. The output of simulations during normal conditions was automatically compared with a set of predefined values. The differences between the simulation output variables and expected values were sorted in order to observe the most questionable parts of the model immediately following the simulation. The scripts sped up the development of the model, because there was no need for the manual examination of graphs for each included variable following each modification of the model.

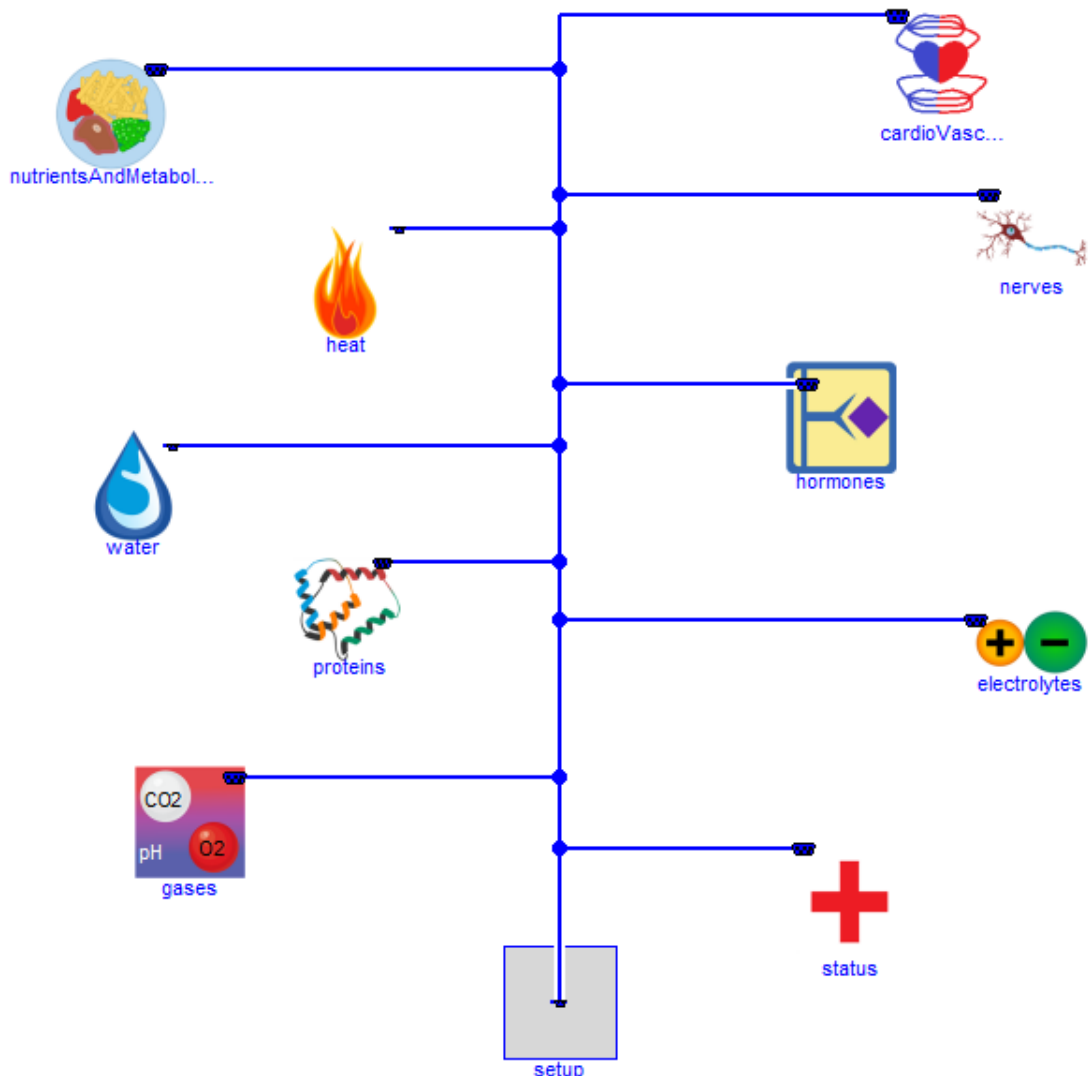


Diagram 1: Physiomodel subsystems, top-level diagram implementation.

5.1 CARDIOVASCULAR SYSTEM

The cardiovascular system is composed of the heart, pulmonary circulation and systemic circulation, as implemented in Diagram 2. These components are connected using the Physiolibrary's hydraulic connectors (Table II), where pressure and volumetric flow is hidden behind the black line connections. Both pulmonary and systemic circulation has the same behavior during steady state as the simple hydraulic resistor. The heart behaves as a continuous hydraulic pump during steady state. However, during dynamic middle-term simulation, the situation is more complex and blood volumes can dynamically spillover between blood vessels, changing blood pressure and blood flow. The pumping heart is more complexly described in the 'Heart' subsection and both dynamic circulations are described in detail in the 'Circulation' subsection using tissue arterioles, capillaries and venules from the 'Microcirculation' subsection.

As blood volume and hematocrit strongly influences both blood pressure and blood flow in all areas of the cardiovascular system, their implementation is also shown in Diagram 2 as 'red cells' and 'blood properties'. These components calculate the amount of red blood cells, blood volume, hematocrit and blood viscosity effect on hydraulic conductance, among others and are described in the 'Blood' subsection.

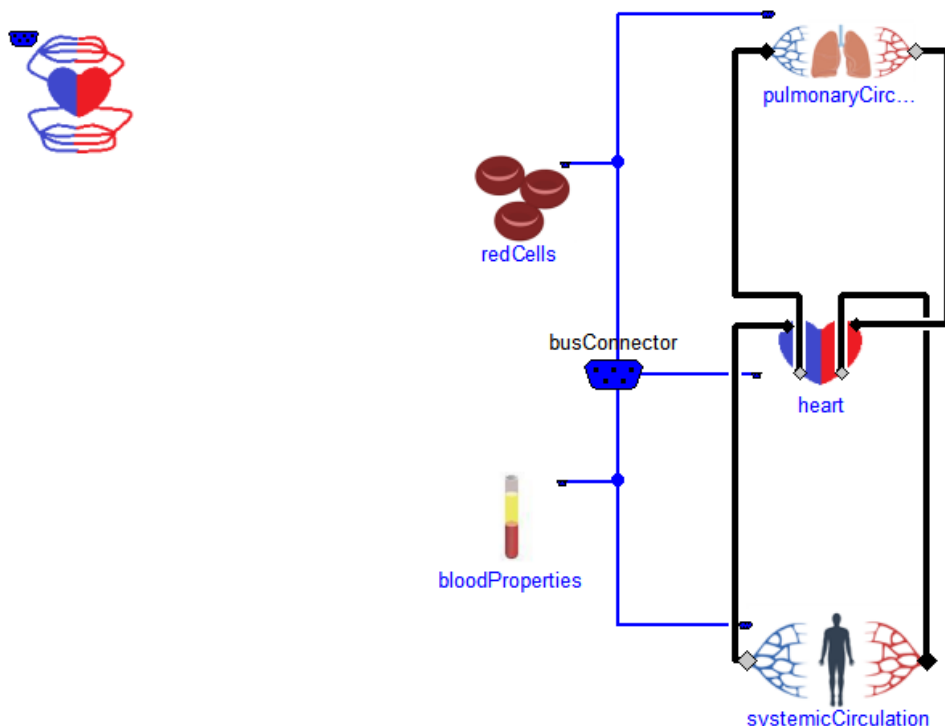


Diagram 2: Cardiovascular system; the black line at the top-right represents the pressure and blood flow at the end of pulmonary veins, while the bottom-right black line notes the start of the aorta, the bottom-left line notes the end of systemic veins and the top-left line shows the start of pulmonary arteries.

5.1.1 Heart

The model for blood pumped by the heart consists of models for heart atriums, ventricles, the sinoatrial node, atrial pressure receptors and atriopeptin. The heart components have four hydraulic connectors that connect the veins and arteries. From systemic veins blood is transferred directly into the right atrium, from which the right ventricle is filled. The right ventricle is emptied into pulmonary arteries using a connector in the left bottom corner of the

heart icon (see on Diagram 2). After oxygenation in the lungs, blood moves to the left atrium and left ventricle, from which it is ejected into the aorta (Diagram 2). The pathological state of mixing deoxygenated blood with oxygenated blood, when the foramen ovale is opened, is not yet implemented. Thus, during steady state, the flow in the connector of veins is the same as the flow in the connector of arteries for both halves of the heart.

The sinoatrial node calculates the heart rate and will be described together with low pressure receptors in a section on autonomic neural activity. Atriopeptin, as a hormone produced by the heart in answer to blood pressure inside heart atriums, will be described in a section about hormones.

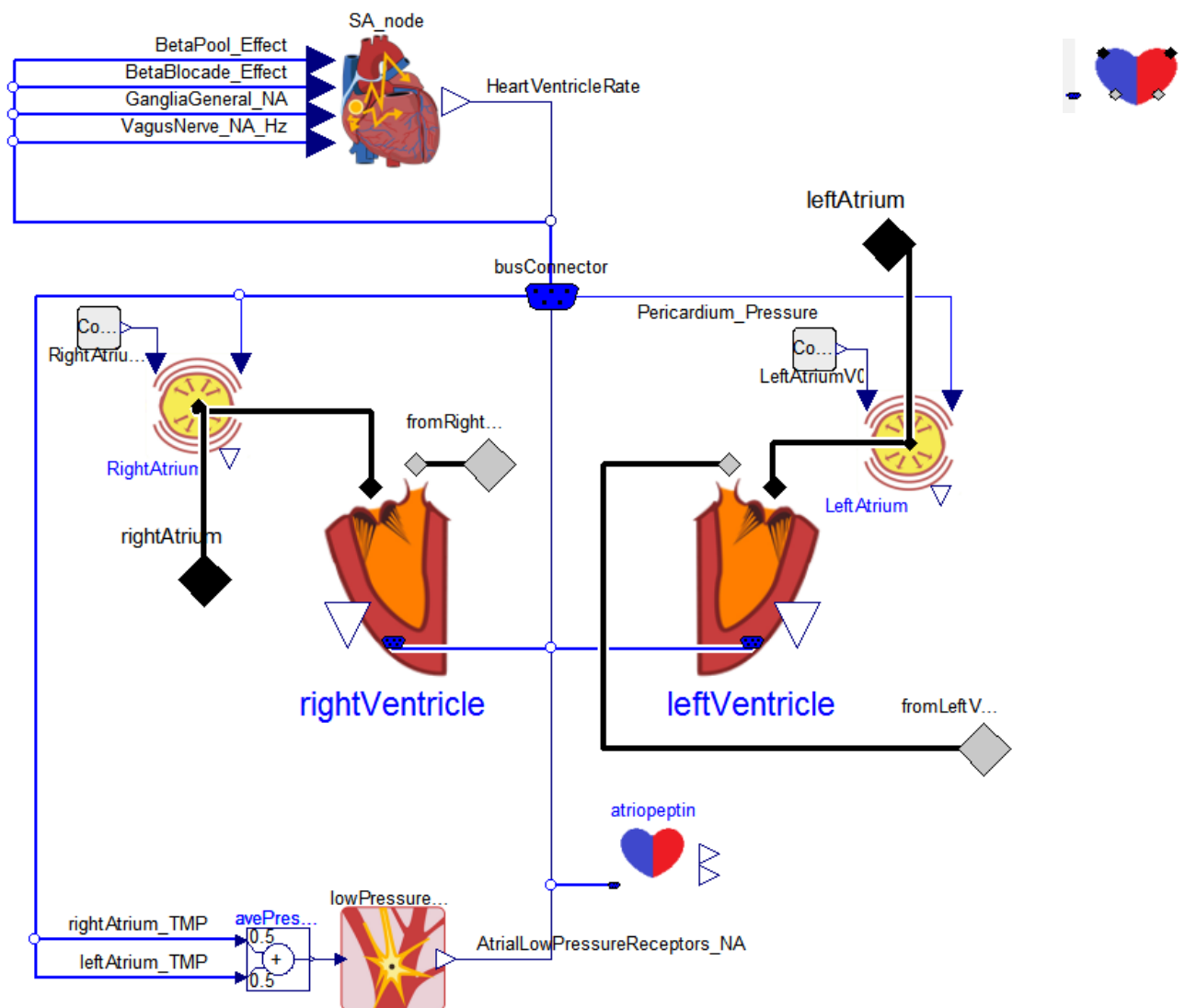


Diagram 3: Heart; deoxygenated (oxygenated) blood goes from systemic (pulmonary) veins to pulmonary (systemic) arteries through the right (left) heart atrium and right (left) ventricle.

As long-term heart activity can be modeled using the mean values of pressures and flows, the heart activity must not be modeled as beat by beat. Instead of using dynamic periodical values, the pressure and the blood flow is precisely calculated in values, which make up their arithmetical average during each heart period and is referred to as mean variables or mean values. In these conditions, the heart atrium can be implemented using the simple elastic

vessels in the Physiolibrary as defined by Equation 26 and Equation 27, and represented by yellow circles in Diagram 3.

The heart ventricle, as implemented in Diagram 4, has two hydraulic connectors, which represent the area prior to the input valve and the area following the output valve. Through this area, some blood flow moves and some pressure is always generated, as is typical within the hydraulic connector. Flow going to the arteries is called cardiac output. Cardiac output (CO) as a mean blood flow from the heart ventricle is heart rate (HR) multiplied by stroke volume (SV), where stroke volume is the difference between end diastolic volume (EDV) and end systolic volume (ESV) (NODA, et al., 1993). The most common descriptions are pressure-volume relations (Sagawa, et al., 1988), as in A-V fistula experiments (Guyton and Sagawa, 1961) or filling pressure experiments (SUGA and SAGAWA, 1974), or less invasive exercise experiments (Little and Cheng, 1993).

This model does not solve the situation where there are very short times for the good filling of the heart ventricle. However, using Physiolibrary, it is possible to create the beat-by-beat implementations as we have described in articles (Kulhánek, et al., 2014a; Kulhánek, et al., 2014b). These publications show the opening and closing valves (Equation 30) that simulate the current pressure and flow during the diastolic filling and systolic ejection of ventricles. Moreover, blood flow inertia is also integrated (Equation 31), which plays a significant role in the shape of blood flow and pressure (e.g., generating dicrotic notch) during these short-term events.

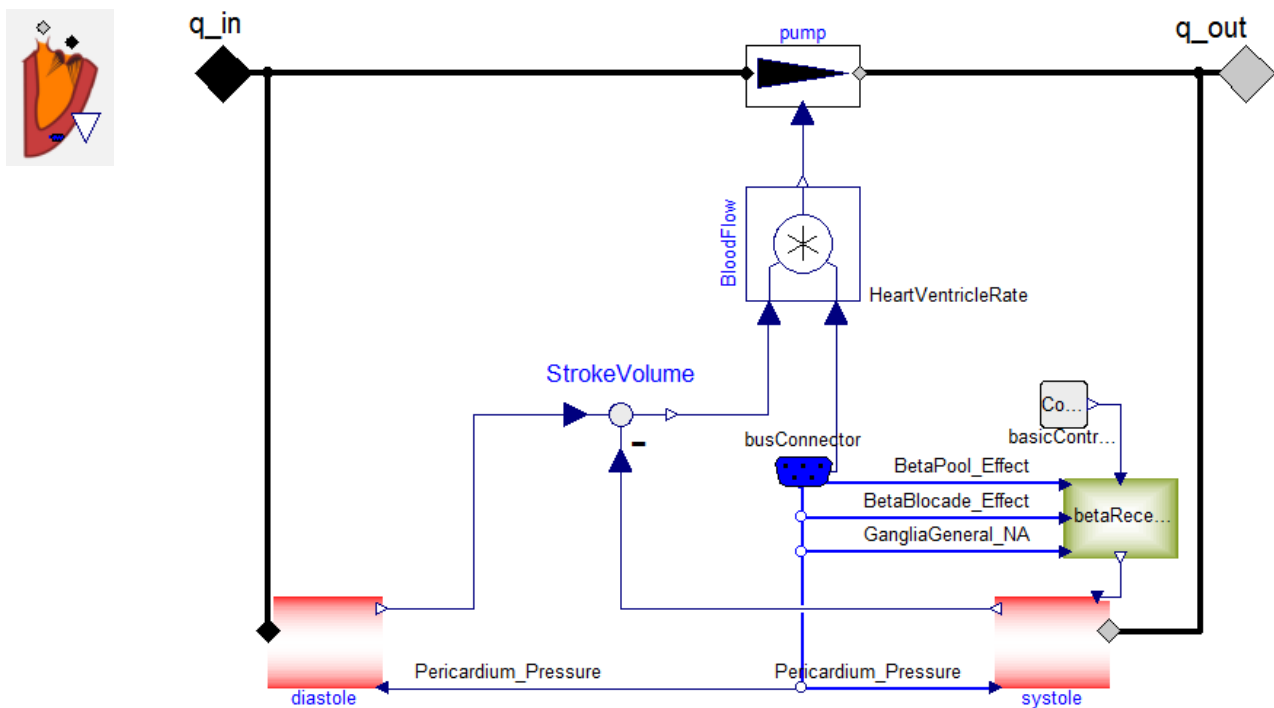


Diagram 4: Heart ventricle; the block diastole calculates the end diastolic volume from mean filling pressure, while the block systole calculates the end systolic volume from mean arterial pressure and contractility, which is a function of the beta receptors' activity.

5.1.2 Circulation

During pulmonary circulation, blood flows through pulmonary arteries, capillaries and veins. All of these are represented in Diagram 5 by the elastic vessel (Equation 26 and Equation 27) and hydraulic resistor (Equation 28). A special block is used for the calculation of perfusion of

ventilated alveoli and is based on total blood flow through pulmonary capillaries, called lungBloodFlow.

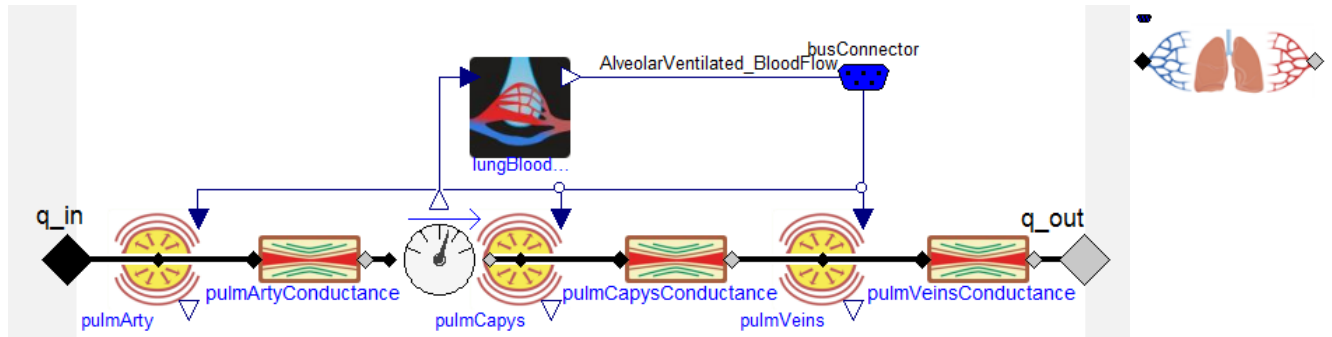


Diagram 5: Pulmonary circulation.

The local regulation of vasoconstriction and vasodilation in lungs (Archer and Michelakis, 2002) is not implemented, but can easily be inserted in the follow-up versions.

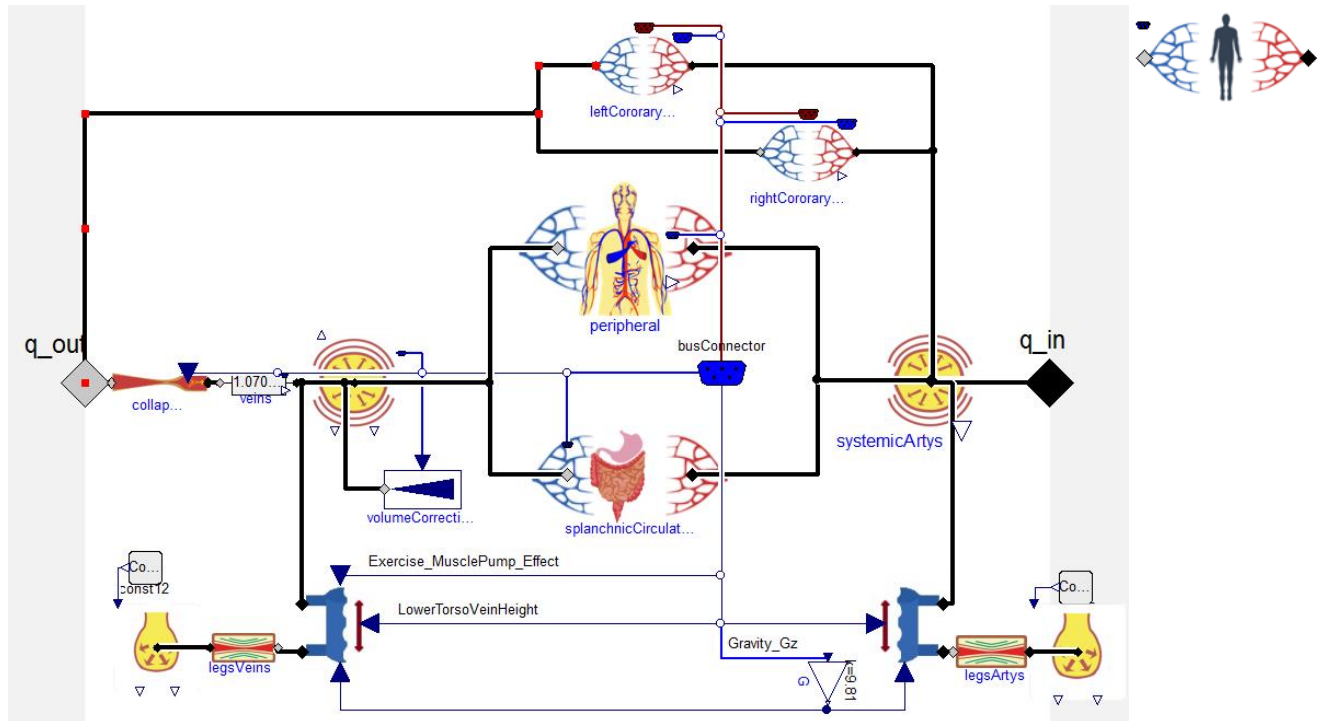


Diagram 6: Systemic circulation.

In systemic circulation, blood flow from systemic arteries (Roach and Burton, 1957) is divided into branches for different tissues. The upper part of Diagram 6 shows coronary (micro)circulation through the heart; next is shown all other circulation for peripheral organs except for renal circulation and splanchnic circulation, where the blood from gastrointestinal tract mixed with blood from hepatic arteries. The lower part of Diagram 6 represents the sequestered blood in lower parts of the body caused by the hydrostatic gravitation effect (Equation 29). The characteristics of sequestered blood in leg vessels can be measured using a variety of orthostatic experiments (Bevegård and Lodin, 1962; Bock, et al., 1930; Henry and Gauer, 1950; Mayerson, et al., 1939; OCHSNER, et al., 1951; Pollack and Wood, 1949; Thompson, et al., 1928). The blood pumping effect is caused by vein valves during contraction

and relaxation of surrounding skeletal muscle (Armstrong, et al., 1985; LAUGHLIN, 1987; Laughlin and Armstrong, 1983).

After flowing through tissues, blood moves into systemic veins, where zero-pressure-volume is driven by venoconstriction. Venoconstriction is driven by sympathetic neural pathways such as part of the baroreflex (ECHT, et al., 1974; GAUER, et al., 1956; Shigemi, et al., 1994). The vein can collapse between abdominal and thorax cavity. This is caused by small negative intrathorax pressure, which can suck all volume from the veins at the diaphragm and restrict blood flow, which occurs in collapsing vessels if there is not enough blood volume.

Peripheral circulation is composed of eight types of tissues: bone, neural, adipose, skeletal and respiratory muscle, renal, skin tissues and the rest. These organs are implemented by the same class of microcirculation but with different parametrical settings. The exception to general microcirculation is the renal circulation of kidneys (Diagram 10). This type is very specific, because blood flow after renal arcuate artery and afferent arterioles access the glomerular capillary network. After the glomerular capillaries and efferent arterioles is blood divided to the capillary network of the vasa recta or interlobular capillary network. The differences in renal circulation are significant, because renal blood flow is typically around 20% of cardiac output.

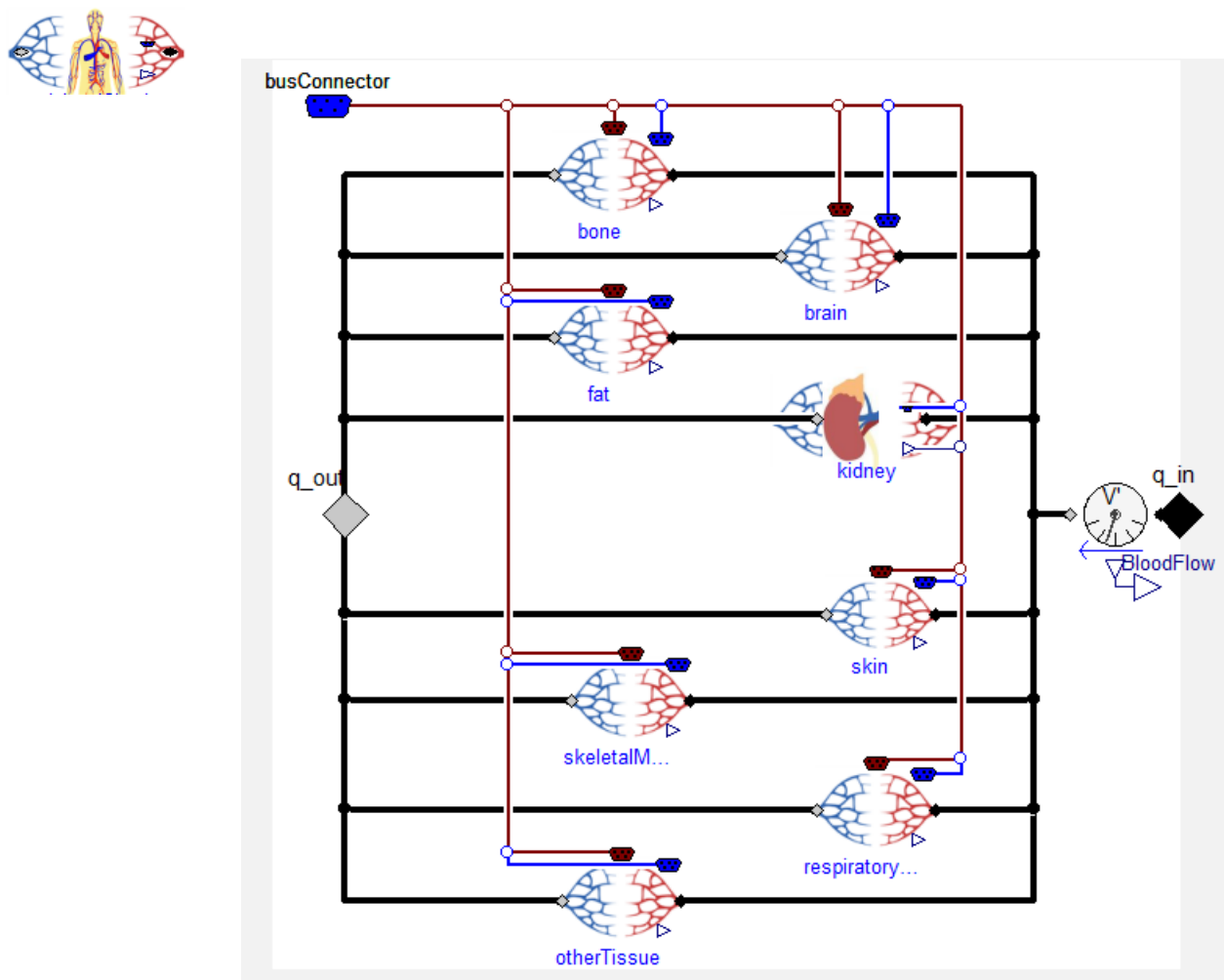


Diagram 7: Peripheral circulation.

Splanchnic circulation delivers all blood from the gastrointestinal tract to the liver via the portal vein (Bradley, et al., 1953). In the liver hepatic blood flow is determined by the portal vein and hepatic artery blood flow. Normal hepatic blood flow can vary from 1 to 2.5 l/min (BRADLEY, et al., 1952), depending on gastro-intestinal blood flow. Splanchnic circulation can function as a blood reservoir during hemorrhage or during blood infusion (Greenway and Lister, 1974; Maass-Moreno and Rothe, 1992).

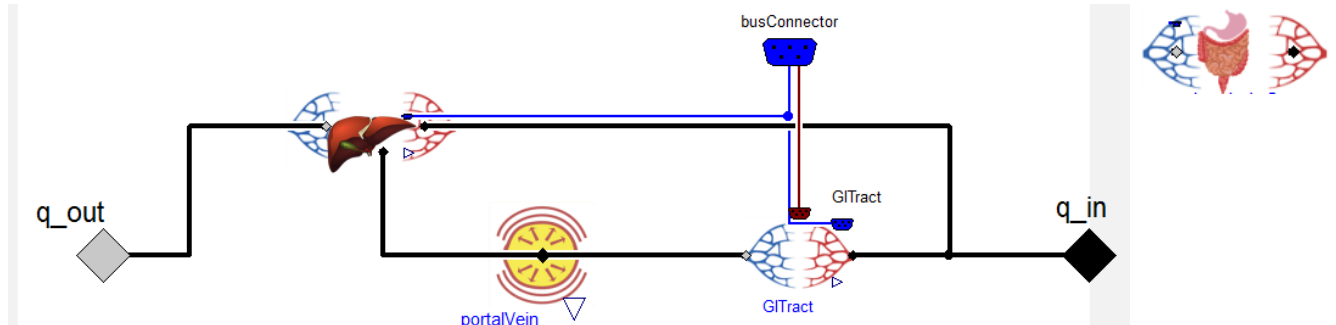


Diagram 8: Splanchnic circulation.

5.1.3 Microcirculation

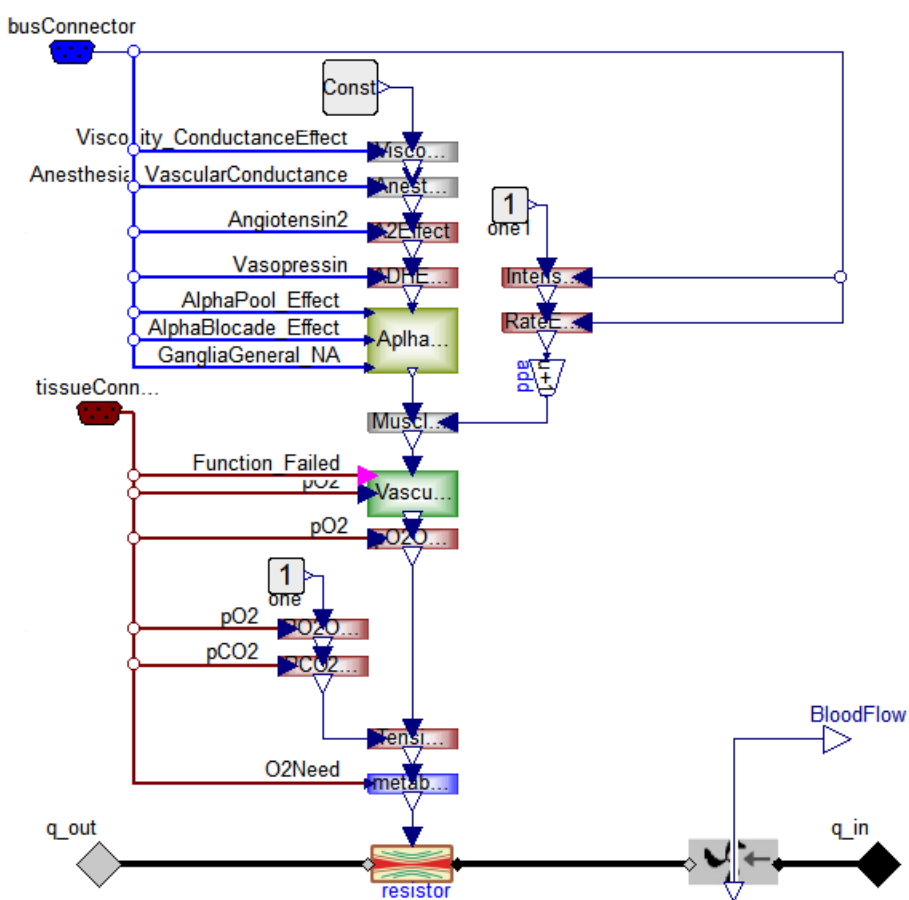


Diagram 9: Microcirculation.

Blood flow through blood vessels depends on blood viscosity (Whittaker and Winton, 1933), as shown by the upper factor of Diagram 9. Below this factor is shown the vasodilation/vasoconstriction effect of anesthesia, then the effect of angiotensin 2, vasopressin and catecholamines. Catecholamines such as epinephrine and norepinephrine that freely dissolve in extracellular fluids are described in the ‘Hormones’ section and their effect on alpha receptors are calculated as the variable AlphaPool_Effect. The alpha receptors can also be stimulated by sympathetic neural activity (GangliaGeneral_NA) or inhibited using alpha blockers (AlphaBlocade_Effect), as will be described in section addressing neural activity. The next factor applies to skeletal muscles, where a metaboreflex dilates the arterioles to bring more oxygen and nutrients into working tissues. The next factor is an adaptation to a long-term low hypoxic condition by angiogenesis, where new branches between arterioles and venules cause lower resistance for blood flow. The partial pressure of oxygen can also have an acute effect on vasodilation (or local vasoconstriction in lungs). However, the brain must also calculate the effect of carbon dioxide (Kety and Schmidt, 1948), which increases blood conductance in a situation where it needs to be washed out or where it decreases blood conductance, where it must be accumulated to eliminate local rapid pH changes. The local metabolic demand for oxygen is also one of the factors of vascular resistance. The final factor is an embolism, where the perceptual part of tissue circulation can be blocked by an embolus in the form of a blood clot, gas bubble or any solid blockage in the blood stream.

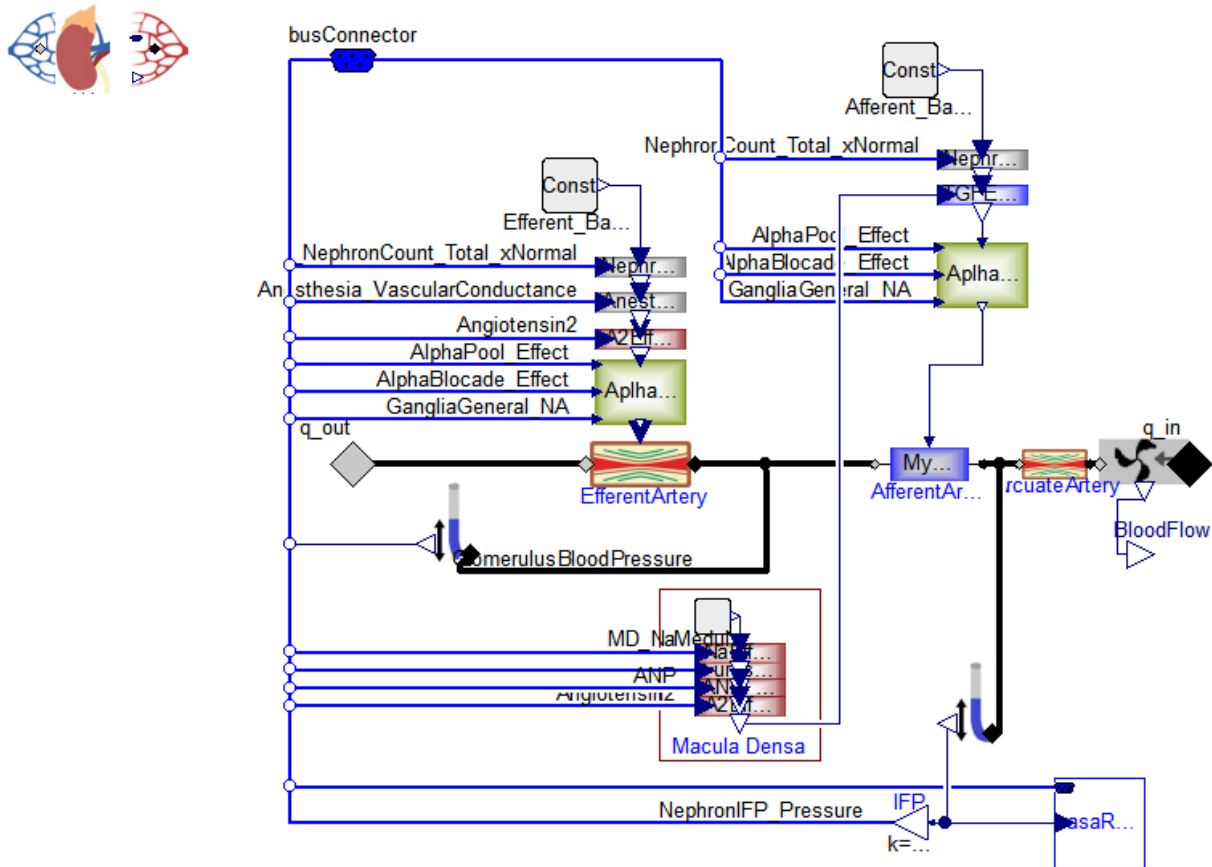


Diagram 10: Renal (micro-) circulation of kidneys.

An exception in terms of microcirculation is the renal circulation of kidneys, where only the efferent interlobar part is driven by some of the abovementioned factors. The strictly regulated renal blood flow by both afferent and efferent arterioles (Diagram 10) needs to set an optimal filtration pressure (Manning, 1987; Manning, 1990) and prevent the washout of kidney medulla concentrations. This process is driven by a number of working nephrons, tubule-glomerular-feedback (Ito and Carretero, 1990; Moore and Casellas, 1990), baroreflex-like patterns (Skarlatos, et al., 1993), local mechanoreceptor-myogenic patterns (Aukland, 1989; Drummond, et al., 2008) and by efferent interlobar microcirculation (Heyeraas and Aukland, 1987).

Hydraulic resistance (reciprocal value of conductance) is regulated by a cross-sectional area of vessels. The higher the cross-area the faster the blood stream will be at the same pressure gradient. The radius of this area is a function of circumference, which is determined by the current length of surrounded vascular smooth muscle. The vascular smooth muscle tone is regulated by many factors, as described previously (Mellander and Bjornberg, 1992; Shigemi, et al., 1994). Vasoconstriction causes increasing resistance and pressure, together with decreasing blood flow. Vasodilation has the opposite effect. These types of vascular regulations are specific for different tissues, where any of the factors can be disabled or enabled, or set to different sensibilities for different tissues.

5.1.4 Blood properties

Blood volume is calculated as plasma volume plus the volume of red blood cells. Blood plasma volume is calculated by the water subsystem, but the amount of erythrocytes is integrated inside the cardiovascular subsystem alongside the components shown in Diagram 11. Using population components from the Physiolibrary (Equation 32 and Equation 33), increasing the number of erythrocytes by erythropoiesis or transfusion is increased, while erythrocytes are decreased as a result of their natural mortality or by hemorrhage. The rate of erythropoiesis is determined by the concentration of erythropoietin, which is modeled in section on hormones.

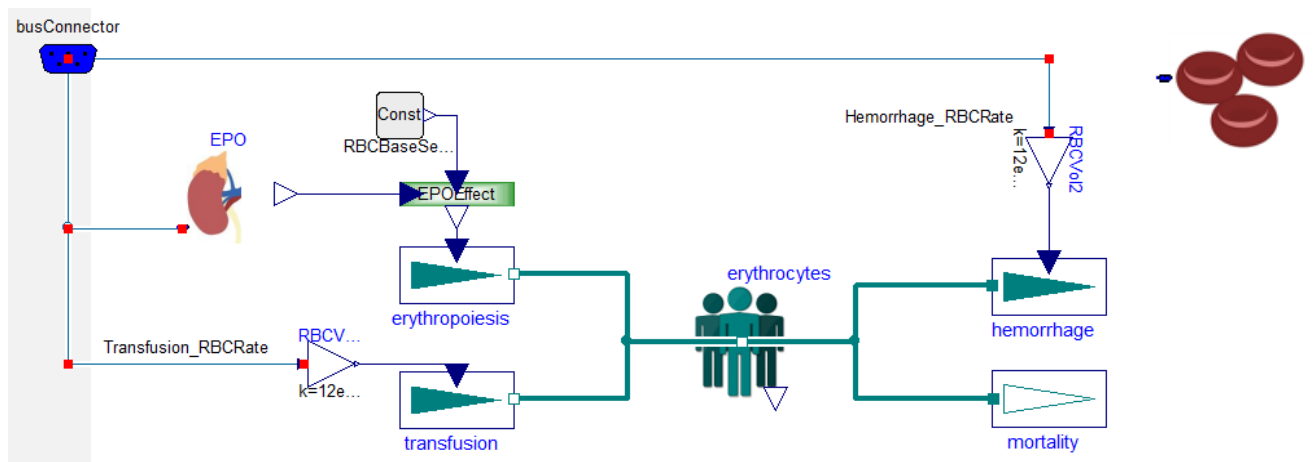


Diagram 11: Red cells.

The final additional component of the cardiovascular system is a block with general blood properties such as total blood volume, hematocrit and viscosity or the viscosity conductance effect. Viscosity of blood is strongly dependent on hematocrit (Begg and Hearns, 1966; Schrier, et al., 1970; Stone, et al., 1968); therefore, the higher the number of erythrocytes, the less ability blood has to move. However, if there are more red blood cells, then more oxygen can be connected to hemoglobin. As a result, optimal hematocrit for oxygen transport between

these two conditions can experimentally be estimated as 40-60% in most tissues (Fan, et al., 1980; Jan and Chien, 1977).

5.1.5 Comparison with HumMod v1.6

The cardiovascular system shows many differences when comparing the Physiomodel and HumMod 1.6, but yields very similar results in terms of simulations.

In our Physiomodel, the accumulation of blood volume in systemic veins is implemented with the same component (Equation 27: Elastic Vessel) as in other areas of circulation. The total blood volume is calculated as the sum of these compartments. The original HumMod v1.6 calculates the integration of total blood volume instead of systemic venous blood volume, which is calculated as the rest of the blood volume from all other places in the body. These reformulations lead to the same steady state equations; therefore, in a normal situation when blood volume remains constant, the simulation results are the same. Additionally, after stabilization and equilibration to the new blood volume, the same results must be reached. However, our component-based solution has better properties in a dynamic situation, where rapid blood changes can be applied to the specific parts of circulation with local dynamic responses. Cross-checking in the Physiomodel is done using the conservation law of blood volume alongside known changes of total blood volume. Change in the sum of blood volume of all circulation components must be the same as external changes from/to circulation. These tests can also uncover non-correctly-defined changes in the blood volume of heart ventricles and their connection with end systolic pressures, which are also corrected in the Physiomodel, in contrast with HumMod 1.6.

As each circulation component must be connected in the circuit diagrams, all blood flows are correctly defined by these diagrams in the Physiomodel. The original textual representation of the HumMod has no form of connection checking and as such, it is easy to forget to connect, for example, blood flow from splanchnic circulation to the systemic veins. In Modelica diagrams, it can be observed when some physical connectors are not connected. Thus, the user sees blood outflow from components that are unconnected. Even when noting flows from/to the environment, the user should use the specific component such as flow pumps or fixed pressure source.

The graphical diagrams illustrate the connections of blood pressures and blood flows. Finding all the equations for blood flows in the original HumMod and applying an understanding of these equations must lead to very similar visual representations. If these representations have mathematical meaning, as in Modelica, understanding and upgrading of the model will be easy. Using diagrams, for example, it must be immediately evident that the coronary circulation in the HumMod accesses the systemic veins, as in other peripheral blood flows. The Physiomodel changes this to a more anatomically precise idea, i.e., that coronary circulation ends directly into the right atrium. As a result, the resistance parameter of coronary vessels was recalculated to a new pressure gradient (between the aorta and right atrium) in order to reach the same coronary blood flow.

There remains small cardiovascular system disproportions in both models. For example, the changing of pulmonary blood flows through ventilated alveoli is not connected to the circulation circuit. The total pulmonary circulation in these versions is independent of this process, which in reality must be interconnected. Additionally, renal blood flow through the vasa recta is not correctly connected within the model's cardiovascular system. All of these parts can be upgraded in future versions of the models.

5.2 BODY WATER

The model for water (Diagram 12), for example, the model for extracellular proteins, is divided into eight main compartments: blood plasma (plasma), red blood cells (RBC) and interstitial (IST)/intracellular (ICF) water of the upper torso (UT), middle torso (MT) and lower torso (LT). These compartments are connected by chemical connectors, which also support the osmotic processes. Selected distribution of body water (41L for 70kg, male) between compartments is shown in Table IV. From these values, the total interstitial, extracellular or intracellular volume used for simplified pharmacokinetic calculations can also be expressed.

Table IV: Typical steady state water volume of compartments [L].

Plasma	RBC	UT_IST	UT_ICF	MT_IST	MT_ICF	LT_IST	LT_ICF
3.0	1.6	2.3	5.0	5.7	12.5	3.4	7.5

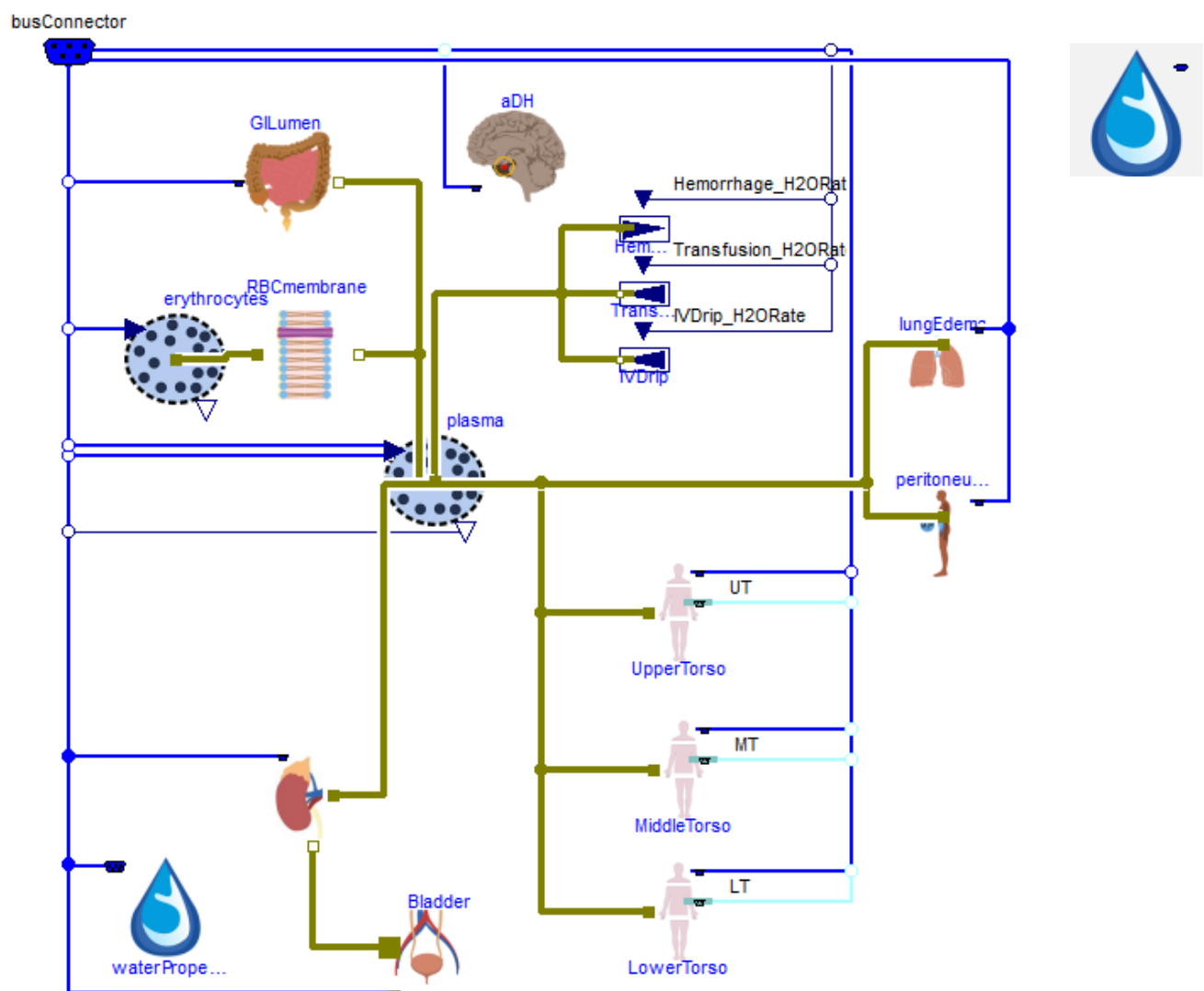


Diagram 12: Water subsystem.

Selected mean water flow between all compartments are listed in Table V, as examined in a range of studies (Eisenhoffer, et al., 1994; Engeset, et al., 1973; Henriksen, 1985; Xie, et al., 1995). The steady state of Table V reverts the sum of each row and each column to zero. Table rows represent flow description while columns refer to different areas. The areas into which

water flows are indicated according to whether the value is positive, or whether the places from which the water flows has a negative value.

For example, in the first line, the water is absorbed from diet in the gastrointestinal tract; the food comes from the environment (ENV) and goes into the blood plasma (Plasma). In each torso the water is metabolically produced and excreted through sweating or by vaporization. Flows such as hemorrhage, transfusion, intravenous drip, flow to the peritoneum, to the lungs and edema are zero in normal conditions. Excretion in the form of urine is modeled by the kidney component.

Table V: Selected steady state water flows between compartments [ml/min].

	Plasma	UT	MT	LT	ENV
From diet	1.4				-1.4
Across capillaries	-3.01	0.38	1.23	1.40	
Lymph	2.41	-0.32	-0.75	-1.34	
From metabolism		0.06	0.11	0.06	-0.23
Evaporation		-0.12	-0.59	-0.12	0.83
Urination	-0.8				0.8

5.2.1 Extracellular proteins

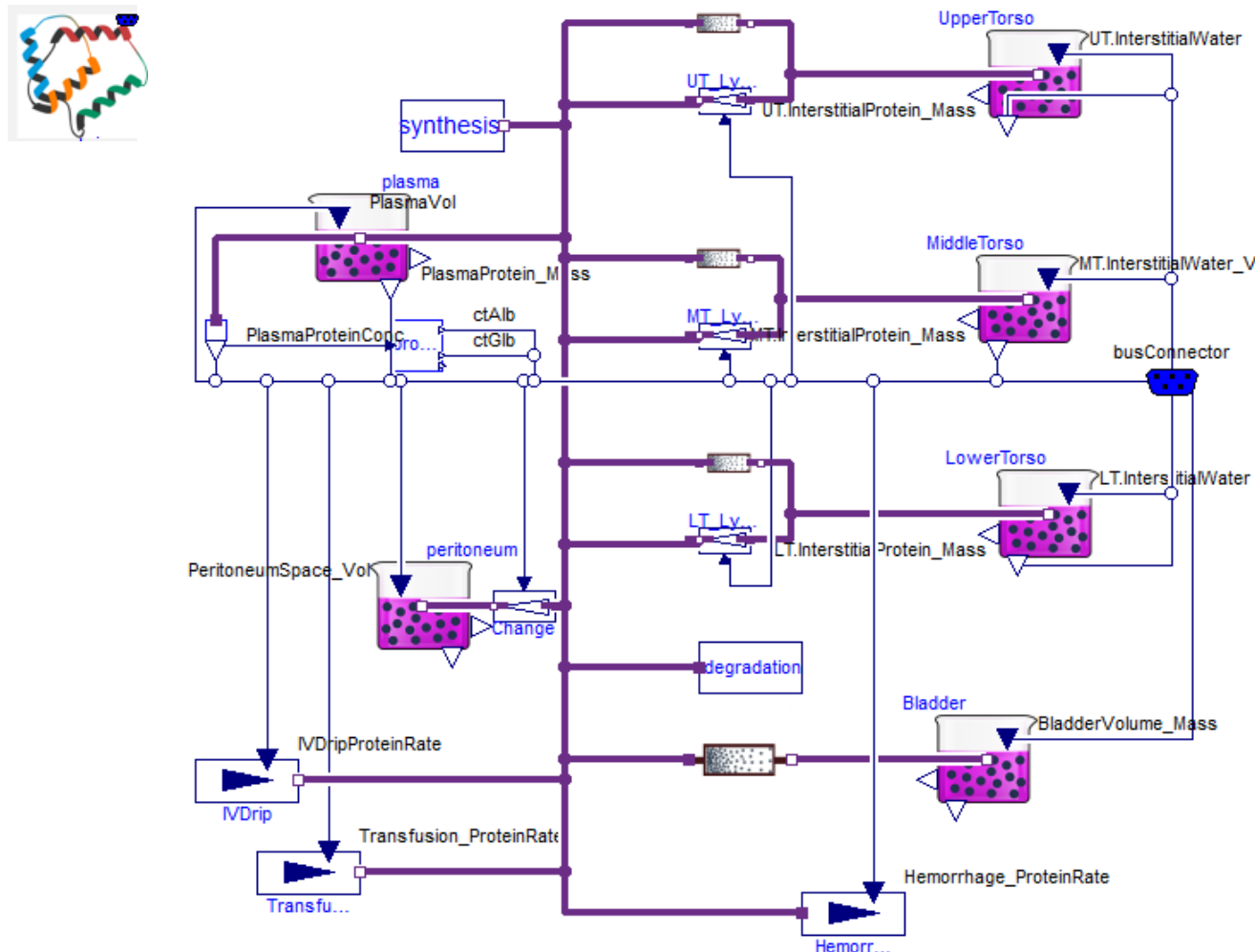


Diagram 13: Subsystem of extracellular proteins.

Water distribution between cardiovascular and interstitial spaces occurs concurrently with colloid osmotic pressures, which leads to the calculation of extracellular proteins of the same compartments, as described in the previous section. Usually, proteins are calculated in units of mass; however, our implementation calculates their amount of substance, because mole fractions play a role in osmotic equilibrium (Equation 8). The molar mass of albumin is 66.5 kDa and the mass of albumins in blood plasma is about 60% of the total plasmatic protein mass. The rest of significant colloid proteins are globulins. The typical molar amount of plasmatic proteins is as presented in Table VI. The general approach for recalculating mass-molar units is by joining an osmotic pressure equation as a mass function (Ahlqvist, 2003; Manning, 1987) with Equation 8, where the molar volume of water is around 0.018 L/kg.

Table VI: Typical plasma proteins concentrations

Total	Albumin	Globulins
1.44 mmol/L	0.63 mmol/L	0.81 mmol/L
28 µmol/mol	12 µmol/mol	16 µmol/mol

As already noted, the model of proteins (Diagram 13) has four main compartments: blood plasma, upper torso interstitial space, middle torso interstitial space and lower torso interstitial space. Normal concentrations in interstitial compartments are listed in Table VII. Normal mean proteins synthesis is the same as it is for protein degradation. Their current values can be changed alongside deviation of their plasmatic concentrations. Movement between compartments is caused by capillary membrane concentration gradient or by lymph flow (Mayerson, et al., 1960) from interstitial spaces to blood, as implemented in the diagram of Diagram 13. Special changes in plasmatic concentrations can be effected by intravenous therapy, hemorrhage or pathological states. Pathological states include proteins entering the peritoneal space or crossing the glomerular membrane in primary urine filtrate.

Table VII: Typical protein concentrations in interstitium.

Upper torso	Middle torso	Lower torso
0.6 mmol/L	0.48 mmol/L	0.4 mmol/L

5.2.2 Gastrointestinal water absorption

As presented in Table V, the mean water in diet should be about 2 l/day, which is the sum of all water in food and drinks. Firstly, water is accumulated in the gastrointestinal lumen (GILumen). From the lumen, water can cross the cellular membrane of gastrointestinal cells (OsmBody_CellWall) using aquaporins to equilibrate its extracellular and intracellular mole fractions (Diagram 14).

The absorption of water from the gastrointestinal lumen into the intestinal cells is here driven only by osmotic forces. The typical mean intake of 2 L/day is caused by a mean osmotic pressure gradient of 25 kPa at a temperature of 37°C. From these assumptions, the permeability parameter can easily be expressed as 0.08 L/(kPa.day).

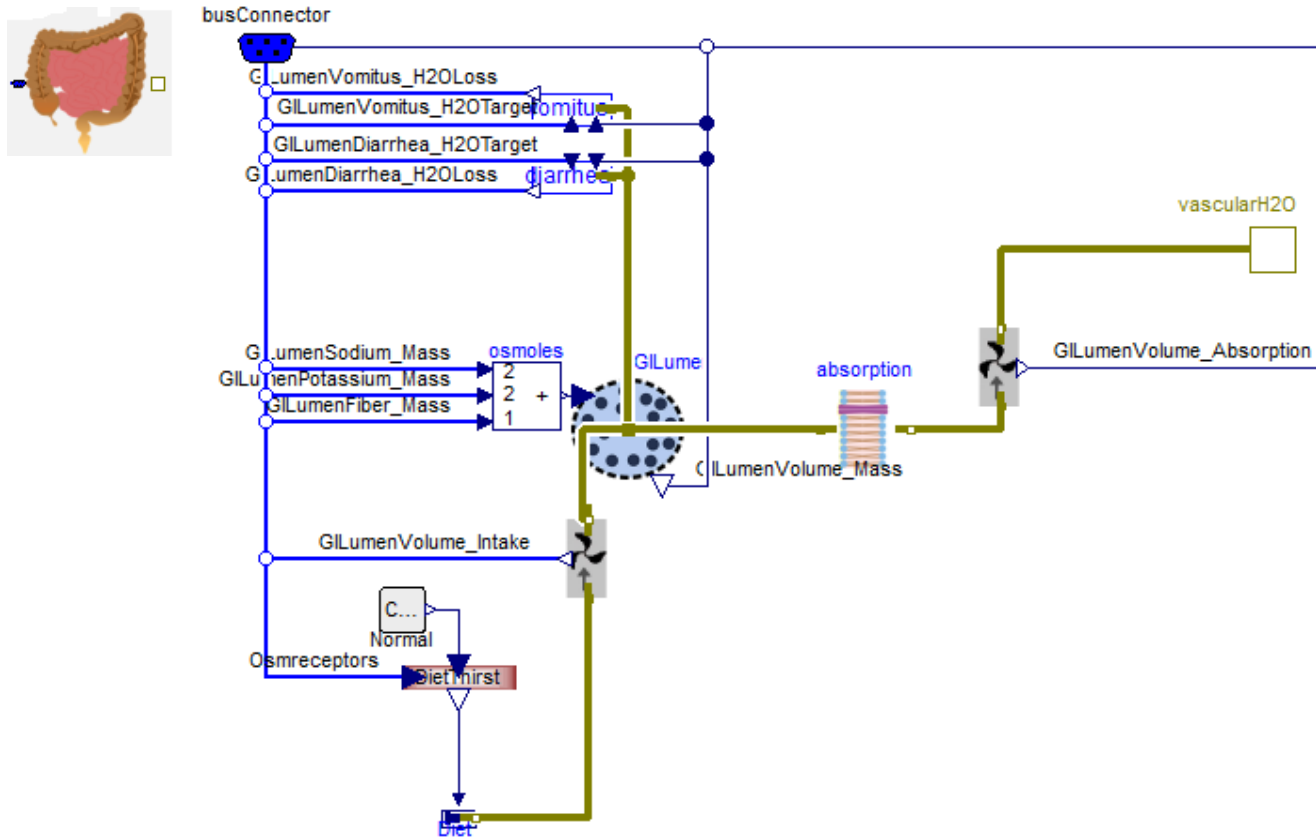


Diagram 14: Water absorption in the gastrointestinal tract.

5.2.3 Upper/middle/lower torso water

Flow between plasma and the interstitium is determined by colloid osmolarity on the capillary walls. This way is typically coming water to the tissue interstitium. Another way is the one directional lymph flow from the interstitium to blood plasma (Eisenhoffer, et al., 1994; Engeset, et al., 1973; Henriksen, 1985), as presented in Table V. These flows can be influenced by the internal pressure in tissues caused by their volume and skin, as examined by Guyton (Guyton, 1965) and Xie et al. (Xie, et al., 1995). Water crossing the capillary wall is driven by hydrostatic-oncotic pressure gradients, as expressed by Equation 8.

However, the flow of water between the interstitium and cells is determined by its model's fraction equilibrium. In cellular membrane, proteins' osmolarity plays a minor role, because their concentration is only about 1 mol/L. In the extracellular space the total amount of substances is divided into water, electrolytes, urea, glucose and other solutes. In the intracellular space, these substances are water, electrolytes, urea and other solutes. The small total amount of solution in interstitial fluid is caused by large molecules, which take up the highest solution volume (60-74%) with their small amount of substance (less than 10 mmol/L).

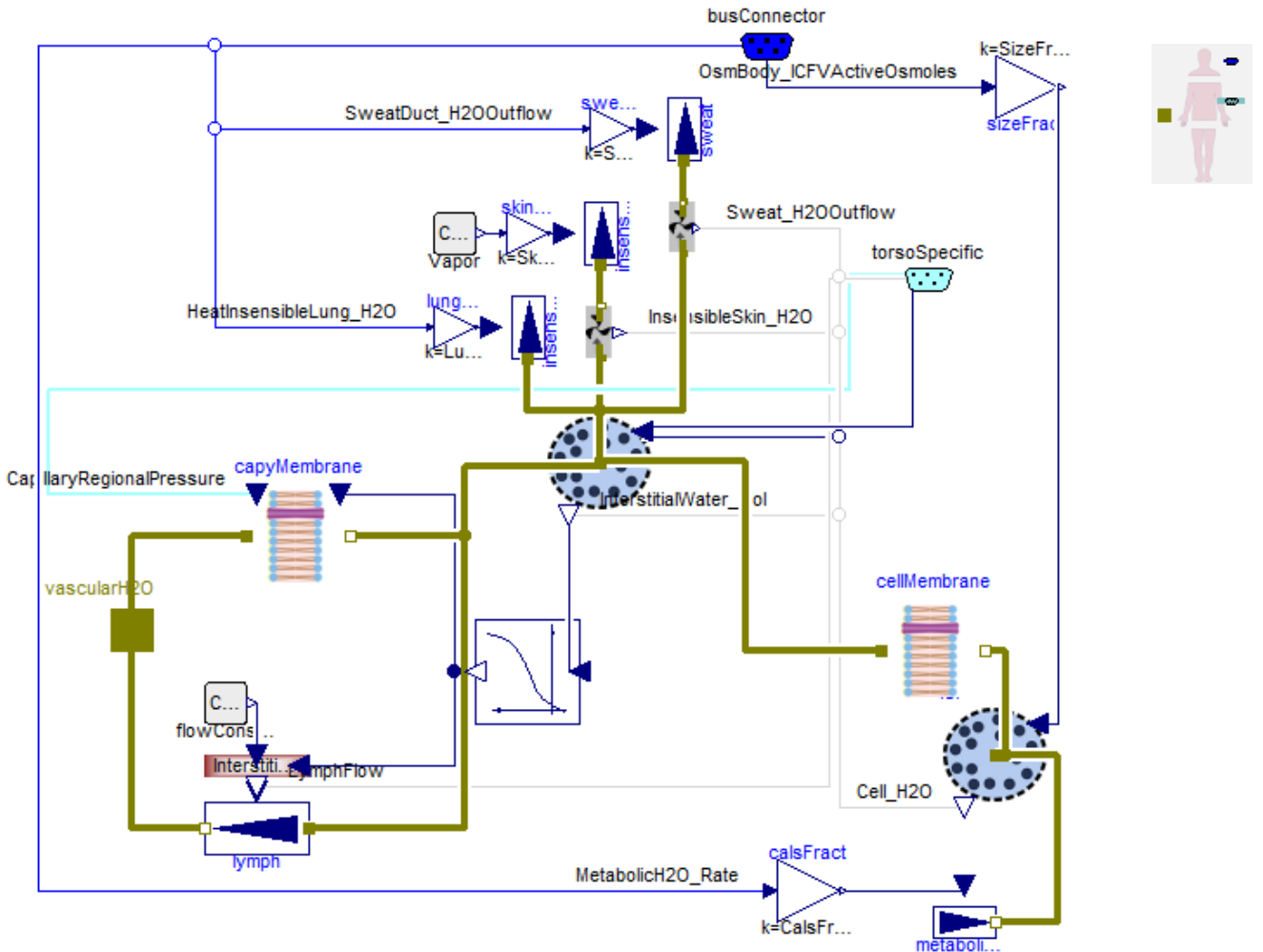


Diagram 15: Water exchanges for upper, middle or lower torso.

5.2.4 Kidney water excretion

In the kidneys, water is delivered by blood to the glomerulus, where blood plasma is filtrated into glomerular filtrate (GFR). Most of this filtrate is reabsorbed in nephrotic parts: the proximal tubule (PT), the loop of Henle (LH), the distal tubule (DT) and the collecting ducts (CD); the rest is accumulated in the bladder as urine.

Table VIII: Typical average steady state flows through nephrons [ml/min.]

GFR	to LH	to DT	to CD	to Bladder
120 ml/min	57 ml/min	41 ml/min	4.6 ml/min	0.8 ml/min

Proximal tubule

Glomerular filtrate in the glomerulus has the same pressure as blood in the glomerulus and this pressure pushes it into nephrons. The reabsorption fraction in the proximal tubule is determined only by sodium reabsorption of the proximal tubule.

Loop of Henle

Only the short coronary nephrons contain the aquaporin channels inside the loop of Henle, which reabsorbs the water of 37% fraction of the sodium reabsorption fraction (Gottschalk and Mynlie, 1959; Nielsen, et al., 2000).

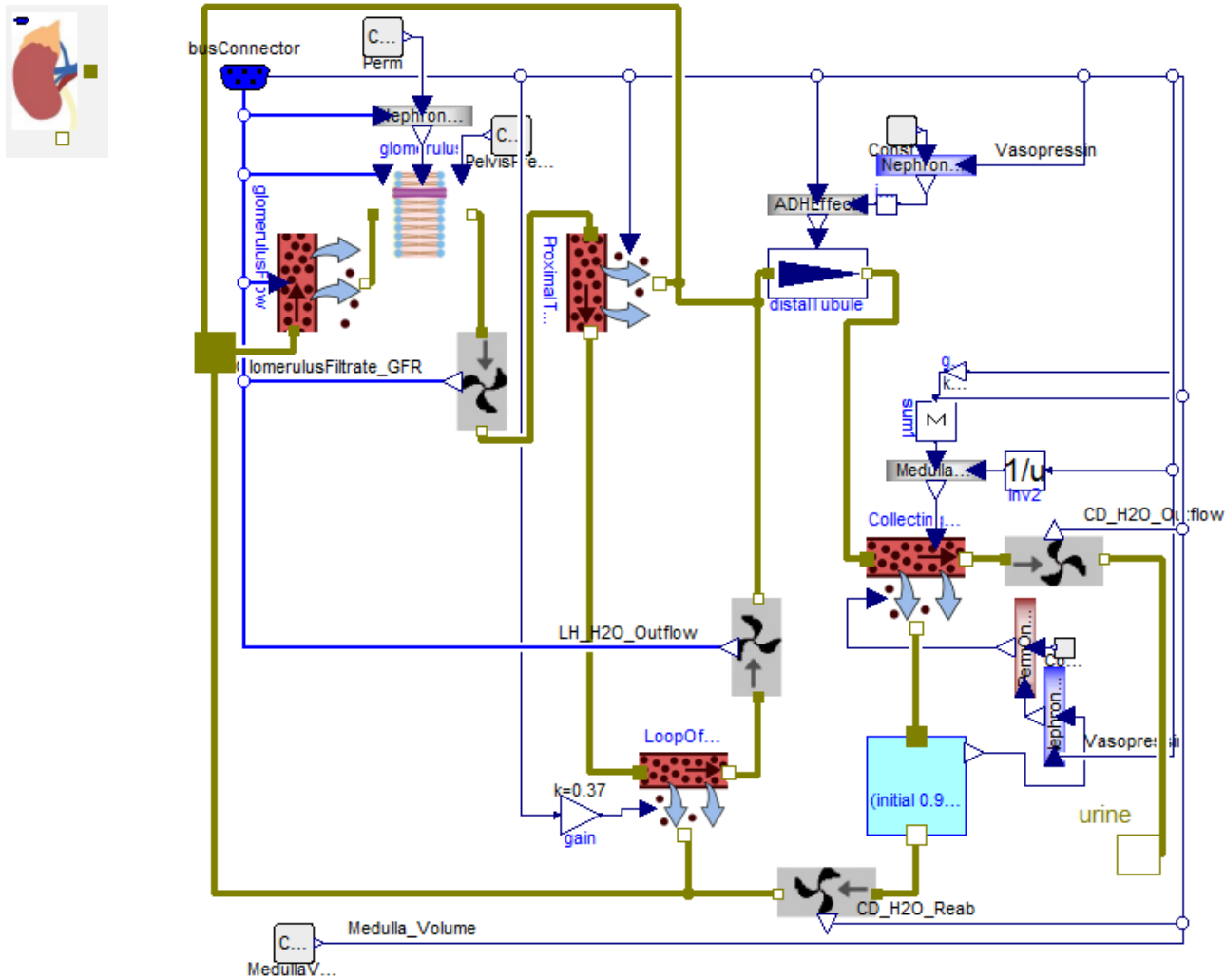


Diagram 16: Water excretion by kidney nephrons.

Distal tubule

Outflow of filtrate to the collecting duct is determined by the outflow of sodium, where it is dependent on ADH nephron concentration, as described in Khokhar et al. and Atherton et al. (Atherton, et al., 1971; Khokhar, et al., 1976).

Collecting duct

In the collecting duct, the number of active aquaporin channels are driven by ADH; proportionally, this indicates the volumetric flow rate of reabsorbed water by the collecting duct tubules (Jamison and Lacy, 1972; Jamison, et al., 1971). Changing the activity of aquaporin channels is modeled by the integration of inactive channels driven by ADH concentration as simulating the process of their intracellular vesicular storage. There is minimal water outflow to urine, which is determined by sodium outflow to urine and medulla osmolarity.

5.2.5 Hydrostatic spillover

Orthostatic position also plays a role in water transport. The hydrostatic pressure component can be calculated using Equation 29. Together with hydrodynamic blood pressure and osmotic

pressure components, it forms the pressure gradient on the capillary walls of tissues. The values of blood hydrostatic pressure and interstitium hydrostatic pressure are different in an upright position. The pressure gradients are caused by the different heights of compact liquid columns, which generate the pressure. Blood vessels are mostly compact tubes, where the highest position determines the hydrostatic pressure of the position below. These hydrostatic pressure components can be calculated only from the height difference, while the interstitial space can be more hydrostatically independent, meaning that the weight of the tissue water can be maintained using a system of cavity membranes, which generates smaller heights of hydrostatic columns. In the lower torso, veins are enabled as a result of motions made by the leg's skeletal muscle, which has a pumping effect similar to that of the heart. The reason for this is the availability of vein valves, between which accumulates a volume of blood from lower parts of the body during skeletal muscle relaxation, which is ejected to upper parts of systemic veins during skeletal muscle contraction. This pumping effect not only reduces hydrostatic pressure, but also actively increases the blood flow of systemic veins during walking, running or cycling.

5.2.6 Relational comparison with HumMod 1.6.1

The primary differences between the HumMod and Physiomodel in terms of water calculation is that the latter is more physically-based, but yielding almost the same results as the former.

This means that, for example, osmosis is calculated by the equilibrium of chemical potentials, as indicated in physical chemistry textbooks (Mortimer, 2008). The impermeable proteins of plasma and interstitial fluid are in the Physiomodel recalculated to molar amounts. These molar amounts were selected by mass amounts of the HumMod to reach the same normal values of osmotic pressures on capillary membrane. Oncotic pressure is calculated in both models from these proteins, which cannot freely cross the capillary membrane. Their molar concentrations in Table VI and in Table VII are consistent with both physical osmotic pressure calculation and with their original mass concentration (Ahlqvist, 2003), where the ratio between mass and molar concentration is the average molar mass of these proteins.

In textual representation, it is easy to misuse one variable in the place of another. As a result, equations can be entirely wrong, which can immediately be observed in simulation results. Worse, if the both variables have similar values, all results will appear in order up to the point where a specific setting is applied. This is the case for regional capillary blood pressure in HumMod 1.6. If the patient is lying down on a bed, all regional pressures will be the same. If the patient stands up, hydrostatic pressures will change according to different heights relative to position of heart (Equation 29). As a result, there will be higher regional capillary pressure in the lower torso and lower regional capillary pressure in the upper torso. The Physiomodel calculates results by taking these factors into account; however, in the HumMod 1.6, these tissue capillary pressure gradients are always calculated only from the upper torso capillaries' pressure, or from the middle or lower torso.

The Physiomodel also makes improvements in the relationship regarding losing water by vaporization in respiratory pathways. In the HumMod 1.6, it is assumed that all water in expired air arises from vaporization. However, there can be significant humidity in the inspired air. The Physiomodel inserts this humidity to slow down the expiration of water in hot and humid environments.

The final differences between the Physiomodel and the HumMod 1.6 concerns the behavior of tissue water in an initial state and during steady state. For example, lymph flow in the upper torso was too slow to deliver the same amount of water from the upper torso interstitial space

as the amount of water crossing the capillary membranes at the same time and in the same place. Thus, the interstitial water of the upper torso slowly increases from the start of the simulation to pathophysiological values. To prevent this instability in the model, we recalculated the permeability coefficient of the upper capillaries in order to meet the steady state of these flows. As a result, there are initial steady states of interstitial water in the Physioworld.

5.3 HORMONES

5.3.1 Anti-Diuretic Hormone (ADH, Vasopressin)

Arginine vasopressin, known as an antidiuretic hormone (ADH), has a molecular weight of 1084 Dalton. ADH as a hypothalamic neurohormone is synthesized in the cell bodies of magnocellular neurons of paraventricular and supraoptic nuclei and is intracellularly transported to the lower side of these neurons in the posterior pituitary.

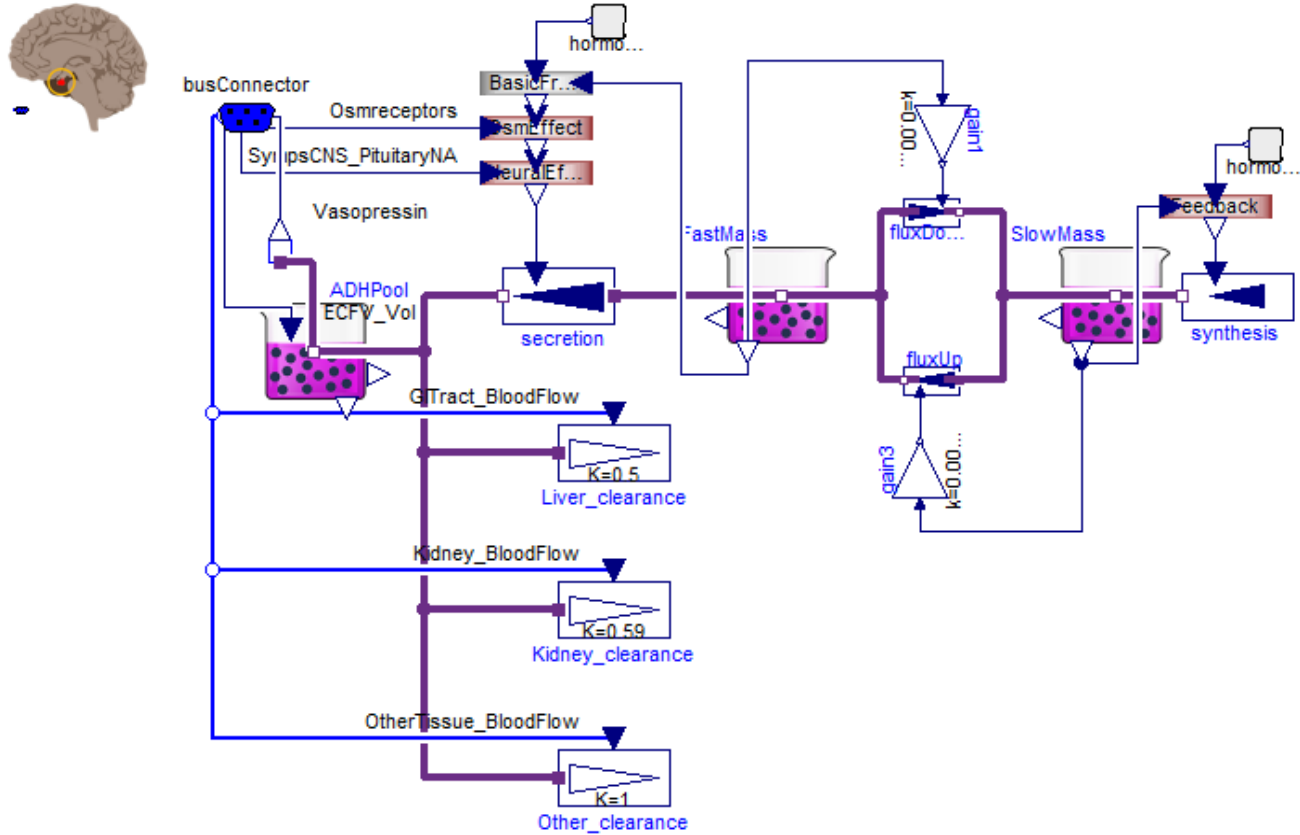


Diagram 17: Vasopressin

The model (Diagram 17) accumulates an amount of this hormone in four areas: in the cell bodies of magnocellular neurons (Slow Mass), from where it needs to be transported to the posterior pituitary part of the cells; in the posterior pituitary side of neurons (Fast Mass), where ADH is prepared for secretion into the blood; in the entire body's extracellular fluid (ECF); in the kidney tissue, where it plays a role in water reabsorption. The normal long-time amounts of ADH in these compartments are listed in Table IX; however, during regulation, their concentration can be increased a hundred- or thousand-fold (Lankford, et al., 1991). The normal long-term mean rate of synthesis, secretion and degradation should be the same at

steady state. However, secretion in the form of a short-time process can achieve much larger changes. The effect of various changes and concentrations has been demonstrated in dosage experiments (Atherton, et al., 1971). Internal secretion is determined by osmoreceptors and pituitary activity. Osmoreceptors are the cells in the anterior hypothalamus near the supraoptic nuclei. When the osmolarity increases, the osmoreceptors shrink and send a neural signal to release ADH (Young, et al., 1977). Another possibility for regulating ADH secretion is through cardiovascular centrum reflexes (Erwald and Wiechel, 1978).

Table IX: Selected long-term steady state amounts of vasopressin.

Slow Mass	Fast Mass	ECF	Kidney Medulla
15.7 nmol	2.95 nmol	0.028 nmol	0.000 057 nmol

The vasopressin within cells is modeled using instances of the chemical Substance class; the intracellular vesicular mole fraction is 1, because ADH is transported as a pure substance by vesicles down the cell. The degradation is divided into liver, kidney and other tissue blood clearance. To reach the mean constant level of ADH, the sum of all long-term mean losses must be the same as the long-term mean synthesis and secretion. The loss of ADH in these organs as an enzymatic degradation in liver, kidney and other tissues is dependent on blood flow.

A typical concentration in blood plasma and extracellular fluid is in the order of ng/l, pg/ml, pmol/l or mIU/l. An increase in these concentrations causes water reabsorption in the kidneys (Lankford, et al., 1991) as implemented in Diagram 16.

5.3.2 Atriopeptin

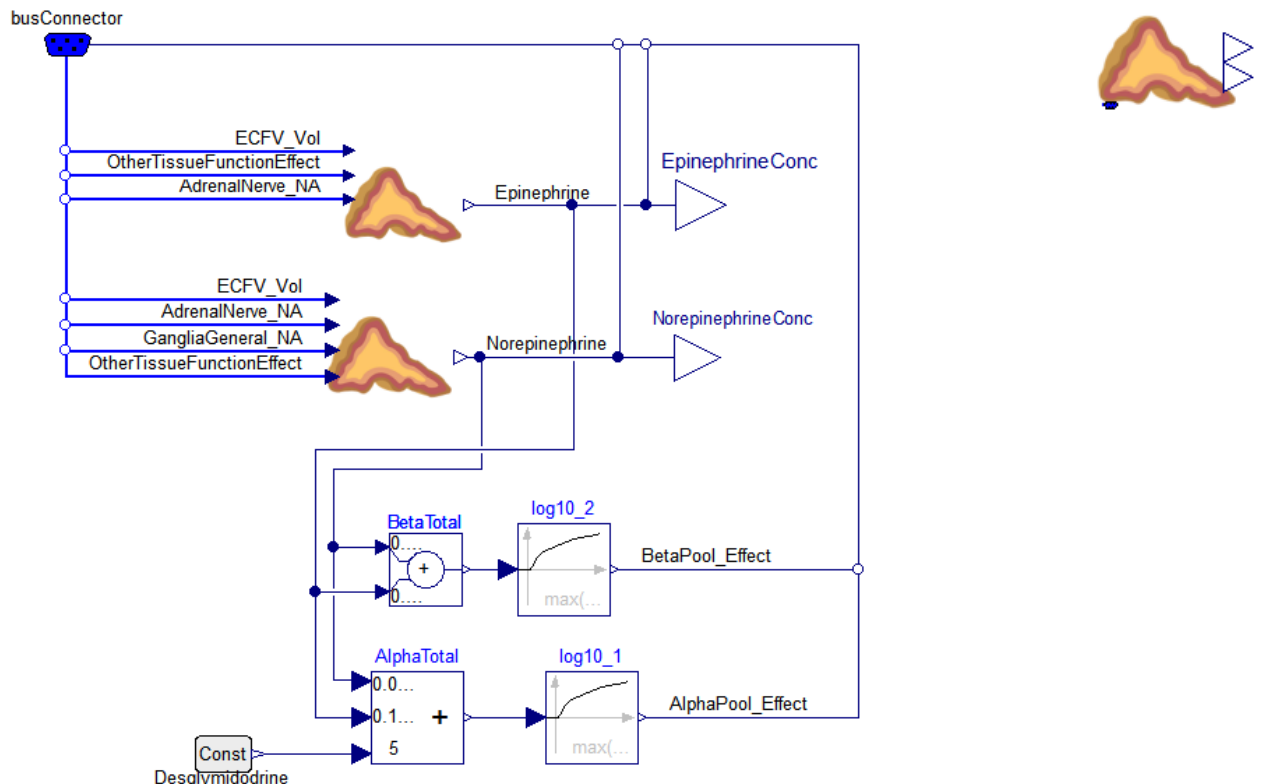


Diagram 18: A catecholamines model integrated with a model of epinephrine and norepinephrine.

The secretion of atrium natriuretic peptide (ANP) is driven by mean blood pressure in both atria. These pressures are relative to pericardium pressure and noted with the suffix ‘_TMP’ in Diagram 18. There is an adaptation of secretion to current pressures with half time about fifteen minutes, what makes from ANP the middle-term regulator of blood pressure and blood volume

5.3.3 Catecholamines (epinephrine; norepinephrine)

The model of catecholamine accumulation, secretion and clearance is very simple. Driven by sympathetic neural activity, epinephrine and norepinephrine is secreted in the adrenal gland. It is then accumulated in extracellular space and continuously degraded by clearance, which at a long-term steady state causes the same mean degradation as the mean secretion. This model accurately describes an experiment of 60-minutes’ continuous intravenous epinephrine infusion, where different nominal rates caused different steady state plasma epinephrine concentrations (Clutter, et al., 1980).

The effect of catecholamine in alpha- or beta-receptors on the effector organs is expressed as a decimal logarithm of the concentration. This effect is combined with sympathetic neural activity on the receptors and can be blocked by alpha- or beta-blockers.

Erythropoietin (EPO)

Erythropoietin (EPO) secretion is driven by partial oxygen pressure in the kidneys (Goldberg and Schneider, 1994; Jacobson, et al., 1957; Pagel, et al., 1988; Porter and Goldberg, 1993). In contrast with previous hormones, the distribution space of EPO is not all extracellular fluid, but only about 40% of this fluid (Miller, et al., 1982; Reissmann, et al., 1965). The mean degradation must be the same as the mean secretion during typical mean concentration in a steady state.

The role of erythropoietin is connected with erythropoiesis in the bone marrow (Jacobson, et al., 1957; Roush, 1995; Winearls, et al., 1986).

5.3.4 Insulin and glucagon

Insulin is one of the most widely studied hormones. Molar mass of insulin is 5.808 kDa. The first standard international unit of insulin was noted in 1958 (Standardization and Organization, 1958); the most recently discontinued definition from 1986 has been improved to 38.46 µg/IU (Standardization and Organization, 1987). Using this definition, it is possible to deduce a conversion factor from pharmacological units to amount of substance as 6.621 pmol per 1 IU of insulin.

The insulin pharmacokinetic and pharmacodynamics obeys the same principles as the model of glucose-insulin homeostasis put forward by Guyton et al. (Guyton, et al., 1978). Insulin is synthetized and stored in beta-cells and its secretion is driven primarily by glucose and secondarily by keto acids (Imai, et al., 2008; Rutter and Hill, 2006). Portal and peripheral vein insulin has different concentrations (Blackard and Nelson, 1970), because insulin is transported directly after its secretion by portal veins to the liver. Absorbance and clearance of insulin have been measured using a range of infusion experiments (Dobson, et al., 1967; DOEDEN and RIZZA, 1987; GINSBERG, et al., 1973).

Problems with insufficient insulin secretion results in type 1 diabetes mellitus and receptor insensibility leads to type 2 diabetes mellitus (George, et al., 2004; Prager, et al., 1987; Summers, et al., 1997), where many differences between normal and obese individuals have

been observed (Prager, et al., 1986). Insulin has significant effects on glucose absorption into hepatocytes (Iwanishi, et al., 2000; Previs, et al., 2000; Rother, et al., 1998), where glucose is stored and released to/from glycogen (glycogenesis, glycogenolysis), glucose is created from amino-acids (gluconeogenesis) or glucose is transformed to fats (lipogenesis) (Guyton, et al., 1978; Miles, et al., 1995; Prager, et al., 1986). The similar effects on glucose absorption and storage is modeled in skeletal muscle tissue. Insulin also facilitates storing of fatty acids in adipose tissue, as modeled in the lipid submodel of metabolism (Diagram 32).

In contrast to the storage effect of insulin, glucagon helps to increase the glucose and fatty acid concentration in the extracellular space. However, the secretion of glucagon is dependent on the insulin concentration (and the glucose concentration), rendering it the secondary regulator of blood glucose concentration.

5.3.5 Leptin

Leptin is secreted by adipose tissue as a signal from accumulated lipids (JÉquier, 2002). The notion of curing obesity using leptin is not valid, due to leptin resistance in instances of obesity (Friedman-Einat, et al., 2003). The clearance of leptin is primarily effected by the kidneys (Cumin, et al., 1996). Leptin has multiple effects on higher metabolic centers (Mantzoros, et al., 2011; Wong, et al., 2004), which is modeled primarily according to the influence of diet composition and the amount of food eaten as a result of changes in taste caused by leptin concentration.

5.3.6 Renin-angiotensin-aldosterone system

The secretion of renin in the kidneys is driven by tubuloglomerular feedback (TGF) (Braam, et al., 1993; Seeliger, et al., 1999), as well as adrenergic receptors (Almgård and Ljungqvist, 1975; WINER, et al., 1969). Clearance is primarily conducted by the liver (Christlieb, et al., 1968). Renin is an enzyme that converts angiotensinogen into angiotensin I. This conversion obeys Michaelis-Menton dynamics, which creates linear dependence between the amount of renin and the rate of conversion (Goldblatt, et al., 1953). The same dynamic is observed in the lungs regarding angiotensin converting enzyme (ACE), where angiotensin I is transformed into angiotensin II. In optimal regulation conditions, enzymatic reactions give linear dependence between renin concentration and angiotensin II concentration (Claassen, et al., 2013).

5.3.7 Thyroid hormones

The main purpose of thyroid hormones in our model is to maintain the basal metabolism in connection with long-term thermoregulation (Edelman, 1974). The concentrations, secretions and clearance of thyroid hormones are well known, because of the relative easy measurement of iodine radioactive isotopes (HAYS, 1993; Chopra, 1976; Larsen, 1972; Nicoloff, et al., 1972). During cold months, increasing triiodothyronine (T_3) (Hesslink, et al., 1992) increases the basal metabolism (Osiba, 1957), which improves heat regulation in cold conditions. The impulse for the production and secretion of T_3 and thyroxine (T_4) is thyrotropin (TSH) (Jackson, 1982). The secretion of TSH is driven by thermoreceptors and is directly suppressed by T_3 (Gross and Pitt-Rivers, 1953; Hesslink, et al., 1992; SURKS and LIFSCHITZ, 1977; SURKS and OPPENHEIMER, 1976). The clearance of TSH happens much quicker than the clearance of T_3 or T_4 (Ridgway, et al., 1974); as a result, TSH concentration can be directly estimated from the secretion of these thyroid hormones, which is determined by current thyroxines concentrations and temperature.

5.3.8 Comparison with HumMod 1.6

There are also small corrections of hormonal equations in the Physiomodel; however, the mean levels of hormones are almost the same as in HumMod 1.6.; this solves, for example, the mish-mash of physical units or the potential confusion of variables.

The primary aim of modeling all organic chemical substances was to calculate the amount of their molecules. This was the impetus for using molar units. The amount of substance in moles multiplied by the Avogadro constant yields the relevant number of particles. However, currently, even the Avogadro constant is approximated and as a decimal number, only the first eight of its 23 digits are exactly determined. This means that the precision of counting the particles of a solution is limited and we do not know exactly how to measure and work with very small molar concentrations (such as piko- or femtooles per liter). These very small concentrations are biologically significant for some hormones, enzymes or cytokines. Instead of physical units, some pharmacokinetic units must therefore be used (u or iu – international unit defined by [WHO](#)); these are defined by the solution extract as a result of the described purification process. In the Physiomodel, this situation is solved using a redefinition of the Physiolibrary, where all moles are switched to international units of the specific hormone, enzyme or cytokine. These redefined library components must be used for each block calculation with the relevant substance. For example, if we want to create the chemical reaction of this ‘unmeasurable’ hormone with its receptor, the concentration and amount of receptors must also be in the same international units as the hormone. Hormones, enzymes or cytokines with already known conversions should be used in their physical amount of substance rather than in international units.

It is not surprising that physical units can be a source of many mistakes in the models, especially in the case of hormones, where unusual prefixes such as micro-, nano-, piko- and fento are used together with more alternatives for expressing concentrations such as molar concentration, mass concentration, molar fraction, mass fraction and international units. For example, in HumMod 1.6, this combination of units with thyroid hormones, where a concentration is 100 x higher due to switching ‘ug/ml’ for ‘ug/dl’ when compared to data presented by (CHOPRA, et al., 1975). When using the Physiolibrary in some user-friendly Modelica environments, there is automatic support for recalculation of non-SI units into/from SI units, including those with different prefixes. Using this automated physical unit support for inputs and outputs of simulation the modeling process becomes more error-free in the area of unit conversions.

The other example of changes in variable names in HumMod 1.6 is in the case of intracellular renin fluctuation calculations. Instead of calculating the flux from free renin synthesis to renin granules, the same variable is used for the intake and outtake of the renin granules. Thus, the renin granules have the same concentration every time for each simulation experiment, even if rapid secretion occurs. Using the diagram modeling of the Physiolibrary it becomes very clear *from* which or *to* which compartment the renin flows move. The likelihood of mistakes occurring in this area therefore decreases, because the connections are visually self-descriptive.

Changes in physical units can hide more contextual errors. For example, a change in vasopressin as a result of blood clearance in circulating blood through tissue must be less or equal than the amount of vasopressin inflowing as a result of blood moving to this tissue. Because of the recalculation from milliliters to liters, values higher than 1 is hidden by physical unit conversion. This confusion is also visible in other instances of tissue clearance of vasopressin in HumMod 1.6; in the Physiomodel, it is resolved by selecting full clearance in this type of tissue, which generates only a small differences in vasopressin degradation.

5.4 ELECTROLYTES AND ACID-BASE

5.4.1 Acid-base

The acid-base balance calculation is based on electroneutrality. In the case of plasma, in extracellular and in intracellular fluid, the charges of strong ions that do not significantly change their charge at a pH from 5 to 9 are summarized. This is called strong ion difference (**SID**) (Stewart, 1981). As an analogy of SID, the variable anion gap (**AG**) can be used, which is the same as SID with a charge of bicarbonates ($AG = SID - [HCO_3^-]$), where the amounts and properties of other non-bicarbonates acid-base buffers are also not included. The acid-base buffers (HCO_3^- and other weak ions) are calculated as the **negative** summary charge concentration at normal conditions (prefix N); this is called normal strong ion difference (**NSID**). The **normal conditions** are defined as **plasma pH=7.4, full oxygen saturation, CO₂ partial pressure 40mmHg and temperature 37°C**.

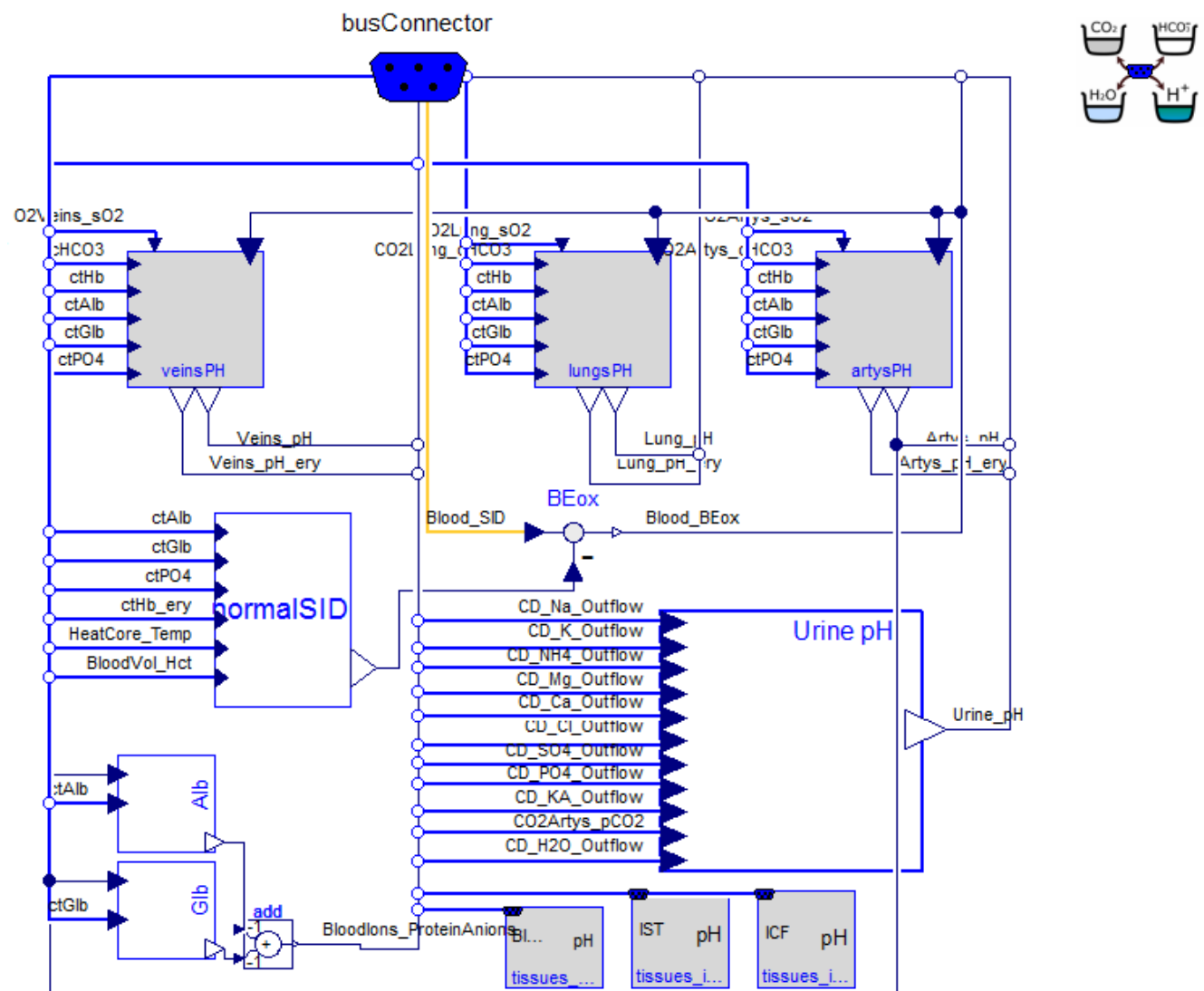


Diagram 19: Acid-base subsystem.

NSID describes the potential of acid-base buffers. In normal conditions it has the same value as SID. In a situation where there is a higher value of NSID than SID (for example, there is an excess of strong acids) the arterial pH<7.4 during a normal state of respiration at 37°C. If $NSID < SID$, then $pH > 7.4$ (for example, an excess of strong bases) during a normal state of

respiration at 37°C. Both SID and NSID can be calculated in plasma (suffix P) and inside erythrocytes (suffix E). The titration of one liter of blood in order to reach normal conditions must use the same amount of strong acid as the differences between SID and NSID in plasma and in erythrocytes (Mateják, 2013). This hypothetical titration is expressed as $\text{BE}_{\text{ox}} = \text{Hct} * (\text{SID}_E - \text{NSID}_E) + (1 - \text{Hct}) * (\text{SID}_P - \text{NSID}_P)$, where Hct is the hematocrit and BE_{ox} is the base excess of oxygenated blood, as defined by (Kofránek, 2009; Kofranek, et al., 2007). The measurable amount of titrant can also be expressed as a negative value, referred to as titratable hydrogen ions of oxygenated blood ($\text{cTH}_{\text{ox}} = -\text{BE}_{\text{ox}}$), as applied by Siggaard using the Van-Slyke equation (Siggaard-Andersen, 2005). The BE_{ox} and cTH_{ox} are independent of blood gases (CO₂, HCO₃⁻, O₂), which renders them perfect candidates for describing the metabolic parts of acid-base disorders. Respiratory problems or additional regulation of acid-base disorders should be immediately observable from the arterial blood partial pressure of CO₂, which should normally be regulated by respiration to 40mmHg.

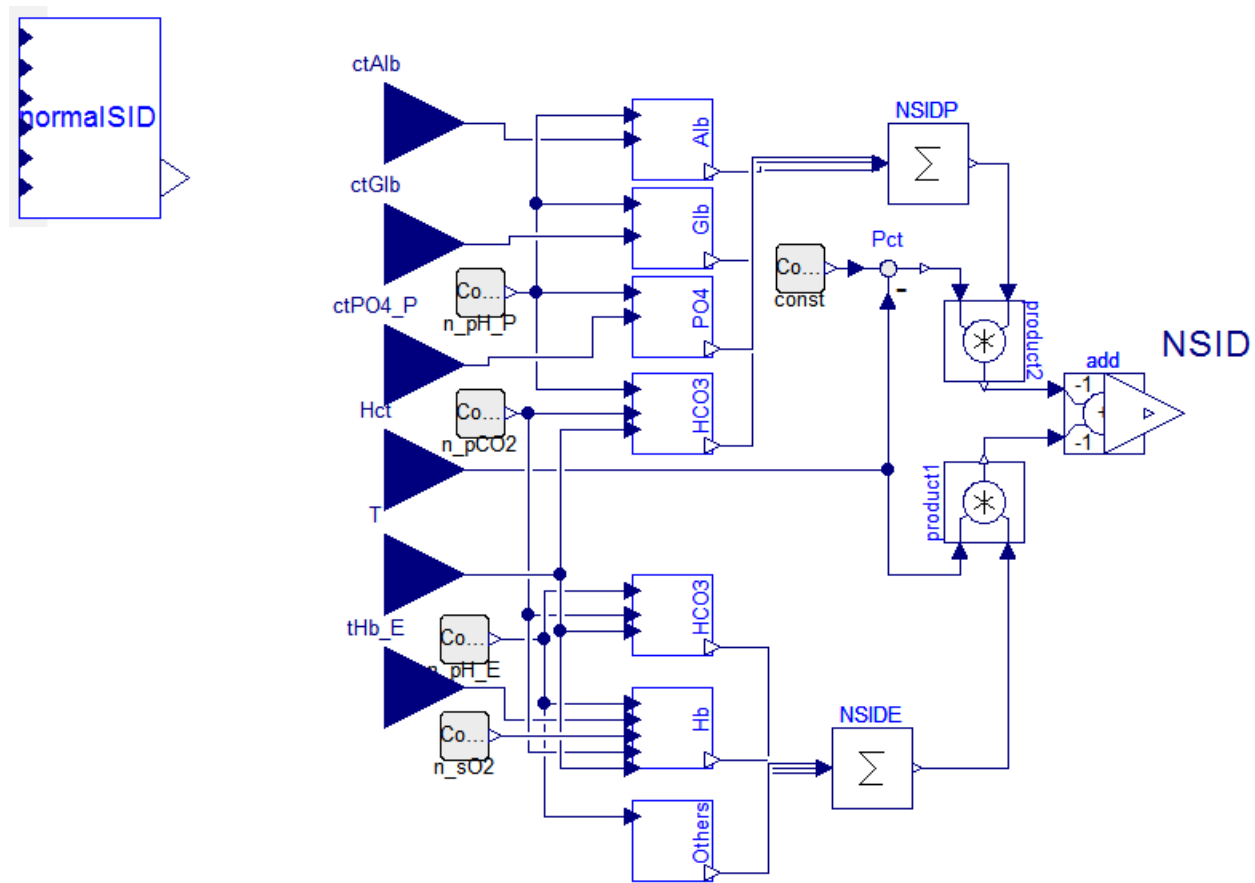


Diagram 20: Acid buffers (normal strong ion difference).

The acid-base equilibrium is connected to all charged substances by electroneutrality. The charges of substances are calculated in physical units called equivalent (eq) or milliequivalent (1 meq = 0.001 eq). A positive value means a positive charge, while a negative value indicates a negative charge. One equivalent is the charge of one mol of protons, which is the same as one mol of sodium cations Na⁺ or the same as half a mole of calcium cations Ca²⁺. The typical SID_P is composed of Na⁺, K⁺, Cl⁻, SO₄²⁻, Lactate⁻ and the typical NSID_P is calculated as a negative sum of normal bicarbonate HCO₃⁻, albumin, phosphates and globulins charges at a

hypothetical pH=7.4 and a temperature of 37°C. In erythrocytes, the SID_E is typically the sum of the charges of K⁺, Cl⁻, Na⁺, Mg²⁺ and SO₄²⁻. The NSID_E is the negative sum of the charges of HCO₃⁻, hemoglobin, phosphates such as 2,3-DPG, ATP, ADP and GSH at hypothetical plasma pH=7.4, full oxygen saturation of hemoglobin and a temperature of 37°C. Other electrolytes and buffers are neglected, because of their small concentration and/or small charge. This calculation in the Physiomodel is similar as the calculation of Raftos et al. (Raftos, et al., 1990), Wolf et al. (Wolf, 2013; Wolf and DeLand, 2011).

The calculation of charge of the weak ions (weak acids) is dependent on pH, because they are equilibrated as chemical reactions in Table X. The first schematic reaction is called the Henderson-Hasselbalch equation and is generally used to calculate the carbonic acid dissociation to bicarbonate, which is often connected with CO₂ dissolution in water (Equation 13) and CO₂ hydration to H₂CO₃ and accelerated by carbonic anhydrase inside red cells. The acid-base equilibrium can be calculated as in Equation 11, where the dissociation constant K can be defined using a negative decimal logarithm such as pK = -log₁₀(K).

Table X: Schemes of acid-base reactions.

Group of acid	Type of reaction	Example of acids
Monoprotic	HA ↔ A ⁻ + H ⁺	HCl, -COOH, some protein side chains
Diprotic	H ₂ A ↔ HA ⁻ + H ⁺ ↔ A ²⁻ + 2H ⁺	H ₂ SO ₄ , H ₂ CO ₃
Polyprotic	H _n A ↔ H _{n-1} A ⁻ + H ⁺ ↔ ...	H ₃ PO ₄
Brønsted	AH ⁺ ↔ AH + H ⁺	NH ₄ ⁺ , -NH ₃ ⁺ , some protein side chains

Table XI: Dissociation constants (pK) of selected acid-base reactions.

Chemical reaction	pK	Temperature of pK
CO ₂ (aq) + H ₂ O ↔ H ⁺ + HCO ₃ ⁻	6.103	37°C
HCO ₃ ⁻ ↔ H ⁺ + CO ₃ ²⁻	10.329	25°C
AcAc ↔ H ⁺ + AcAc ⁻	3.6	37°C
β-Hb ↔ H ⁺ + β-Hb ⁻	4.7	37°C
HSO ₄ ⁻ ↔ H ⁺ + SO ₄ ²⁻	1.99	25°C
H ₃ PO ₄ ↔ H ⁺ + H ₂ PO ₄ ⁻	1.91	37°C
H ₂ PO ₄ ⁻ ↔ H ⁺ + HPO ₄ ²⁻	6.66	37°C
HPO ₄ ²⁻ ↔ H ⁺ + PO ₄ ³⁻	11.78	37°C
NH ₄ ⁺ ↔ H ⁺ + NH ₃	9.25	25°C

The special attention was served to hemoglobin titration (Mateják, et al., 2015), because during deoxygenation hemoglobin change the affinity for some hydrogen ions called Bohr protons noted as ΔH⁺ in Figure 1. This process is connected with Bohr's effect on oxygen dissociation curve and can be described as the oxygen stabilize the relaxed quaternary structure form of hemoglobin tetramer while protons stabilized the tensed form. However, in the same time the third ligand – carbon dioxide is presented, which is competitively binding with one of the Bohr proton to the amino terminus of each of four hemoglobin subunits. This way the CO₂ also stabilize the tense form of hemoglobin tetramer. As a result each three ligands are nonlinearly connected using principle of macromolecule equilibria described in section 3.1.5.

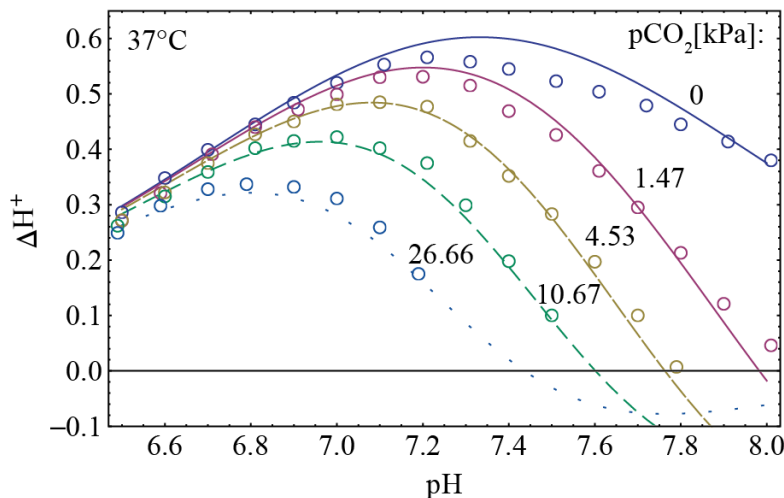


Figure 1, Hemoglobin subunit titration change caused by deoxygenation. Curve are results from our model (Mateják, et al., 2015), circles are data from Siggaard-Andersen (Siggaard-Andersen, 1971).

5.4.2 Kidney acid-base regulation

In the kidneys, pH is regulated by the excretion of titratable hydrogen ions H^+ and ammonium ions NH_4^+ . In contrast with weak acids, the protons connected to NH_4^+ remains more bounded than separated as H^+ and NH_3 . Urine pH can vary between 4.6 and 8. To connect the flowing acidity of urine (pH_u) with the flow of all charged substances, electroneutrality is used. The total molar flow of each substance is described in the subsections about electrolytes. The charge of substances in urine does not always remain the same as in the extracellular fluid. This is caused by different pH levels. For example, in more acidic urine conditions (more H^+ , lower pH), the H^+ joins organic acids and phosphates ($H_2PO_4^-$), and during more basic urine conditions (less H^+ , higher pH), the H^+ separates from phosphates (HPO_4^{2-}); some H^+ can even be separated from NH_4^+ and HCO_3^- . Electrolytes such as HPO_4^{2-} , PO_4^{3-} , CO_3^{2-} and $C_2O_4^{2-}$ can react with calcium Ca^{2+} to create solid salts crystals known as kidney stones. The charge of each substance is calculated using its scheme of chemical reaction (Table X) in equilibrium with Equation 11, using dissociation constants from Table XI.

5.4.3 Sodium

The sodium (Na^+) concentration is modeled in extracellular space to reach a typical value from 140 to 150 mmol/L. Sodium intake results from diet in the gastrointestinal tract, while its outtake to urine is regulated by the kidneys; outtake by sweating is expressed via the sweat glands (Diagram 21). Other mechanisms that can change sodium mass (often together with changes in fluid volumes) are modeled as dialysis, intravenous drip, transfusion or hemorrhage.

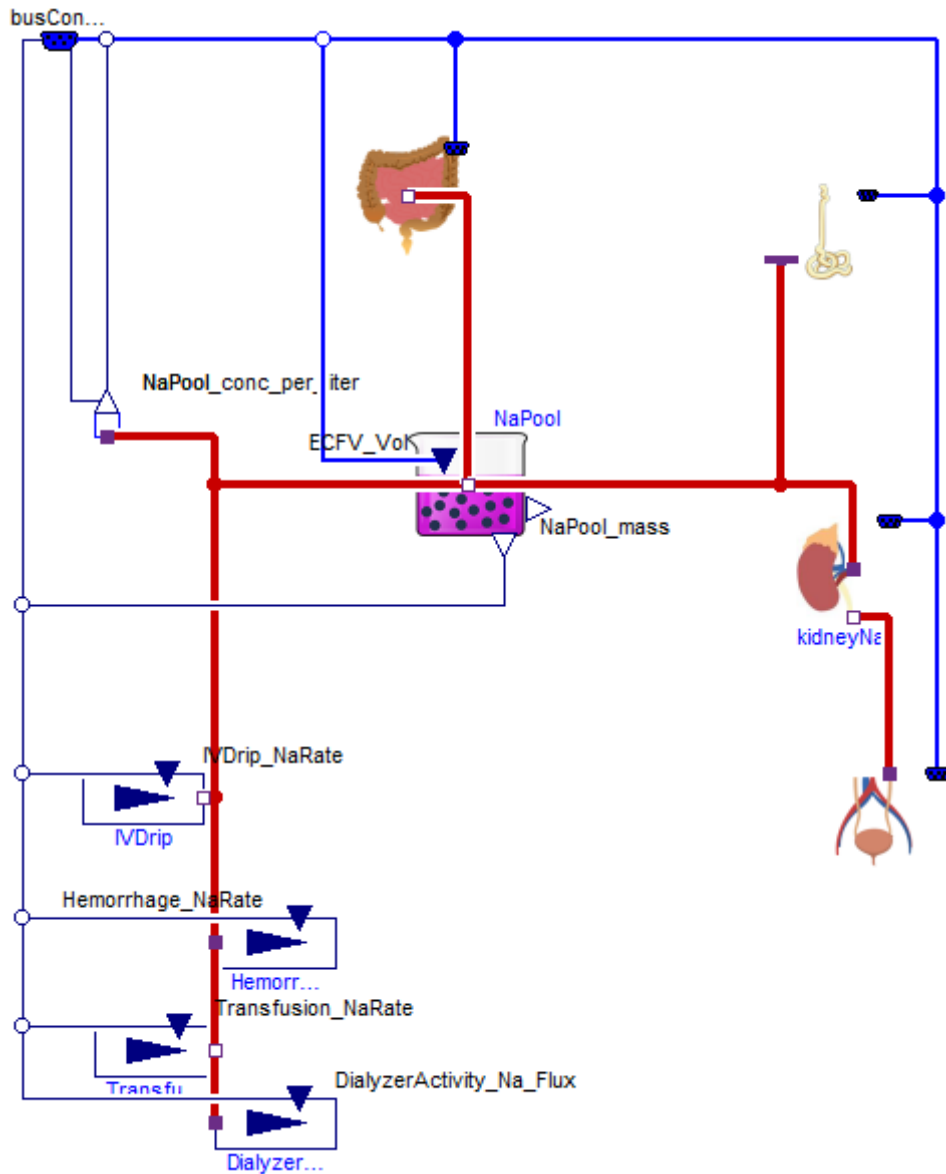


Diagram 21: Sodium in extracellular fluid.

In the kidneys, sodium cations are filtered by the glomerulus into the primary urine of the nephrons. In each part of the nephrons, the sodium is actively reabsorbed into the kidney medulla (Diagram 22). After glomerular filtration, the sodium is reabsorbed in the proximal tubule, the loop of Henle, the distal tubule and finally in the collecting duct. Reabsorption is driven by aldosterone, atrial natriuretic peptides and angiotensin 2. Reabsorbed sodium from collecting duct is accumulated inside the kidney medulla, where it is the secondary determinant of osmolarity, the first being urea. From the kidney medulla, sodium is washed out by vasa recta blood flow, where the equilibrium between tubular reabsorption and vasa recta outflow sets a high intramedullary sodium concentration.

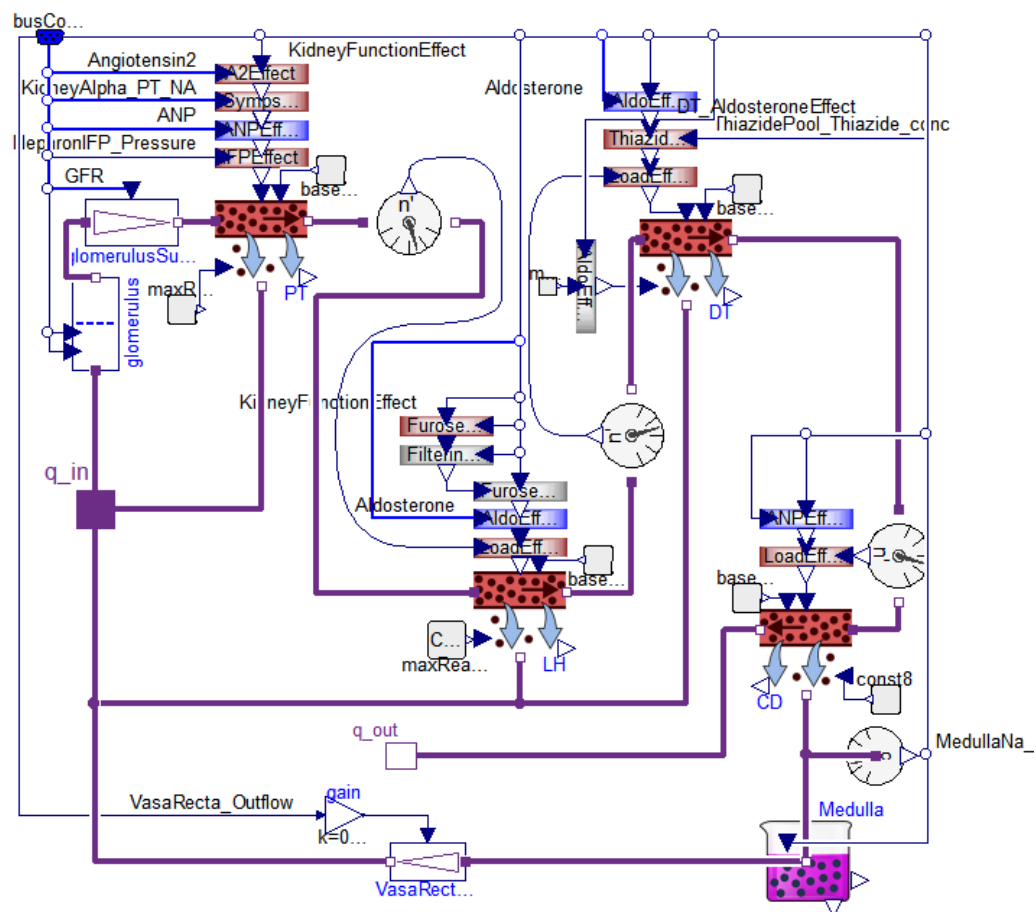
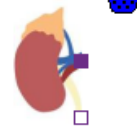


Diagram 22: Kidney excretion of sodium.

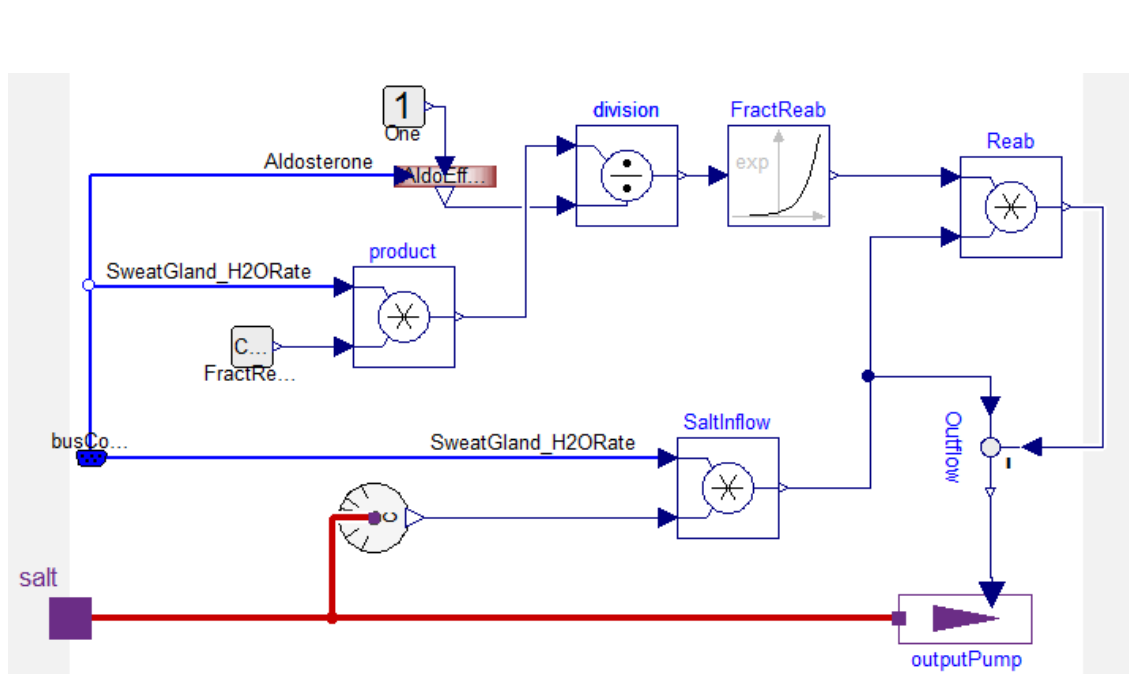


Diagram 23: Sodium excretion by sweat glands.

The backward reabsorption of sodium from excreted sweat is driven by aldosterone. When the amount of excreted water by sweat glands is high, all sodium from sweat is not reabsorbed and it remains as salt on the surface of the skin.

5.4.4 Potassium

The highest concentrations of potassium (K^+) are stored inside cells; therefore, the potassium model must be composed of at least with two compartments – intracellular and extracellular (Diagram 24). Potassium intake results mainly from the gastrointestinal tract while its main outtake occurs through kidney nephrons to urine. Potassium flow through cellular membrane is regulated by Nernst potential, by aldosterone and by glucose intake to the cells. Additionally, kidney excretion and sweating of potassium is affected by a number of channels, the expression of which is affected by aldosterone.

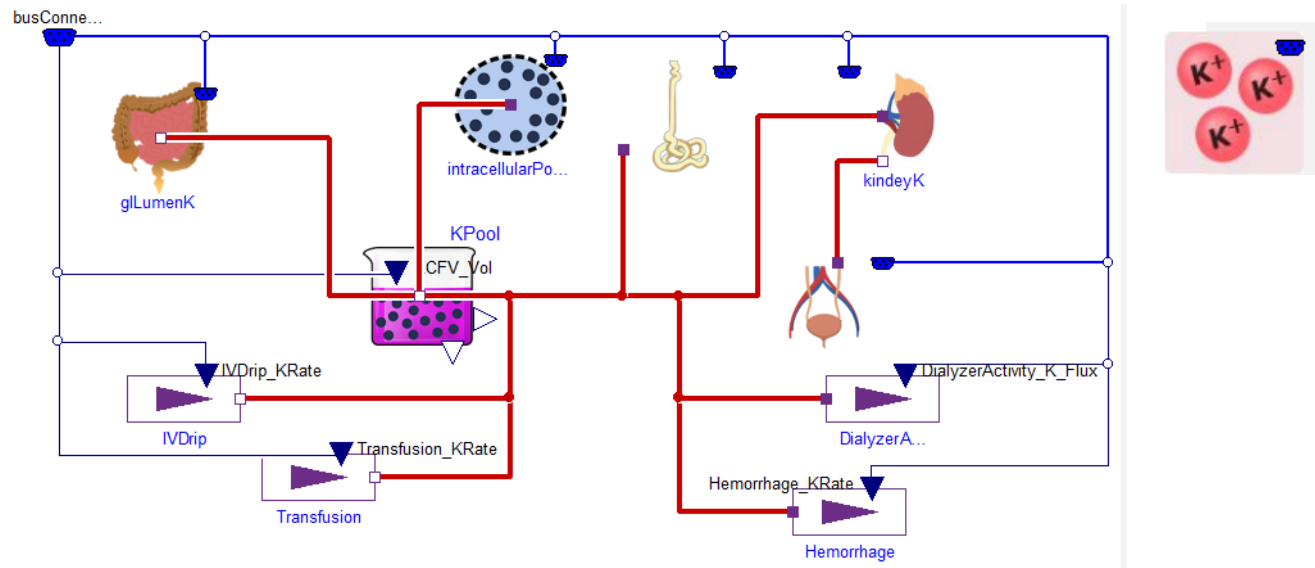


Diagram 24: Potassium in intracellular and extracellular fluids.

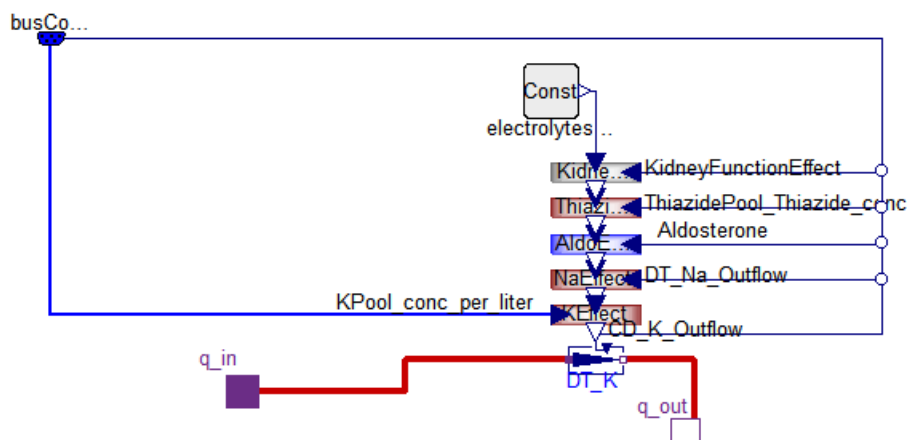


Diagram 25: Kidney potassium excretion.

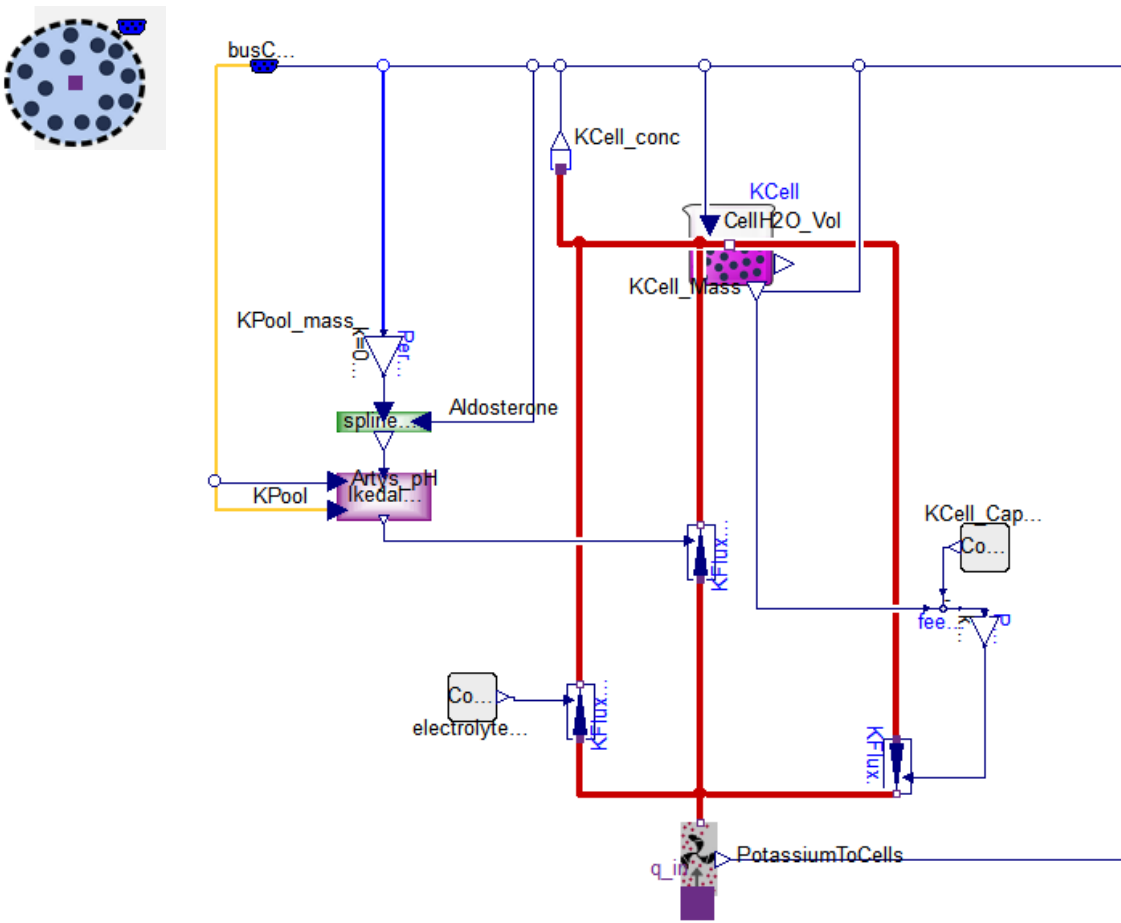


Diagram 26: Cellular membrane potassium transport.

5.4.5 Phosphates and Sulfates

Sulfates (SO_4^{2-}) and phosphates (HPO_4^{2-} , H_2PO_4^-) are accumulated in extracellular fluid. Their intake occurs from diet and unregulated outtake to urine undergoes Donnan's equilibrium at the glomerular membrane (Equation 9).

5.4.6 Comparison with HumMod 1.6

Acid-bases in the Physiomodel is entirely different than in HumMod 1.6. The new calculation uses the original electrolyte models of strong ions. However, the pH is calculated from the electroneutrality equation applied to significantly weak ions such as phosphates, proteins and carbonic acid. The charge of these weak ions is dependent on pH, known as titration curve; thus, the idea is to find the value of a pH that generates sufficient charges for the weak ions at electroneutrality with the rest of solution. The state variables are the total amounts of substances, which in the case of weak ions includes all their protonated and deprotonated forms. For example, inorganic extracellular phosphates refer to H_3PO_4 , H_2PO_4^- , HPO_4^{2-} and PO_4^{3-} forms. The total amount of these inorganic phosphates is independent of pH; however, the total charge of phosphates is pH dependent. The same calculation can also be applied for the total amount of albumin, globulins, hemoglobin or carbon dioxide. For example, if we assume some constant total concentrations of all weak acids in blood plasma, then we can propose a titration curve of the plasma as a function of SID on pH. However, this function is dependent on the type and total concentrations of weak acids; thus, all charged solutes in a solution must be included in the calculation. This renders our acid-base model in the Physiomodel better than the acid-base calculation of HumMod 1.6, because there is no

calculation of weak ion charges, except for bicarbonate. Moreover, the inorganic phosphate is calculated as a strong ion, which does not change form alongside a change of pH.

The same style of acid-base model is also applied to urine in the Physiomodel. The acidity of urine was not calculated in HumMod 1.6; however, all the necessary data for acidity of the primary urine was calculated. In future, this calculation can be used, for example, for the modeling of kidney stones or for establishing more precise functions of membrane channels in nephrons.

During simulation of metabolic acidosis such as ketoacidosis (Mateják, 2013), we found that the original pH regulation was so strong that even apparently non-existing chloride was excreted from the body. This confusing notion leads to negative chloride concentrations. To prevent this confusion, we added the stopper function to the Physiomodel, which stops chloride excretion if the extracellular concentration falls below 50 mmol/L. We do not have the exact data for this pathological function, but the insufficiency of chloride during acidosis is a known phenomenon (Levitin, et al., 1958).

5.5 BLOOD GASES

To support the metabolism of every cell, oxygen (O_2) must be delivered to it and carbon dioxide (CO_2) must be transported out of the body. Both of these blood gases are critical to life. Blood gas transport begins through lung ventilation in order to achieve optimal alveolar partial pressures of carbon dioxide (pCO_2) and oxygen (pO_2). These pressures play a role in gases dissolving in the blood. However, the total amount of transported gases is also dependent on blood flow, the binding properties of hemoglobin, temperature and hydrogen ion activity. The blood is delivered so close to cells by tissue microcirculation that no other active delivery is needed and as a result, only diffusion takes place here.

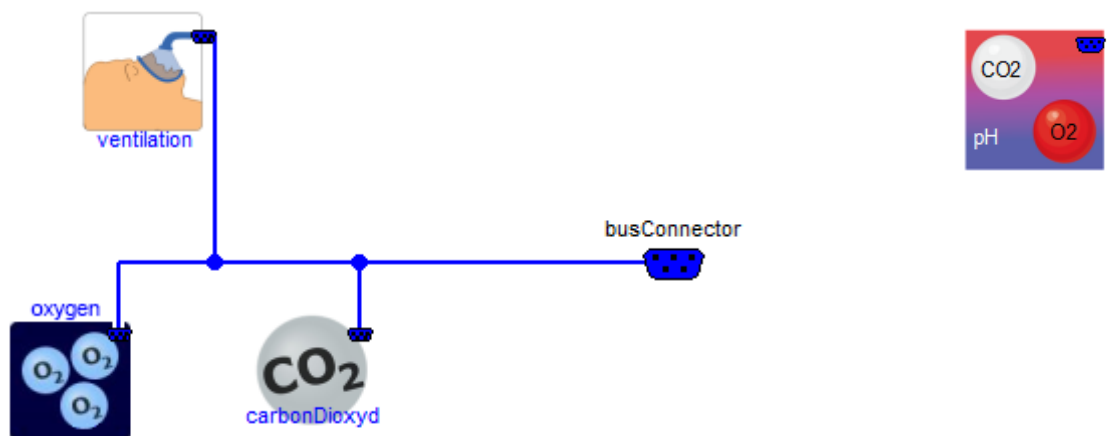


Diagram 27: Gases subsystem.

The submodels of gas transport are: ventilation, where air flow, water vapor dilution, temperatures and pressure effects are calculated; oxygen transport; carbon dioxide transport.

5.5.1 Ventilation

Natural ventilation is mainly driven by neural reflexes, the sensors of which are central chemoreceptors, which answer to changes in intracellular pH; peripheral chemoreceptors located in the arterial sinus and aorta, which detects changes in blood gases; receptors of the skeletal muscle metaboreflex. The entire afferent path of respiratory reflexes is summarized in

the model as one normalized value called TotalDrive; from within this value, the efferent part calculates the respiratory rate and normalized respiratory center's motoric nerve activity.

From the lung properties are calculated current tidal volume (for example, 450 ml at body conditions of a temperature of 37°C and 100% humidity) and current dead space volume (for example, 150ml at body conditions). As the temperature and humidity in lungs differ from the air in the surrounding environment, alveolar ventilation is recalculated to the inspired air conditions in a submodel called alveolarVentilation.

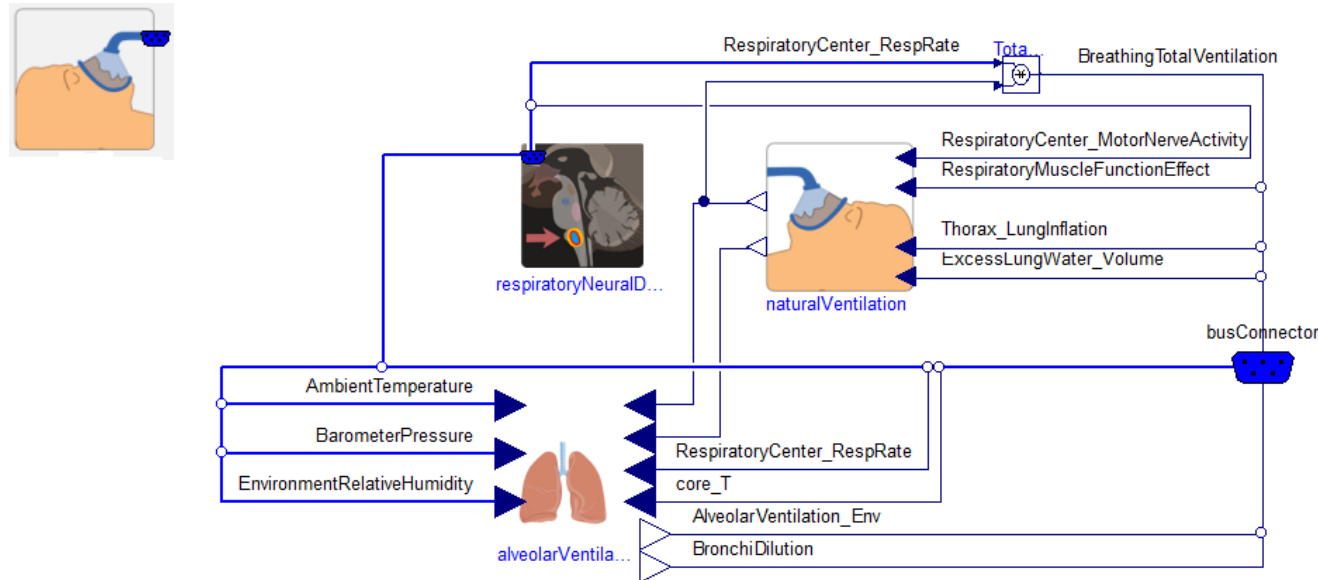


Diagram 28: Regulation of ventilation.

5.5.2 Oxygen

The content of air oxygen in the earth's atmosphere is typically 21%, with atmospheric pressure at 101325 Pa, which yields a partial pressure in air of around 21 kPa. However, the amount of oxygen molecules is still dependent on temperature driven by an ideal gas equation. For example, in 0°C (273.15 K), dry air is a molar concentration of oxygen at 9.2 mmol/l, while in 40°C, dry air oxygen molar concentration is only 8.1 mmol/l at the same oxygen partial pressure of 21 kPa.

In respiratory paths, air is heated to body temperature and diluted by water. The volume of inspired air changes, which is reflected in the variable AlveolarVentilation, recalculated to inspired air conditions. Once the air is transported to the alveolus, an exchange takes place. Oxygen dissolves in blood plasma and red blood cells, where it chemically bounds the hemoglobin molecules. The dissolving of oxygen in water is driven by Henry's law (Equation 13).

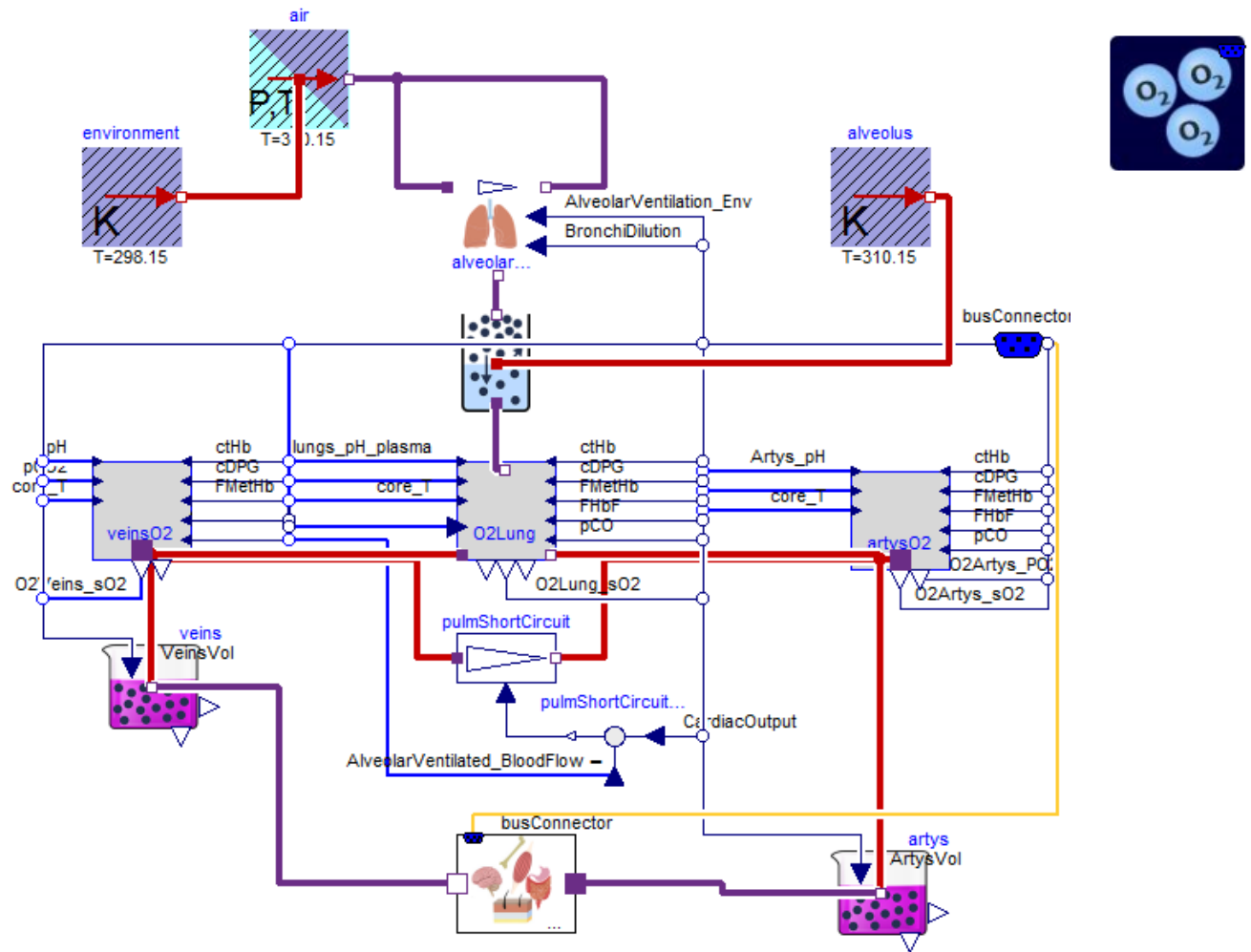


Diagram 29: Oxygen.

5.5.3 Hemoglobin

Hemoglobin allosterically binds oxygen, carbon dioxide and hydrogen ions, creating cross-dependences between concentrations of all three substances in the blood (Mateják, et al., 2015).

The most common hemoglobin in adults is hemoglobin A. As a protein tetramer it is symmetrically composed of four subunits, two alpha and two beta units. In the middle of each subunit is heme with a central iron atom (Fe^{2+}), where the oxygen molecule is bounded. The bounding of oxygen (oxygenation) causes small changes in the shape of heme, which increase the probability of relaxed space conformation for the entire tetramer. Otherwise, tensed conformation is more common for fully deoxygenated tetramers. The binding of CO_2 into a terminal $-\text{NH}_2$ group of each subunit is known as carboxylation and competes with H^+ binding in the same area to form $-\text{NH}_3^+$. These reactions also have different dissociation constants in tensed and in relaxed conformations. In beta-cleft there are more than ten other amino acid side chains that bind H^+ (Bohr's protons) with different dissociation constants in relaxed and tensed states. In normal conditions, the release of two oxygen molecules is connected with the binding of one H^+ and vice versa (Figure 1).

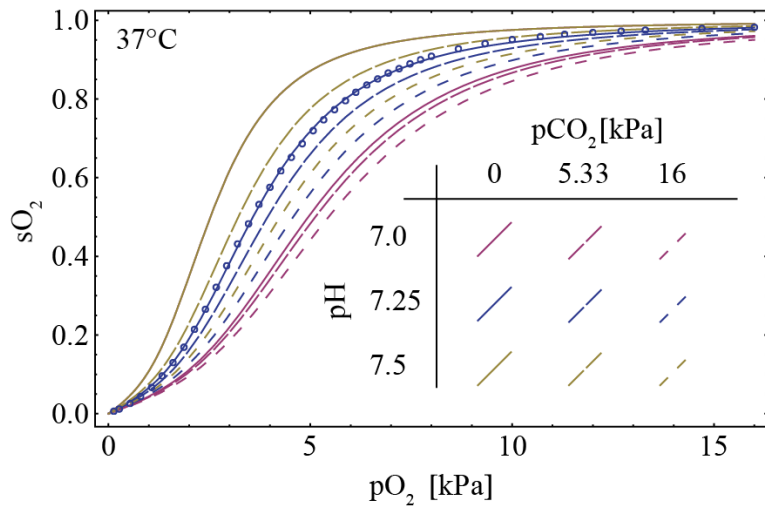


Figure 2, Oxygen dissociation curve described by our model (Mateják, et al., 2015) fitted to data collected by (Severinghaus, 1979).

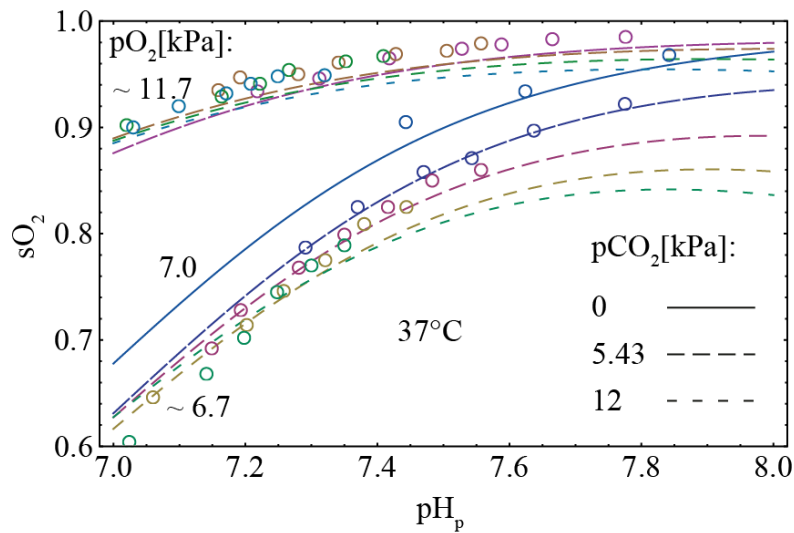


Figure 3, Bohr's effect as oxygen saturation dependence on pH. Lines are our model (Mateják, et al., 2015) and circles are data measured by (Naeraa, et al., 1963).

5.5.4 Carbon dioxide

Most carbon dioxide is transported by blood from tissues to the lungs as bicarbonate (HCO_3^-). Even small amounts are bounded to hemoglobin and form a significant part of transported CO_2 (about 23%), due to its connection with oxygen binding. As noted in a previous section, changes in hemoglobin also change the binding properties of CO_2 .

HCO_3^- is a salt of carbonic acid (H_2CO_3). It significantly affects the acid-base, as mentioned in section 5.4.1. The hydration of free dissolved CO_2 to H_2CO_3 in blood is enzymatically accelerated by carbonic anhydrases inside the erythrocytes, from which the HCO_3^- is transported to plasma in exchange for the chloride ion Cl^- , using Hamburger shift channels to reach Donnan's equilibrium (Equation 9).

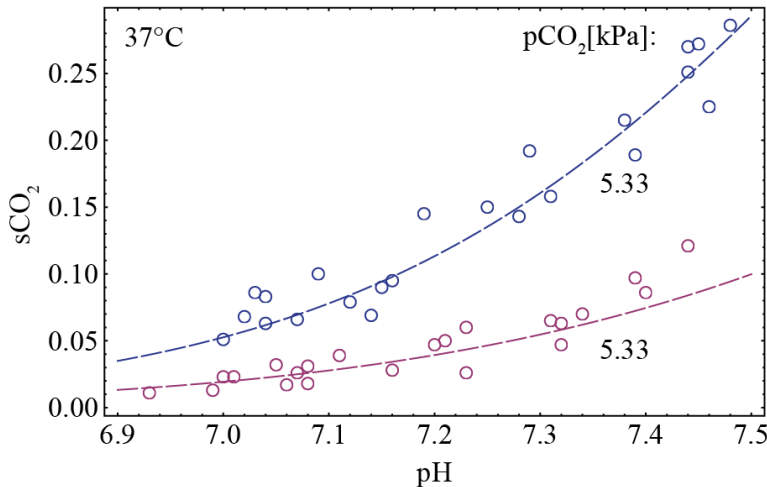


Figure 4, Carbon dioxide deoxyhemoglobin and oxyhemoglobin saturation at different pH. Lines are from our model (Mateják, et al., 2015). Circle are real observations from (Bauer and Schröder, 1972).

5.5.5 Comparison with HumMod 1.6

The primary notion of the blood gas transport subsystem is the same in both models and composed of exchange of oxygen and carbon dioxide within the lungs, systemic arteries, exchange in tissues, and through systemic veins back to the lungs. The difference is in the calculation of the total amount of gases in the blood, from their partial pressure and vice versa. The Physiomodel uses more precise calculations, based on our approach (Mateják, et al., 2015) and approach of Siggaard-Andersen's (Siggaard-Andersen and Siggaard-Andersen, 1990). Our calculation of hemoglobin oxygen saturation is dependent on pH, temperature and carbon dioxide. Additionally, the recalculation between carbon dioxide partial pressure and carbon dioxide content in blood is in the Physiomodel also improved. This divides the total amount of carbon dioxide in blood into free dissolved carbon dioxide in plasma and in erythrocytes, into bicarbonate in plasma, and into bicarbonate and carboxylated hemoglobin amino-terminals in erythrocytes. These calculations are better than the simplified calculations of HumMod 1.6, where the carbon dioxide is calculated only as one bicarbonate concentration for the blood as a whole, independent of hematocrit or oxygen saturation.

5.6 NUTRIENTS AND METABOLISM

Almost all mechanical energy in the human body is taken from food, metabolized into small high energy compounds such as ATP, which is used by muscles, membrane channels and vesicular transports. The body can metabolize three groups of organic compounds: saccharides, proteins and lipids. After eating these, they are absorbed in the form of base nutrients such as glucose, lactate, amino acids, fatty acids, triglycerides and keto acids. The regulation of uptake, usage, storage, release and transformation of these nutrients is managed primarily by hormones such as leptin, insulin, glucagon and thyroxine.

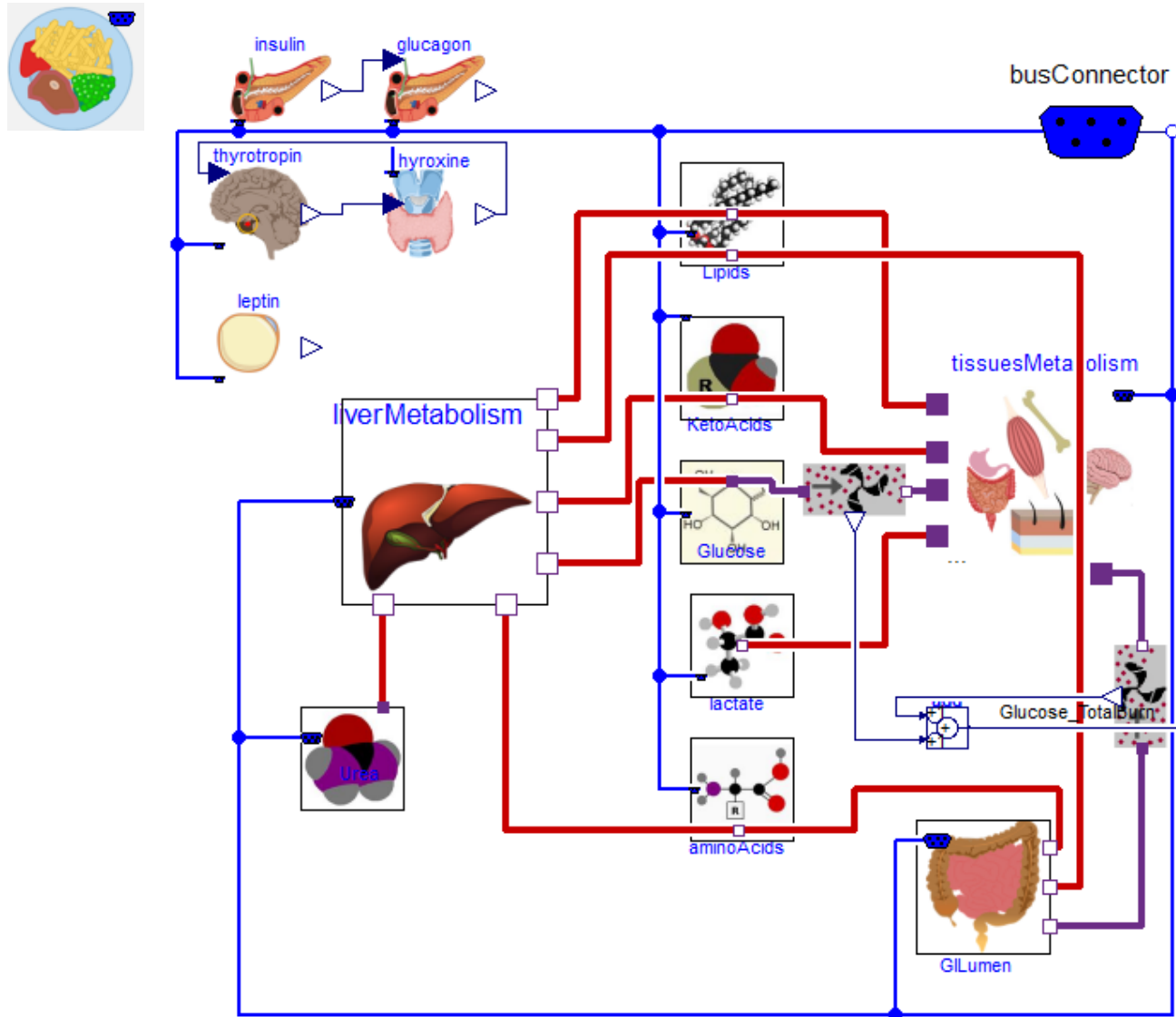


Diagram 30: Nutrients and metabolism subsystems.

5.6.1 Cellular metabolism

Base nutrients can be changed in cellular cytosol by glycolysis or lipolysis into acetyl coenzyme A, which is used directly by the mitochondrial citric acid cycle to produce high energy electrons (bound to NADH or FADH), which helps to move the hydronium ions (H_3O^+ noted as H^+) into the mitochondrial intermembrane space. Finally, to equilibrate electrochemical potentials, the hydronium ions have to go back to the mitochondrial matrix through the ATP synthase. The new synthetized ATP is exchanged for ADP and one phosphate across mitochondrial membranes using the electroneutral symporter mechanism.

The ratio between using the base nutrients can differ according to the type of cell (Randle, 1986). For example, the heart muscle prefers lactate more than other organs, while neural tissue metabolizes glucose and keto-acids and does not use any fatty acids or triglycerides (Owen, et al., 1967). Amino acids can be metabolized only by the liver or in kidney tubules (Hannaford, et al., 1982), because only there can the toxic ammonia (NH_4^+) be eliminated.

5.6.2 Liver metabolism

To support good function of all cells, it is necessary to have balanced extracellular concentrations of the base nutrients, even if food is monotone and does not explicitly contain

all types of these nutrients in sufficient ratios. The transforming processes from one base nutrient to another takes place in the liver and is known as gluconeogenesis (Wahren and Ekberg, 2007), ketogenesis (McGarry and Foster, 1976) and lipogenesis (Kotani, et al., 2004). Gluconeogenesis creates new glucose from amino acids, ketogenesis creates keto-acids from lipids and lipogenesis can create triglycerides from glucose or amino acids.

The base nutrients can also be stored as lipids in adipose tissue or as glycogen in the liver or in muscles. Stored lipids are long-time reservoirs of energy in contrast with glucose, which is stored as glycogen and which can be used much faster (Chiasson, et al., 1976). The process of storing glucose in glycogen granules is known as glycogenesis and the reversal process – releasing glucose from glycogen – is known as glycogenolysis (Diagram 31).

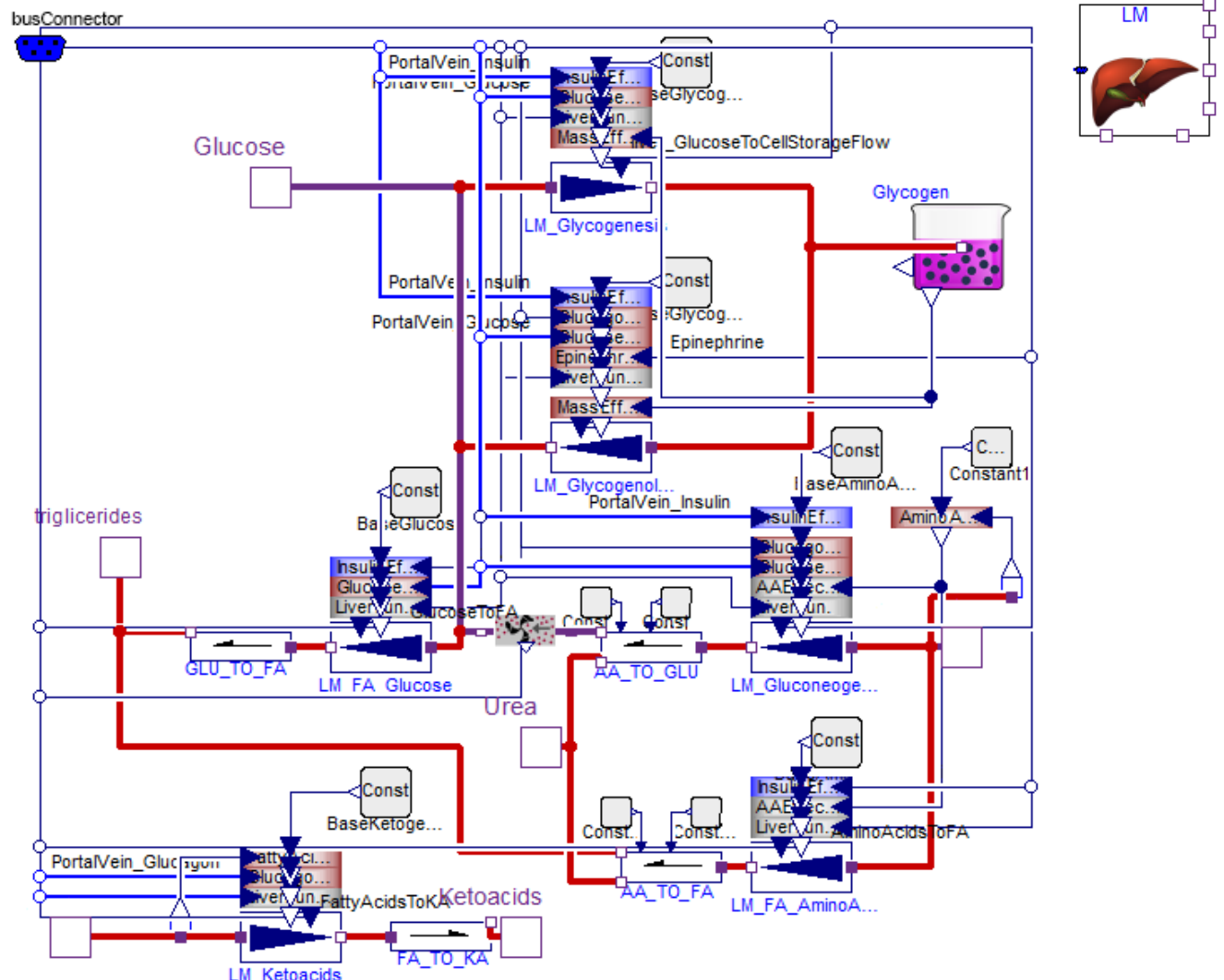


Diagram 31: Liver transformations of base nutrients.

5.6.3 Lipids

Lipids are transported from the gastrointestinal tract by lymph to blood plasma using chylomicrons. Chylomicrons contain primarily triglycerides, which are hydrolyzed into fatty acids. These fatty acids can be stored in lipid deposits or used for the metabolic purposes of cells.

In the capillary walls of adipose tissue or muscles, the enzyme lipoprotein lipase is expressed, which transform the triglycerides of chylomicrons into fatty acids and glycerol. These fatty acids can very easily cross the cellular membrane and be stored in adipose tissue or used as metabolism fuel in the form of energy. Only a small amount of free fatty acids is transported by the cardiovascular system and is typically connected to albumin. However, their turnover is extremely fast: every two-to-three minutes, half of these free fatty acids is used as energy by the metabolism and replaced by new fatty acids from lipid deposits (Frayn, 2002).

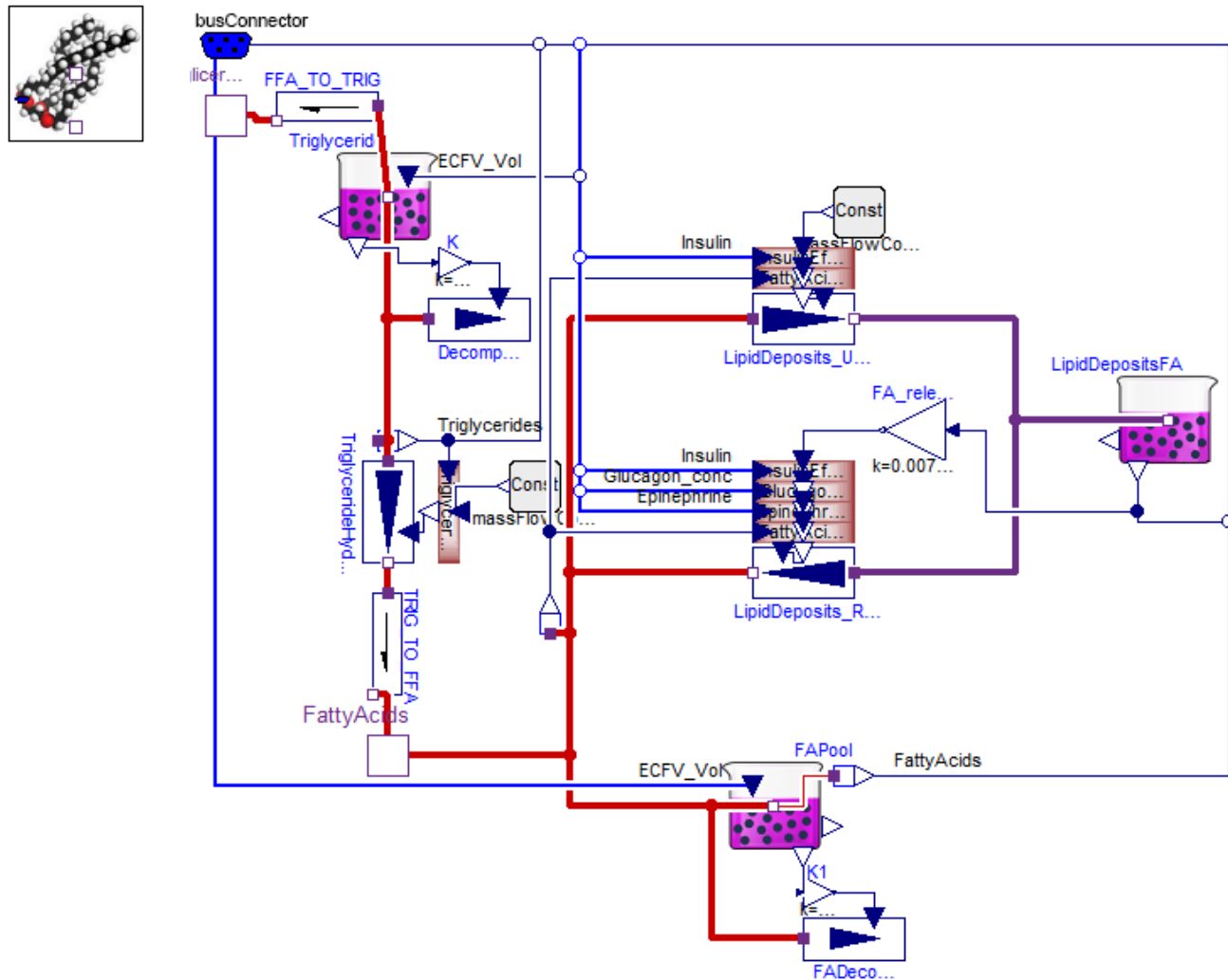


Diagram 32: Transformation between triglycerides, free fatty acids and lipid deposits.

5.6.4 Proteins, amino-acids and urea

Almost all proteins from diet are absorbed as amino-acids. There are only 20 types of amino acids and 10 of these are essential. The essential amino acids cannot be synthetized inside the human body and must therefore be ingested as part of food. The primary role of amino acids is to build new proteins; however, they can also be used as fuel for the metabolism. The degradation of amino acids (deamination) takes place almost entirely in liver hepatocytes, because only there can the toxic byproduct NH_4^+ be transformed into urea. The other area for deamination is in the kidney nephron tubular cells, from which NH_4^+ is excreted directly to urine in the form of an extremely efficient mechanism of H^+ excretion; this is done without decreasing urine pH. The deamination of amino acids in the liver will prepare new glucose or triglycerides as a source of energy for other cells. The new synthetized urea diffuses

into the blood and takes on a primary role in high kidney medulla osmolarity, which is necessary for water balance (Sands, 1999).

5.6.5 Keto acids

Keto-acids are not the primary fuel for the body's metabolism, but in some critical situations they can temporarily act as a substitute for missing primary nutrients, especially for neural tissue. During ketoacidosis, there are elevated levels of acetyl acetate and beta-hydroxybutyrate in the body. Keto acid are synthetized in the liver from acetyl coenzyme A, which is created mainly from free fatty acids, acetic acid or ethanol (McGarry and Foster, 1976). They can be metabolized in various tissues, but the speed of their degradation is limited to the speed of the mitochondrial metabolism. Thus, if their production is higher than these limits, they can cause metabolic acidosis accompanied by their elevated renal excretion (Angielski and Lukowicz, 1978; Mateják, 2013).

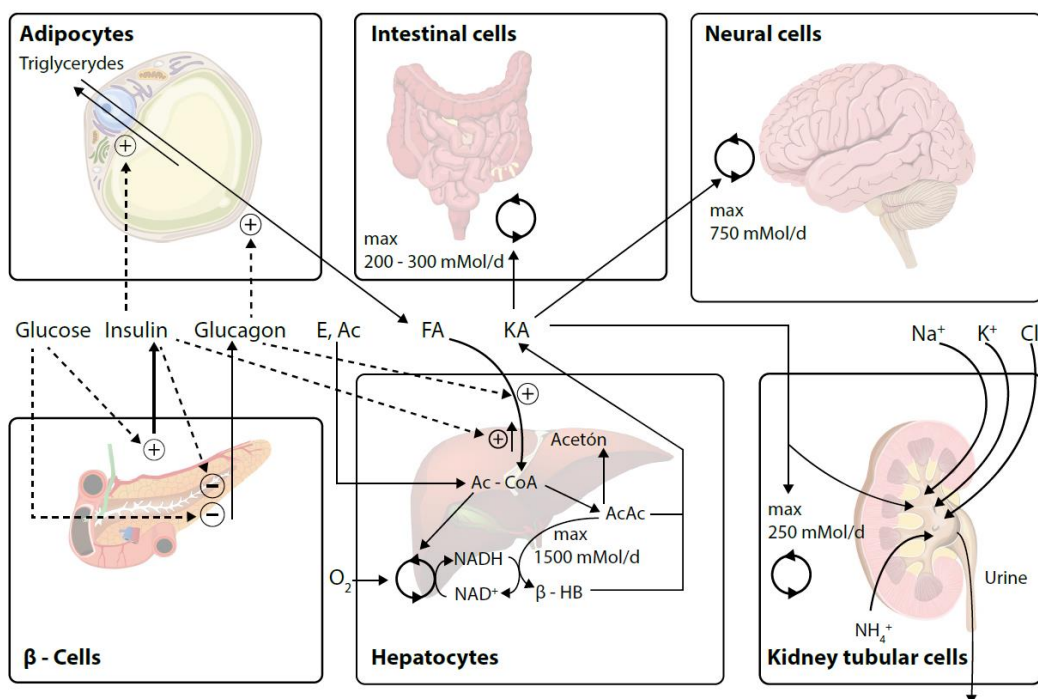


Figure 5: Keto-acids.

5.6.6 Comparison with HumMod 1.6

The nutrient metabolism in the Physiomodel has only small differences to the HumMod 1.6 such as in the case of correcting units, stabilizing the shape of approximated curves and the setting of an optimal diet for long simulations.

For example, the physical unit of glucose consumed during anaerobic metabolism by tissue is in HumMod 1.6 expressed in mg/min and this value is assigned by mistake as a variable given in cal/min. In Modelica, a user is not allowed to connect incompatible physical quantities or physical units without converting them first. Thus, this type of error should automatically be prevented in the Physiomodel, because glucose is in this instance always represented by 'amount of substance' and 'molar flows' as physical quantities using 'moles' and 'moles per second' as SI-units. These units are used in each instance of the Physiomodel – in chemical reactions, in glucose transports and in glucose storage.

Some approximations of effects use the cubic interpolation splines to express empirical dependences. Using these splines is easy: the user sets only a small number of points on the x-y graph between the dependent variables. For example, for the definition of the linear line, setting one point is enough; for more nonlinear functions, two or three points are typically used. These points contain the value of the x-axis, the value of the y-axis and the value of the slope. The slope poses the biggest problem, because it determines the shape of the function between two points. If the slope is too sharp, a small fluctuation can occur. This means that the shape of the function can leave the interval defined by the y-coordinates of the points. In this situation, the function loses its invertibility and can be inconsistent for some types of nonlinear solvers such as “Newton solver”. Therefore, if it is not necessary, it is better to avoid this fluctuation by correcting the nearest slope to a better comfort value or by adding more definition points. In HumMod 1.6, these fluctuations can be observed, for example, in the mass effect of the glycogen to glycogenesis process in the liver, or in the effect of the glucagon to ketogenesis process in the liver. These situations are solved in the Physiomodel by rotating the slope of the middle point to a slightly more horizontal direction.

For the Physiomodel, the optimal diet for the default setting (for a 75kg male with a metabolic rate of 2500kcal/day) was prepared. A diet of 2000kcal of carbohydrates, 300kcal of proteins and 200kcal of fats per day was selected. In a long-term simulation including this diet, adipose tissue stabilized at 3.6 kg as 5% of body mass – typical for a healthy state.

5.7 THERMOREGULATION

5.7.1 Heat

The human body works best at a core temperature of around 37°C. All chemical processes are dependent on temperature (Equation 6). If the temperature rises, protein structures become unstable. Even, actually the gene expression of at least 394 genes are upregulated or downregulated after 20 minutes' exposure to 43°C, as examined by Sonna et al. (Sonja, et al., 2002). At higher temperatures, heat-shocked proteins are expressed, while at lower temperatures more cold-shocked proteins are expressed (Katschinski, 2004). Both of these instances can change cellular processes, help with protein refolding and if the situation becomes worse, cellular apoptosis can also occur. Additionally, cellular membrane processes are affected. Therefore, the regulation of body temperature is extremely important. The primary mechanism for regulating body temperature is the regulation of blood flow in the skin (Hardy and Soderstrom, 1938; Hsieh, et al., 1965; Kamon and Belding, 1968), as well as the amount of clothes worn. There is also long-term (in terms of months) regulation of heat by thyroid hormones (Osiba, 1957), which increases or decreases the speed of the basal metabolism as the source of heat in each cell. Short-term heat production is typically based on the working of muscles (Saltin and Hermansen, 1966) or by shivering (Florez-Duquet and McDonald, 1998). The efficiency of skeletal muscle is about 30%; thus, a significant part of consumed energy is released as heat during motion. It is assumed that for the heat transfer of any microcirculation, the temperature of outgoing blood is the same as the temperature of tissue (Equation 24) and as such, blood flow will directly determine the amount of transferred heat between the body core and body tissue. Typically, heat is conducted from a warmer to a colder area, but heat can be also transferred by chemical processes as evaporation against the temperature gradient.

5.7.2 Evaporation

Significant loss of heat is connected with the evaporation of water (Equation 23) in upper respiratory pathways during air inspiration (Brennan, et al., 1957). Cold dry air from the

environment is here heated to body temperature and fully saturated with water. Water is also evaporated directly from the surface of the skin. In contrast with water loss by respiration, the function of sweat glands can be regulated (Dodd and Zotterman, 1952; HENSEL, 1953; Piwonka and Robinson, 1967; Sato, 1977; Wyndham, et al., 1966). The regulation of sweating sets the amount of water excreted by the skin. During higher physical activity, this evaporated water bounds heat as enthalpy of vaporization, which is more effective in dry, warm and windy environments. However, it works even if the environmental temperature is higher than the body temperature. Therefore, there must be adequate water intake to prevent dehydration.

5.7.3 Hemoglobin heat transport

The dependence of oxygen dissociation on temperature as presented in Figure 6 is described by first principles of elementary chemical reactions of the hemoglobin equilibrium model (Mateják, et al., 2015). This means that the elementary reaction enthalpies was identified to fit the shift of dissociation constants described as base principle of chemical reaction equilibrium (Equation 12). The reaction rate of reactions during hemoglobin oxygenation directly provide the heat consumed by reactions as the enthalpy change of the system. The hemoglobin transfer about 4-7% of produced heat from aerobic-metabolically active tissue to lungs thanks to these relations (Adair, et al., 1929; Mateják, et al., 2015; Weber and Campbell, 2011; Weber, et al., 2014).

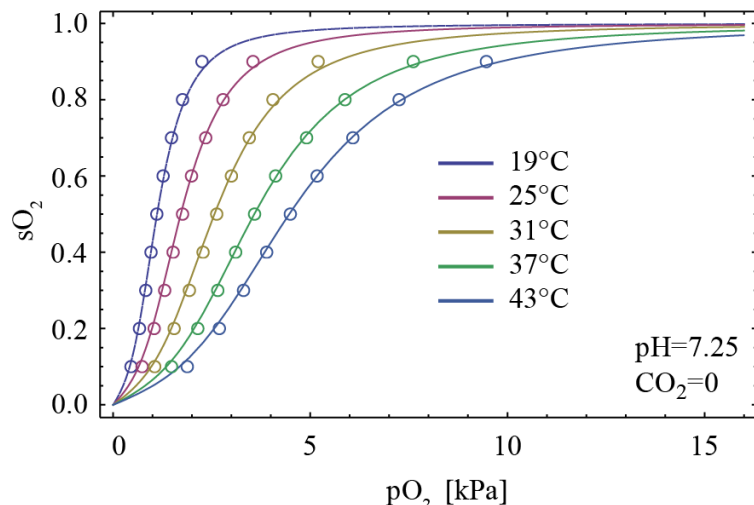


Figure 6, Temperature dependence of oxygen dissociation curve described by our model (Mateják, et al., 2015) compared with observation by (Reeves, 1980; Weber, et al., 2014).

5.7.4 Comparison with HumMod 1.6

Thermoregulation add the heat transport with hemoglobin and change one small difference, that is, in the fatigue of sweat glands. The use of fuel in sweat glands is in the Physiomodel dependent on the current rate of sweating water, not on the constant default base value of this rate, as in HumMod 1.6.

5.8 NEURAL REGULATIONS

The integrative model of human physiology also contains the primary neural regulations, because the autonomic nerves directly drive base processes such as the vasoconstriction of blood vessels, heart rate, heart contractility (SUGA, et al., 1976), kidney functions, secretion of hormones, respiration, sweating, etc. The inputs to the autonomic neural reflexes are from

specialized cells, which measure the current state of the system: baroreceptors (carotid sinus, aorta, heart atria), osmoreceptors (hypothalamus), chemoreceptors (carotid sinus, aorta, medulla oblongata) and thermoreceptors (skin). In these cells, the neural impulses starts. There are two autonomic pathways: sympathetic and parasympathetic. When a signal reaches the end of the last neuron in a pathway, noradrenaline is typically released for sympathetic stimulation and acetylcholine is typically released for parasympathetic stimulation. The synapse receptors of the effector cells are typically muscarinic in the parasympathetic pathways and adrenergic in the sympathetic pathways. There are two groups of adrenergic receptors: alpha and beta receptors. Both adrenergic receptor groups react on epinephrine and on norepinephrine. As a result, the model for the alpha/beta receptors may be dependent on sympathetic stimuli, together with the extracellular concentration of these catecholamines and other agonists (e.g., desglymidodrine) or antagonists (alpha/beta-blockers). The model of alpha receptors can be used in many instances such as for the model of microcirculation, which is used for many tissues with different parametrical settings.

Autonomic regulations simply correct the functions of cells, tissues and organs. In many cases, they are not necessary for life. They can even be removed through surgery (vagotomy, endoscopic thoracic sympathectomy). However, quality of life rapidly decreases, because the loss of regulation decreases the limits to where the body can function properly. For example, the loss of regulation of heart rate is critical in instances of increased physical activity, when higher cardiac output is needed to support oxygen transport to muscles. Without external innervation, the heart still beats using autonomic oscillations of sinoatrial node cells (Bootsma, et al., 1994; Warner and Cox, 1962), but without receiving useful information (Xenopoulos and Applegate, 1994) about muscle metabolism, current blood status and about blood pressure (Ferguson, et al., 1985; Takeshita, et al., 1979).

Neural pathway	Receptors	Effectors
Baroreflex	carotid sinus artery and atrial baroreceptors	heart, vasoconstriction/vasodilation
Metaboreflex	skeletal muscle chemoreceptors	heart, vasoconstriction/vasodilation
Thermoregulation	skin thermoreceptors, core thermoreceptors	vasoconstriction/vasodilation of skin vessels, sweating
Respiration reflexes	central chemoreceptors, peripheral chemoreceptors, skeletal muscle pH	respiration rate, tidal volume
Renal reflexes	atrial low pressure receptors	proximal tubule sodium reabsorption

5.8.1 Comparison with HumMod 1.6

In the Physiometer, the reaction of central chemoreceptors is shifted to new and more precise values of their intracellular pH=7.08 (Kintner, et al., 2000) as a result of detailed tissues and respiratory quotients, based on the metabolic consumption of base nutrients. The details of this shift is described in section 6.1.

6 DISCUSSION

6.1 SELECTION OF FIRST PRINCIPLES

The main problem with the most implementations of the physiological models is that calculations are causal and redundant. Almost all physical and chemical laws as equations are repeated as many times as it occurs within the human body. Modelica provides the opportunity to define one law only in one place and to use it simply by referencing this place (Fritzson and Engelson, 1998; Tummescheit, 2002). It does not matter which variable is used as an output from the equation, because Modelica tools make automatically algebraic manipulation during compilation time (Mattson, et al., 1997; Mattsson, et al., 1998).

For example, consider that only one component defines each chemical reaction. Improving this component will improve all chemical reactions in the model. My first implementation of a chemical reaction had two main parameters: dissociation constant and reaction forward rate. At equilibrium, all is calculated only from the dissociation constant. The next investigation of chemical bases told us that dissociation constant is not really a constant, but dependent on temperature; thus, the Van't Hoff's law was added to this component with a default setting at zero reaction enthalpy. In other words, if reaction enthalpy as a parameter is not set by the user, it will have the same behavior as before. However, it also offers the possibility of defining non-zero enthalpy for reactions with equilibrium dependent on temperature. The investigation of the meaning of reaction enthalpy also gave rise to another idea: to calculate the flow of heat energy from/to a reaction and using the conditional thermal heat port, this allowed the chemical reaction to be a multidomain (chemical and thermal) component. Thus, as in the chemical theory, positive reaction enthalpy means the endothermic reaction and the negative value of reaction enthalpy implies the exothermic reaction. Moreover, because the heat port was hidden by default, all instances of chemical reactions in the model remained the same, with the same settings and connections as before these thermal extensions.

The next approach in the field of physical chemistry (Mortimer, 2008) showed us that we can also calculate the dissociation coefficient at a defined temperature from the thermodynamic properties of substrates and products of the reaction. The idea was to simplify the use of chemical reaction components. The user simply selects the type of substrates and products and the dissociation coefficient is automatically calculated. This approach uses a database of chemical substances alongside their free enthalpies of formation (Δ_fH) and free Gibbs energy of formation (Δ_fG). The enthalpy of the reaction is the sum of formation enthalpies of products minus the sum of formation enthalpies of substrates (Hess's law). Having Gibbs energies of all products and all substrates, the Gibbs energy of the reaction (Δ_rG) is also the result of Hess's law (Equation 11), while the dissociation coefficient (K) of the reaction at temperature T is defined from the Gibbs energy of the reaction as in Equation 34 (Mortimer, 2008), where R is the gas constant.

$$\Delta_rG = -R \cdot T \cdot \ln(K)$$

Equation 34:
Gibbs free
energy of the
reaction.

Chemical processes in the body occur in the water solution of electrolytes. The adaptation to water conditions can be done using activity coefficients. Water surrounds the charged particles and creates solvation shells, which decrease the activity of the substance. This behavior is driven by the Poisson-Boltzmann model, which can be simplified using the Debye-Hückel theory (Debye and Huckel, 1923). The creation of metabolic pathways should be simple, i.e.,

by connecting substances with the implementation of chemical reactions. The user selects the names of substances instead of odd values of dissociation coefficients for each reaction. If these reactions are all in equilibrium, it is not even necessary to apply the value of kinetic rate coefficients in order to start the simulation.

This type of improvement also guarantees the more sophisticated rule of chemical systems called the “Principle of Detailed Balance” (Shiryaeva, 2010). This principle states that in a closed equilibrated chemical system, equilibrium is reached at each chemical reaction. As a result of this law, the product of dissociation constants in chemical circles is equal to 1. Therefore, if the user defines the chemical system as chemical reactions in a circle and wishes to set all dissociation constants as parameters, he must always think about the dependences between them. However, the new proposal based on Gibbs energies does not allow for breaking this fundamental rule of chemical systems. For example, having a closed system with the following chemical reaction: $A_1 \rightleftharpoons A_2$, $A_2 \rightleftharpoons A_3$ and $A_3 \rightleftharpoons A_1$ after an extended time, when the concentrations of A_1 , A_2 and A_3 are constant. The $K_{12} = A_2/A_1$, $K_{23} = A_2/A_3$ and $K_{31} = A_3/A_1$ are dissociation constants of the reactions at temperature T. If the user wants to set the dissociation constants, the following requirements must be verified by the user: $K_{123} = K_{12} * K_{23} * K_{31} = 1$. However, if the system is calculated from Gibbs energies of formation of each substance $\Delta_f G_1$, $\Delta_f G_2$ and $\Delta_f G_3$, then this relation will be automatically fulfilled as relation $0 = (\Delta_f G_2 - \Delta_f G_1) + (\Delta_f G_3 - \Delta_f G_2) + (\Delta_f G_1 - \Delta_f G_3) = \Delta_r G_{12} + \Delta_r G_{23} + \Delta_r G_{31} = \Delta_r G_{123}$, because $\Delta_r G = 0$ if and only if $K = 1$ as in Equation 34.

6.2 DEVELOPMENT OF INTEGRATIVE PHYSIOLOGICAL THEORIES

After we implemented the HumMod model in Modelica, we realized that improving the model is possible without impacting work conducted previously. Comparing the resulting model with the original one, alongside the correct consultation of measured data yielded better equations and a more stable model in each improving step.

For example, in the original model the production of carbon dioxide is calculated in all tissues using the same global respiration quotient (RQ). The flow of produced carbon dioxide was proportional to the flow of consumed oxygen and was independent according to the types of tissues. The right flow of consumed oxygen with the right type and amount of consumed metabolites had already been calculated. Furthermore, because we knew the respiration quotient for each of these metabolites, we improved the amount of produced carbon dioxide per tissue. As a result, there was higher production of CO_2 in neural tissues, because neurons cannot metabolize fats ($RQ=0.7$) and their primary source of energy is glucose ($RQ=1$). Comparing the results of the simulation before and after this modification, it was observed that the patient began to hyperventilate. After a short investigation, it was found that this hyperventilation was caused by the neural regulation of respiration. Observing this was quite easy, because the total effect of neural respiratory regulation (TotalDrive) in a normal situation should have the value one as each normalized multiplicative effect. Looking at appropriate diagram, the connected systems from which the TotalDrive is calculated can be seen. After examination of these few systems, it became clear that the TotalDrive goes from central chemoreceptors, which fire the impulses in answer to the intracellular pH of these neural cells in the brain. Logically, there is a shift in the intracellular pH of neurons (pH_{in}), caused by the higher production of CO_2 . It must be established whether the new value of the calculated pH_{in} reflects the reality of the situation any better. The measured value of pH_{in} in physiological papers were found to be closer to our new value (Kintner, et al., 2000), which was automatically calculated from the model acid-base equations of each intracellular environment. As a result, it was necessary to shift the interpolation curve, which was estimated to lower

values of pH_{in} . These effects of central chemoreceptors had to be shifted to have normal value at a normal pH_{in} . After this correction, the model had the same or better neural respiratory regulations and the same or a better normal state of other variables, and with more precise local status of tissues and blood. These results indicated that all changed values had to be consulted and compared with other research, as the pH_{in} had been in our case.

The other example of physiological expandability concerns the addition of the new acid-base module. At first we tried to calculate the blood acidity from the base excess of oxygenated blood (BE_{ox}) using the empirical Van Slyke equation, as Siggaard Andersen did with $cTH=BE_{ox}$ (Siggaard-Andersen, 2005). Because the BE_{ox} was not calculated in the original model, it had to somehow be defined. The first idea was to create the state variable. Some sources for acids or bases (mainly from the metabolism) and some losses of acids and bases (mainly through the kidneys) were found. The change in bases was the same as the change of BE_{ox} ; the change of acids inferred the negative change of BE_{ox} . However, this implementation failed after a few hours of simulation time. After a short examination of the simulation results, the lost electroneutrality of blood plasma was observed. The model had already integrated all main electrolytes and all main acid-base buffers; as such, it was possible each time to calculate strong ion differences (SID) or the charge on acid-base buffers at the calculated pH. As a result of electroneutrality, the sum of all these charges must be zero, which was not the case. A first generator of these problems was assumed to be the changes in BE_{ox} ; had there been more properly connected flows of electrolytes and flows of all organic acids alongside the changes in BE_{ox} , the stability of the model would have increased from hours to days or even months of simulation time. However, it failed because of electroneutrality. This gave rise to a new idea: if the model includes all electrolytes and acid-base buffers as state variables, then the BE_{ox} is not a state variable and it can be directly calculated from the equation of electroneutrality, as is described in section 5.4.1. After improving BE_{ox} , the model became stable for more than a year of simulation time. As a result of this added equation, it never again lost electroneutrality.

6.3 SENSITIVITY ANALYSIS AND IDENTIFICATION

This work does not describe how to fit or estimate large numbers of parameters in the presented model. However, the references to appropriate scientific papers are the inseparable part of the model. Some parameters are patient-specific, such as weight and body volume, organs and tissues. However, most parameters are properties of chemical substances, membranes, tissues and organs, which are typically not patient-specific and are invariant in terms of other variables or parameters. On the other hand, there are also interpolation curves, which simplify empirical observations such as hormone effects and neural reflexes. In follow-up model developments, these interpolations should be more complexly modeled using both the physical and chemical bases of processes. For example, shifting of the interpolation curve of hemoglobin saturation with oxygen, as implemented in HumMod 1.6, does not allow for examining this process together with the binding of Bohr's protons, or with the binding of carbon dioxide, as in our model. It also does not show the transfer of heat using these chemical processes.

The new approach of integrative physiology for working with complex models indicates that these large models can even be used for describing *in vivo* experiments in cases where all elementary processes are included in the model. After a reproducible experiment has been designed and set into the model, a sensitivity analysis can be conducted (Moss et al., 2012; Pruett et al., 2013). This is an automatic tool for finding parameters correlated with the experiment. Typically, the experiment can only identify a small set from a vast amount of parameters. Having a sufficient set of observed data, the identification of the values of these selected parameters can provide sufficient results for conducting simulations. For example, the

complex models of the University of Mississippi Medical Centre was used for the simulation of exercise experiments (Carter et al., 2009; Hodnett et al., 2009), for the simulation of carotid baroreflex receptors' stimulation (Lohmeier and Iliescu, 2011), as well as for simulating hemorrhaging (Zhang et al., 2015).

6.4 VERIFICATION

The goal of this integrative approach is to integrate already validated physical processes. The advantage of implementation using hierarchical graphical diagrams is that the verification is based on observation of visual connections in the diagram. However, the details and appropriate setting must have the correct reference to original article as inseparable part of the implementation. The observed parameters from articles must be used in the form of selected first principles. Usually, some recalculation is needed; however, in almost all mentioned cases, a conversion to the parameters of selected first principles existed; for example, the need for recalculating the dissociation coefficient to Gibbs energies using **Equation 12**.

The compact implementation of first principles as Modelica libraries can be applied in many ways that have also been designed for verification purposes. The expected values are compared with the results of small separable experiments and these models are shown to the user as examples for using of the library. The advantage of having one physical law in one component is that implementation mistakes can be detected almost immediately, because the component is used in many examples and many instances within a large and complex model. For example, the mistake in our ElasticVessel compartment (**Equation 27**) was detected one day after submitting source code of the model to the shared repository. This error was discovered in Sweden, because there was automatically received our last version of the Physiolibrary for testing the OpenModelica environment (Fritzson et al., 2006). Using distributed revision control system [GitHub](#) (Dabbish, et al., 2012), anybody can join the development process and report a mistake or error in our development.

Connecting the first principles of integrative physiology together must also achieve the exact rules associated with the physical principles. The verification of these connections is done in the level of Modelica language where the smart support of the definitions of physical quantities and physical units can generate a warning or error to the user if connections are not driven by these rules. However, achieving these implementation rules does not mean that the newly implemented theory will be valid. The validation of the simulation results of integrated first principles must be conducted via experimental observation of the physiological system. Many integrative theories have already been conducted and published using this approach; each *in vivo* experiment must take into account all the processes involved.

The overlap of these integrated theories can be so strong that in general, no more relations are needed and a new theory can be deduced imply by eliminating redundant mathematical equations from the collected set of equations from each integrated theory. This was the case for my new integrative hemoglobin allosteric equilibrium theory (Mateják, et al., 2015), where the principle of detailed balance (Shiryaeva, 2010) was integrated with the chemical reactions with oxygen (Adair, 1925; Severinghaus, 1979), carbon dioxide (Bauer and Schröder, 1972; Vandegriff et al., 1991) and Bohr's protons (Siggaard-Andersen, 1971). The result of the integration is not the only possible result achievable; in general, there also exist alternative explanations for each integrated process. For example, oxygen binding to a hemoglobin tetramer can be described using at least five distinguished theories:

1. Allosteric theory (Eaton et al., 2007; Monod et al., 1965)
2. Adair's theory (Adair, 1925; Imai and Yonetani, 1975)

3. Siggaard-Andersen's approximation (Siggaard-Andersen, 1990)
4. Severinghaus' approximation (Severinghaus, 1979)
5. Hill's approximation (Hill, 1913)

Each of these theories accurately describes oxygen dissociation curve in selected conditions. However, for integration purposes, theories based on physical and chemical principles (allosteric or Adair's theory) are better than empirical approximations of collected data (the other three theories noted above). Since both allosteric theory and Adair's theory are already in the level of elementary chemical reactions of oxygen binding, they are very suitable for integration.

However, many researchers have attempted to extend the approximation of oxygen binding to different ligands (Dash and Bassingthwaite, 2010; Rees and Andreassen, 2005; Severinghaus, 1979; Siggaard-Andersen and Garby, 1973). This approach shifts the oxygen dissociation curve to the left or right, based on empirical observations, but other ligand saturations are not included. These integrations are insufficient, because the relations between ligands are critical for having complex answers to complex processes.

Each new theory built upon first principles is automatically improved whenever these principles are improved on in more detail. For example, the model of hemoglobin equilibrium based on chemical reactions automatically inherited the thermal properties already hidden behind reaction enthalpies, with good agreement when including the observation of heat transfers and temperature dependences (Reeves, 1980; Weber and Campbell, 2011; Weber et al., 2014).

The thesis presents the new approach for integrative physiology based on visual verification. Using graphical diagrams in Modelica language the implementation is equal to the integrative physiological theory. Therefore, these diagrams rapidly increase readability even for non-Modelica users. This intelligibility makes from the proposed libraries and model the platform for theoretical research, which need to be integrated into one model.

7 CONCLUSION

This work began with the reimplementation of different physiological models into MATLAB/Simulink (MathWorks, Inc., U.S.). This approach was very time-consuming, with its only purpose being consistency-verification. The models in Simulink were neither simplified nor self-describing. Moreover, these models could not be easily extended or modified. This was the reason why we moved away from causal simulation tools and started to look for new possibilities for formalizing the physiological model for computer simulation (Mateják, et al., 2008). The solution to our computer language criteria was provided by the Modelica language, into which I was able to easily implement the original Guyton model from 1972 (Mateják, et al., 2009). One year later, I implemented the QHP model into Modelica (Mateják and Kofránek, 2010). This model was one of the main results of our very successful national project, “E-Golem: medical learning simulator of human physiological functions as a background of e-learning teaching of critical care medicine” (2006–2009, MSM/2C, 2C06031). The next model I implemented into Modelica was HumMod 1.6 (Mateják and Kofránek, 2011). This implementation involved the automatic comparison of output values with the original model, so it could describe all experiments for which the original one was described. Having achieved this implementation, it became very easy to extend the model with new acid-base theories, or new blood gas transport and cardiovascular details. Thus, in 2012, I implemented into the model Siggaard-Andersen’s new blood oxygen status model (Siggaard-Andersen and Siggaard-Andersen, 1990). The model was able to simulate the support of artificial ventilation, for example, and even extravascular oxygenation (Mateják, et al., 2012). These and many other inputs, such as infusions, dialyses, transfusions and hemorrhages, were designed for educational simulations, as part of the project entitled “Virtual patient – Simulator for medical education” (2011–2014, MPO/FR, FR-TI3/869). In the same manner of educational simulation, different scenarios of acid-base and respiratory disorders—for example, ketoacidosis (Mateják, 2013)—were also tested in the model, into which the new acid-base calculations had already been implemented, as a result of electroneutrality, along with calculations for each significant chemical substance. One of the most significant results of this work was my separation of the main principles from the model into a Modelica library, called “Physiolibrary” (Mateják, et al., 2014). This library won the free Modelica library awards at the 10th International Modelica Conference in 2014, in Lund, Sweden. By having these first principles—for the hydraulic calculation of cardiovascular system, for example—we were able to implement and identify more detailed cardiovascular models (Kulhánek, et al., 2014). Through working on the physical chemistry theory behind physiology, I was able to formalize the first principles of electrochemical processes in 2015. Using these chemical formalizations, it was possible to implement almost any equilibrium from physical chemistry. Furthermore, I also designed the general principle of allosteric equilibria, which could be used, for example, to calculate the hemoglobin model with three ligands: oxygen, carbon dioxide and hydrogen ions (Mateják, 2015b; Mateják, et al., 2015a). As shown in the thesis, all these physiological descriptions can be easily integrated into a single model, which I have named “Physiomodel”.

The integrative description of human physiology using Modelica opens up new possibilities of scientific examination and the interconnection of physiology within many scientific disciplines. One must realize that according to a physiological description there are always some chemical, hydraulic, thermal, osmotic or population-based domains. Furthermore, the laws of these physical domains can be exactly described by mathematical equations. As was shown, the entire human physiology can be described as a large set of these mathematical equations. Without the object-orienting equation-based approach of computer science, it is not

possible to easily create, extend, modify or understand such extremely large mathematical models.

The integration and image extension of an integrative physiological model is often also connected with domain extension, which is not assumed as an improvement of the model (section 4). In many instances in the Chemical library and Physiolibrary, this is solved using the “default” setting. This means that the new parameters are designed as unnecessary if the user does not want to use them. In this case, the user does not need to set them, because they have a default value. An example is the kinetics coefficient of chemical processes, which are set to be fast enough to equilibrate the process in a very short time. The user, who is interested only in viewing the chemical equilibrium, will simply ignore setting the kinetics coefficient.

Therefore, if possible, it is better to design parameters that have already been scaled and that are almost independent of other settings. For example, the weight of organs and tissues can be represented by parameters defined as fractions of the entire weight. This automatically scales the size of each organ when we set only one parameter, i.e., the total weight of the individual patient. Furthermore, the default values that solve the switch between preselected genotypes or phenotypes can be considered as part of the model. This can decrease even a complex setting into choosing one type of setting, which is considered a rapid improvement of the model by applying the theory noted above. Modelica has been extremely helpful in solving the initial equations where relations between parameters can be implemented.

As an extension, integration also has the same problems in terms of increasing the parameters and inputs of the model. Solving this problem using default values, scaled parameters or predefined datasets is not always a good idea. Mass should be guaranteed, so that during integration, redundant relations do not occur in the model. This state is very dangerous and is not automatically detectable. The redundant equation or redundant variable is an alternative equation of something that is already present in model. If this redundant variable is the state variable, its change as a type of flow is calculated twice; however, there must not be twice the amount of flows in any model. If an entirely new subsystem is inserted to the model that already calculates some parts of that subsystem, then the regulations and answers to the state of the new subsystem will be incorrect. The only clear solution to this problem is to remove all duplicated variables and duplicated relations, even if they calculate the same data but in a different way. In this way, the trusted relations can be selected and relations with lower credibility can be eliminated. An example of this is rendering our extension of the acid-base model as described in sections 6.1, 5.4.1 and 5.4.2.

The methodology of integrative model development has been formalized (Section 4). Using these rules, the Physiomodel (Section 5), a large integrative model of human physiology was created in Modelica, a computer language standardized by the Modelica Association. The model is an extension and integration of the HumMod 1.6 model, created by the Mississippi University of Medical Center. The Physiomodel integrates the original HumMod model with the new acid-base model (Section 5.4.1, 5.4.6 and Section 6.1) and new blood gases transport approach (Section 5.5). As part of the acid-base and gases transport model, a new general model of complex chemical equilibria on macromolecules was developed, as demonstrated by the $O_2\text{-}H^+\text{-}CO_2\text{-}HemoglobinA$ system (Section 5.5.3, 3.1.5, 5.5.4 and 5.7.3). The primary results of this work include also the new Modelica libraries called Physiolibrary and Chemical library (Section 3), which have already been integrated to the open-source Modelica environment called OpenModelica. These graphical and hierarchical implementations confirms the formalization hypothesis.

The results of the formalized theory of model development (Section 4) are the rules for comparison, reduction, extension and integration of models. The comparison between models was based on real experiments that can be described by the models. Reduction here refers to the elimination of correlated parameters. Extension refers to the addition of new relations with new variables to the model, which does not collide with aspects of the rest of model. Finally, integration refers to the development of a new theory that can describe all real experiments of previously separated models. The integration rules have been designed to always achieve the best model, better from those models preceding it. Whole section 5 confirms that the physiological knowledge in HumMod can be integrated using physical diagrams as predicted in integrative hypothesis,

During the compilation of the Physiomodel (Section 5), more than 80000 variables were presented. Most of these variables were generated from graphical connection of Modelica connectors (Table II), so that the number of real physically distinguishable variables was between 4000 and 5000. There were also more than 4000 parameters. However, each of these had a default value and they were designed using the reduction rule to be invariant of other parameters or variables. For example, instead of a parameter containing the basal metabolism of tissue, there is a parameter that contains a basal metabolism per one kilogram for each type of selected tissue. Therefore, it was easy to simulate the experiments, because they could be described only by a few parameters, while the rest remained set as default values.

During implementation of the HumMod, we corrected more than 30 mistakes in the original implementation, as described in the subsection called “Comparison with HumMod 1.6” when discussing the appropriate position and description of the whole model (Sections: 5.1.5, 5.2.6, 5.3.8, 5.4.6, 5.5.5, 5.6.6, 5.7.4, 5.8.1). Most of these mistakes were caused by the misuse of non-SI units (e.g., mg/L instead of mg/dl) or by the misuse of physical quantities (e.g., mass concentration instead of molar concentration). Other mistakes included the misuse of variable connections (exchanging variable names) or ignoring known facts (e.g., the charge of inorganic phosphates is dependent on pH). Additionally, some subsystems were designed very simply in order to describe the physiological functions that we wanted to examine (e.g., synergy of blood gas binding to hemoglobin).

As has been shown in the section on physical and Modelica backgrounds (Section 2), the first principles and its integration can be implemented at a highly error-proof level. The correctly defined basis can generate errors or warnings almost every time when the user wishes to use a variable or class in a questionable way. In Modelica, the user can design predefined submodules with well-defined inputs, outputs, parameters and connectors. For future usage of these components, it is almost impossible to confuse physical units or physical quantities.

The object-oriented equation-based Modelica language allowed us to create extremely robust support of integrative physiology based on selected first principles. Similar support has already been implemented for technical sciences such as libraries for electrical, magnetic, mechanical and thermal processes. However, in physiology, we need models for more sophisticated domains such as electrochemical (for chemical reactions, membrane transports, water evaporation, diffusion, etc.), hydraulic (for cardiovascular systems), thermal (for thermoregulation) and population (for cell populations). By creating an analogy to existing systems we created Physiolibrary 2.3, a library for physiological processes, which was named by the Modelica Association in the Modelica Library Awards as the best free Modelica library in 2014. The result of the year 2015 is a new general library for electrochemical processes, called Chemical library. It is helpful for more general electrochemical equilibration processes. This library is a by-product of our integration of membrane electrochemical equilibria, based

on Donnan's electrolytes equilibrium and Nernst membrane potential in the field of physical chemistry, as described by first principles of chemical domain.

Having the formalized first principles of physiology, the building of new integrative physiological theories can be approached more easily. Through the use of graphical diagrams of Modelica language, the differences between theory and implementation can almost be made to disappear. As a result of the automatic generation of computer code arising from these graphical representations of physical processes, correctly defined physiological systems can be directly simulated using a computer.

REFERENCES

- Abram, S.R., et al. Quantitative circulatory physiology: an integrative mathematical model of human physiology for medical education. *Advances in physiology education* 2007;31(2):202-210.
- Adair, G., Cordero, N. and Shen, T. The effect of temperature on the equilibrium of carbon dioxide and blood and the heat of ionization of haemoglobin. *The Journal of physiology* 1929;67(3):288-298.
- Adair, G.S. The hemoglobin system VI. The oxygen dissociation curve of hemoglobin. *J. Biol. Chem.* 1925;63(2):529-545.
- Ahlqvist, J. Plasma protein osmotic pressure equations for humans. *Journal of Applied Physiology* 2003;94(3):1288-1289.
- Almgård, L. and Ljungqvist, A. Effect of circulating norepinephrine on the renin release from the denervated kidney. *Scandinavian journal of urology and nephrology* 1975;9(2):119-124.
- Angielski, S. and Lukowicz, J. The role of the kidney in the removal of ketone bodies under different acid-base status of the rat. *The American Journal of Clinical Nutrition* 1978;31(9):1635-1641.
- Archer, S. and Michelakis, E. The Mechanism(s) of Hypoxic Pulmonary Vasoconstriction: Potassium Channels, Redox O₂ Sensors, and Controversies. 2002.
- Armstrong, R., Vandenakker, C. and Laughlin, M. Muscle blood flow patterns during exercise in partially curarized rats. *Journal of Applied Physiology* 1985;58:698-701.
- Atherton, J., Green, R. and Thomas, S. Influence of lysine-vasopressin dosage on the time course of changes in renal tissue and urinary composition in the conscious rat. *J. Physiol. (Lond.)* 1971;213(2):291-309.
- Aukland, K. Myogenic mechanisms in the kidney. *Journal of hypertension. Supplement: official journal of the International Society of Hypertension* 1989;7(4):S71-76; discussion S77.
- Bassingthwaighe, J.B. Strategies for the physiome project. *Annals of biomedical engineering* 2000;28(8):1043-1058.
- Bauer, C. and Schröder, E. Carbamino compounds of haemoglobin in human adult and foetal blood. *J. Physiol.* 1972;227(2):457-471.
- Begg, T. and Hearns, J. Components in blood viscosity. The relative contribution of haematocrit, plasma fibrinogen and other proteins. *Clinical science* 1966;31(1):87-93.
- Bevegård, S. and Lodin, A. Postural Circulatory Changes at Rest and during Exercise in five Patients with Congenital Absence of Valves in the Deep Veins of the Legs. *Acta Medica Scandinavica* 1962;172(1):21-29.
- Blackard, W.G. and Nelson, N.C. Portal and Peripheral Vein Immunoreactive Insulin Concentrations Before and After Glucose Infusion. *Diabetes* 1970;19(5):302-306.

Bock, A.V., Dill, D.B. and Edwards, H.T. ON THE RELATION OF CHANGES IN BLOOD VELOCITY AND VOLUME FLOW OF BLOOD TO CHANGE OF POSTURE. *The Journal of Clinical Investigation* 1930;8(4):533-544.

Bootsma, M., et al. Heart rate and heart rate variability as indexes of sympathovagal balance. *American Journal of Physiology* 1994;266:H1565-H1565.

Braam, B., et al. Relevance of the tubuloglomerular feedback mechanism in pathophysiology. *Journal of the American Society of Nephrology* 1993;4(6):1257-1274.

BRADLEY, S.E., INGELFINGER, F.J. and BRADLEY, G.P. Hepatic Circulation in Cirrhosis of the Liver. *Circulation* 1952;5(3):419-429.

Bradley, S.E., et al. The circulating splanchnic blood volume in dog and man. *Transactions of the Association of American Physicians* 1953;66:294-302.

Brebbia, D.R., Goldman, R.F. and Buskirk, E.R. Water Vapor Loss From the Respiratory Tract During Outdoor Exercise in the Cold. 1957.

Carter, C.B., Hodnett, B.L. and Hester, R. Modeling of gender differences in respiratory function during exercise using Quantitative Human Physiology. *The FASEB Journal* 2009;23(1_MeetingAbstracts):LB118.

Carter, Y.M., et al. Diastolic properties, myocardial water content, and histologic condition of the rat left ventricle: effect of varied osmolarity of a coronary perfusate. *J Heart Lung Transplant* 1998;17(2):140-149.

Claassen, K., et al. A detailed physiologically-based model to simulate the pharmacokinetics and hormonal pharmacodynamics of enalapril on the circulating endocrine renin-angiotensin-aldosterone system. *Frontiers in Physiology* 2013;4.

Clutter, W.E., et al. Epinephrine plasma metabolic clearance rates and physiologic thresholds for metabolic and hemodynamic actions in man. *The Journal of Clinical Investigation* 1980;66(1):94-101.

Coleman, T., et al. Long-term regulation of the circulation. *Interrelationships with body fluid volumes, Physical Bases of Circulatory Transport: Regulation and Exchange*, WB Saunders Co, Philadelphia 1967.

Coleman, T.G. and Randall, J.E. A Comprehensive Physiological Model. *The Physiologist* 1983;26(1).

Conte, G., et al. Role of inhibition of atrial natriuretic factor release in the down-regulation of salt excretion. *Kidney Int* 1992;42:673-680.

Cumin, F., Baum, H.P. and Levens, N. Leptin is cleared from the circulation primarily by the kidney. *Int J Obes Relat Metab Disord* 1996;20(12):1120-1126.

Dabbish, L., et al. Social coding in GitHub: transparency and collaboration in an open software repository. In, *Proceedings of the ACM 2012 conference on Computer Supported Cooperative Work*. ACM; 2012. p. 1277-1286.

Dash, R.K. and Bassingthwaigte, J.B. Erratum to: Blood HbO₂ and HbCO₂ dissociation curves at varied O₂, CO₂, pH, 2, 3-DPG and temperature levels. *Ann. Biomed. Eng.* 2010;38(4):1683-1701.

Debye, P. and Huckel, E. Theory of electrolytes, part 1. *Freezing point depression and cognate phenomena Phys. Zeits* 1923;24:185-206.

Dobson, H.L., et al. Absorption of ¹³¹I labeled modified insulin. *Metabolism* 1967;16(8):723-732.

Dodt, E. and Zotterman, Y. Mode of action of warm receptors. *Acta physiologica scandinavica* 1952;26(4):345-357.

DOEDEN, B. and RIZZA, R. Use of a Variable Insulin Infusion to Assess Insulin Action in Obesity: Defects in Both the Kinetics and Amplitude of Response. *The Journal of Clinical Endocrinology & Metabolism* 1987;64(5):902-908.

Drummond, H.A., Grifoni, S.C. and Jernigan, N.L. A new trick for an old dogma: ENaC proteins as mechanotransducers in vascular smooth muscle. *Physiology* 2008;23(1):23-31.

Eaton, W.A., et al. Evolution of allosteric models for hemoglobin. *IUBMB Life* 2007;59(8-9):586-599.

Edelman, I.S. Thyroid Thermogenesis. *New England Journal of Medicine* 1974;290(23):1303-1308.

ECHT, M., et al. Effective Compliance of the Total Vascular Bed and the Intrathoracic Compartment Derived from Changes in Central Venous Pressure Induced by Volume Changes in Man. *Circulation Research* 1974;34(1):61-68.

Eisenhoffer, J., Lee, S. and Johnston, M. Pressure-flow relationships in isolated sheep prenodal lymphatic vessels. *American Journal of Physiology-Heart and Circulatory Physiology* 1994;36(3):H938.

Engeset, A., et al. Studies on human peripheral lymph. I. Sampling method. *Lymphology* 1973;6(1):1-5.

Erwald, R. and Wiechel, K. Effect of vasopressin on central and splanchnic hemodynamics in awake man. *Acta chirurgica Scandinavica* 1978;144(6):347.

Fan, F.C., et al. Effects of hematocrit variations on regional hemodynamics and oxygen transport in the dog. 1980.

Ferguson, D.W., Abboud, F.M. and Mark, A.L. Relative contribution of aortic and carotid baroreflexes to heart rate control in man during steady state and dynamic increases in arterial pressure. *The Journal of Clinical Investigation* 1985;76(6):2265-2274.

Figge, J.J. The Figge-Fencl Quantitative Physicochemical Model of Human Acid-Base Physiology (Version 2.0). *An Educational Web Site about Modern Human Acid-Base Physiology*.

Florez-Duquet, M. and McDonald, R.B. Cold-induced thermoregulation and biological aging. *Physiological reviews* 1998;78(2):339-358.

- Frayn, K. Adipose tissue as a buffer for daily lipid flux. *Diabetologia* 2002;45(9):1201-1210.
- Friedman-Einat, M., et al. Serum leptin activity in obese and lean patients. *Regulatory peptides* 2003;111(1):77-82.
- Fritzson, P., et al. OpenModelica-A free open-source environment for system modeling, simulation, and teaching. In, *IEEE International Symposium on Computer-Aided Control Systems Design*. 2006. p. 1588-1595.
- Fritzson, P. and Engelson, V. Modelica—A unified object-oriented language for system modeling and simulation. In, *ECOOP'98—Object-Oriented Programming*. Springer; 1998. p. 67-90.
- Gaasch, W.H., et al. Dynamic determinants of left ventricular diastolic pressure-volume relations in man. *Circulation* 1975;51(2):317-323.
- GAUER, O.H., HENRY, J.P. and SIEKER, H.O. Changes in Central Venous Pressure after Moderate Hemorrhage and Transfusion in Man. *Circulation Research* 1956;4(1):79-84.
- Gedde, M.M. and Huestis, W.H. Membrane potential and human erythrocyte shape. *Biophys. J.* 1997;72(3):1220.
- George, S., et al. A family with severe insulin resistance and diabetes due to a mutation in AKT2. *Science* 2004;304(5675):1325-1328.
- GINNSBERG, S., et al. Serum Insulin Levels Following Administration of Exogenous Insulin. *The Journal of Clinical Endocrinology & Metabolism* 1973;36(6):1175-1179.
- Goldberg, M.A. and Schneider, T.J. Similarities between the oxygen-sensing mechanisms regulating the expression of vascular endothelial growth factor and erythropoietin. *Journal of Biological Chemistry* 1994;269(6):4355-4359.
- Goldblatt, H., Lamfrom, H. and Haas, E. Physiological Properties of Renin and Hypertensin. 1953.
- Gottschalk, C.W. and Mynlie, M. Micropuncture study of the mammalian urinary concentrating mechanism: evidence for the countercurrent hypothesis. *American Journal of Physiology--Legacy Content* 1959;196(4):927-936.
- Greenway, C.V. and Lister, G.E. Capacitance effects and blood reservoir function in the splanchnic vascular bed during non-hypotensive haemorrhage and blood volume expansion in anaesthetized cats. *J. Physiol. (Lond.)* 1974;237(2):279-294.
- Grodins, F.S., Buell, J. and Bart, A.J. Mathematical analysis and digital simulation of the respiratory control system. In.: DTIC Document; 1967.
- Grodins, F.S., et al. Respiratory responses to CO₂ inhalation. A theoretical study of a nonlinear biological regulator. *Journal of applied physiology* 1954;7(3):283-308.
- Gross, J. and Pitt-Rivers, R. 3: 5: 3'-Triiodothyronine. 2. Physiological activity. *Biochemical Journal* 1953;53(4):652.
- Guyton, A.C. Interstitial fluid pressure: II. Pressure-volume curves of interstitial space. *Circulation research* 1965;16(5):452-460.

- Guyton, A.C. The relationship of cardiac output and arterial pressure control. *Circulation* 1981;64(6):1079-1088.
- Guyton, A.C. Blood pressure control--special role of the kidneys and body fluids. *Science* 1991;252(5014):1813-1816.
- Guyton, A.C. and CE Coleman, T. Circulatory physiology: cardiac output and its regulation. 1973.
- Guyton, A.C., Coleman, T.G. and Granger, H.J. Circulation: overall regulation. *Annual review of physiology* 1972;34(1):13-44.
- Guyton, A.C. and Sagawa, K. Compensations of cardiac output and other circulatory functions in areflex dogs with large AV fistulas. *Am. J. Physiol* 1961;200:1157.
- Guyton, A.C., Taylor, A.E. and Granger, H.J. Dynamics and control of the body fluids. Saunders; 1975.
- Guyton, J.R., et al. A Model of Glucose-insulin Homeostasis in Man that Incorporates the Heterogeneous Fast Pool Theory of Pancreatic Insulin Release. *Diabetes* 1978;27(10):1027-1042.
- Hall, J.E. Guyton and Hall textbook of medical physiology. Elsevier Health Sciences; 2010.
- Hannaford, M.C., et al. Protein wasting due to acidosis of prolonged fasting. 1982.
- Hardy, J.D. and Soderstrom, G.F. Heat Loss from the Nude Body and Peripheral Blood Flow at Temperatures of 22°C. to 35°C.: Two Figures. *The Journal of Nutrition* 1938;16(5):493-510.
- HAYS, M.T. Colonic excretion of iodide in normal human subjects. *Thyroid* 1993;3(1):31-35.
- Henriksen, J.H. Estimation of lymphatic conductance: A model based on protein-kinetic studies and haemodynamic measurements in patients with cirrhosis of the liver and in pigs. *Scandinavian journal of clinical & laboratory investigation* 1985;45(2):123-130.
- Henry, J.P. and Gauer, O.H. THE INFLUENCE OF TEMPERATURE UPON VENOUS PRESSURE IN THE FOOT. *The Journal of Clinical Investigation* 1950;29(7):855-861.
- HENSEL, H. The time factor in thermoreceptor excitation. *Acta Physiologica Scandinavica* 1953;29(1):109-116.
- Hesslink, R.L., et al. Human cold air habituation is independent of thyroxine and thyrotropin. 1992.
- Hester, R.L., et al. HumMod: A Modeling Environment for the Simulation of Integrative Human Physiology. *Frontiers in physiology* 2011;2:12.
- Hester, R.L., Coleman, T. and Summers, R. A multilevel open source integrative model of human physiology. *The FASEB Journal* 2008;22(1_MeetingAbstracts):756.758.
- Hester, R.L., et al. Systems biology and integrative physiological modelling. *The Journal of physiology* 2011;589(5):1053-1060.

- Heyeraas, K.J. and Aukland, K. Interlobular arterial resistance: Influence of renal arterial pressure and angiotensin II. *Kidney Int* 1987;31(6):1291-1298.
- Hill, A.V. The combinations of haemoglobin with oxygen and with carbon monoxide. I. *Biochem. J.* 1913;7(5):471.
- Hodgkin, A.L. and Huxley, A.F. A quantitative description of membrane current and its application to conduction and excitation in nerve. *The Journal of physiology* 1952;117(4):500-544.
- Hodnett, B.L., Carter, C.B. and Hester, R. Modeling of gender differences in cardiovascular function during exercise using Quantitative Human Physiology. *The FASEB Journal* 2009;23(1_MeetingAbstracts):LB117.
- Hsieh, A.C.L., Nagasaka, T. and Carlson, L.D. Effects of immersion of the hand in cold water on digital blood flow. 1965.
- Chiasson, J., et al. Differential sensitivity of glycogenolysis and gluconeogenesis to insulin infusions in dogs. *Diabetes* 1976;25(4):283-291.
- Chopra, I.J. An assessment of daily production and significance of thyroidal secretion of 3, 3', 5'-triiodothyronine (reverse T3) in man. *The Journal of Clinical Investigation* 1976;58(1):32-40.
- CHOPRA, I.J., HERSHMAN, J.M. and HORNABROOK, R.W. Serum Thyroid Hormone and Thyrotropin Levels in Subjects from Endemic Goiter Regions of New Guinea. *The Journal of Clinical Endocrinology & Metabolism* 1975;40(2):326-333.
- Christlieb, A.R., et al. Renin extraction by the human liver. *Experimental Biology and Medicine* 1968;128(3):821-823.
- Ikeda, N., et al. A model of overall regulation of body fluids. *Annals of biomedical engineering* 1979;7(2):135-166.
- Imai, J., et al. Regulation of Pancreatic β Cell Mass by Neuronal Signals from the Liver. *Science* 2008;322(5905):1250-1254.
- Imai, K. and Yonetani, T. PH dependence of the Adair constants of human hemoglobin. Nonuniform contribution of successive oxygen bindings to the alkaline Bohr effect. *J. Biol. Chem.* 1975;250(6):2227-2231.
- Ito, S. and Carretero, O.A. An in vitro approach to the study of macula densa-mediated glomerular hemodynamics. *Kidney Int* 1990;38(6):1206-1210.
- Iwanishi, M., Czech, M.P. and Cherniack, A.D. The Protein-tyrosine Kinase Fer Associates with Signaling Complexes Containing Insulin Receptor Substrate-1 and Phosphatidylinositol 3-Kinase. *Journal of Biological Chemistry* 2000;275(50):38995-39000.
- Jackson, I.M.D. Thyrotropin-Releasing Hormone. *New England Journal of Medicine* 1982;306(3):145-155.
- Jacobson, L.O., et al. Role of the Kidney in Erythropoiesis. *Nature* 1957;179(4560):633-634.

- Jamison, R. and Lacy, F.B. Evidence for urinary dilution by the collecting tubule. *Am. J. Physiol* 1972;223:898-902.
- Jamison, R.L., et al. A micropuncture study of collecting tubule function in rats with hereditary diabetes insipidus. *Journal of Clinical Investigation* 1971;50(11):2444.
- Jan, K.M. and Chien, S. Effect of hematocrit variations on coronary hemodynamics and oxygen utilization. 1977.
- JÉQuier, E. Leptin Signaling, Adiposity, and Energy Balance. *Annals of the New York Academy of Sciences* 2002;967(1):379-388.
- Kamon, E. and Belding, H.S. Heat uptake and dermal conductance in forearm and hand when heated. 1968.
- Katschinski, D.M. On heat and cells and proteins. *Physiology* 2004;19(1):11-15.
- Kety, S.S. and Schmidt, C.F. THE EFFECTS OF ALTERED ARTERIAL TENSIONS OF CARBON DIOXIDE AND OXYGEN ON CEREBRAL BLOOD FLOW AND CEREBRAL OXYGEN CONSUMPTION OF NORMAL YOUNG MEN 1. *The Journal of Clinical Investigation* 1948;27(4):484-492.
- Khokhar, A., et al. Effect of vasopressin on plasma volume and renin release in man. *Clinical Science* 1976;50(Pt 5):415-424.
- Kintner, D., et al. 31P-MRS-based determination of brain intracellular and interstitial pH: its application to in vivo H⁺ compartmentation and cellular regulation during hypoxic/ischemic conditions. *Neurochemical research* 2000;25(9-10):1385-1396.
- Kittnar, O. and Mlček, M. Atlas fyziologických regulací. Grada Publishing as; 2009.
- Kofránek, J. Complex model of blood acid-base balance. In: Ziethamlová, M., editor, *MEDSOFT 2009*. Creative Connections; 2009. p. 23-60.
- Kofránek, J., Mateják, M. and Privitzer, P. Leaving toil to machines - building simulation kernel of educational software in modern software environments. In, *Mefanet 2009*. Masaryk University, Brno; 2009.
- Kofranek, J., Matousek, S. and Andrlík, M. Border flux balance approach towards modelling acid-base chemistry and blood gases transport. In, *In: Proceedings of the 6th EUROSIM congress on modelling and simulation. Ljubljana: University of Ljubljana*. 2007. p. 1-9.
- Kofránek, J., Matoušek, S., Rusz, J., Stodulka, P., Privitzer, P., Mateják, M. and Tribula, M.: The Atlas of Physiology and Pathophysiology: Web-based multimedia enabled interactive simulations. *Computer Methods and Programs in Biomedicine* 2011;104(2):143-153
- Kotani, K., et al. GLUT4 glucose transporter deficiency increases hepatic lipid production and peripheral lipid utilization. *The Journal of clinical investigation* 2004;114(11):1666-1675.
- Kulhánek, T., Kofránek, J. and Mateják, M. Modeling of short-term mechanism of arterial pressure control in the cardiovascular system: Object-oriented and acausal approach. *Computers in Biology and Medicine* 2014;54(0):137-144.

Kulhánek, T., et al. Simple models of the cardiovascular system for educational and research purposes. *MEFANET Journal* 2014.

Lankford, S.P., et al. Regulation of collecting duct water permeability independent of cAMP-mediated AVP response. *American Journal of Physiology-Renal Physiology* 1991;261(3):F554-F566.

Larsen, P.R. Direct immunoassay of triiodothyronine in human serum. *The Journal of Clinical Investigation* 1972;51(8):1939-1949.

LAUGHLIN, M.H. Skeletal muscle blood flow capacity: role of muscle pump in exercise hyperemia. *Am J Physiol* 1987;253:1004.

Laughlin, M.H. and Armstrong, R. Rat muscle blood flows as a function of time during prolonged slow treadmill exercise. *Am J Physiol Heart Circ Physiol* 1983;244:H814-H824.

Levitin, H., Branscome, W. and Epstein, F.H. The pathogenesis of hypochloremia in respiratory acidosis. *Journal of Clinical Investigation* 1958;37(12):1667.

Little, W.C. and Cheng, C.P. Effect of exercise on left ventricular-arterial coupling assessed in the pressure-volume plane. *AMERICAN JOURNAL OF PHYSIOLOGY* 1993;264:H1629-H1629.

Lohmeier, T.E. and Iliescu, R. Chronic lowering of blood pressure by carotid baroreflex activation mechanisms and potential for hypertension therapy. *Hypertension* 2011;57(5):880-886.

Maass-Moreno, R. and Rothe, C.F. Contribution of the large hepatic veins to postsinusoidal vascular resistance. *Am J Physiol Gastrointest Liver Physiol* 1992;262:G14-G22.

Manning, R.D. Renal hemodynamic, fluid volume, and arterial pressure changes during hyperproteinemia. 1987.

Manning, R.D. Effects of hypoproteinemia on blood volume and arterial pressure of volume-loaded dogs. 1990.

Mantzoros, C.S., et al. Leptin in human physiology and pathophysiology. 2011.

Mateják, M. Simulovanie ketoacidózy. In, *Medsoft 2013*. 2013. p. 140-150.

Mateják, M. Adairove viazanie O₂, CO₂ a H⁺ na hemoglobín In, *Medsoft 2015*. 2015. p. 140-149.

Mateják, M. and Kofránek, J. Rozsáhlý model fyziologických regulací v Modelice. In, *Medsoft 2010*. 2010. p. 126-146.

Mateják, M. and Kofránek, J. HumMod–Golem Edition–Rozsáhlý model fyziologických systémů. In, *Medsoft 2011*. 2011. p. 182-196.

Mateják, M., Kofránek, J. and Rusz, J. Akauzální "vzkříšení" Guytonova diagramu. In, *Medsoft 2009*. 2009. p. 105.

- Mateják, M., Kulhánek, T. and Matoušek, S. Adair-based hemoglobin equilibrium with oxygen, carbon dioxide and hydrogen ion activity. *Scandinavian Journal of Clinical & Laboratory Investigation* 2015;1-8.
- Mateják, M., et al. Physiolibrary - Modelica library for Physiology. In, *10th International Modelica Conference*. Lund, Sweden; 2014.
- Mateják, M., et al. Model ECMO oxygenátoru. *Medsoft* 2012:205-2014.
- Mateják, M., Privitzer, P. and Kofránek, J. Modelica vs. blokovo-orientované jazyky matematického modelovania. In: Janech, J., editor, *OBJEKTY 2008*. Žilina, SR: Edis Žilina; 2008. p. 79-94.
- Matthew, J.B., et al. Quantitative determination of carbamino adducts of alpha and beta chains in human adult hemoglobin in presence and absence of carbon monoxide and 2, 3-diphosphoglycerate. *J. Biol. Chem.* 1977;252(7):2234-2244.
- Mattson, S.E., Elmquist, H. and Broenink, J.F. Modelica: An international effort to design the next generation modelling language. *Journal A* 1997;38(3):16-19.
- Mattsson, S.E., Elmquist, H. and Otter, M. Physical system modeling with Modelica. *Control Engineering Practice* 1998;6(4):501-510.
- Mayerson, H.S., Sweeney, H.M. and Toth, L.A. THE INFLUENCE OF POSTURE ON CIRCULATION TIME. 1939.
- Mayerson, H.S., et al. Regional differences in capillary permeability. 1960.
- McCulloch, W.S. and Pitts, W. A logical calculus of the ideas immanent in nervous activity. *The bulletin of mathematical biophysics* 1943;5(4):115-133.
- McGarry, J.D. and Foster, D.W. Ketogenesis and its regulation. *Am J Med* 1976;61(1):9-13.
- McGarry, J.D. and Foster, D.W. Ketogenesis and its regulation. *The American Journal of Medicine* 1976;61(1):9-13.
- Mellander, S. and Björnberg, J. Regulation of Vascular Smooth Muscle Tone and Capillary Pressure. 1992.
- METZLER, C.H., et al. Increased right or left atrial pressure stimulates release of atrial natriuretic peptides in conscious dogs. *Endocrinology* 1986;119(5):2396-2398.
- Miles, P.D., et al. Kinetics of insulin action in vivo: identification of rate-limiting steps. *Diabetes* 1995;44(8):947-953.
- Miller, M.E., Cronkite, E.P. and Garcia, J.F. Plasma levels of immunoreactive erythropoietin after acute blood loss in man. *British journal of haematology* 1982;52(4):545-549.
- Mizelle, H.L., et al. Atrial natriuretic peptide induces sustained natriuresis in conscious dogs. *American Journal of Physiology-Regulatory, Integrative and Comparative Physiology* 1990;258(6):R1445-R1452.
- Monod, J., Wyman, J. and Changeux, J.-P. On the nature of allosteric transitions: a plausible model. *J. Mol. Biol.* 1965;12(1):88-118.

Moore, L.C. and Casellas, D. Tubuloglomerular feedback dependence of autoregulation in rat juxtapamedullary afferent arterioles. *Kidney Int* 1990;37(6):1402-1408.

Mortimer, R.G. 8 - The Thermodynamics of Electrical Systems. In: Mortimer, R.G., editor, *Physical Chemistry (Third Edition)*. Burlington: Academic Press; 2008. p. 297.

Mortimer, R.G. Physical Chemistry (Third Edition). In: Mortimer, R.G., editor. Burlington: Academic Press; 2008. p. 1-1385.

Moss, R., et al. Virtual patients and sensitivity analysis of the Guyton model of blood pressure regulation: towards individualized models of whole-body physiology. *PLoS Comput Biol* 2012;8(6):e1002571-e1002571.

Naeraa, N., Petersen, E.S. and Boye, E. The influence of simultaneous, independent changes in pH and carbon dioxide tension on the in vitro oxygen tension-saturation relationship of human blood. *Scand. J. Clin. Lab. Invest.* 1963;15(2):141-151.

Nicoloff, J.T., et al. Simultaneous Measurement of Thyroxine and Triiodothyronine Peripheral Turnover Kinetics in Man. *The Journal of Clinical Investigation* 1972;51(3):473-483.

Nielsen, S., et al. Key roles of renal aquaporins in water balance and water-balance disorders. *Physiology* 2000;15(3):136-143.

Nicholls, M. and Richards, A. Human studies with atrial natriuretic factor. *Endocrinology and metabolism clinics of North America* 1987;16(1):199-223.

NODA, T., et al. Curvilinearity of LV end-systolic pressure-volume and dP/dt,-end-diastolic volume relations. 1993.

OCHSNER, A., COLP, R. and BURCH, G.E. Normal Blood Pressure in the Superficial Venous System of Man at Rest in the Supine Position. *Circulation* 1951;3(5):674-680.

Osiba, S. THE SEASONAL VARIATION OF BASAL METABOLISM AND ACTIVITY OF THYROID GLAND IN MAN. *The Japanese Journal of Physiology* 1957;7:355-365.

Owen, O.E., et al. Brain Metabolism during Fasting*. *The Journal of Clinical Investigation* 1967;46(10):1589-1595.

Pagel, H., Jelkmann, W. and Weiss, C. A comparison of the effects of renal artery constriction and anemia on the production of erythropoietin. *Pflugers Arch.* 1988;413(1):62-66.

Piwonka, R.W. and Robinson, S. Acclimatization of highly trained men to work in severe heat. 1967.

Pollack, A.A. and Wood, E.H. Venous Pressure in the Saphenous Vein at the Ankle in Man during Exercise and Changes in Posture. 1949.

Porter, D. and Goldberg, M. Regulation of erythropoietin production. *Experimental hematology* 1993;21(3):399-404.

Prager, R., Wallace, P. and Olefsky, J.M. In vivo kinetics of insulin action on peripheral glucose disposal and hepatic glucose output in normal and obese subjects. *The Journal of Clinical Investigation* 1986;78(2):472-481.

- Prager, R., Wallace, P. and Olefsky, J.M. Hyperinsulinemia Does Not Compensate for Peripheral Insulin Resistance in Obesity. *Diabetes* 1987;36(3):327-334.
- Previs, S.F., et al. Contrasting effects of IRS-1 versus IRS-2 gene disruption on carbohydrate and lipid metabolism in vivo. *J Biol Chem* 2000;275(50):38990-38994.
- Privitzer, P., Kofránek, J., Tribula, M., Ježek, F., Kulhánek, T., Mateják, M. and Šilar, J.: Virtual reality in advanced simulations of intensive care scenarios. In *Mefanet 2014*. Brno, Czech Republic, 2014
- Pruett, W.A., et al. A population model of integrative cardiovascular physiology. *PloS one* 2013;8(9).
- Raftos, J.E., Bulliman, B.T. and Kuchel, P.W. Evaluation of an electrochemical model of erythrocyte pH buffering using ³¹P nuclear magnetic resonance data. *The Journal of general physiology* 1990;95(6):1183-1204.
- Randle, P.J. Fuel selection in animals. *Biochemical Society Transactions* 1986;14(5):799.
- Rees, S.E. and Andreassen, S. Mathematical models of oxygen and carbon dioxide storage and transport: the acid-base chemistry of blood. *Crit. Rev. Biomed. Eng.* 2005;33(3).
- Reeves, R.B. The effect of temperature on the oxygen equilibrium curve of human blood. *Respir. Physiol.* 1980;42(3):317-328.
- Reissmann, K.R., et al. Influence of disappearance rate and distribution space on plasma concentration of erythropoietin in normal rats. *J Lab Clin Med* 1965;65:967-975.
- Renkin, E. and Tucker, V. Atrial Natriuretic Peptide as a Regulator of Transvascular Fluid Balance. *Physiology* 1996;11(3):138-143.
- Ridgway, E.C., Weintraub, B.D. and Maloof, F. Metabolic Clearance and Production Rates of Human Thyrotropin. *The Journal of Clinical Investigation* 1974;53(3):895-903.
- Roach, M.R. and Burton, A.C. THE REASON FOR THE SHAPE OF THE DISTENSIBILITY CURVES OF ARTERIES. *Canadian Journal of Biochemistry and Physiology* 1957;35(8):681-690.
- Rother, K.I., et al. Evidence That IRS-2 Phosphorylation Is Required for Insulin Action in Hepatocytes. *Journal of Biological Chemistry* 1998;273(28):17491-17497.
- Roush, W. An "off switch" for red blood cells. *Science* 1995;268(5207):27-28.
- Rutter, G.A. and Hill, E.V. Insulin Vesicle Release: Walk, Kiss, Pause ... Then Run. 2006.
- Sagawa, K., et al. Cardiac contraction and the pressure-volume relationship. Oxford University Press New York; 1988.
- Saltin, B. and Hermansen, L. Esophageal, rectal, and muscle temperature during exercise. 1966.
- Sands, J.M. Urea Transport: It's Not Just "Freely Diffusible" Anymore. 1999.

- Sato, K. The physiology, pharmacology, and biochemistry of the eccrine sweat gland. In, *Reviews of Physiology, Biochemistry and Pharmacology, Volume 79*. Springer; 1977. p. 51-131.
- Seeliger, E., et al. Pressure-dependent renin release: effects of sodium intake and changes of total body sodium. *American Journal of Physiology-Regulatory, Integrative and Comparative Physiology* 1999;277(2):R548-R555.
- Severinghaus, J.W. Simple, accurate equations for human blood O₂ dissociation computations. *J. Appl. Physiol.* 1979;46(3):599-602.
- Sheppard, C. The Theory of the Study of Transfers within a Multi-Compartment System Using Isotopic Tracers. *Journal of Applied Physics* 1948;19(1):70-76.
- Shigemi, K., Brunner, M.J. and Shoukas, A.A. -and -Adrenergic mechanisms in the control of vascular capacitance by the carotid sinus baroreflex system. *AMERICAN JOURNAL OF PHYSIOLOGY* 1994;267:H201-H201.
- Shiryaeva, A. On the stationary state of a mixture of reacting gases. *Russian Journal of Physical Chemistry B* 2010;4(3):413-422.
- Schrier, R.W., et al. Influence of hematocrit and colloid on whole blood viscosity during volume expansion. *Am. J. Physiol* 1970;218(346):77.
- Siggaard-Andersen, O. Oxygen-Linked Hydrogen Ion Binding of Human Hemoglobin. Effects of Carbon Dioxide and 2, 3-Diphosphoglycerate I. Studies on Erythrolysate. *Scand. J. Clin. Lab. Invest.* 1971;27(4):351-360.
- Siggaard-Andersen, O. Acid-base balance. *Encyclopedia of respiratory medicine* 2005:1-6.
- Siggaard-Andersen, O. and Garby, L. The Bohr effect and the Haldane effect. *Scand. J. Clin. Lab. Invest.* 1973;31(1):1-8.
- Siggaard-Andersen, O. and Siggaard-Andersen, M. The oxygen status algorithm: a computer program for calculating and displaying pH and blood gas data. *Scand. J. Clin. Lab. Invest.* 1990;50(S203):29-45.
- Skarlatos, S., et al. Spontaneous pressure-flow relationships in renal circulation of conscious dogs. *Am J Physiol* 1993;264(5 Pt 2):H1517-1527.
- Sonna, L.A., et al. Invited review: effects of heat and cold stress on mammalian gene expression. *Journal of Applied Physiology* 2002;92(4):1725-1742.
- Standardization, W.E.C.o.B. and Organization, W.H. WHO Expert Committee on Biological Standardization [meeting held in Geneva from 22 to 27 September 1958]: Twelfth report. 1958:10.
- Standardization, W.E.C.o.B. and Organization, W.H. WHO Expert Committee on Biological Standardization: Thirty-seventh Report. 1987:26.
- Stewart, P.A. How to understand acid-base: a quantitative acid-base primer for biology and medicine. Edward Arnold London; 1981.

- Stokes, R.H. and Robinson, R.A. Ionic Hydration and Activity in Electrolyte Solutions. *J. Am. Chem. Soc.* 1948;70(5):1870-1878.
- Stone, H., Thompson HK and Schmidt-Nielsen, K. Influence of erythrocytes on blood viscosity. 1968.
- SUGA, H. and SAGAWA, K. Instantaneous Pressure-Volume Relationships and Their Ratio in the Excised, Supported Canine Left Ventricle. *Circulation Research* 1974;35(1):117-126.
- SUGA, H., SAGAWA, K. and KOSTIUK, D.P. Controls of ventricular contractility assessed by pressure-volume ratio, Emax. *Cardiovascular Research* 1976;10(5):582-592.
- Summers, R. and Coleman, T. Computer systems analysis of the cardiovascular mechanisms of reentry orthostasis in astronauts. In, *Computers in Cardiology, 2002*. IEEE; 2002. p. 521-524.
- Summers, R.L., et al. Theoretical analysis of the mechanisms of chronic hyperinsulinemia. *Computers in Biology and Medicine* 1997;27(3):249-256.
- SURKS, M.I. and LIFSCHITZ, B.M. Biphasic Thyrotropin Suppression in Euthyroid and Hypothyroid Rats. *Endocrinology* 1977;101(3):769-775.
- SURKS, M.I. and OPPENHEIMER, J.H. Incomplete Suppression of Thyrotropin Secretion after Single Injection of Large L-Triiodothyronine Doses into Hypothyroid Rats. *Endocrinology* 1976;99(6):1432-1441.
- Takeshita, A., et al. Effect of central venous pressure on arterial baroreflex control of heart rate. 1979.
- Thompson, W.O., Thompson, P.K. and Dailey, M.E. THE EFFECT OF POSTURE UPON THE COMPOSITION AND VOLUME OF THE BLOOD IN MAN 1. *The Journal of Clinical Investigation* 1928;5(4):573-604.
- Tummescheit, H.: Lund University; 2002. Design and implementation of object-oriented model libraries using modelica.
- Tummescheit, H. Design and implementation of object-oriented model libraries using modelica. 2002.
- Vandegriff, K., et al. Carbon dioxide binding to human hemoglobin cross-linked between the alpha chains. *J. Biol. Chem.* 1991;266(5):2697-2700.
- Wahren, J. and Ekberg, K. Splanchnic regulation of glucose production. *Annu. Rev. Nutr.* 2007;27:329-345.
- Warner, H.R. and Cox, A. A mathematical model of heart rate control by sympathetic and vagus efferent information. 1962.
- Weber, R.E. and Campbell, K.L. Temperature dependence of haemoglobin-oxygen affinity in heterothermic vertebrates: mechanisms and biological significance. *Acta Physiologica* 2011;202(3):549-562.
- Weber, R.E., Fago, A. and Campbell, K.L. Enthalpic partitioning of the reduced temperature sensitivity of O₂ binding in bovine hemoglobin. *Comparative Biochemistry and Physiology Part A: Molecular & Integrative Physiology* 2014.

Weidmann, P., et al. Blood levels and renal effects of atrial natriuretic peptide in normal man. *Journal of Clinical Investigation* 1986;77(3):734.

Whittaker, S.R.F. and Winton, F.R. The apparent viscosity of blood flowing in the isolated hindlimb of the dog, and its variation with corpuscular concentration. *J. Physiol. (Lond.)* 1933;78(4):339-369.

Winearls, C., et al. EFFECT OF HUMAN ERYTHROPOIETIN DERIVED FROM RECOMBINANT DNA ON THE ANAEMIA OF PATIENTS MAINTAINED BY CHRONIC HAEMODIALYSIS. *The Lancet* 1986;328(8517):1175-1178.

WINER, N., et al. Adrenergic receptor mediation of renin secretion. *The Journal of Clinical Endocrinology & Metabolism* 1969;29(9):1168-1175.

Wolf, M.B. Whole body acid-base and fluid-electrolyte balance: a mathematical model. 2013.

Wolf, M.B. and DeLand, E.C. A mathematical model of blood-interstitial acid-base balance: application to dilution acidosis and acid-base status. *J. Appl. Physiol.* 2011;110(4):988-1002.

Wong, S.L., et al. Leptin hormonal kinetics in the fed state: effects of adiposity, age, and gender on endogenous leptin production and clearance rates. *The Journal of Clinical Endocrinology & Metabolism* 2004;89(6):2672-2677.

Wyndham, C.H., et al. Fatigue of the sweat gland response. 1966.

Xenopoulos, N.P. and Applegate, R.J. The effect of vagal stimulation on left ventricular systolic and diastolic performance. *American Journal of Physiology-Heart and Circulatory Physiology* 1994;35(6):H2167.

Xie, S., et al. A model of human microvascular exchange. *Microvascular research* 1995;49(2):141-162.

Yandle, T.G., et al. Metabolic clearance rate and plasma half life of alpha-human atrial natriuretic peptide in man. *Life Sci* 1986;38(20):1827-1833.

Young, D.B., Pan, Y. and Guyton, A.C. Control of extracellular sodium concentration by antidiuretic hormone-thirst feedback mechanism. *Am J Physiol* 1977;232(5).

Zhang, S., Pruett, W.A. and Hester, R. Visualization and classification of physiological failure modes in ensemble hemorrhage simulation. In, *IS&T/SPIE Electronic Imaging*. International Society for Optics and Photonics; 2015. p. 93970O-93970O-93978.

<http://www.hummod.org> – model HumMod, University of Mississippi Medical Center, 2015

<http://www.physiolibrary.org> - Physiolibrary, Charles University in Prague, M. Mateják, 2015

<http://www.physiomodel.org> – Physiomodel, Charles University in Prague, M. Mateják, 2015

<http://www.wikipedia.org> – Wikipedia, Wikimedia Foundation, 2015

APPENDIX A – LIST OF PUBLICATIONS OF AUTHOR

Publications related to thesis

1. Mateják Marek, Kulhánek Tomáš, Matoušek Stanislav. Adair-based hemoglobin equilibrium with oxygen, carbon dioxide and hydrogen ion activity. Scandinavian Journal of Clinical and Laboratory Investigation, **IF: 2.009**, ISSN: 0036-5513 (print), 1502-7686 (electronic).
2. T. Kulhánek, J. Kofránek, and M. Mateják. Modeling of short-term mechanism of arterial pressure control in the cardiovascular system: Object oriented and acausal approach. Computers in Biology and Medicine, Received 15 May 2014, Accepted 22 August 2014, Available online 1 September 2014.<http://dx.doi.org/10.1016/j.combiomed.2014.08.025>, **IF: 1.475**, ISSN: 0010-4825
3. T. Kulhanek, M. Matejak, J. Silar, and J. Kofranek. Parameter estimation of complex mathematical models of human physiology using remote simulation distributed in scientific cloud. In Biomedical and Health Informatics (BHI), 2014 IEEE EMBS International Conference on, pages 712–715, June 2014.
4. Marek Mateják, Tomáš Kulhánek, Jan Šilar, Pavol Privitzer, Filip Ježek, Jiří Kofránek: Physiolibrary -Modelica library for Physiology, In Conference Proceeding, 10th International Modelica Conference 2014, March 12, 2014 (1st price)
5. Tomáš Kulhánek, Marek Mateják, Jan Šilar, Jiří Kofránek: Identifikace fyziologických systémů, sborník příspěvků MEDSOFT 2014, ISSN 1803-8115, 148-153
6. Marek Mateják: Physiolibrary - fyziológia v Modelice, sborník příspěvků MEDSOFT 2014, ISSN 1803-8115, 165-172
7. Filip Ježek, Anna Doležalová, Marek Mateják: Vývoj modelu pro výukovou aplikaci ECMO, sborník příspěvků MEDSOFT 2014, ISSN 1803-8115, 82-89
8. Mateják,M.: Krvné plyny, acidobáza a hemoglobín. 19. Konferencia Slovenských a Českých Patofyziológov, Lekárska fakulta MU Brno, 5.-6. září 2013, GRIFTART s.r.o. Brno, ISBN 978-80-905337-3-8
9. Mateják, Marek: Simulovanie ketoacidózy. In MEDSOFT 2013, (Milena Ziethamlová Ed.) Praha: Agentura Action M, Praha, str.140-150, ISSN 1803-8115.
10. Mateják, Marek, Nedvědová, Barbora, Doležaloví, Anna, Kofránek, Jiří, Kulhánek, Tomáš: Model ECMO oxygenátoru. In MEDSOFT 2012, (Milena Ziethamlová Ed.) Praha: Agentura Action M, Praha, str. 205-214, ISSN 1803-8115.

11. Jiří Kofránek, Marek Mateják, Pavol Privitzer: HumMod - large scale physiological model in Modelica. 8th International Modelica Conference 2011, Dresden.
12. Marek Mateják, Jiří Kofránek: HUMMOD - GOLEM EDITION - ROZSÁHLÝ MODEL FYZIOLOGICKÝCH SYSTÉMŮ. In Medsoft 2011
13. Jiří Kofránek: KOMPLEXNÍ MODELY FYZIOLOGICKÝCH SYSTÉMŮ JAKO TEORETICKÝ PODKLAD PRO VÝUKOVÉ SIMULÁTORY. In Medsoft 2011
14. Filip Ježek, Marek Mateják, Pavol Privitzer: Simulace tlakových a průtokových křivek u různě velikých pacientů s pulsatilní srdeční podporou. In Medsoft 2011
15. Mateják,M., Kofránek,J.: Quantitative human physiology – rozsiahly model fyziologických regulácií ako podklad pre lekársky výukový simulátor. 18. Konferencia Slovenských a Českých Patofyziológov, Lekárska fakulta UPJŠ Košice, 9.-10. september 2010, (Roman Beňačka Ed.), Equilibria s.r.o. Košice
16. Privitzer,P., Mateják,M., Šilar,J., Tribula,M., Kofránek,J.: Od modelu k simulátoru v internetovom prehliadači. 18. Konferencia Slovenských a Českých Patofyziológov, Lekárska fakulta UPJŠ Košice, 9.-10. september 2010, (Roman Beňačka Ed.), Equilibria s.r.o. Košice
17. Marek Mateják, Jiří Kofránek: Rozsáhlý model fyziologických regulací v modelice. MEDSOFT 2010. Praha: Agentura Action M, Praha 2010, str. 66-80. ISSN 1803-81115
18. Jiří Kofránek, Matoušek Stanislav, Marek Mateják: Modelování acidobazické rovnováhy. MEDSOFT 2010. Praha: Agentura Action M, Praha 2010, str. 66-80. ISSN 1803-81115
19. Jiří Kofránek, Marek Mateják: Electrophysiology in Modelica, Introduction to large models: Quantitative Human Physiology; Modeling Multiscale Cardiovascular and Respiratory System Dynamics, Physiome Project – National Simulation Project. August 23-27,2010, N140 William H.Foege Building, Univesity of Washington, Seattle, WA 98195; http://www.physiome.org/Course/Session_1/index.html
20. Jiří Kofránek, Marek Mateják, Pavol Privitzer: Dřinu strojům – moderní softwarové nástroje pro tvorbu simulačního jádra výukových programů, MEFANET 2009, 3. Konference lékařských fakult ČR a SR s mezinárodní účastí na téma e-learning a zdravotnická informatika ve výuce lékařských oborů, Masarykova Univerzita, Brno, 2009, ISBN 978-80-7392-118-7
21. Jiří Kofránek, Marek Mateják, Pavol Privitzer: Kreativní propojení objektových technologií pro tvorbu výukových biomedicínských simulátorů. **OBJEKTY 2009**, Ročník konference, Hradec Králové, 5.-6.11.2009, (Pavel Kříž Ed.), Gaudeamus, Hradec Králové, s. 1-21. ISBN 978-80-7435-009-2
22. Jiří Kofránek, Pavol Privitzer, Marek Mateják, Martin Tribula: Akauzální modelování – nový přístup pro tvorbu simulačních her. MEDSOFT 2009. (Milena Zeithamlová Ed.) Praha: Agentura Action M, Praha 2008, str. 31-37. ISBN 978-80-904326-0-4
23. Jiří Kofránek, Marek Mateják, Pavol Privitzer: Causal or acausal modeling: labour for humans or labour for machines. In Technical Computing Prague 2008, 16th Annual Conference Proceedings. (Cleve Moler, Aleš Procházka, Robert bartko, Martin Folin, Jan

Houška, Petr Byron Eds). Humusoft s.r.o., Prague, 2008, ISBN 978-80-7080-692-0. CD ROM, str. 1-16, [Online] http://www2.humusoft.cz/kofranek/058_Kofranek.pdf.

24. Marek Mateják, Jiří Kofránek, Jan Rusz: Akauzální „vzkřísení“ Guytonova diagramu. MEDSOFT 2009. (Milena Zeithamlová Ed.) Praha: Agentura Action M, Praha 2008, str. 105-120. ISBN 978-80-904326-0-4
25. Jiří Kofránek, Jan Rusz, Marek Mateják: From Guyton's graphic diagram to multimedia simulators for teaching physiology. (Resurrection of Guyton's Chart for educational purpose) **Proceedings of the Jackson Cardiovascular-Renal Meeting 2008**. (Stephanie Lucas Ed,), CD ROM, 11. pp.
26. Marek Mateják, Jiří Kofránek: Modelica vs. blokovo-orientované jazyky matematického modelovania. In **OBJEKTY 2008** (Žilina SR): Žilinská Univerzita, 20.-21.11.2008, (Jan Janech Ed.), Edis, Žilina, s. 79-94. ISBN 978-80-8070-923-3
27. Marek Mateják: SVK 9/ Jazyky pre fyziologické modelovanie
28. Kofránek Jiří, Andrlík Michal, Mateják Marek, Matoušek Stanislav, Privitzer Pavol, Stodulka Petr, Tribula Martin, Vacek Ondřej: Škola (multimediální simulační) hrou: využití multimediálních aplikací a simulačních modelů ve výuce patologické fyziologie, Sborník 17. Konference českých a slovenských patofyziologů, 11-12. září 2008, ISBN 978-80-254-0863-6, CD ROM příloha

Publications not related to thesis

1. Jiří Kofránek, Stanislav Matoušek, Jan Rusz, Petr Stodulka, Pavol Privitzer, Marek Mateják, Martin Tribula,: Atlas of physiology and pathophysiology - web-based multimedia teaching tool with simulation games. Computer Methods and Programs in Biomedicine 2011, **IF: 1.516**, ISSN: 0169-2607.
2. Kulhánek T., Mateják M., Šilar J.,Privitzer P., Tribula M., Ježek F., Kofránek J.: Hybridní architektura pro webové simulátory. MEDSOFT 2013, str. 115-121, ISSN 1803-8115
3. Šilar J., Staváker K., Mateják M., Privitzer P., Nagy J.: Modeling with Partial Differential Equations - Modelica Language Extension Proposal. OpenModelica Annual Workshop February 3, 2014
4. Kulhánek T., Mateják M., Šilar J., Privitzer P., Tribula M., Ježek F., Kofránek J.: RESTful web service to build loosely coupled web based simulation of human physiology: IEEE EMBC 2013, Osaka, Japan 3-7 July 2013, late breaking research poster, published in August 2013, Trans JSMBE, ONLINE ISSN: 1881-4379
5. Kulhánek T, Mateják M., Šilar J., Privitzer P., Tribula M., Ježek F., Kofránek J. Hybrid architecture for web simulators of pathological physiology. EFMI STC 2013 Prague 17-19 April 2013. WS1 workshop.
6. Privitzer P., Šilar J., Kulhánek T., Mateják M., Kofránek J.: Simulation Applications in Medical Education. EFMI STC 2013 Prague 17-19 April 2013. WS1 workshop.

7. Ježek, Filip, Kroček, Tomáš, Mateják, Marek, Kofránek, Jiří: Zkušenosti z inovace výuky modelování a simulace na FEL ČVUT. In MEDSOFT 2012, (Milena Ziethamlová Ed.) Praha: Agentura Action M, Praha, str. 139-146, ISSN 1803-8115.
8. Jiří Kofránek, Pavol Privitzer, Marek Mateják, Stanislav Matoušek: Use of Web Multimedia Simulation in Biomedical Teaching, Worldcomp 2011, Las Vegas.
9. Martin Tribula, Marek Mateják, Pavol Privitzer: Webový simulátor ledvin. MEDSOFT 2010. Praha: Agentura Action M, Praha 2010, str. 201-210. ISSN 1803-81115
10. Jiří Kofránek, Pavol Privitzer, Marek Mateják, Ondřej Vacek, Martin Tribula, Jan Rusz: Schola ludus in modern garment: use of web multimedia simulation in biomedical teaching. Proceedings of the 7th IFAC Symposium on Modeling and Control in Biomedical Systems, Aalborg, Denmark, August 12-14, 2009, 425-430
11. Jiří Kofránek, Marek Mateják, Stanislav Matoušek, Pavol Privitzer, Martin Tribula, Ondřej Vacek: School as a (multimedia simulation) play: use of multimedia applications in teaching of pathological physiology. In MEFANET 2008. (Daniel Schwarz, Ladislav Dušek, Stanislav Štípek, Vladimír Mihál Eds.), Masarykova Univerzita, Brno, 2008, ISBN 978-80-7392-065-4, CD ROM, str. 1-26, [Online]
<http://www.mefanet.cz/res/file/articles/prispevek-mefanet-anglicky-kofranek.pdf>
12. Kofránek Jiří, Mateják Marek, Matoušek Stanislav, Privitzer Pavol, Stodulka Petr, Tribula Martin, Vacek Ondřej, Hlaváček Josef: Škola (simulační) hrou. Sborník 17. Konference českých a slovenských patofyziologů, 11-12. září 2008, str.14
13. Kofránek Jiří, Privitzer Pavol, Stodulka Petr, Tribula Martin, Mateják Marek: Metodologie tvorby webových výukových simulátorů. Sborník 17. Konference českých a slovenských patofyziologů, 11-12. září 2008, str.19-20

APPENDIX B – SELECTED EQUATIONS

Chemical equations	
$n_A = \int \partial n_A$	Amount of substance A
$x_A = \frac{n_A}{n_{solution}} = c_A \cdot \frac{V_{solution}}{n_{solution}} = b_A \cdot \frac{m_{solvent}}{n_{solution}}$	Mole fraction of the substance A
$a_A = \gamma_A \cdot x_A$	Mole fraction based activity of the substance A
$\mu_A = \mu_A^0 + T \cdot R \cdot \ln(a_A) + F \cdot z_A \cdot \varphi$	Electrochemical potential of the substance A in the solution
$\mu_A^0 = H_{m,A} - T \cdot S_{m,A}$	Chemical potential of the pure substance A
$\partial n_p = -k_C \cdot \sum (v_i \cdot \mu_{A_i})$	Rate of chemical process $O \rightleftharpoons v_1 A_1 + v_2 A_2 + \dots$, where v_i is negative for reactants
$\partial n_j = v_j \cdot \partial n_p$	Molar change of the substance
$n = \sum n_j$	$H = \sum (n_j \cdot H_{m,j})$
$m = \sum (n_j \cdot M_{m,j})$	$S = \sum (n_j \cdot S_{m,j})$
$V = \sum (n_j \cdot V_{m,j})$	$Q = \sum (n_j \cdot Q_{m,j})$
$U = H - p \cdot V$	Internal energy of the chemical solution
$G = H - T \cdot S$	Gibbs energy of the chemical solution
$x_S = x_Q \cdot \prod_i \frac{x_{P_i}}{x_Q}$	Equilibrium of the specific macromolecule form S composed from the specific independent primary structure subunits P_i in the macromolecule quaternary structure Q
$\sum \partial n_i = 0$	Kirchhoff's junction rule for molar flows

Recalculation of chemical parameters from substance properties

$K = \prod a_j^{v_j} = e^{-\left(\frac{\sum(v_j \mu_j^0)}{R \cdot T}\right)}$	Equilibrium (dissociation) coefficient of the chemical reaction
$\Pi = \frac{\mu_{out}^0 - \mu_{in}^0}{V_m} = \frac{R \cdot T}{V_m} \ln\left(\frac{a_{in}}{a_{out}}\right)$	Osmotic pressure (equilibrium of each uncharged permeable substance across membrane)
$\varphi = \varphi_{out} - \varphi_{in} = \frac{R \cdot T}{F \cdot z_j} \ln\left(\frac{a_{in}}{a_{out}}\right)$	Membrane potential (equilibrium of each charged permeable substance across membrane)
$k_{xH} = \frac{a_d}{a_g} = e^{\frac{\mu_g^0 - \mu_d^0}{R \cdot T}}$	Henry's coefficient (equilibrium of gas dissolution in liquid)
$\Delta_f H_{dissolved} = \Delta_f H_{gaseous} + 298 \cdot C$	Molar enthalpy change of gass dissolution from Henry's constant C at 25°C
$k_{xH} = M \cdot k_{H,NIST}$ Water solution: $k_{xH} = 0.018 \cdot k_{H,NIST}$	Recalculation of Henry's coefficients. M is molar mass of solvent in 'kg/mol', $k_{H,NIST}$ is Henry's coefficient in 'mol/kg*bar' as presented by NIST ² at 25°C and 1 bar.
$p_{vap} = p_{air} \cdot e^{-\left(\frac{\mu_g^0 - \mu_d^0}{R \cdot T}\right)} \cdot a_d$	Raoult's vapor pressure (vaporization equilibrium)
$k_s = \frac{a_d}{a_g} = e^{\frac{\mu_g^0 - \mu_d^0}{R \cdot T}}$	Sieverts' coefficient (equilibrium of gas dissolution in solids)
$V_{m,A} = \frac{2478 \cdot \ln(a_A)}{\Pi_A}$	Molar volume of the incompressible substance A from its osmotic pressure at 25°C and 1 bar.
$D = \frac{a_{in}}{a_{out}} = e^{38.93 \cdot \varphi}$	Donnan's equilibrium coefficient of ions with charge +1 at 25°C and 1 bar: D=Cation _{in} /Cation _{out}

² U.S. Department of Commerce: National Institute of Standards and Technology (<http://webbook.nist.gov/chemistry/>)

Thermal equations

$H = \int \partial H$	Heat accumulation
$T = 310.15 + \frac{H}{n \cdot c_p}$	Temperature
$\partial H = Cond \cdot (T_{in} - T_{out})$	Heat convection
$\partial H = \partial n \cdot (T \cdot c_{p,H_2O} + (H_{m,H2O(g)} - H_{m,H2O(l)}))$	Change of heat by vaporization of water
$T_{outflowing} = T_{environment}$	Ideal radiator (e.g. microcirculation)
$\sum \partial H_i = 0$	Kirchhoff's junction rule for heat flows

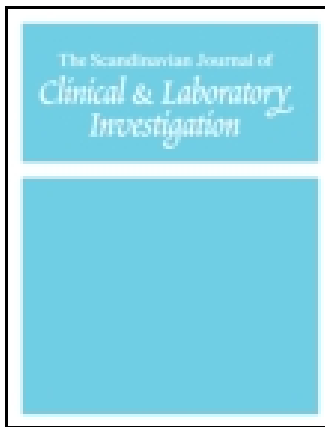
Population equations

$sz = \int \partial sz$	Size of population
$\partial sz = \partial sz p_m \cdot sz$	Change of population
$\sum \partial sz_i = 0$	Kirchhoff's junction rule for population flows

Hydraulic equations

$V = \int \partial V$	Volume accumulation
$p = \begin{cases} \frac{V - V_0}{C} + p_{Ext}, & V_0 \leq V \\ p_{Ext}, & V \leq V_0 \end{cases}$	Pressure in container with elastic walls (e.g. blood or lymph vessels)
$\partial V = \frac{(p_{in} - p_{out})}{R}$	Hydraulic resistance /conductance
$p_{down} = p_{up} + g \cdot \rho \cdot h$	Pascal's law
$\partial V = \begin{cases} G_{off} \cdot (p_{in} - p_{out}), & closed \\ G_{on} \cdot (p_{in} - p_{out}), & open \end{cases}$	Idealized hydraulic valve
$\partial V = \int \frac{p_{in} - p_{out}}{Inertance}$	Hydraulic inertia
$\sum \partial V_i = 0$	Kirchhoff's junction rule for volumetric flows

APPENDIX C – PUBLICATIONS IN EXTENSO



Scandinavian Journal of Clinical and Laboratory Investigation

Publication details, including instructions for authors and subscription information:
<http://www.tandfonline.com/loi/iclb20>

Adair-based hemoglobin equilibrium with oxygen, carbon dioxide and hydrogen ion activity

Marek Mateják^a, Tomáš Kulhánek^a & Stanislav Matoušek^a

^a The Institute of Pathological Physiology, First Faculty of Medicine, Charles University in Prague, Czech Republic

Published online: 15 May 2015.

To cite this article: Marek Mateják, Tomáš Kulhánek & Stanislav Matoušek (2015) Adair-based hemoglobin equilibrium with oxygen, carbon dioxide and hydrogen ion activity, Scandinavian Journal of Clinical and Laboratory Investigation, 75:2, 113-120

To link to this article: <http://dx.doi.org/10.3109/00365513.2014.984320>

PLEASE SCROLL DOWN FOR ARTICLE

Taylor & Francis makes every effort to ensure the accuracy of all the information (the "Content") contained in the publications on our platform. However, Taylor & Francis, our agents, and our licensors make no representations or warranties whatsoever as to the accuracy, completeness, or suitability for any purpose of the Content. Any opinions and views expressed in this publication are the opinions and views of the authors, and are not the views of or endorsed by Taylor & Francis. The accuracy of the Content should not be relied upon and should be independently verified with primary sources of information. Taylor and Francis shall not be liable for any losses, actions, claims, proceedings, demands, costs, expenses, damages, and other liabilities whatsoever or howsoever caused arising directly or indirectly in connection with, in relation to or arising out of the use of the Content.

This article may be used for research, teaching, and private study purposes. Any substantial or systematic reproduction, redistribution, reselling, loan, sub-licensing, systematic supply, or distribution in any form to anyone is expressly forbidden. Terms & Conditions of access and use can be found at <http://www.tandfonline.com/page/terms-and-conditions>

ORIGINAL ARTICLE

Adair-based hemoglobin equilibrium with oxygen, carbon dioxide and hydrogen ion activity

MAREK MATEJÁK, TOMÁŠ KULHÁNEK & STANISLAV MATOUŠEK

*The Institute of Pathological Physiology, First Faculty of Medicine, Charles University in Prague, Czech Republic***Abstract**

As has been known for over a century, oxygen binding onto hemoglobin is influenced by the activity of hydrogen ions (H^+), as well as the concentration of carbon dioxide (CO_2). As is also known, the binding of both CO_2 and H^+ on terminal valine-1 residues is competitive. One-parametric situations of these hemoglobin equilibria at specific levels of H^+ , O_2 or CO_2 are also well described. However, we think interpolating or extrapolating this knowledge into an ‘empirical’ function of three independent variables has not yet been completely satisfactory. We present a model that integrates three orthogonal views of hemoglobin oxygenation, titration, and carbamination at different temperatures. The model is based only on chemical principles, Adair’s oxygenation steps and Van’t Hoff equation of temperature dependences. Our model fits the measurements of the Haldane coefficient and CO_2 hemoglobin saturation. It also fits the oxygen dissociation curve influenced by simultaneous changes in H^+ , CO_2 and O_2 , which makes it a strong candidate for integration into more complex models of blood acid-base with gas transport, where any combination of mentioned substances can appear.

Key Words: Acid-base equilibrium, blood gas analysis, carboxyhemoglobin, hemoglobin A, oxyhemoglobins

Abbreviations: ODC, hemoglobin oxygen dissociation curve; 2,3-DPG, 2,3-diphosphoglycerate; [X], molar concentration of X in mol.m⁻³; aH⁺, activity of hydrogen ions, where pH = $-\log_{10}(aH^+)$; αO₂, O₂ solubility in mol.m⁻³.Pa⁻¹; αCO₂, CO₂ solubility in mol.m⁻³.Pa⁻¹; pO₂, partial pressure of O₂ in Pa; pCO₂, partial pressure of CO₂ in Pa; Hb_u, hemoglobin alpha or beta subunit; Hb_{uD}, deoxygenated Hb_u; Hb_{uO}, oxygenated Hb_u; Hb_uNH₃⁺, Hb_u with protonated Nterminus; Hb_{uD}NH₃⁺, Hb_{uD} with protonated Nterminus; Hb_{uO}NH₃⁺, Hb_{uO} with protonated Nterminus; Hb_uNH₂, Hb_u with -NH₂ form of Nterminus; Hb_{uD}NH₂, Hb_{uD} with -NH₂ form of Nterminus; Hb_{uO}NH₂, Hb_{uO} with -NH₂ form of Nterminus; Hb_{uD}COO⁻, Hb_{uD} with carboxylated Nterminus; Hb_{uD}COO⁻, Hb_{uD} with carboxylated Nterminus; Hb_uAH, Hb_u with protonated side-chains; Hb_{uD}AH, Hb_{uD} with protonated side-chains; Hb_{uO}AH, Hb_{uO} with protonated side-chains; Hb_uA⁻, Hb_u with deprotonated side-chains; Hb_{uD}A⁻, Hb_{uD} with deprotonated side-chains; Hb_{uO}A⁻, Hb_{uO} with deprotonated side-chains; Hb_uA⁻NH₂, selected normalized form of Hb_u with deprotonated side-chains and NH₂ form of Nterminus; Hb_{uD}A⁻NH₂, deoxygenated form of Hb_uA⁻NH₂; Hb_{uD}A⁻NH₂, oxygenated form of Hb_uA⁻NH₂; f_{uD}, fraction of Hb_{uD}A⁻NH₂ from Hb_{uD}; f_{uO}, fraction of Hb_{uD}A⁻NH₂ from Hb_{uD}; f_{zCD}, fraction of Hb_{uD}NH₂ form Hb_{uD}; f_{zCO}, fraction of Hb_{uD}NH₂ form Hb_{uD}; f_{hD}, fraction of Hb_{uD}A⁻ form Hb_{uD}; f_{hO}, fraction of Hb_{uD}A⁻ form Hb_{uD}; ΔH⁺_h, change of valence (charge) on side-chains during deoxygenation per one Hb_u; ΔH⁺_z, protonation of -NH₂ form of Nterminus during deoxygenation per one Hb_u; ΔH⁺_c, decarboxylation of carboxylated Nterminus during deoxygenation per one Hb_u; ΔH⁺, Haldane coefficient per hemoglobin subunit; Hb_t, hemoglobin tetramer without bound O₂ molecules; (O₂)_iHb_t, hemoglobin tetramer with the number of i bound O₂ molecules; (O₂)_iHb_{tn}, hemoglobin tetramer composed only of Hb_uA⁻NH₂ subunit forms with the number of i bound O₂ molecules; sO₂, O₂ saturation of hemoglobin; sCO_{2D}, CO₂ saturation of deoxyhemoglobin; sCO_{2O}, CO₂ saturation of oxyhemoglobin; sCO₂, CO₂ saturation of hemoglobin; tCO₂, total concentration of CO₂ = free dissolved CO₂ + HCO₃⁻ + CO₃²⁻ + Hb_uCOO⁻; dTH, shift of titration curve with the change of both pO₂ and pCO₂ to zero, which equals to how many moles of strong acid must be added to one mole of Hb_u to reach the pH of the chosen standard titration curve (O₂ and CO₂ free); pH, acidity/basicity of hemoglobin solution (e.g. inside erythrocytes); pH_p, pH in plasma (e.g. acidity/basicity of blood).

Correspondence: Marek Mateják, U Nemocnice 5, Prague 2, 128 53, Czech Republic. Tel: + 420 776 301 395. Fax: + 420 224 965 916. E-mail: marek.matejak@lf1.cuni.cz

(Received 20 June 2014; accepted 2 November 2014)

Introduction

Human hemoglobin A is one of the most extensively studied protein macromolecules. The composition and 3D conformation of both α and β chains is known [1,2] and the binding of O_2 , H^+ and 2,3-DPG has been described [2,3]. Since the 1930s it has generally been believed that CO_2 binding to Hb occurs by carbamination of the amino-terminus, i.e. forming a carboxylate compound [4–6]. This hemoglobin carbamination was verified by Morrow et al. [7], who used nuclear magnetic resonance of $^{13}CO_2$ to find its exact binding sites at valine-1. The shift of titration between oxygenated and deoxygenated forms is also well known. Called the Bohr or Haldane effect [8–10], it is caused by the same valine-1 side and by more than 10 other acid-base residues [2,11].

The most common descriptions of the hemoglobin oxygen dissociation curve (ODC) are the allosteric models [12,13], the model based on Hill equation [14,15], and Adair's four-step model [16]. Some of the ODC models [15,17,18] also include the effects of varying pH and CO_2 concentration. However, these models operate only with interpolation or extrapolation of ODC from normal pH or normal pCO_2 and do not take into account the chemical dependences between titration [8] and carbamation [19]. They fail when both pH and CO_2 are not at normal values, especially in the alkaline pH range.

Based on these findings, we propose a hemoglobin binding equilibrium model that starts with a description of hemoglobin-oxygen dissociation using a slightly modified version of Adair's approach [16]. We continue by describing the relationship between CO_2 and H^+ as competitive inhibition in the amino group of terminal valine-1 residue on each chain (suffixes z and c), which is in accordance with the known facts [4,6,20]. Finally, we lump all other acid-base side chains residues in a hemoglobin subunit into one Bohr proton-binding site of the side chain residues. These are denoted by the suffix h in the article.

Methods

The model is built in Mathematica 9.0 (Wolfram, Champaign, IL, USA) and also in Dymola FD01 2014 (Dassault Systemes, Paris, France) as an example of chemical package in open-source Modelica library Physiolibrary 2.2.0 (<http://www.physiolibrary.org>) [21,22] according to the model structure defined in the following section. The model contains only physiological parameters such as gas solubilities and dissociation coefficients of defined reactions. The unknown parameters are fitted to the data of Sigaard-Andersen [23], Bauer and Schröder [24], Severinghaus [18], Matthew et al. [1] and Reeves [25]

using Mathematica function FindFit and also using parameter estimation method suggested by Kulhanek et al. [26].

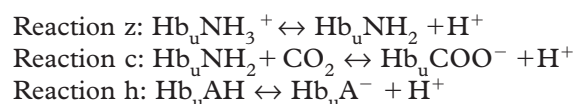
Free dissolved concentrations of $[O_2]$ and $[CO_2]$ in red blood cells are calculated from gas partial pressures using Henry's law ($[O_2] = \alpha O_2 * pO_2$ and $[CO_2] = \alpha CO_2 * pCO_2$) with solubility coefficients $\alpha O_2 = 1.005 * 10^5 \text{ mol.m}^{-3}.\text{Pa}^{-1}$ measured at 38°C by Sendroy et al. [27], and $\alpha CO_2 = 2.3 * 10^4 \text{ mol.m}^{-3}.\text{Pa}^{-1}$ at 37°C , as proposed by Maas et al. [28]. These solubilities are slightly different from solubilities in pure water or in plasma because of the effects of salts and proteins inside erythrocyte [27].

Model structure

The model is built upon several simplifying assumptions. Firstly, each of four hemoglobin tetramer subunits is treated as identical, even though (slight) differences are known to exist between α and β subunits. Secondly, CO_2 or H^+ binding is supposed not to affect the CO_2 or H^+ affinities in the other three subunits. Thus, the interaction between the subunits is modeled purely through the varying affinities of oxygen in each oxygenation step. The third simplifying assumption has already been mentioned; it is lumping all Bohr proton binding sites of subunit into two (first for the valine-1 amino-terminus and second for the side chains residues), a simplification first suggested by Antonini [29].

Model structure of hemoglobin subunit

The three reactions that participate in the Bohr and Haldane effect of each subunit are as follows:



where the reactions z and c are competitive on the valine-1 amino-terminus, and the reaction h is independent of z or c .

The chemical equilibrium equations of these three reactions are Equations 1–3, where K_x is the equilibrium dissociation coefficients of the reaction x (i.e. z , c or h).

$$\text{Reaction z: } K_z = \frac{[Hb_u NH_2] * aH^+}{[Hb_u NH_3^+]} \quad (1)$$

$$\text{Reaction c: } K_c = \frac{[Hb_u COO^-] * aH^+}{[CO_2] [Hb_u NH_2]} \quad (2)$$

$$\text{Reaction h: } K_h = \frac{[Hb_u A^-] * aH^+}{[Hb_u AH]} \quad (3)$$

These dissociation coefficients are different between oxy and deoxy subunits, which are distinguished by the subscripts O and D in the following text. They can be also written in their logarithmic

form, where pK_x means $-\log_{10}(K_x)$. Thus, for instance, pK_{z0} denotes the equilibrium coefficient of the reaction z for the oxy form of the hemoglobin subunit. Similar notation is used for describing the activity of hydrogen ions (acidity), where $\text{pH} = -\log_{10}(aH^+)$.

Using Equations 1–3 it is possible to express fractions of chosen species for deoxy and oxy subunits. We label these fractions as follows: $Hb_u^{NH_2}$ fractions are called f_{zcD} (f_{zcO}), $Hb_u^{A^-}$ fractions f_{hD} (f_{hO}), $Hb_u^{A^-NH_2}$ fractions fn_D (fn_O) and $Hb_u^{COO^-}$ fractions sCO_{2D} (sCO_{2O}) as in Equation 4–7. The selection of form $Hb_u^{A^-NH_2}$ from the orthogonal division into $Hb_u^{NH_2}$ and $Hb_u^{A^-}$ is also illustrated in Figure 1A, B.

$$f_{zcD} = \frac{[Hb_{uD}^{NH_2}]}{[Hb_{uD}]} = \frac{1}{1 + 10^{pKzD - pH} + [CO_2]10^{pH - pKcD}} \quad (4)$$

$$f_{hD} = \frac{[Hb_{uD}^{A^-}]}{[Hb_{uD}]} = \frac{1}{10^{pKhD - pH} + 1} \quad (5)$$

$$fn_D = \frac{[Hb_{uD}^{A^-NH_2}]}{[Hb_{uD}]} = f_{zcD} \times f_{hD} \quad (6)$$

$$sCO_{2D} = \frac{[Hb_{uD}^{COO^-}]}{[Hb_{uD}]} = 10^{pH - pKcD} f_{zcD} [CO_2] \quad (7)$$

We define a titration shift as the amount of acid that must be added to achieve the same pH after full

deoxygenation of the hemoglobin subunit. This change of subunit charge during deoxygenation (by the Bohr protons) is also called Haldane coefficient ΔH^+ . The coefficient can be divided into contributions of the previously mentioned reactions $\Delta H^+_{h^*}$, $\Delta H^+_{z^*}$ and $\Delta H^+_{c^*}$, as is algebraically expressed by Equations 8–11.

$$\Delta H^+_h = -\frac{[Hb_{uD}^{A^-}] - [Hb_{uD}^{A^-}]}{[Hb_u]} = -(f_{hD} - f_{hO}) \quad (8)$$

$$\begin{aligned} \Delta H^+_z &= \frac{[Hb_{uD}^{NH_3^+}] - [Hb_{uD}^{NH_3^+}]}{[Hb_u]} \\ &= \left(\frac{10^{pKzD}}{10^{pH}} f_{zcD} - \frac{10^{pKzO}}{10^{pH}} f_{zcO} \right) \end{aligned} \quad (9)$$

$$\begin{aligned} \Delta H^+_c &= -\frac{[Hb_{uD}^{COO^-}] - [Hb_{uD}^{COO^-}]}{[Hb_u]} \\ &= -(sCO_{2D} - sCO_{2O}) \end{aligned} \quad (10)$$

$$\Delta H^+ = \Delta H^+_z + \Delta H^+_c + \Delta H^+_h \quad (11)$$

Model structure of hemoglobin tetramer

Chemical speciation of the hemoglobin tetramer molecule can be considered at various levels of detail; the one chosen as appropriate in our approach is indicated in Figure 1C. The possible forms include different combinations of oxygenated and deoxygenated

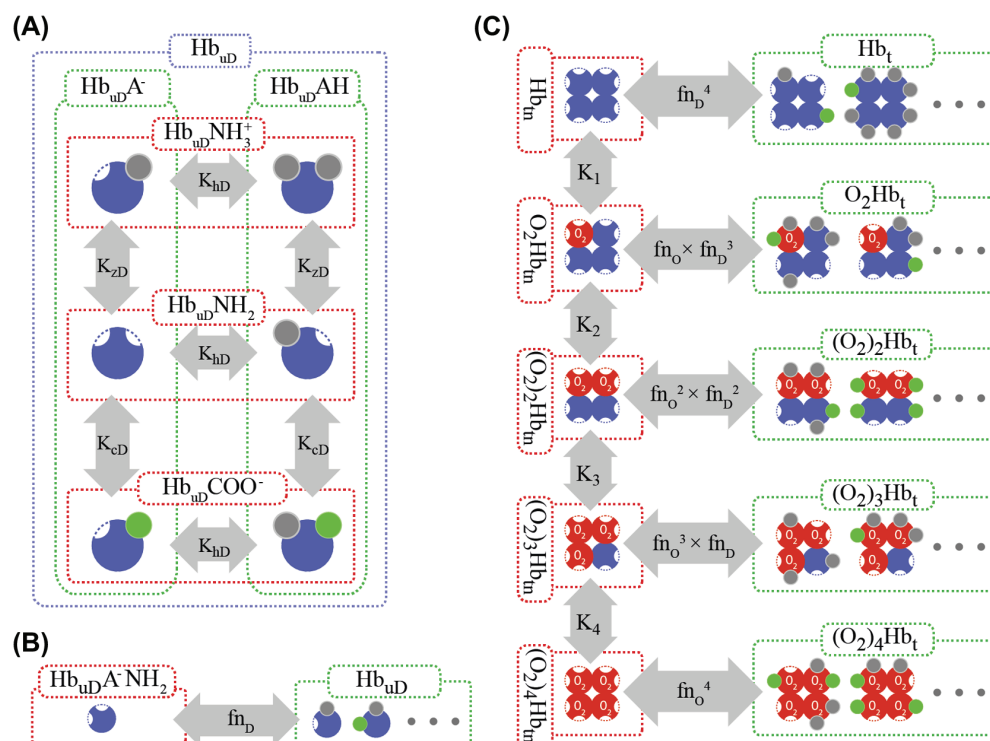
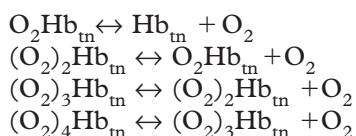


Figure 1. Schema of hemoglobin calculation. (A) Possible forms of deoxyhemoglobin subunit (the blue circles). The gray circles represent hydrogen ions, and the green circles represent carbon dioxide. The arrows with dissociation coefficients represent the reactions z , c and h . (B) Schema of chemical speciation of deoxyhemoglobin subunit. (C) Schema of chemical speciation and Adair's oxygenation steps of hemoglobin tetramer. This Figure is reproduced in color in the online version of *The Scandinavian Journal of Clinical & Laboratory Investigation*.

hemes, protonated and deprotonated oxygen-linked acid groups, and free or carboxylated amino endings of each chain. Yet because of the law of detailed balance in equilibrium [30], it is not necessary to calculate all reactions between these forms. As a result, only four oxygenation reactions need be selected for the calculation. This is done in accordance with Figure 1C, by selecting a tetramer form $(O_2)_4 Hb_{tn}$ composed only of four subunits in the form $Hb_u A^- NH_2$ (H^+ and CO_2 free), and modeling oxygen binding to these forms with Adair-type coefficients of the following reactions:



where dissociation coefficients are defined by Equation 12, which are also represented by vertical arrows at Figure 1C.

$$K_i = \frac{[(O_2)_{i-1} Hb_{tn}] \cdot [O_2]}{[(O_2)_i Hb_{tn}]} \quad (12)$$

For the next calculation, all forms can be expressed as a fraction of the deoxy-tetramer form $(O_2)_0 Hb_{tn}$, as shown in Equation 13.

$$[(O_2)_i Hb_{tn}] = \frac{[(O_2)_0 Hb_{tn}] \cdot [O_2]^i}{\prod_{j=1}^i K_j} \quad (13)$$

Let us move the attention from specific forms of Hb_{tn} to the description of the equilibrium within the whole group of Hb_t . Looking at Figure 1C, one can see that for each oxygenation step we can calculate the equilibrium in each horizontal line using Equation 14.

$$[(O_2)_i Hb_t] \cdot f n_D^{4-i} \cdot f n_O^i = [(O_2)_i Hb_{tn}] \quad (14)$$

The CO_2 - and pH-dependent oxygen saturation equation in the Adair style (Equation 15) is algebraically derived from Equation 13–14, where $a_i = \frac{1}{(\prod_{j=1}^i K_j)}$
 $x = (f n_D(pH, [CO_2]) / f n_O(pH, [CO_2])) * [O_2]$.

$$sO_2 = \frac{a_1 x + 2 a_2 x^2 + 3 a_3 x^3 + 4 a_4 x^4}{4 + 4 a_1 x + 4 a_2 x^2 + 4 a_3 x^3 + 4 a_4 x^4} \quad (15)$$

Hemoglobin saturation with CO_2 (sCO_2) is calculated separately in oxygenated and deoxygenated subunits forms (sCO_{2O} and sCO_{2D}) using Equation 16.

$$sCO_2 = sO_2 \cdot sCO_{2O} + (1 - sO_2) \cdot sCO_{2D} \quad (16)$$

Finally, the shift of titration after deoxygenation and decarbamination of the hemoglobin subunit can be expressed by Equation 17.

$$dTH = sO_2 \cdot \Delta H^+ + sCO_{2D} + \frac{sCO_{2D}}{1 + 10^{pH - pK_{zD}}} \quad (17)$$

Temperature dependences

The temperature dependences are integrated using the Van't Hoff equation (Equation 18), where $R = 8.314 \text{ J.K}^{-1}.\text{mol}^{-1}$ is gas constant, ΔH^θ is the standard enthalpy change, i.e. an amount of heat consumed by a reaction changing one mole of substrates to products, and K_2 and K_1 are Henry's coefficients of solution or the dissociation coefficient of the chemical reaction at temperature T_2 and T_1 (expressed in Kelvin).

$$\ln\left(\frac{K_2}{K_1}\right) = \frac{-\Delta H^\theta}{R} \left(\frac{1}{T_2} - \frac{1}{T_1} \right) \quad (18)$$

Results

The Adair's coefficients are fitted to the collection of ODC measurements by Severinghaus [18] at $pCO_2 = 0 \text{ Pa}$ and $pH_p = 7.4$, see Figure 2A and Table I. The dissociation coefficients of carboxylation are determined in close agreement with Bauer and Schröder using their data [24]; the resulting fit can be seen in Figure 2B, the coefficients are in Table II. The lumped acid dissociation coefficients for the side-chains pK_{hD} and pK_{hO} are estimated by optimization of Siggaard-Andersen's data [23] at $DPG/Hbt = 0.84$, $pH = 6.5–8.0$ and 37°C ; the resulting fit can be seen in Figure 2C, and the coefficients complete Table II.

We conclude that the model also describes the ODC shifts by comparing with Naerea et al.'s [31] oxygen saturation measurements at different plasma pH and CO_2 levels, see Figure 2D. The recalculation of data from plasma pH_p to intracellular erythrocyte pH uses the equation $pH = 7.2464 + 0.796(pH_p - 7.4)$, as presented by Siggaard-Andersen and Salling [32].

The gas solubility as Henry's coefficient at different temperatures can be recalculated using the enthalpy of gas solution (-14 kJ.mol^{-1} for O_2 , and -20 kJ.mol^{-1} for CO_2 [33]). If we assume that the examined hemoglobin of Matthew et al. [1] is at compatible conditions, but at a temperature of 30°C with $pK_{zD} = 7.53$, $pK_{zO} = 7.28$, $pK_{cD} = 4.77$ and $pK_{cO} = 5.20$ as plotted in Figure 2E, then the enthalpies of these reactions are -51 , 8 , 59 and -41 kJ.mol^{-1} .

Atha and Ackers measured the heat of hemoglobin oxygenation under conditions independent of carbon dioxide and Bohr protons and not including the oxygen heat of solution, coming to the value of 59 kJ.mol^{-1} [34]. Using this value for each Adair oxygenation step, one can optimize other enthalpies to fit the Reeves data [25] measured at $19–43^\circ\text{C}$ (Figure 2F). Resulting enthalpies are 59 kJ.mol^{-1} for the deoxy and 127 kJ.mol^{-1} for the oxy version of reaction h.

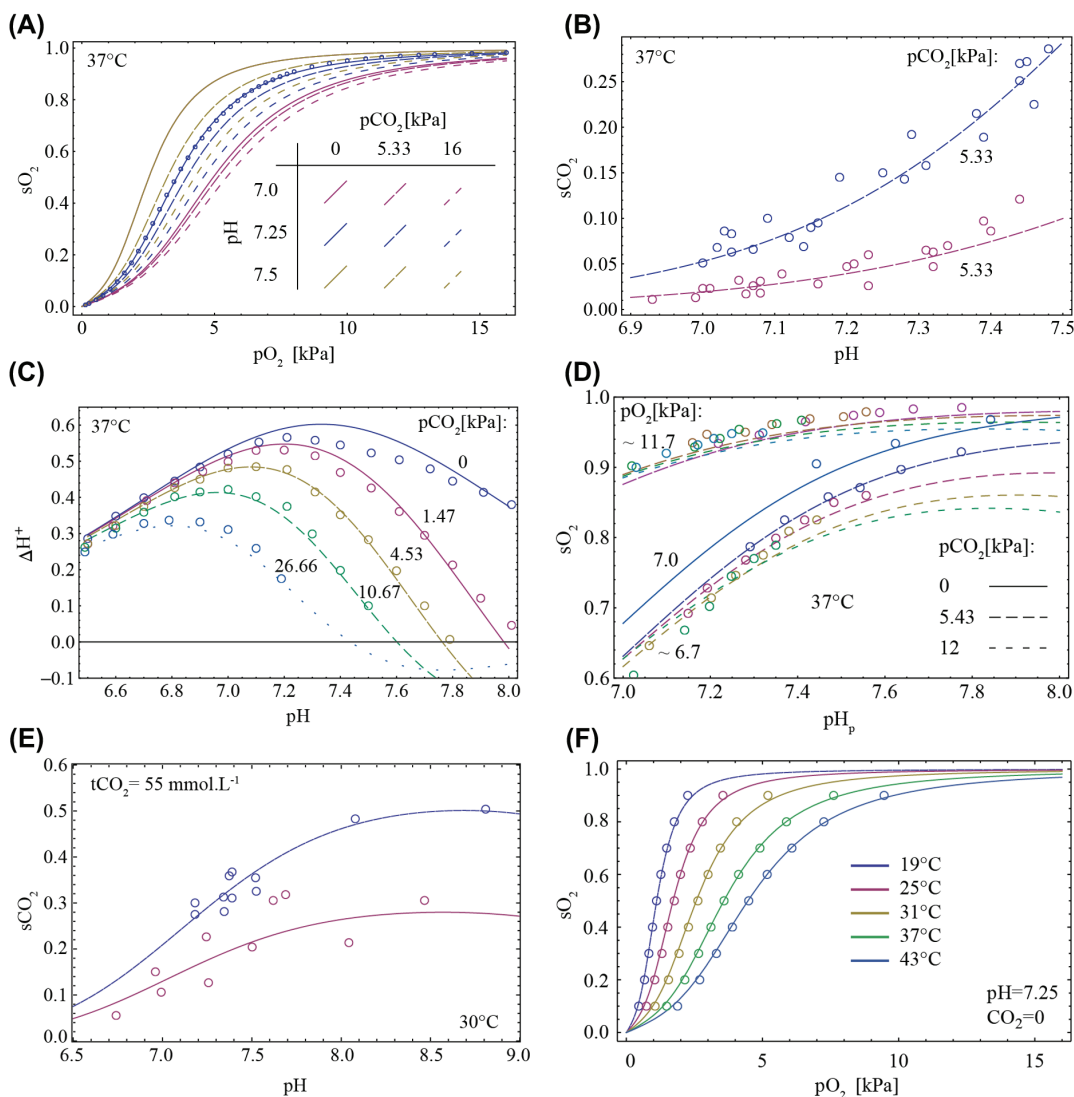


Figure 2. Model curves and measured data points. (A) Points are from Severinghaus's oxygen dissociation curve collection [18] at $pCO_2 = 0$ Pa, erythrocyte intracellular pH = 7.25 and temperature 37°C. Lines are sO_2 defined by Equation 15. (B) Carboxylation of hemoglobin measured and estimated by Bauer and Schröder [24]. The lines (Equation 7) are sCO_{2D} and sCO_{20} at $pCO_2 = 5.33$ kPa. (C) Bohr protons released during oxygenation of one hemoglobin subunit. Dots are data measured by Siggaard-Andersen [23] in erythrolysate at 37°C, DPG/Hb_t = 0.84. Lines are calculated from Equation 11 using coefficients from Table II. From top to bottom data are plotted for different $pCO_2 = 0$ kPa, 1.47 kPa, 4.53 kPa, 10.67 kPa and 26.66 kPa. (D) Naeraa et al.'s [31] oxygen saturation data comparison. The two groups of lines (Equation 15) are determined mainly by pO_2 around 6.7 kPa and 11.7 kPa. The small nuances in each group are caused by different pCO_2 changed from 0–12 kPa. (E) Matthew et al.'s [1] carbamination data measured at 30°C with constant content of all carbonates 55 mmol.L⁻¹. Fitted dissociation constants, which determine the lines, are used to estimate enthalpies of their reactions to be consistent with Bauer and Schröder [24]. (F) Reeves [25] oxygen saturation data at different temperatures. Enthalpies of reaction h and specific Adair oxygenation step enthalpy is estimated (lines) to fit the data (circles). This Figure is reproduced in color in the online version of *The Scandinavian Journal of Clinical & Laboratory Investigation*.

Discussion

Having a precise quantitative description of hemoglobin behavior is a crucial aspect in describing the behavior of whole blood, which has numerous uses in medicine today. It is important in areas such as blood gas analysis [15,34], the building of complex

models [35], simulation for teaching purposes [36], or rebreathing-based methods for cardiac output estimation, which represent a more specific use [37]. For instance, the precision of the latter methods is crucially dependent on the exact calculation of the total amount of carbon dioxide in blood for various

Table I. Estimated form-specific Adair's coefficients [mol.m⁻³] at 37°C.

K_1	K_2	K_3	K_4
0.0121	0.0117	0.0871	0.000386

Table II. Estimated acid dissociation coefficients at 37°C.

Reaction z	Reaction c	Reaction h
$pK_{zD} = 7.73$	$pK_{cD} = 7.54$	$pK_{hD} = 7.52$
$pK_{zO} = 7.25$	$pK_{co} = 8.35$	$pK_{ho} = 6.89$

(abnormal) patient conditions, as has been recently pointed out [38].

This model offers a precise description of various phenomena that take place with hemoglobin, based on relatively simple starting points, such as competitive binding of H^+ and CO_2 at valine-1 amino terminus or the law of detailed balance [30]. Even with a simple structure, it offers a remarkably good fit to the data of hemoglobin oxygenation, titration, and carbamination at different temperatures, as shown in Figure 2A–E. These can be calculated with any combination of oxygen, carbon dioxide and hydrogen ions defined as open system (lungs), where the partial pressures are equilibrated, and also in a closed system (tissues), where mass conservation laws and the total amount of substances take place, as was also modeled by Rees and Andreassen [39], among others.

The results of our model (Figure 2A–E) show strong nonlinear dependences between variables, which is in agreement with the known data [1,23–25,40]. Looking at Figure A, one can compare sets of ODCs, where each color represents a different pH. Various curves of each color represent ODCs for various levels of pCO_2 for a given pH. As can be seen, the effect of pCO_2 on the ODC is stronger at high (alkaline) pH, which is in agreement with the data [23]. Similarly, one can compare the curves within the sets of solid or dashed lines, where each set represents dissociation curves for various values of pH at a given level of pCO_2 . The variation between the curves of each line type represents the Bohr effect for the given level of CO_2 , this effect can also be appreciated from data of Figure 2C, which shows the average amount of released H^+ upon oxygenation of one hemoglobin subunit.

The model uses enthalpies to calculate temperature dependences of hemoglobin behavior (Figure 2F, E), which allows examination of the heat transfers during single chemical processes. For instance, binding of aqueous oxygen onto hemoglobin produces 30–40 kJ/mol of heat [41–44], and the same amount of heat is consumed by deoxygenation process in metabolically active tissues, thus helping to cool them down. When the hemoglobin model is used in the standard conditions of a large-scale HumMod model [35], the resulting heat transfer due to the exothermy of the hemoglobin oxygen reaction is 4–7% of the total heat produced by muscle, which is in agreement with experimental results [41,43,44]. It is interesting to note that this heat transfer occurs without any increase in blood temperature.

The integration of chemical processes in a macromolecule requires a precise view into their underlying principles. Some physiologists use the elementary chemical equations [39], but do not implement the principle of detailed balance [30]. Other physiologists make empirically-based equations with a raw linear gradient approximation of possible combinations of model values [15]. We feel that it is almost

impossible to see the problem as this type of black-box function with more than two inputs. Instead, it is better to have an integrated model of oxygenation, titration and carbamination.

Today, allosteric hemoglobin oxygenation models do exist that seem more in agreement with the structural knowledge of hemoglobin [12,45–47]. These models take into account two or more structurally different forms: relaxed and tensed. However, these models have so far been limited to hemoglobin oxygenation only. Our Adair-based model can explain not only oxygen and carbon dioxide saturation, but also their cooperation with acid-base buffering properties of hemoglobin. All three of these connected phenomena fit to measured data in physiological ranges.

As any work, the presented model has its limitations. First of all, it does not include the effects of changes in Hb tetramer conformations. Also the model could be extended with dependences on electrolytes such as chloride, 2,3-bisphosphoglycerate or other organic phosphates and their binding reactions, as many research studies show these interactions [48–51]. The next extension of this model could be performed by the integration of an intracellular red cell environment to calculate with phosphate acid-base buffers, and finally the membrane changes with blood plasma, where the chloride shift reaches a Gibbs-Donnan equilibrium and establishes chloride, bicarbonate and hydrogen ion activity ratios. Having an integrated model of blood gases and acid-base is crucial if we want the precise computational algorithms of the current state of a patient. These calculations could be used, for example, inside the next generation of medical devices to estimate not only blood properties, but also the connected properties of circulation [37] or metabolic functions [39].

In this article, we present a hemoglobin model that integrates O_2 , CO_2 and H^+ binding. The model is not just empirical, but is based on sound theoretical principles, such as the competitive binding of CO_2 and H^+ on the valine-1 NH_2 terminus, the Bohr and Haldane effect [9,52] and on the principle of detailed balance. The principle of detailed balance is used for the first time in the Adair type of model. The advantages of this approach include explicit formulation of mass and energy conservation principles: The model accumulates substances and heat inside hemoglobin forms, making it very useful for integration in higher-scale dynamic models.

Acknowledgements

In addition, the authors want to thank doc. MUDr. Jiří Kofránek, CSc, and Prof. MUDr. Emanuel Nečas, DrSc, for critical review and Austin Schaefer for English language editing.

This work was supported by grants from the Ministry of Industry and Trade of the Czech Republic: MPO TIP TI3/869 – Virtual patient for medical education; and by The Ministry of Education, Youth and Sports via the grant SVV-2014-260033.

Declaration of interest: The authors report no conflict of interest. The authors alone are responsible for the content and writing of the paper.

References

- [1] Matthew JB, Morrow J, Wittebort RJ, Gurd F. Quantitative determination of carbamino adducts of alpha and beta chains in human adult hemoglobin in presence and absence of carbon monoxide and 2, 3-diphosphoglycerate. *J Biol Chem* 1977;252:2234–44.
- [2] Perutz M. Species adaptation in a protein molecule. *Mol Biol Evol* 1983;1:1–28.
- [3] Perutz M, Kilmartin J, Nishikura K, Fogg J, Butler P, Rollema H. Identification of residues contributing to the Bohr effect of human haemoglobin. *J Mol Biol* 1980;138:649–68.
- [4] Rossi-Bernardi L, Roughton F. The specific influence of carbon dioxide and carbamate compounds on the buffer power and Bohr effects in human haemoglobin solutions. *J Physiol* 1967;189:1–29.
- [5] Forster R, Constantine H, Craw MR, Rotman H, Klocke R. Reaction of CO₂ with human hemoglobin solution. *J Biol Chem* 1968;243:3317–26.
- [6] Stadie WC, O'Brien H. The carbamate equilibrium I. The equilibrium of amino acids, carbon dioxide, and carbamates in aqueous solution; with a note on the Ferguson-Roughton carbamate method. *J Biol Chem* 1936;112:723–58.
- [7] Morrow J, Matthew J, Wittebort R, Gurd F. Carbon 13 resonances of ¹³CO₂ carbamino adducts of alpha and beta chains in human adult hemoglobin. *J Biol Chem* 1976;251:477–84.
- [8] Bohr C, Hasselbalch K, Krogh A. Concerning a biologically important relationship—the influence of the carbon dioxide content of blood on its oxygen binding. *Scand Arch Physiol* 1904;16:402.
- [9] Sigaard-Andersen O, Garby L. The Bohr effect and the Haldane effect. *Scand J Clin Lab Invest* 1973;31:1–8.
- [10] Tyuma I. The Bohr effect and the Haldane effect in human hemoglobin. *Jpn J Physiol* 1984;34:205.
- [11] Matthew J, Hanania G, Gurd F. Electrostatic effects in hemoglobin: hydrogen ion equilibria in human deoxy-and oxyhemoglobin A. *Biochemistry* 1979;18:1919.
- [12] Monod J, Wyman J, Changeux J-P. On the nature of allosteric transitions: a plausible model. *J Mol Biol* 1965;12:88–118.
- [13] Eaton WA, Henry ER, Hofrichter J, Bettati S, Viappiani C, Mozzarelli A. Evolution of allosteric models for hemoglobin. *IUBMB Life* 2007;59:586–99.
- [14] Hill AV. The combinations of haemoglobin with oxygen and with carbon monoxide. I. *Biochem J* 1913;7:471.
- [15] Sigaard-Andersen O, Sigaard-Andersen M. The oxygen status algorithm: a computer program for calculating and displaying pH and blood gas data. *Scand J Clin Lab Invest* 1990;50:29–45.
- [16] Adair GS. The hemoglobin system VI. The oxygen dissociation curve of hemoglobin. *J Biol Chem* 1925;63:529–45.
- [17] Dash RK, Bassingthwaite JB. Erratum to: Blood HbO₂ and HbCO₂ dissociation curves at varied O₂, CO₂, pH, 2, 3-DPG and temperature levels. *Ann Biomed Eng* 2010;38:1683–701.
- [18] Severinghaus JW. Simple, accurate equations for human blood O₂ dissociation computations. *J Appl Physiol* 1979;46:599–602.
- [19] Christiansen J, Douglas C, Haldane J. The absorption and dissociation of carbon dioxide by human blood. *J Physiol* 1914;48:244–71.
- [20] Perrella M, Bresciani D, Rossi-Bernardi L. The binding of CO₂ to human hemoglobin. *J Biol Chem* 1975;250:5413–8.
- [21] Mateják M, Kulhánek T, Šilar J, Privitzer P, Ježek F, Kofránek J. Physiobinary-Modelica library for Physiology. 10th International Modelica Conference; 2014 March 12; Lund, Sweden: Linköping University Electronic Press; 2014. pp. 499–505.
- [22] Mateják M. Physiology in Modelica. *Mefanet J* 2014; 2:10–4.
- [23] Sigaard-Andersen O. Oxygen-linked hydrogen ion binding of human hemoglobin. effects of carbon dioxide and 2, 3-diphosphoglycerate I. Studies on erythrolysate. *Scand J Clin Lab Invest* 1971;27:351–60.
- [24] Bauer C, Schröder E. Carbamino compounds of haemoglobin in human adult and foetal blood. *J Physiol* 1972;227:457–71.
- [25] Reeves RB. The effect of temperature on the oxygen equilibrium curve of human blood. *Respir Physiol* 1980; 42:317–28.
- [26] Kulhanek T, Mateják M, Šilar J, Kofránek J. Parameter estimation of complex mathematical models of human physiology using remote simulation distributed in scientific cloud. Biomedical and Health Informatics (BHI), 2014 IEEE-EMBS International Conference on 1–4 June 2014; pp. 712–5.
- [27] Sendroy J, Dillon RT, Van Slyke DD. Studies of gas and electrolyte equilibria in blood XIX. The solubility and physical state of uncombined oxygen in blood. *J Biol Chem* 1934;105:597–632.
- [28] Maas A, Rispens P, Sigaard-Andersen O, Zijlstra W. On the reliability of the Henderson-Hasselbalch equation in routine clinical acid-base chemistry. *Ann Clin Biochem* 1984;21:26.
- [29] Antonini E, Wyman J, Brunori M, Fronticelli C, Bucci E, Rossi-Fanelli A. Studies on the relations between molecular and functional properties of hemoglobin V. The influence of temperature on the Bohr effect in human and in horse hemoglobin. *J Biol Chem* 1965;240:1096–103.
- [30] Sauro HM. Enzyme kinetics for systems biology. Future Skill Software (Ambrosius Publishing); 2011. pp. 20–1.
- [31] Naeraa N, Petersen ES, Boye E. The influence of simultaneous, independent changes in pH and carbon dioxide tension on the in vitro oxygen tension-saturation relationship of human blood. *Scand J Clin Lab Invest* 1963;15:141–51.
- [32] Sigaard-Andersen O, Salling N. Oxygen-linked hydrogen ion binding of human hemoglobin. Effects of carbon dioxide and 2, 3-diphosphoglycerate. II. Studies on whole blood. *Scand J Clin Lab Invest* 1971;27:361–6.
- [33] Lide DR. CRC handbook of chemistry and physics. Boca Raton, FL: CRC Press; 2004.
- [34] Atha DH, Ackers GK. Calorimetric determination of the heat of oxygenation of human hemoglobin as a function of pH and the extent of reaction. *Biochemistry* 1974;13:2376–2382.
- [35] Hester RL, Brown AJ, Husband L, Iliescu R, Pruitt D, Summers R, Coleman TG. HumMod: a modeling environment for the simulation of integrative human physiology. *Front Physiol* 2011;2.
- [36] Kofránek J, Matousek S, Rusz J, Stodulka P, Privitzer P, Mateják M, Tribula M. The Atlas of Physiology and Pathophysiology: Web-based multimedia enabled interactive simulations. *Comput Methods Programs Biomed* 2011;104: 143–53.
- [37] Jarvis SS, Levine BD, Prisk GK, Shykoff BE, Elliott AR, Rosow E, Blomqvist CG, Pawelczyk JA. Simultaneous determination of the accuracy and precision of closed-circuit cardiac output rebreathing techniques. *J Appl Physiol* 2007; 103:867–74.

- [38] Sun X-G, Hansen JE, Ting H, Chuang M-L, Stringer WW, Adame D, Wasserman K. Comparison of exercise cardiac output by the Fick Principle using oxygen and carbon dioxide. *CHEST J* 2000;118:631–40.
- [39] Rees SE, Andreassen S. Mathematical models of oxygen and carbon dioxide storage and transport: the acid-base chemistry of blood. *Crit Rev Biomed Eng* 2005;33.
- [40] Imai K, Yonetani T. PH dependence of the Adair constants of human hemoglobin. Nonuniform contribution of successive oxygen bindings to the alkaline Bohr effect. *J Biol Chem* 1975;250:2227–31.
- [41] Adair G, Cordero N, Shen T. The effect of temperature on the equilibrium of carbon dioxide and blood and the heat of ionization of haemoglobin. *J Physiol* 1929;67:288–98.
- [42] Chipperfield J, Rossi-Bernardi L, Roughton F. Direct calorimetric studies on the heats of ionization of oxygenated and deoxygenated hemoglobin. *J Biol Chem* 1967; 242:777–83.
- [43] Weber RE, Campbell KL. Temperature dependence of haemoglobin-oxygen affinity in heterothermic vertebrates: mechanisms and biological significance. *Acta Physiolog* 2011; 202:549–62.
- [44] Weber RE, Fago A, Campbell KL. Enthalpic partitioning of the reduced temperature sensitivity of O₂ binding in bovine hemoglobin. *Comparat Biochem Physiol A: Molec Integrat Physiol* 2014;176:20–5.
- [45] Szabo A, Karplus M. A mathematical model for structure-function relations in hemoglobin. *J Mol Biol* 1972; 72:163–97.
- [46] Brunori M, Coletta M, Di Cera E. A cooperative model for ligand binding to biological macromolecules as applied to oxygen carriers. *Biophys Chem* 1986;23:215–22.
- [47] Henry ER, Bettati S, Hofrichter J, Eaton WA. A tertiary two-state allosteric model for hemoglobin. *Biophys Chem* 2002;98:149–64.
- [48] de Bruin SH, Rollema HS, Janssen LH, van Os GA. The interaction of chloride ions with human hemoglobin. *Biochem Biophys Res Commun* 1974;58:210–5.
- [49] Rollema HS, de Bruin SH, Janssen L, Van Os G. The effect of potassium chloride on the Bohr effect of human hemoglobin. *J Biol Chem* 1975;250:1333–9.
- [50] Benesch R, Benesch RE, Yu CI. Reciprocal binding of oxygen and diphosphoglycerate by human hemoglobin. *Proc Natl Acad Sci USA* 1968;59:526.
- [51] Bunn HF, Briehl RW. The interaction of 2, 3-diphosphoglycerate with various human hemoglobins. *J Clin Invest* 1970; 49:1088.
- [52] Sigaard-Andersen O, Salling N, Nørgaard-Pedersen B, Rørth M. Oxygen-linked hydrogen ion binding of human hemoglobin. effects of carbon dioxide and 2, 3-diphosphoglycerate: III. Comparison of the Bohr effect and the Haldane effect. *Scand J Clin Lab Invest* 1972;29:185–93.



Letter to the Editor

Modeling of short-term mechanism of arterial pressure control in the cardiovascular system: Object-oriented and acausal approach

ARTICLE INFO

Keywords:
 Acausal modeling
 MODELICA programming language
 OPENMODELICA modeling environment
 DYMOLA modeling environment
 Cardiovascular system

ABSTRACT

This letter introduces an alternative approach to modeling the cardiovascular system with a short-term control mechanism published in *Computers in Biology and Medicine*, Vol. 47 (2014), pp. 104–112. We recommend using abstract components on a distinct physical level, separating the model into hydraulic components, subsystems of the cardiovascular system and individual subsystems of the control mechanism and scenario. We recommend utilizing an acausal modeling feature of Modelica language, which allows model variables to be expressed declaratively. Furthermore, the Modelica tool identifies which are the dependent and independent variables upon compilation. An example of our approach is introduced on several elementary components representing the hydraulic resistance to fluid flow and the elastic response of the vessel, among others.

The introduced model implementation can be more reusable and understandable for the general scientific community.

© 2014 Elsevier Ltd. All rights reserved.

1. Introduction

Fernandez de Canete et al. [1] described a closed loop cardiovascular model and short-term and long-term mechanisms of arterial pressure control in the Modelica language and DYMOLA tool. The model is decomposed into several distinct components, which express computation of output volume, pressure and flow, based on elastance input, input flow and pressure. The basic blocks from standard Modelica libraries are composed together to model the whole hemodynamics with the control mechanism [1]. The process of computing of similar flowrate/volume, pressure, elastance and resistance is repeated in multiple blocks of pulmonary circulation, systemic circulation and heart circulation [1].

Redundant definition of similar relations and the mixing of more phenomenon in a single component were identified as antipatterns (bad practices) by Tiller [2], who recommends expressing single phenomenon as a general component model. This should be conducted by composing a subsystem model with instances of component models and utilizing the object-oriented features of the Modelica language.

Additionally the model [1] defines the flow of the computation of output values from input values. It is identified as causal or signal-oriented modeling. Modelica allows the expression of models not only in the causal (signal) manner, but also in an acausal manner. The acausal modeling technique is based on the fact that model variables are expressed declaratively, and the Modelica tool identifies which are the dependent and independent variables upon compilation. We have shown that an acausal description captures the essence of the modeled reality much better, and the simulation models are much more legible and, thus, also less prone to mistakes [3]. With the greatest respect to the authors of the above-mentioned publication, we would like to

introduce an alternative implementation of the original model with recommendations to reduce redundancy and utilize acausal and object-oriented modeling techniques. An example of our approach is shown with respect to an elastic vessel component with unstressed volume and external pressure.

As a result of the acausal approach we believe that the alternative implementation method introduced can be more reusable by the scientific community for educational as well as for research purposes.

Additionally, Modelica tools allow rich sets of numerical solving methods for further simulation and analysis, as well as export to third party tools used by computational physiologists.

Supplementary materials contain a full source code of the alternative model implementation derived from the original publication in the Modelica language together with dependent libraries.

2. Methods

Model behavior (equations) can be expressed in Modelica in text form and in graphical form – diagram. Later in this paper we present text form as a source code listing and graphical form as detailed by the figures.

To introduce an alternative implementation of the original model, the following recommendations should be followed:

- (a) Introduce an acausal connector for a hydraulic domain with “flow” variable q –flowrate and “non-flow” variable p –pressure. Introduce a single component for an elastic vessel, a hydraulic resistor and a cardiac valve with one or two acausal connectors and describe equations of volumetric flow, volume and pressure based on the parameters of elastance and resistance.

- (b) Separate a general model from a control model and a specific experiment. Utilize object-oriented features of the Modelica language to reuse the architecture model and replace the

The component is declared by icon () and by the statements and equations in the following Modelica listing (shortened):

```
model AortaFlowMeasurement "measures flow, diastolic, systolic and mean pressure"
...
discrete Boolean b(start=false) "beat signal";
Time T0(start=0) "start of cardiac cycle";
discrete Time HP(start=1) "length of cardiac cycle";
initial algorithm
Ps := q_in.pressure;
Pd := q_in.pressure;
equation
Pmax = max(Pmax, q_in.pressure);
Pmin = min(Pmin, q_in.pressure);
b = der(q_in.pressure) > 0;
when {b and not pre(b)} then
T0 = time "initial time of current cardiac cycle";
HP = if (pre(T0) > 0) then time - pre(T0) else 1;
Pmean = SumPressure / pre(HP) "mean pressure";
Ps = Pmax "systolic pressure = maximum pressure during cardiac cycle";
Pd = Pmin "diastolic pressure=minimal pressure during cardiac cycle";
reinit(SumPressure, 0) "reinitialisation of sum pressure";
reinit(Pmax, q_in.pressure) "reinitialisation of maximal pressure";
reinit(Pmin, q_in.pressure) "reinitialisation minimal pressure";
end when;
der(SumPressure) = q_in.pressure;
end AortaFlowMeasurement;
```

concrete implementation of the subsystem model with a derived model experiment.

- (c) Prefer the text form of Modelica notation to define equations on a component level model. Prefer the diagram form of Modelica notation to express relations between components on a higher subsystem and system level model.

We have recently published a Modelica library, referred to as Physiolibrary [4], to support modeling in the physiological domain. The library contains several hydraulic components that can be directly used to model the cardiovascular system following the recommendation (a). Table 1 contains icon, description and equations characterizing the components. The equations of these components are defined in Modelica using text form following the recommendation (c) and can be seen in supplementary materials. The models of the pulmonary circulation and the systemic circulation are defined by diagrams in Figs. 1 and 2 utilizing the components from Physiolibrary (from Table 1). The models are almost equivalent to the pulmonary and systemic blocks from the original work [1], apart from the pulmonary and aortic valves, that we moved to the model of the heart subsystem described later.

Additionally the systemic circulation contains a block to measure blood properties in aorta, it extends the existing block from Physiolibrary that measures flow. Additionally it computes systolic, diastolic and mean pressure during a single cardiac cycle. The mean arterial pressure P_{mean} during the cardiac cycle is counted as the average of pressure going into the component ($q_{in,pressure}$) from the beginning of the cardiac cycle (T_0) during the heart period (HP) by formula:

$$P_{mean} = \frac{\int_{T_0}^{T_0+HP} q_{in,pressure} dt}{HP} \quad (1)$$

We separate out the variable elastance(compliance) generator from the heart subsystem in Fig. 3.

The block “pulsos” (identified by icon ()) generates the relative heart phase within the heart period during a simulation time based on the heart rate signal [1]. However, in contrast to the original implementation we define it in text form per recommendation (c), and with the changed behavior: the heart period HP is changed per the input signal heart rate only at the moment when the new cardiac cycle begins. The output signal “heartphase” modeled in the original work can be presented as the following equation:

$$\text{heartphase} = \frac{\text{time} - T_0}{HP} \quad (2)$$

Thus, the model behavior is defined by the following listing:

```
model pulsos "relative position in heart period"
  discrete Physiolibrary.Types.Time HP(start = 0)
    "heart period - duration of cardiac cycle";
  Boolean b(start = false);
  discrete Physiolibrary.Types.RealIO.TimeOutput T0
    "start time of cardiac cycle";
  Physiolibrary.Types.RealIO.FrequencyInput HR;
  Modelica.Blocks.Interfaces.RealOutput heartphase;
equation
  b = time - pre(T0) >= pre(HP); //new cycle begins?
  when {initial(), b} then
    T0 = time; //update start time of cardiac cycle
    HP = 1 / HR; //update heart period
  end when;
  heartphase = (time - pre(T0)) / pre(HP);
end pulsos;
```

Table 1

Icon and description of hydraulic components used from Physiolibrary [4].

Icon	Description
◆◆	Hydraulic connectors – the MODELICA tool generates the following equations to keep “Kirchhoff law” analogy for all connected component’s non-flow variables $p_1 \dots p_n$ – pressure and “flow” variable $q_1 \dots q_n$ – flowrate: $p_1 = p_2 = \dots = p_n \quad (3)$ $\sum_{i=1}^n q_i = 0 \quad (4)$
	Hydraulic Resistor – characterized by G-conductance parameter (reciprocal value of resistance $G = 1/R$) and defined by relation among quantities from both hydraulic connectors, q -flowrate and $(p_{out} - p_{in})$ –pressure gradient: $q = G * (p_{out} - p_{in}) \quad (5)$
	Elastic compartment – characterized by C-compliance parameter(reciprocal value of elastance $C = 1/E$), V_0 –unstressed volume parameter, p_0 –external pressure parameter and by equation among p –pressure, V –volume and q –flowrate: $p - p_0 = \begin{cases} 0 & \text{if } V < V_0 \\ \frac{V - V_0}{C} & \text{otherwise} \end{cases} \quad (6)$ $\frac{dV}{dt} = q \quad (7)$
	Valve is characterized by the direction where the flow is allowed, by inflow and backflow conductance
	2D natural cubic interpolation spline defined by x, y and slope points. Used to define curve determined by empirical data

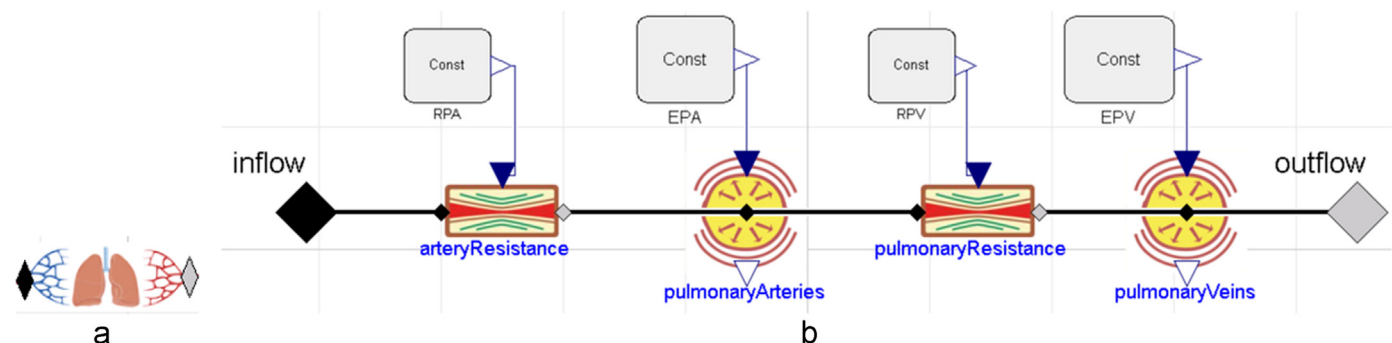


Fig. 1. Pulmonary circulation model icon (a) and its constitutive diagram (b). The elastic compartments and the resistors are connected via hydraulic connectors. The model parameters are presented as block Const with an appropriate type and value.

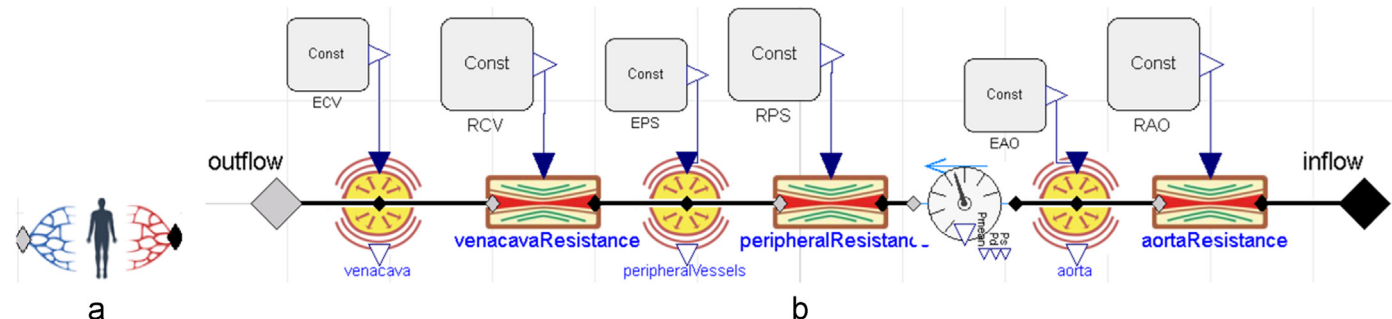


Fig. 2. Systemic circulation icon (a) and its constitutive diagram (b). The elastic compartments and the resistors are connected via hydraulic connectors. The model parameters are presented as block Const with an appropriate type and value.

The heart model in Fig. 4 consists of the left and right parts; they are driven separately by the appropriate elastance generator, but with the same heart rate signal.

Finally, the generic model of the hemodynamics without any control mechanism is shown in Fig. 5. Note that the diagram looks

very similar to the usual conceptual decomposition of the cardiovascular system.

Following recommendation (b), the model defines heart, systemicCirculation and pulmonaryCirculation components as “replaceable” to allow replacement with some derived subtype

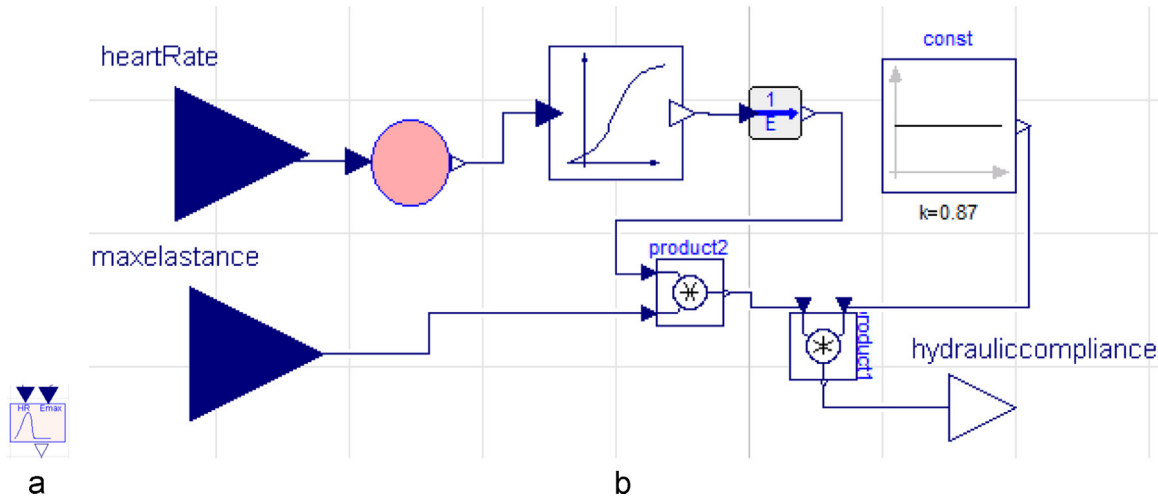


Fig. 3. Compliance generator icon (a) and its constitutive diagram (b). The relative elastance is generated from the relative time position in the heart period via empirical curves generated from points. As Physioblock uses a connector for compliance – reciprocal value of elastance – we convert elastance to compliance with a block $1/E$.

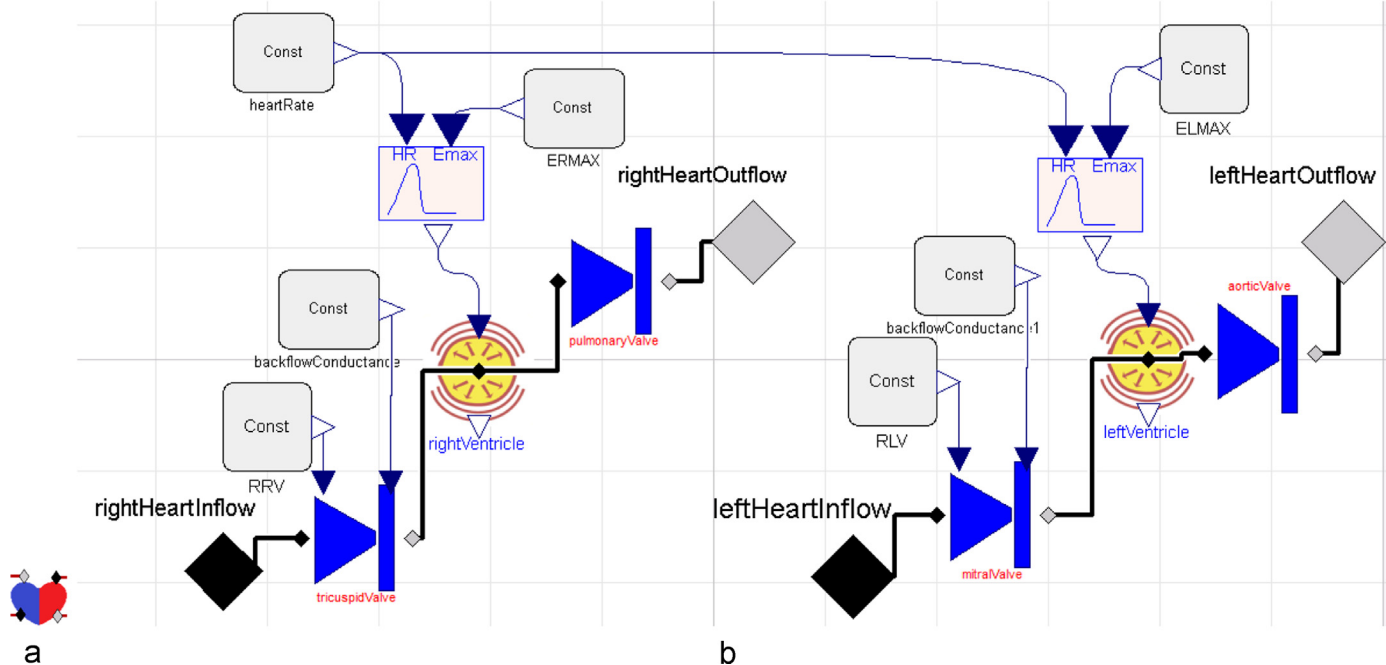


Fig. 4. Heart model icon (a) and its constitutive diagram (b). The valves are connected with the elastic compartment modeling the ventricle driven by the variable elastance component. Heart rate is shared but other parameters are different for each part.

of the model as seen from the text form of the model in the following listing:

```
model Hemodynamics_pure
  replaceable Parts.Heart heart;
  replaceable Parts.SystemicCirculation systemicCirculation;
  replaceable Parts.PulmonaryCirculation pulmonaryCirculation;
  ...
```

To simulate a particular scenario or control mechanism, selected parameters of the model need to be manipulated externally during simulation. We introduced derived model *SystemicCirculation_baro* and redeclared the constant block with a compatible control block as seen in the following listing which allows manipulation with the model parameter by an external

component.

```
model SystemicCirculation_baro
  extends FernandezModel.Parts.SystemicCirculation(
    redeclare HydraulicConductanceControl RPS,
    redeclare HydraulicComplianceControl ECV);
  ...
```

The subsystem *SystemicCirculation_baro* contains additional input connectors connected with the previously redeclared control blocks as shown in Fig. 6.

A similar technique is used for the heart component in Fig. 7. The model of controllable hemodynamics is an extension of the generic model of hemodynamics. The model uses new implementation of the controllable heart and systemic circulation and introduces input and output connectors specific for the baroreceptor control system,

as seen in the following listing and in Fig. 8.

```
model Hemodynamics_controllable
  extends Models.Hemodynamics_pure (
    redeclare Heart_baro heart,
    redeclare SystemicCirculation_baro systemicCirculation);
  ...

```

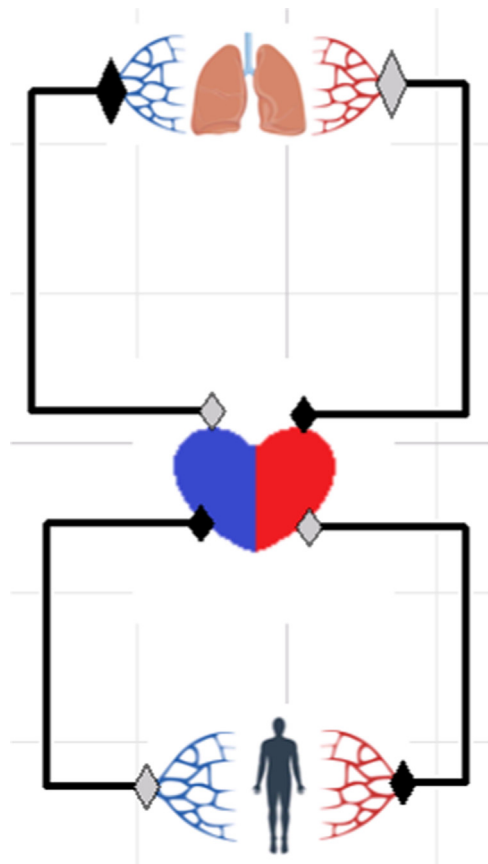


Fig. 5. Complete model of the cardiovascular system without any regulation.

The controllable model of hemodynamics is connected with baroreceptor module and with the module driving the simulation of stenosis, as shown in Fig. 9

3. Results

The implementation was changed in the case of block *pulos* and block *AortaFlowMeasurement*. Other parts are equivalent to the original work and use the same initial values of state variables and parameters [1]. The model can be executed in a free OPEN-MODELICA tool developed by Open Source Modelica Consortium [5]. The dynamics of the aortic pressure during a sudden change of elastance of vena cava shown in Fig. 10 gives similar results as the original work. The evolution of heart rate and ventricle elastance is smoother because the mean arterial pressure and the heart period signals are changed only at the beginning of the next cardiac cycle.

4. Discussion and summary

We believe that the recommendation (a) applied to the model allows it to better capture the essence of the modeled reality, in contrast to the original “signal”-like approach where it might be hard to deduce the concept of the model for a user who is not familiar with this modeling technique. Additionally further modification or enhancements of the basic component, e.g., elastic vessel by adding non-linear compliance or active tone, will be propagated to the existing model using this component with no or minimal need for further modification of the model. Such modification will appear in the model within the modified components as modified behavior or new parameters which can be set.

For example, the original model expresses the pressure p , volume V and compliance C (reciprocal value of elastance) as equation $p = V/C$. In contrast to the original model, the alternative implementation modifies the basic element of elastic compartment with unstressed volume V_0 and external pressure p_0 as Eq. (6). V_0 and p_0 are set to 0 by default and can be changed in further model experiments.

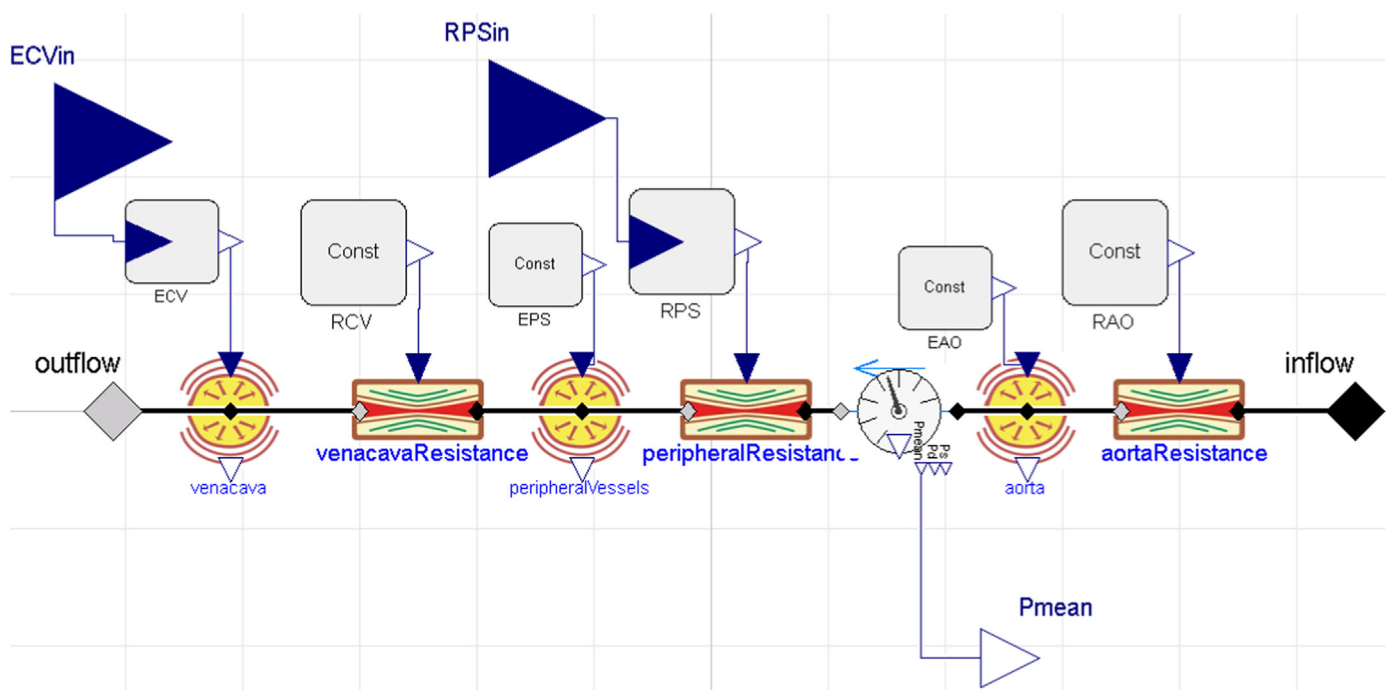


Fig. 6. SystemicCirculation prepared to be driven by elastance of vena cava and peripheral resistance coming from outside.

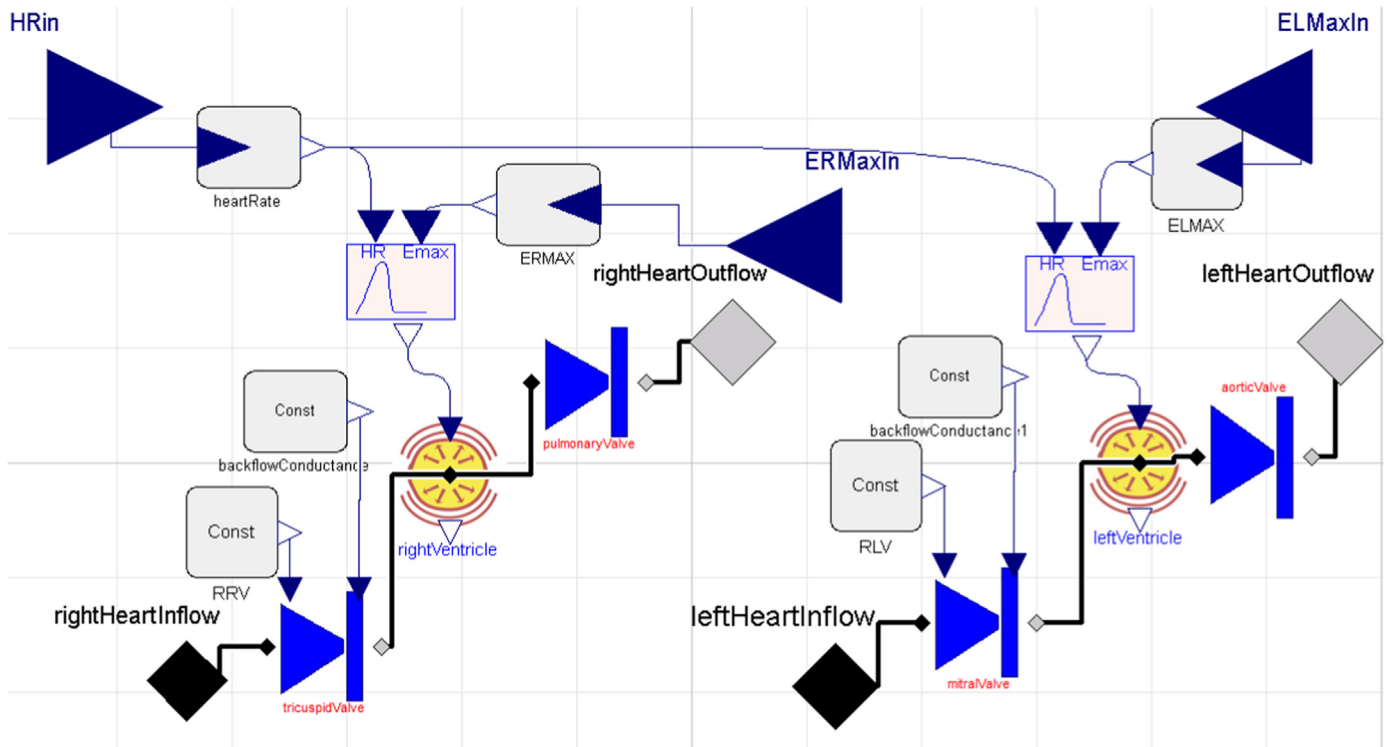


Fig. 7. The Heart model prepared to be driven by an elastance, and a change of the heart rate from outside control mechanism.

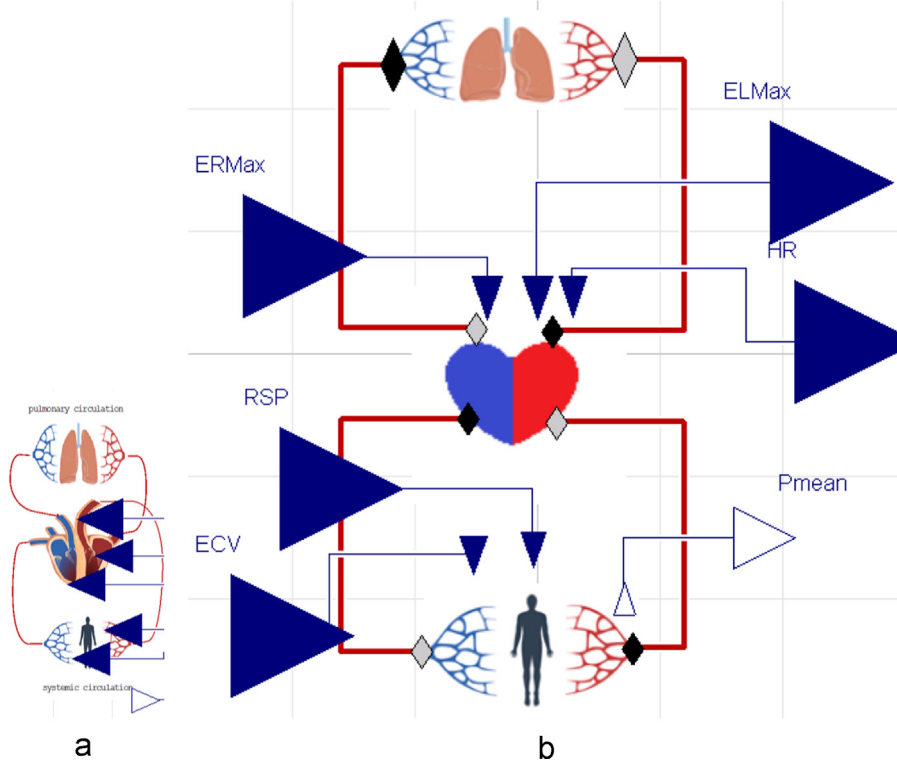


Fig. 8. Icon of the controllable model of hemodynamics (a) extended by input and output connectors and its constitutive diagram (b) connecting new connectors with the redeclared implementation of controllable heart and systemic circulation.

Such enhancement is propagated by inheritance to all elastic compartments used within the model. When the original model [1] needs to be enhanced with such features of unstressed volume or external pressure effect, then more than one component

(compartment with valve, compartment without valve and systemic circulation) needs to be modified.

The recommendation (b) applied to the generic model brings the advantage of a major feature of object-oriented programming –

polymorphism. A model (e.g. Hemodynamics_pure) comprises a subsystem model of a certain type (e.g. Heart) will work correctly with another subsystem that is compatible with the certain type (e.g. Heart_baro). The subsystem models might be reimplemented and

replaced in an existing model without touching the generic model. Therefore, it may be appropriate for specific in silico experiments.

The Modelica standard library allows equations to be expressed using blocks in diagrams; however, it should not be overused. For example, the recommendation (c) applied to the component "pulos" shows the Eq. (2) cleanly in the text form of Modelica notation (see the listing above). During the reimplementation of this block, we reformulated the method of changing the heart rate signal where heart period and pulse generation are updated at the beginning of the next cardiac cycle. This facilitates the computation. In the original work, the heart period and pulse generation are changed immediately. This difference is seen in simulating the baroreflex control, where the control mechanism is smoother, as seen in Fig. 10.

On the higher subsystem level, the recommendation (c) is optional. If there are more relations among components then a diagram form may be more understandable than a textual form. For example, the block VariableElasticityGenerator in Fig. 3 can be expressed in an equivalent text form as seen in the following model listing:

```
model VariableElasticityGenerator_text
...
equation
  pulsos.HR = heartRate;
  curve.u = pulsos.heartPhase;
  hydrauliccompliance = 0.87 * (maxelastance/curve.val);
end VariableElasticityGenerator_text
```

The original work contains a long-term pressure control mechanism, which was not implemented within this alternative implementation. However, it can be done following the above recommendations similar to the presented short-term "baroreflex" pressure control.

We believe that the introduced alternative approach to modeling the cardiovascular system will enhance the understandability

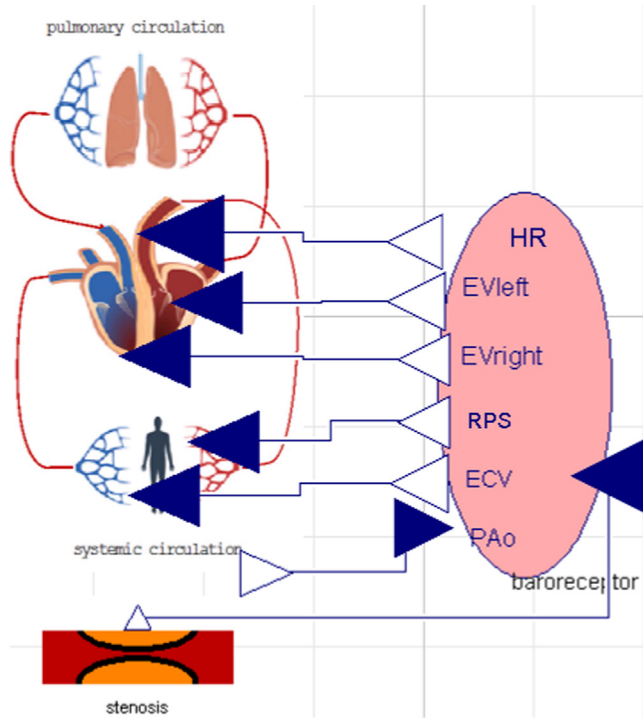


Fig. 9. The model of hemodynamics with baroreceptor control and a module manipulating the elastance during simulation – stenosis of vena cava simulation.

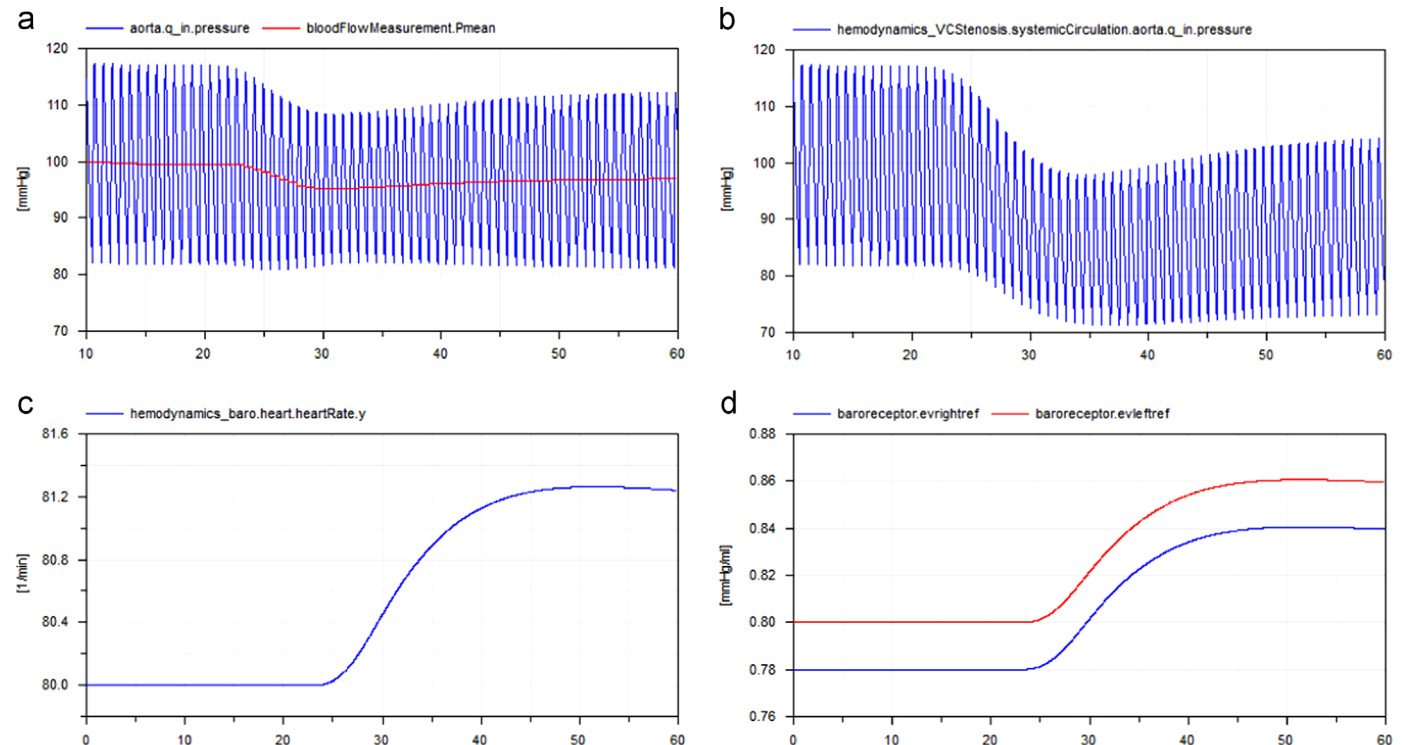


Fig. 10. Simulation of the aortic pressure response on vena cava elastance reduction at the simulation time 20 s for model with (a) and without (b) baroreceptor control showing the evolution of heart rate (c) and ventricle elastance (d).

and reusability of the excellent work done by the authors of the original model.

Conflict of interest statement

None declared.

Acknowledgments

This paper describes the outcome of research that has been accomplished as part of a research program funded by the Ministry of Industry and Trade of the Czech Republic via the grant FR-TI3/869; and by The Ministry of Education, Youth and Sports via the grant SVV-2014-260033.

Appendix A. Supplementary data

Supplementary data associated with this article can be found in the online version at <http://dx.doi.org/10.1016/j.combiomed.2014.08.025>.

References

- [1] J. Fernandez de Canete, J. Luque, J. Barbancho, V. Munoz, Modelling of long-term and short-term mechanisms of arterial pressure control in the cardiovascular system: an object-oriented approach, *Comput. Biol. Med.* 47 (2014) 104–112. <http://dx.doi.org/10.1016/j.combiomed.2014.01.006>.
- [2] M. Tiller, Patterns and anti-patterns in Modelica, in: Proceedings Modelica 2008 Conference, 2008, pp. 647–655.
- [3] J. Kofránek, M. Mateják, P. Privitzer, M. Tribula, Causal or acausal modeling: labour for humans or labour for machines, Technical Computing Prague, 2008, pp. 1–16.
- [4] M. Mateják, T. Kulhánek, J. Šilar, P. Privitzer, F. Ježek, J. Kofránek, Physiobrery—modelica library for physiology, in: Proceedings of the Tenth Modelica Conference, March 10–12, 2014, Lund, Sweden, 2014, pp. 499–505. URL <http://dx.doi.org/10.3384/ecp14096499>.
- [5] P. Fritzson, P. Aronsson, H. Lundvall, K. Nyström, A. Pop, L. Saldamli, D. Broman, The OpenModelica modeling, simulation, and software development environment, *Simul. News Eur.* 44 (45) (2005).

Tomáš Kulhánek, Jiří Kofránek*, Marek Mateják

Institute of Pathological Physiology, Charles University in Prague, U Nemocnice 5, 12853 Praha 2, Czech Republic
E-mail address: kofranek@gmail.com (J. Kofránek)

Received 15 May 2014; accepted 22 August 2014

* Corresponding author.

10th INTERNATIONAL **MODELICA** CONFERENCE

LIBRARY AWARD

The Board of the 10th International Modelica Conference awards

Marek Mateják,

Tomáš Kulhánek, Jan Šilar,

Pavol Privitzer, Filip Ježek and

Jiří Kofránek

1st price of 500€

for contributing the free Modelica library:



Physiolibrary

Lund, March 12th 2014

The Chairman of the Modelica Association

Prof. Dr. Martin Otter

A handwritten signature in black ink, appearing to read "Martin Otter".

Program Chair

Dr. Hubertus Tummescheit

A handwritten signature in blue ink, appearing to read "Hubertus Tummescheit".

Physiolibrary - Modelica library for Physiology

Marek Mateják*, Tomáš Kulhánek*, Jan Šilar*, Pavol Privitzer*, Filip Ježek**, Jiří Kofránek*

*Institute of Pathological Physiology, 1st Faculty of Medicine, Charles University in Prague

U nemocnice 5, Prague 2, 128 53, Czech Republic

**Department of Cybernetics, Faculty of Electrical Engineering, Czech Technical University in

Prague, Technicka 2, Prague 6

marek@matfyz.cz

Abstract

Physiolibrary is a free open-source Modelica library designed for modeling human physiology. It is accessible on the Modelica Libraries web page at <https://www.modelica.org/libraries>. This library contains basic physical laws governing human physiology, usable for cardiovascular circulation, metabolic processes, nutrient distribution, thermoregulation, gases transport, electrolyte regulation, water distribution, hormonal regulation and pharmacological regulation.

Keywords: *Physiolibrary; HumMod; Modelica library; Physiology; Integrative physiology; System biology*

1 Introduction

Our laboratory have a long tradition building physiological libraries, starting with the Matlab/Simulink environment [2]. The origin of this Modelica Physiolibrary was in the first version of our HumMod Golem Edition model implementation [3-6], where it was called HumMod.Library. As the successors of Guyton's Medical Physiology School write, the original HumMod model [7] is "The best, most complete, mathematical model of human physiology ever created" [8].

We are also developing many types of smaller physiological models for use in medical education [9-11], so it was essential to separate this library from our HumMod Modelica implementation. Some other Modelica models and libraries covering the biological domain already existed, e.g. [12-17], which are useful in the process of system modeling and parameter identification. Especially BioChem Modelica library, that implements large part of SBML library in Modelica language [14-18].

Our Physiolibrary contains only carefully-chosen elementary physiological laws, which are the basis of more complex physiological processes. For example from only three type of blocks (ChemicalReaction, Substance and MolarConservationMass) it is possible to compose the allosteric transitions [19] or the Michaelis-Menten equation.

2 Physiology

Physiology is a very progressive discipline, that examines how the living body works. And it is no surprise that all processes in the human body are driven by physical laws of nature. The great challenge is to marry old empirical experiments with the "new" physical principles. Many teams and projects in the word deal with this formalization of physiology, for example: Physiome[20], SBML[17, 18], EuroPhysiome[21], VPH[22], CellML[23] etc. It is our hope that this library helps this unflagging effort of physiologists to exactly describe the processes.

2.1 Display units in physiology

Energy in medicine and chemistry has a very long tradition. One must not be confused by its different units and definitions. The researcher must be aware of multiple definitions of calorie, such as the international calorie, the 15°C calorie, the thermal calorie or the Calorie with a capital "C". The origin of this unit is in the thermal energy needed to heat one gram of water by one degree Celsius. But because the measurement conditions may differ, these alternative definitions are necessary. In physiology it is recommended to use only international calorie as defined in Table 1. The flow of heat/energy is usually calculated in kcal/min, but in physics this is called power and is expressed in the SI unit watts.

Pressure units in medicine are also mainly based on historical measurements. For many years blood

pressure was measured by the mercury sphygmomanometer, where the pressure is represented by the change of mercury hydrostatic column height. And because the scale of units on the column is in millimetres the pressure unit is called millimetre of mercury 'mmHg'. There also exists a very small difference between this unit and torrs. It is caused again by variance in measurement conditions.

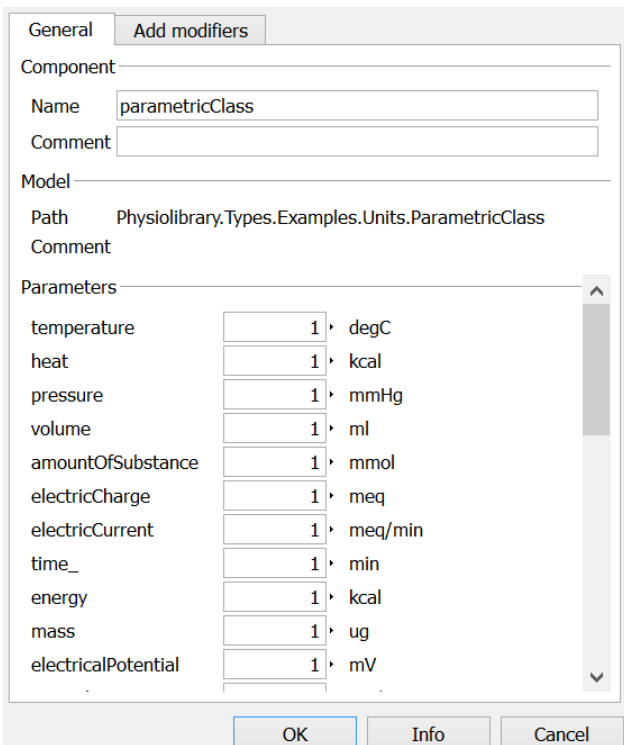


Figure 1, Example parameter dialog for non-SI physiological units. The Dymola environment automatically converts this user's non-SI-values to SI-values to ensure compatibility with any other Modelica library.

Many physiological processes are based on electrical principles in the human body. The main cause of this is that each cell has a nonconductive membrane with molecular structures called channels, through which the fluxes of electrolytes can be precisely regulated. Even more, the cells use energy from metabolism to retain a small electric potential between inside and outside. This view leads to a unit called equivalents or "eq". A charge of 1eq, for example, has 1mol of sodium cations (Na^+). The fluxes of electrically charged ions can be in meq/min, but in physics the SI unit ampere is more generally used.

Unit conversion table (for Modelica environment display-unit setting)

x kcal	=	4186.8*x J
x kcal/min	=	69.78*x W

x mmHg	=	133.322387415*x Pa
x degC	=	273.15 + x K
x meq	=	96.4853365*x C
x meq/min	=	1.60808894*x A
x mosm	=	0.001*x mol
x litreSTP	=	0.044031617*x mol
x litreSATP	=	0.040339548*x mol
x litreNIST	=	0.041571200*x mol

Table 1, Selected Non-SI units in physiology

Another strange unit describing the amount of substance is the osmol ("osm"), which has the same value as the mol, but which highlights the property that this substance cannot cross the membrane together with the flux of its solvent.

For gases, it is common to measure the amount as volume, which for specific measurement conditions is equivalent to the number of molecules. The International Union of Pure and Applied Chemistry (IUPAC) set this standard condition for temperature and pressure (STP) precisely at 0°C and 100kPa. But other standards exist. For example, SATP is measured at 25°C and 100kPa, or the standard measurement condition at the National Institute of Standards and Technology (NIST), which is 20°C and 101.325kPa.

2.2 Chemical domains in physiology

In physiology books, chapters about chemical substances are organized by their types. The main reason for this is that each substance in the human body is regulated in a different way. For example the regulation of sodium is different from the regulation of potassium, and from the regulation of glucose, and so on. This view leads to the idea of having separate models of each substance. The origin of different flows and regulations is the (cellular) membrane. Water and solutions can cross it in different directions at the same time. Crossings occur for different reasons: water is driven mostly by osmotic gradients, electrolytes are driven by charge to reach Donnan's equilibrium, and some solutes can even be actively transported against their concentration or electrical gradients. And all this is specifically driven from the higher levels by neural and hormonal responses.

In Physilibrary flows and fluxes of solutes are supported mostly by the Chemical package. All parts inside this Physilibrary.Chemical package use the connector ChemicalPort, which defines the molar concentration and molar flow/flux rate of one solute. This is the supporting infrastructure for modeling membrane diffusion, accumulations of substances,

reversal chemical reactions, Henry's law of gas solubility, dilution with additional solvent flow, membrane reabsorption, chemical degradation and physiological clearance.

For usage examples, please open the `Chemical.Examples` package, where the chemical reaction shown in Fig. 2 is implemented, along with many other chemical processes.

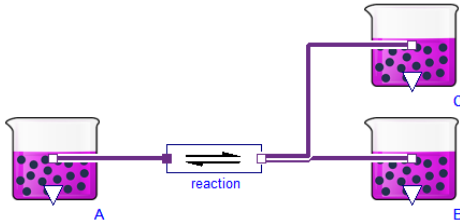


Figure 2, Example of a chemical reaction: $A \leftrightarrow B + C$. Purple beakers (Substance) accumulate one type of substance and generate its concentration in port. Block for chemical reaction (ChemicalReaction) can have any number of substrates or products with any stoichiometric numbers. In this case there is only one substrate and two products. Purple lines represent chemical connectors, are composed of molar concentration and the molar flow of substance.

The graphically-created diagram shown in Fig. 2 generates this Modelica code:

```
model SimpleReaction2
import Physiolibrary.Chemical.Components.*;
Substance A(solute_start=0.9);
ChemicalReaction reaction(K=1, nP=2);
Substance B(solute_start=0.1);
Substance C(solute_start=0.1);
equation
connect(A.q_out, reaction.substrates[1]);
connect(reaction.products[1], B.q_out);
connect(reaction.products[2], C.q_out);
end SimpleReaction2;
```

This means that before the numerical simulation begins, each `Substance.solute_start` parameter must be set to some initial amount of substance. `ChemicalReaction.nP` must also be configured for the number of products, and parameter `ChemicalReaction.K` must be configured for the dissociation constant of reaction in SI-units (please note that concentration of $1 \text{ mol/m}^3 = 1 \text{ mmol/L}$). As mentioned before, the values in text code are in SI-units, but the Dymola environment support non-SI units in the parameter dialog of each component.

2.3 Hydraulic domain in physiology

The main usage of the hydraulic domain in human physiology is modeling of the cardio-vascular system. And because there are no extreme thermo-

dynamic conditions, the system can be really simple—it is only necessary to model conditions for incompressible water, at normal liquid-water temperatures and with relative pressure 5-20kPa. This boring thermodynamic state leads to using very simple blocks of hydraulic resistance, hydrostatic pressure, volumetric flow, inertia and finally a block representing blood accumulation in elastic vessels.

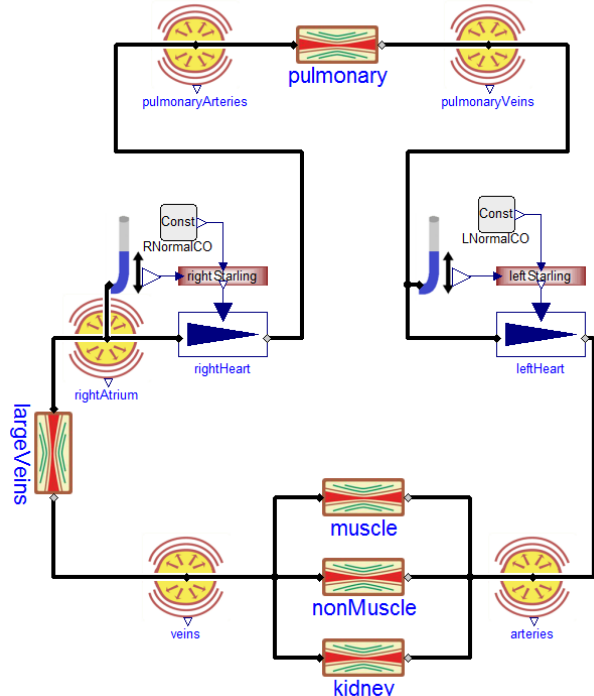


Figure 3, Hydraulic example: the cardiovascular subsystem of the famous Guyton-Coleman-Granger model [1]. Yellow circles (ElasticVessel) represent blood accumulation and pressure generation, rectangles between them are hydraulic resistances (Resistance) of blood vessels, blue triangles (Pump) represent a heart pump driven by the Frank-Starling law. Heart-filling pressures are determined by the block with the blue tube icon (PressureMeasure) and a block-rectangle (Blocks.Factors.Spline) converts filling pressure to their effect on cardiac output. Black lines connect the hydraulic connectors (HydraulicPort), which contains pressure and volumetric flow variables.

2.4 Thermal domain in physiology

For the human body to function optimally, it is critical to hold the core temperature at $35\text{--}39^\circ\text{C}$. A fever of 41°C for more than a short period of time causes brain damage. If the core temperature falls below 10°C , the heart stops. As in the hydraulic domain, the thermal domain is simplified to these conditions.

The `Physiolibrary.Thermal` package extends the package `Modelica.Thermal.HeatTransfer` from

Modelica Standard Library 3.2 (MSL), where the connector is composed of temperature and heat flow. The main blocks in Physiolibrary.Thermal are: Conductor, IdealRadiator and HeatAccumulation. The heat conductor conducts the heat from the source, such us muscles or metabolically active tissue, to its surrounding. IdealRadiator delivers heat to tissues by blood circulation. HeatAccumulation plays a role in accumulating thermal energy in each tissue mass driven by its heat capacity. We recommend using this block instead of Modelica.Thermal.HeatTransfer.HeatCapacitor to allow the possibility of variable mass amounts, and to have support for calculating steady state, described in section 2.7.

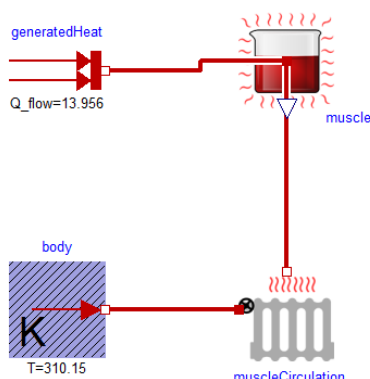


Figure 4, Example of heat flow from a working muscle. The muscle is represented by a red beaker (HeatAccumulation), where heat energy is accumulated in a mass with defined weight and specific heat. Heat transfer is processed by blood circulation (IdealRadiator) with blood flow as its internal parameter. The temperature of blood is set to a fixed value of 37°C to simulate well-regulated core body temperature.

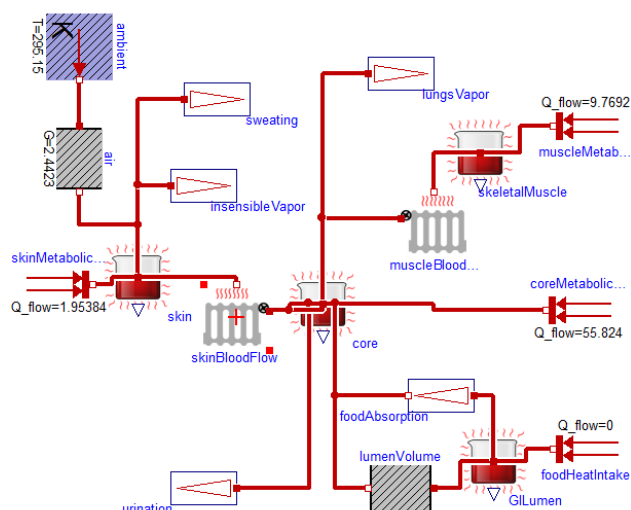


Figure 5, Basic heat flow model of human body. Heat production occurs in each tissue via metabolism, or from warm (to cool) eaten food using the MSL block

with two red arrows (Modelica.Thermal.HeatTransfer.Sources.FixedHeatFlow). This heat is stored in tissues (HeatAccumulation) and transferred out by blood (IdealRadiator) or together with mass (Stream, HeatOutstream), where the model also integrates vaporization heat loss. Heat radiation and conduction to the environment is simplified using an MSL block for heat conductor (Modelica.Thermal.HeatTransfer.Components.ThermalConductor).

2.5 Osmotic domain in physiology

One of the basic phenomenon of biological systems is the osmotically-driven flow of water. This is always connected with semipermeable membranes. The different concentrations of impermeable solutes on both sides of the membrane causes the hydrostatic pressure at the concentrated side to rise[24]. This pressure difference is called osmotic pressure. Osmotic pressure is linearly proportional to the concentration gradient of impermeable solutes. The osmolarity (osmotic concentration) is also one of the main indexes of human body balance, called homeostasis. Its value should not significantly deviate for a long period of time from a value of 285-295mosm/l.

In Physiolibrary the osmotic connector OsmoticPort is composed of the osmotic concentration and the volumetric flux of permeable liquid. The two main blocks are called Membrane and OsmoticCell. Here, inside the membrane blocks, it is of course possible to also define hydraulic pressure and temperatures effects on both sides of membrane.

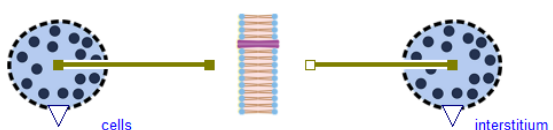


Figure 6, Osmotic example simulating water transfer between intracellular and interstitial compartments in hypertonic or hypotonic conditions.

2.6 Types and units

The most common errors in HumMod Golem Edition were caused by using bad physical units. The main problem of medical research, articles, and experiments is using obscure units from medicine, pharmacology, biology and non-physics disciplines.

The Physiolibrary fulfills the Modelica ideal of using SI units as the main unit for each variable, and the previously described physiological units are also implemented as the displayUnits for each variable. Using these displayUnits the user sets and sees the "physiological" values. The implementation can also be joined to any unit-correct Modelica models and physical equations without crashing due to unit in-

compatibilities. The unit support of Physilibrary is so strong that one can even chose the right unit-typed “input real”/“output real” from the library package Types.RealIO or one can use unit-typed constants (Types.Constants). As can be expected, only the non-specific package Blocks in the Physilibrary has variables without units.

2.7 Steady states

One of the main questions in clinical medicine is how to stabilize the patient. In modeling the oscillating heart, breathing, circadian rhythm or menstruation cycle the model can be designed as non-oscillating, using variables such as period times, amplitudes, frequencies, mean values and other phase space variables. This type of model has better numerical stability for long simulation times, and even more importantly, it can be “stabilized”. This stabilization we call a steady state.

To be mathematically exact, we define a *steady state system* (SSS) as a non-differential system derived from an original differential system (DS) by using zero derivations and by adding additional steady state equations (ASSE). The number of the ASSE must be the same as the number of algebraically dependent equations in the non-differential system derived from DS by setting zero derivations. The ASSE describes the system mostly from the top view, such as the equations of mass conservation laws or the boundary equation of environment sources.

To define a model as an SSS, the user must switch each Simulation parameter in each block to the value Types.SimulationType.SteadyState and must have correctly defined all necessary ASSE. This setting causes the system to ignore any start values for any state and add zero derivation equations instead. There does not currently exist a Modelica environment which can automatically find and remove generated dependent equations by this solution. So the correct number of states must be marked as dependent (parameter isDependent) and the same number of ASSE must be inserted. However, despite the fact that a model in this steady-state setting will not be locally balanced, it must be globally balanced and without any dependent equation.

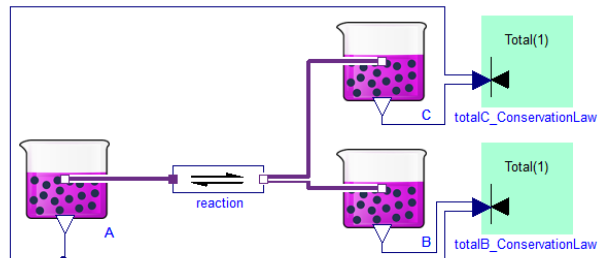


Figure 7, Steady state system example: equilibrium of chemical reaction $A \rightleftharpoons B + C$ is calculated with two ASSE. Zero change of reactant A is automatically propagated through a reaction to both products. So both products must be marked as dependent (parameter `isDependent`), and two mass conservation laws must be added as green square blocks to the right (`MolarConservationLaw`). Please note that conservation laws must be included only after designing the rest of the system, because they are global properties, not properties of individual substances or reactions.

Adding an ASSE is possible by inserting and connecting the energy or mass conservation law block from package SteadyState.Components. Another possibility is using environment sources blocks, where setting the `isIsolatedInSteadyState` parameter adds the equation of the zero mass/volume/energy flow from or to environment.

The steady state model often changes to one big nonlinear strong component, but without solver stiff or convergence problems. Especially in quick chemical kinetics, it is not necessary to have very rapid molar fluxes, when it always reach equilibrium in the end. This design is also useful in creating steady-state parts in a dynamical model without huge rebuilding. It also brings other benefits. To see these possibilities, one has to realize that conservation laws could be invariances in a dynamical simulation. This is really useful for debugging.

For example see the model SteadyStates.Examples.SimpleReaction2_in_Equilibrium (Fig.7), which implements the equilibrium of the closed system from Fig.2 as a solution of three chemical substances with a simple reversible reaction between them extended by two conservation laws. Each of these laws describes the total possible amount of one product in its free form and in its associated form.

It is always a big challenge to nicely solve initial values of differential system. However, it should be possible to solve the SSS in its initial phase. And this is the idea behind the Types.SimulationType.InitSteadyState option for models already extended with ASSE.

2.8 File utilities—input/output manipulations

During the creation and debugging of huge integrated models it is necessary to easily define consistent input, output and test sets of all output variables for some subsystems. Let's imagine that we have a model composed only of subsystems that converge from some constant inputs to constant outputs. It should be possible to substitute each main subsystem for its chosen constant output values as parameters. Comparing the model with these parametric values and the original subsystem can show the wrong part of the simulation.

For example in the huge HumMod model it is necessary to debug smaller parts separately. These tools could be used, because HumMod is the type of constant-converged model. Each subsystem in the first level has the constant input values set for its output variables. Simulating, for example, the cardiovascular subsystem is possible by creating the high-level system with the original cardiovascular subsystem, but with a constant metabolic, constant thermoregulation, constant hormonal, constant water, constant proteins, constant gases, constant electrolytes and constant status subsystem.

Because the number of output variables for each subsystem changes during development, it is a good idea to have only one list for each subsystem. And generating consistent sets to store, restore, compare initial and final values is possible by the same pattern as presented in the package Types.Example. In this package it is also possible to define a customized way to save and load the variables that connect subsystems together. For this purpose, one has to redeclare the package Types.Utilities with simple functions for reading and writing values, such as is done in the default package FileUtilities.

The typical code of a parameter set could be:

```
model MyParameterSet
  replaceable package T = Physiolibrary.Types.RealTypes
  constrainedby Physiolibrary.Types.RealTypes;

  T.Pressure      v1(varName="Bone-Flow.PO2");
  T.VolumeFlowRate v2(varName="Bone-Flow.BloodFlow");
  T.MolarFlowRate v3(varName="Bone-Metabolism.O2-Need");
  T.Volume        v4(varName="Bone-Tissue.LiquidVol");

  BusConnector busConnector;

equation
  connect(v1.y, busConnector.Bone_PO2);
  connect(v2.y, busConnector.Bone_BloodFlow);
  connect(v3.y, busConnector.Bone_O2Need);
  connect(v4.y, busConnector.Bone_LiquidVol);
end MyParameterSet;
```

To redefine these sets of values to use inputs from a file is simple. The user just redeclares the type of the values to type InputParameter and redirects reading functions to FileUtilities:

```
model InputParameterSet
  extends MyParameterSet( T(redeclare block Variable =
    Physiolibrary.Types.RealExtension.InputParameter (
      redeclare package Utilities = Physiolibrary.Types.FileUtilities)));
end InputParameterSet;
```

And the same set of values can also be redefined to file output at the end of the simulation:

```
model OutputFinalSet
  extends MyParameterSet( T(redeclare block Variable =
    Physiolibrary.Types.RealExtension.OutputFinal (
      redeclare package Utilities = Physiolibrary.Types.FileUtilities)));
end OutputFinalSet;
```

3 Conclusion

In our opinion the best way to understand this library is to download it from the Modelica web pages at www.modelica.org/libraries and examine the examples. We recommend examining the package Hydraulic.Examples, which provides an example of a simplified cardiovascular system; the package Chemical.Examples, which provides an example of allosteric hemoglobin oxygen binding; the package Osmotic.Examples, which simulates cell volume in hypertonic and hypotonic environments; and finally the package Thermal.Examples, which simulates the heating of circulated blood inside active muscles.

Acknowledgements

This paper describes the outcome of research that has been accomplished as part of a research program funded by the Ministry of Industry and Trade of the Czech Republic by the grant FR—TI3/869 and by The Ministry of Education, Youth and Sports by the grant SVV-2013-266509.

In addition, the main author wants to thank Jan Obdržálek for consultations about physical units, and Austin Schaefer for English language editing.

References

- [1] Guyton, A.C., T.G. Coleman, and H.J. Granger, *Circulation: overall regulation*. Annual review of physiology, 1972. **34**(1): p. 13-44.

- [2] Teaching, L.o.B.a.C.A. *Physiolibrary in Matlab and Simuling*. 2008; Available from: <http://www.physio.me.cz/simchips>.
- [3] Marek Mateják and J. Kofránek, *HUMMOD-GOLEM EDITION-ROZSÁHLÝ MODEL FYZIOLOGICKÝCH SYSTÉMŮ* Medsoft, 2011: p. 182-196.
- [4] Marek Mateják and J. Kofránek, *Rozsáhlý model fyziologických regulací v Modelice*. Medsoft, 2010: p. 126-146.
- [5] Kofránek, J., M. Mateják, and P. Privitzer. *HumMod - large scale physiological model in Modelica*. in *8th. International Modelica conference*. 2011. Dresden, Germany.
- [6] Kofránek, J., Mateják, M., Privitzer, P., Tribula, M., Kulhánek, T., Šilar, J., Pecinovský, R. *HumMod-Golem Edition: large scale model of integrative physiology for virtual patient simulators*. in *World Congress in Computer Science 2013 (WORLDCOMP'13), International Conference on Modeling, Simulation and Visualisation Methods (MSV'13)*. 2013.
- [7] Hester, R.L., et al., *HumMod: a modeling environment for the simulation of integrative human physiology*. *Frontiers in physiology*, 2011. 2.
- [8] Center, L.b.U.o.M.M., *HumMod*. 2012: p. <http://hummod.org/>.
- [9] Kofránek, J., M. Mateják, and P. Privitzer. *Leaving toil to machines - building simulation kernel of educational software in modern software environments*. in *Mefanet 2009*. 2009. Masaryk University, Brno.
- [10] Kofránek, J., M. Mateják, and P. Privitzer, *Web simulator creation technology*. MEFANET report, 2010. 3: p. 52-97.
- [11] Kofranek, J., et al., *The Atlas of Physiology and Pathophysiology: Web-based multimedia enabled interactive simulations*. *Computer methods and programs in biomedicine*, 2011. 104(2): p. 143-153.
- [12] Proß, S. and B. Bachmann, *An Advanced Environment for Hybrid Modeling and Parameter Identification of Biological Systems*.
- [13] Cellier, F.E. and A. Nebot. *Object-oriented Modeling in the Service of Medicine*. in *Proc. 6th Asia Simulation Conference*. 2005.
- [14] Larsdotter Nilsson, E. and P. Fritzson. *BioChem-A Biological and Chemical Library for Modelica*. in *Proceedings of the 3rd International Modelica Conference (November 3-4, Linköping, Sweden)*. 2003. Modelica Association.
- [15] Nilsson, E.L. and P. Fritzson, *Biochemical and metabolic modeling and simulation with Modelica*. BioMedSim. Linköping, Sweden, 2005.
- [16] Nilsson, E.L. and P. Fritzson. *A Metabolic Specialization of a General Purpose Modelica Library for Biological and Biochemical Systems*.
- [17] in *Paper presented at the 4th International Modelica Conference*. 2005.
- [18] Brugård, J., et al. *Creating a Bridge between Modelica and the Systems Biology Community*. in *7th International Modelica Conference, Como, Italy*. 2009.
- [19] Hucka, M., et al., *The systems biology markup language (SBML): a medium for representation and exchange of biochemical network models*. *Bioinformatics*, 2003. 19(4): p. 524-531.
- [20] Monod, J., J. Wyman, and J.-P. Changeux, *On the nature of allosteric transitions: a plausible model*. *Journal of Molecular Biology*, 1965. 12(1): p. 88-118.
- [21] Bassingthwaite, J.B., *Strategies for the physiome project*. *Annals of Biomedical Engineering*, 2000. 28(8): p. 1043-1058.
- [22] Fenner, J.W., et al., *The EuroPhysiome, STEP and a roadmap for the virtual physiological human*. *Philosophical Transactions of the Royal Society A: Mathematical, Physical and Engineering Sciences*, 2008. 366(1878): p. 2979-2999.
- [23] Hunter, P.J. and M. Viceconti, *The VPH-physiome project: standards and tools for multiscale modeling in clinical applications*. *Biomedical Engineering, IEEE Reviews in*, 2009. 2: p. 40-53.
- [24] Smith, L., et al., *SBML and CellML translation in Antimony and JSim*. *Bioinformatics*, 2013: p. btt641.
- [25] Mortimer, R.G., *Mathematics for physical chemistry*. 1999: Access Online via Elsevier.